# Mathematical Modelling of Mitotic Exit Control in Budding Yeast Cell Cycle

Paula Sofia de Sá Freire

Merton College

Oxford

Dissertation submitted for the degree of Doctor of Philosophy

Department of Biochemistry, University of Oxford

May 2012

# Acknowledgements

I would like to thank Professor Béla Novák for guidance and support. He transmitted me his passion for scientific research, especially for the cell cycle field. He motivated me to always work hard, do my best, and never give up. It was a privilege to work under his supervision and be part of his group.

I would like to thank Vinod Palakkad Krishnanunni for his collaboration and help. Since the early start of my DPhil, Vinod and I were working together on various scientific projects. His experience on the field of systems biology was very important to me, and I have learned much from him.

I thank all the other members of the lab for their constant support: Orsolya Kapuy, Bernhard Schmierer, Maria Domingo-Sananes, Enuo He, Tongli Zhang, Anael Verdugo, Ahmed Rattani, Guido Klingbeil, Elwy Okaz, and Claude Gerard. I am very grateful for all our scientific discussions and for sharing their views with me. In addition, I would like to leave a special acknowledgement to Maria, for her valuable help with the work on robustness.

I would like to thank Frank Uhlmann and Andrea Ciliberto for their collaboration in the work on mitotic exit.

I thank Fundação para a Ciência e Tecnologia (FCT), PhD Program in Computational Biology (PDBC) and Instituto Gulbenkian Ciência for giving me the opportunity to come to Oxford for my DPhil. I am particularly grateful to Jorge Carneiro, the PDBC director,

for having believed in me five years ago. I would also like to thank him for his continuous support.

I am also grateful to my college, Merton, and the UNYCELLSYS project for supporting me in the accomplishment of my work.

I thank my family for always believing in me; my mother, Antónia Freire, and my father, João Pedro Freire, in particular. You both have been a constant source of strength and inspiration.

David Pritchett, thank you for always being there for me.

# Index

# Abbreviations

| | |
|---|---|
| APC | Anaphase Promoting Complex (also called Cyclosome) |
| ATP | Adenosine triphosphate |
| Bir | Baculoviral IAP Repeat-containing protein |
| Bns | Bypasses need for Spo12p |
| Bub | Budding uninhibited by benzimidazole |
| CAK | CDK1-activating kinase |
| CDK1 | Cyclin dependent kinase 1 |
| Cdc | Cell division cycle |
| Cdh1 | Cdc20 homolog 1 |
| CKI | Cyclin dependent kinase inhibitor |
| CV | Covariance |
| Dbf | DumbBell forming |
| DNA | Deoxyribonucleic acid |
| Esp | Extra spindle pole bodies |
| FEAR | cdc Fourteen Early Anaphase Release |
| Fkh | Fork head homolog |
| Fob | Fork blocking less |
| GAP | GTPase-activating protein |
| GEF | Guanine nucleotide exchange factor |
| Grr | Glucose repression-resistant |
| GTP | Guanosine triphosphate |
| Ipl | Increase in ploidy |
| Kar | Karyogamy |

| | |
|---|---|
| Kin | Kinase |
| Lte | Low temperature essential |
| MBF | MCB (Mbp1-Swi6 cell cycle box) binding factor |
| Mbp | MluI-box binding protein |
| Mcm | Minichromosome maintenance |
| MEN | Mitotic exit network |
| Mih | Mitotic inducer homolog |
| min | Minutes |
| Mob | Mps one binder |
| mRNA | Messenger RNA |
| MV1 | Model Version 1 |
| MV2 | Model Version 2 |
| MV3 | Model Version 3 |
| MV4 | Model Version 4 |
| Ndd | Nuclear division defective |
| Net | Nucleolar silencing establishing factor and telophase regulator |
| NLS | Nuclear localization signal |
| NRD | No regulated degradation |
| NRT | No regulated transcription |
| ODE | Ordinary differential equation |
| QM | Queralt's Model |
| PDE | Partial differential equation |
| Pds | Precocious dissociation of sisters |
| RENT | Regulator of nucleolar silencing and telophase |
| RNA | Ribonucleic acid |

| | |
|---|---|
| SAC | Spindle assembly checkpoint |
| SBF | SCB (Swi4-Swi6 cell cycle box) binding factor |
| SCF | Skp-Cullin-F box protein |
| SD | Standard deviation |
| SIN | Septation Initiation Network |
| Sir2 | Silent information regulator |
| Sli | Synthetically lethal with Ipl1 |
| SLK | Synthetic lethal Kar3p |
| SMC | Stability of minichromosomes |
| SPB | Spindle pole body |
| SPO | Sporulation |
| Swe | Saccharomyces Wee1 |
| Swi | Switching deficient |
| Tem | Termination of M phase |
| TEV | Tobacco etch virus |
| Whi | Whiskey |

# Abstract

The operating principles of complex regulatory networks are more easily understood with mathematical modelling than by intuitive reasoning. In this thesis, I study the dynamics of the mitotic exit control system in budding yeast. I present a comprehensive mathematical model, which provides a system's-level understanding of the mitotic exit process. This model captures the dynamics of classic experimental situations reported in the literature, and overcomes a number of limitations present in previous models.

Analysis of the model led to a number of breakthroughs in the understanding of mitotic exit control. Firstly, numerical analysis of the model quantified the dependence of mitotic exit on the proteolytic and non-proteolytic functions of separase. It was shown that the requirement for the non-proteolytic function of separase depends on cyclin-dependent kinase activity. Secondly, APC/Cdc20 is a critical node that controls the phosphatase (Cdc14) branch and both cyclin (Clb2 and Clb5) branches of the cell cycle regulatory network. Thirdly, the model proved to be a useful tool for the systematic analysis of the recently discovered phenomenon of Cdc14 endocycles.

Most proteins belonging to the cell cycle control network are regulated at the level of synthesis, degradation and activity. Presumably, these multiple layers of regulation facilitate robust cell cycle behaviour in the face of genetic and environmental perturbations. To falsify this hypothesis, I subjected the model to global parameter perturbations and tested viability against pre-defined criteria. According to these analyses, the regulated transcription and degradation of proteins make different contributions to cell cycle control. Regulated degradation confers cell cycle oscillations with robustness against perturbations, while regulated transcription plays a major role in controlling the period of these oscillations. Both regulated transcription and degradation

are part of important feedback loops, that combined promote robust behaviour in the face of parametric variations.

# Research Overview

For cells to exit mitosis, a continuous dephosphorylation of mitotic phospho-proteins is required. In budding yeast, cells achieve this dephosphorylation through the downregulation of CDK1 activity and the upregulation of Cdc14, a counteracting CDK1-phosphatase (Queralt and Uhlmann, 2008). In this thesis, I studied the operating principles of the regulatory network that drives mitotic exit, with the use of a mathematical model. More specifically, I developed a quantitative model of the budding yeast cell cycle, based on Queralt's model (QM), which focuses solely on the events occurring between metaphase and the following G1 phase (Queralt and Uhlmann, 2008).

Mathematical modelling is a useful means to incorporate knowledge from various different sources into a single, comprehensive description. Building a model is a sequential process; and there are many intermediate stages which precede the final outcome. The construction of a building provides a helpful analogy for this process; each floor is built on top of the one below, just as each new model builds on the achievements of its predecessor. In this thesis, I describe the model at four distinct stages of its development, referred to MV1, MV2, MV3 and MV4. To extend the analogy, QM can be considered the ground floor, while the final version of the model, MV4, can be considered the top floor (see Figure 1).

QM focuses mainly on the non-proteolytic function of separase in triggering the release of Cdc14. The first version of the model (Model Version 1 – MV1) was built to investigate how the proteolytic and non-proteolytic activities of separase drive not only Cdc14 release, but also mitotic exit. MV1 clearly shows that the requirement for the non-proteolytic function of separase is dependent on cyclin-dependent kinase activity.

The second version of the model (Model Version 2 – MV2) focuses on a different component responsible for mitotic progression, the APC subunit Cdc20. According to the model, APC/Cdc20 is critical for downregulating CDK1 activity and promoting Cdc14 release.

The third version of the model (Model Version 3 – MV3) captures the characteristics of a limit cycle, and is therefore no longer restricted to the time window between metaphase and the following G1 phase. MV3 also incorporates the idea of Cdc14 compartmentalisation; Cdc14 can be localised in the nucleolus, nucleus and cytoplasm.

The final version of the model (Model Version 4 – MV4) can capture the dynamics of experimental situations ranging from single to quintuple genetic mutations. It can be used to make experimental predictions, and can be refined with the emergence of new experimental data. MV4 features an improved description of G1 phase, and unlike its predecessors, provides a comprehensive representation of a complete budding yeast cell cycle. Moreover, MV4 describes the mechanism by which Net1 is phosphorylated, enabling the dissociation of Cdc14 from Net1 (the two-hit model (Manzoni et al., 2010)). Finally, MV4 was used to systematically analyse the recently discovered phenomenon of Cdc14 endocycles (Lu and Cross, 2010; Manzoni et al., 2010).

Once a model has been built and validated against experimental data, it is useful to test its robustness against perturbations (Morohashi et al., 2002). I analysed the robustness of MV4 not only to evaluate how dependent it is on its original parameter set, but also to explore which features of the system are most responsible for the model's fragility/robustness. Most proteins belonging to the cell cycle control network are regulated at the level of synthesis, degradation and activity, and it is possible that these multiple layers of regulation facilitate robust cell cycle behaviour in the face of perturbations. According to my robustness analyses of MV4, the regulated transcription and degradation of proteins make different contributions to cell cycle control. Regulated

degradation confers cell cycle oscillations with robustness against perturbations, while regulated transcription plays a major role in controlling the period of the cell cycle oscillations.

Finally, I showed that regulated transcription and degradation are both part of important feedback loops in the network. Together, these feedback loops promote robust behaviour in the face of parametric variations, which arise from mutations and/or fluctuations in protein levels.

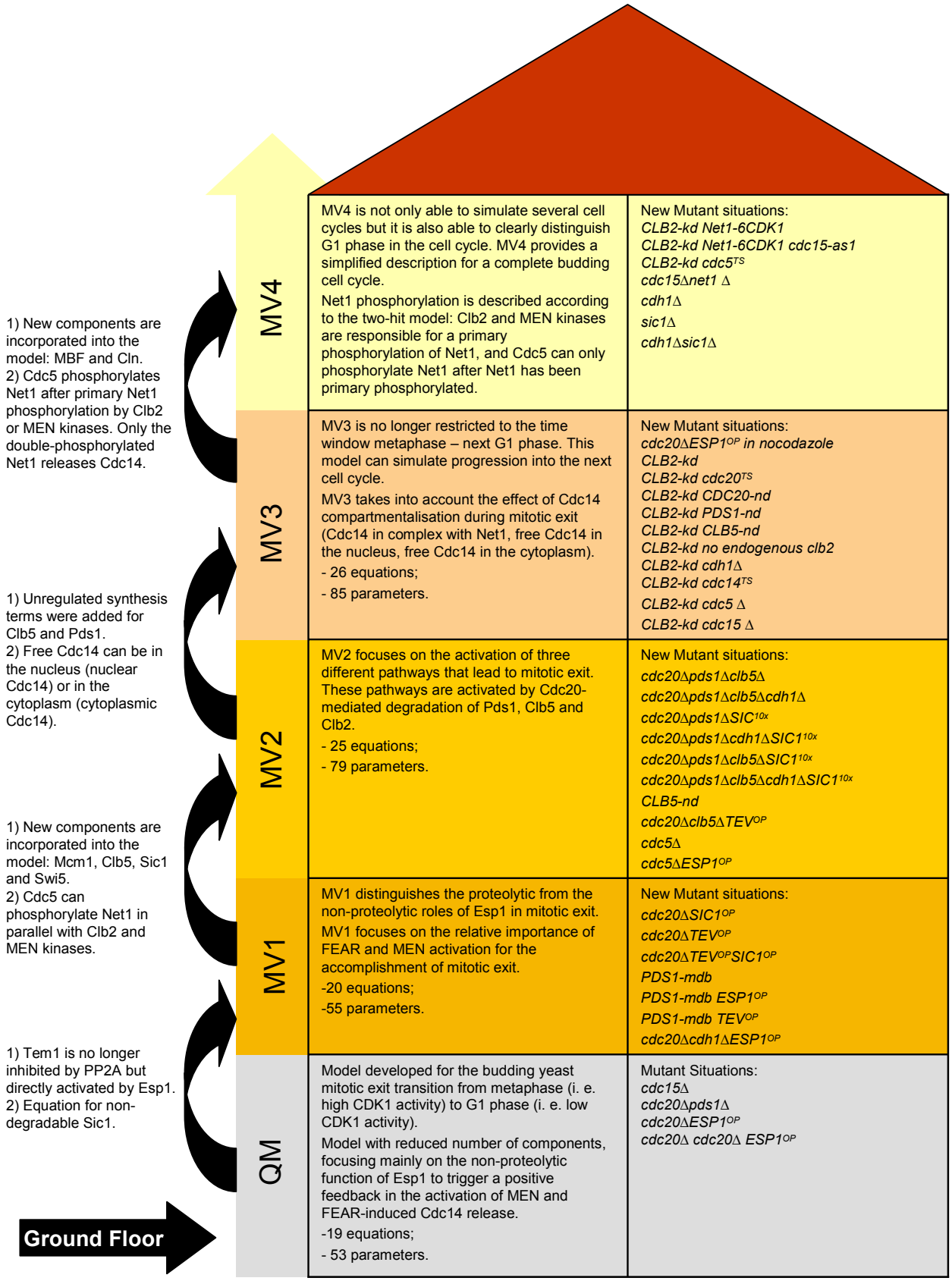


**Figure 1: Building a model is a sequential process. The construction of a building provides a helpful analogy for this process; each floor is built on top of the one below.**

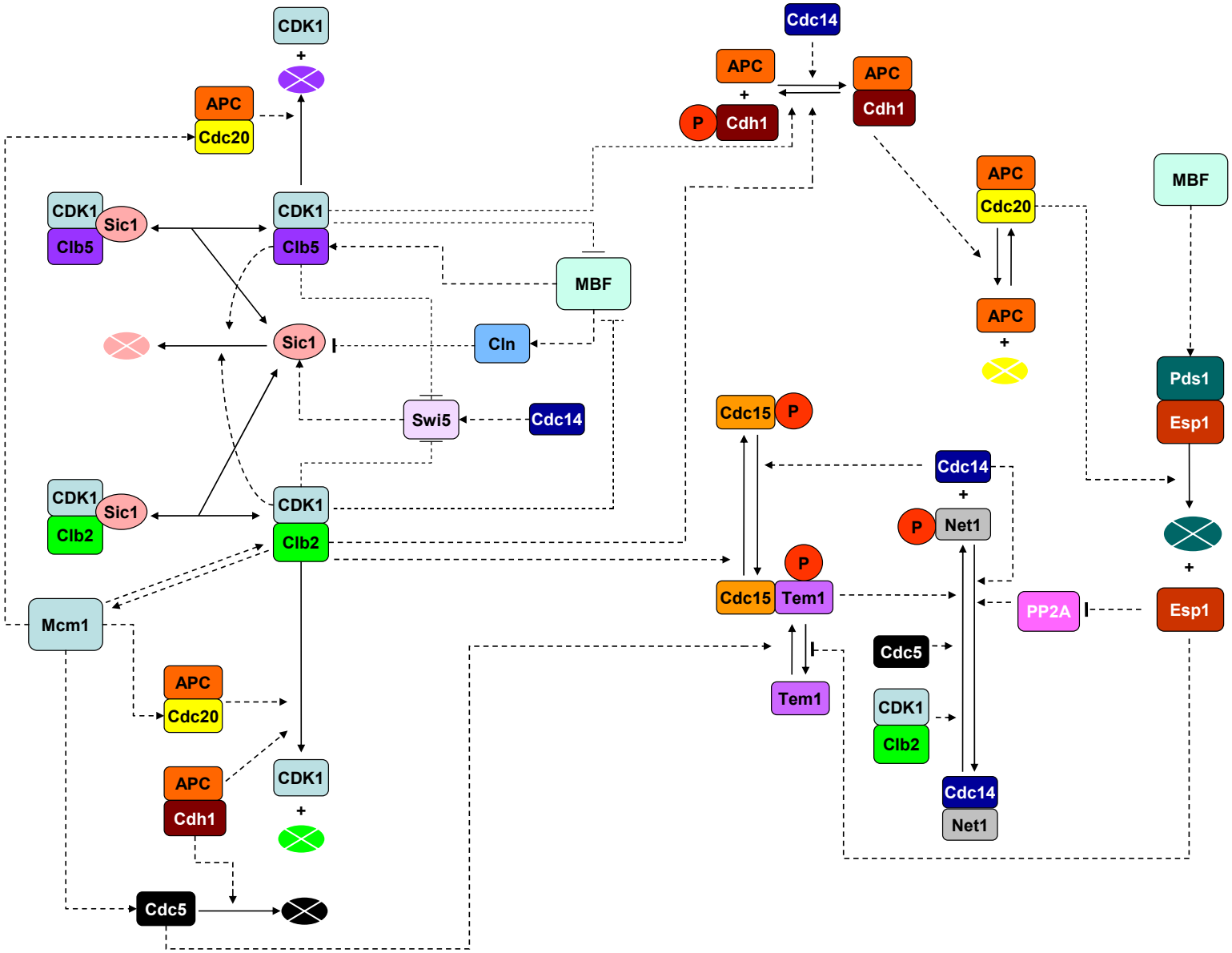


**Figure 2: Wiring Diagram of the molecular network present in MV4.**

# Literature Survey

## *1. Cell Cycle in Eukaryotes*

Cell division is one of the most fundamental physiological processes imaginable. During the mitotic cell cycle, each cell has to accurately duplicate the DNA content of its chromosomes and then precisely segregate the copies into two genetically identical daughter cells. Mitotic cell division is necessary for unicellular organisms to reproduce, and for multicellular organisms to develop and repair themselves. It is therefore no overstatement to suggest that mitotic cell division is essential to the maintenance of life. It is by no means a simple process however; its complexity is reflected in how much we still have to learn about the mechanisms that govern the mitotic cell cycle.

In eukaryotes, the mitotic cell cycle is usually subdivided into four phases, defined on the basis of chromosomal events. In S phase, cells replicate their DNA and duplicate their chromosomes (S stands for synthesis). In M phase, cells divide and distribute the duplicated chromosomes equally between the two daughter cells. Nuclear division is known as mitosis, and cellular division is known as cytokinesis. Between S and M phases, there are two gap phases, G1 and G2, which provide additional time for cell growth and the control of cell cycle progression. G1 occurs before S phase, and G2 occurs before M phase. During both G1 and G2, cells ensure that conditions are suitable and preparations are complete to commit to the next phase of the cell cycle (S phase and mitosis respectively) (Morgan, 2007b). A schematic representation of the events occurring in a generic eukaryotic cell cycle can be seen in Figure 3.

Mitosis is subdivided into four major steps: prophase, metaphase, anaphase and telophase. In prophase, chromosomes undergo condensation and sister chromatids

bound together by the centromere become visible through the microscope. The two centrosomes separate and migrate to opposite poles of the cell. The end result is the formation of a bipolar microtubule array known as the mitotic spindle. Spindle microtubules attach to sister chromatids at the kinetochore, a specialised chromatin structure built on centromeric DNA. This attachment has to be bipolar; that is, microtubules from opposite poles attach to the interconnecting sister chromatid kinetochores. This process leads to all sister chromatids being attached to the mitotic spindle and aligned at its centre. At this point, cells have reached metaphase and the sister chromatids are aligned at the metaphase plate. Anaphase occurs when the proteins holding the sister chromatids together are cleaved, allowing them to separate. The sister chromatids are pulled apart by the shortening of the kinetochore microtubules and move toward the respective centrosomes to which they are attached. The spindle poles also move further apart from each other, resulting in the complete segregation of the sister chromatids to opposite poles of the cell. Mitosis is completed in telophase, when the sister chromatids are repackaged into two identical daughter nuclei and the chromosomes start to decondense (Morgan, 2007b).

After mitosis comes the final stage of the cell cycle: cytokinesis. Here, the two nuclei and other cellular components are distributed into a pair of daughter cells, each containing a single nucleus, centrosome and roughly equal cytoplasmic content. This is achieved by the contraction of a ring composed of actin filaments at the site of cell division, together with the generation of new cellular membrane (Morgan, 2007b).

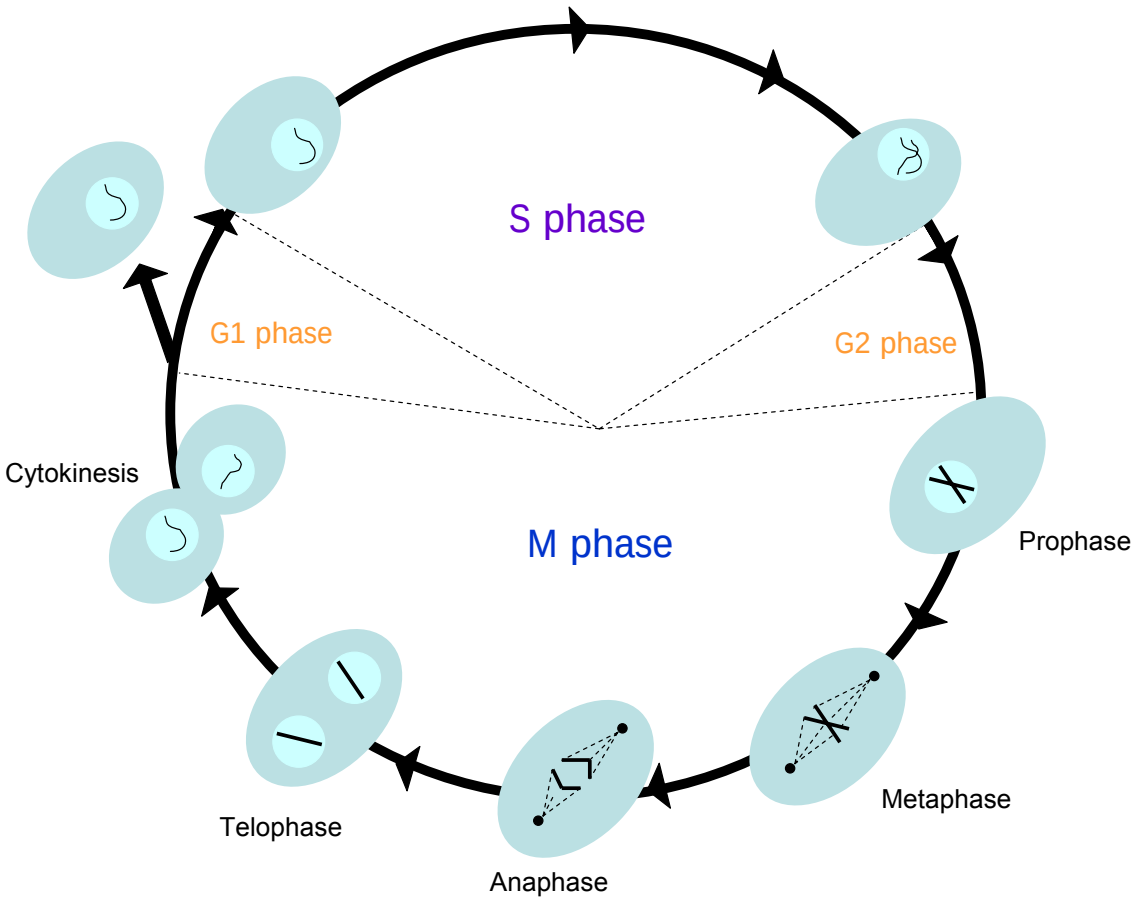


**Figure 3: Schematic Representation of the eukaryotic cell cycle. DNA replication takes place in S phase. Mitosis (nuclear division) and cytokinesis (complete cellular division) take place in M phase. The four major phases of mitosis are also illustrated: prophase, metaphase, anaphase and telophase. Between S and M phases, there are two gap phases: G1 phase that takes place after M phase, and G2 that takes place after S phase.**

## *2. Budding Yeast Cell Cycle*

All eukaryotic cells follow a similar process to duplicate and divide themselves. Therefore, it is common practice to use single celled yeasts to study the basic mechanisms of cell cycle control. These simple organisms divide in a matter of hours and are easy to manipulate genetically.

Nonetheless, each organism has specificities. In the case of *Saccharomyces cerevisae* (budding yeast), cells produce a small bud that keeps growing until the end of the cell cycle. This bud does not reach the size of the mother cell, and therefore budding

yeast has an asymmetric cell division. The nucleus migrates into the bud neck and remains intact while mitosis takes place. Since this phenomenon requires duplication of the spindle pole bodies and reorganization of the microtubules into a mitotic spindle before the conclusion of S phase, budding yeast lacks a clear definition between S, G2 and M phases (Nurse, 1985).

In budding yeast, G1 phase is very well defined. At this point, cells monitor environmental constraints such as nutrition and cell size. If conditions are unfavourable, cells arrest in G1.

Another particularity of this organism is that the nuclear envelope remains unbroken during M phase. Shortly before cytokinesis, it is pinched in two, instead of being re-synthesised as it is in vertebrates (Yeh et al., 1995).

## *3. Cell Cycle Control System*

The sequential events of the cell cycle are controlled by a molecular system which works parallel to the protein machinery that executes the events themselves. This control system determines the precise point at which one event should finish and the next one should start. Moreover, the control system remains operational even if there are abnormalities in the accomplishment of a certain event. In this way, it can monitor for abnormalities and trigger responses to them when they occur. As will become clear, a response usually involves the arrest of the cell cycle until the problem is solved.

### *a. CDK1 and Cyclins*

The cell cycle control system relies mainly on a very specific family of enzymes known as cyclin-dependent protein kinases (CDKs). These kinases phosphorylate a

broad range of proteins, regulating their enzymatic activity or their ability to bind to other proteins.

CDKs target serine and threonine residues, and their activity is dependent on the binding of specific activating subunits, known as cyclins. These subunits were named cyclins because their concentration oscillates during the cell cycle (Evans et al., 1983). Different cyclins are present at different cell-cycle phases, suggesting that the periodic formation of a specific cyclin-CDK complex will trigger a specific event. In this way, the sequence of events in the cell cycle is tightly conserved.

Whereas higher eukaryotes possess multiple CDKs, budding yeast relies on a single CDK (CDK1) to associate with several cyclins and regulate the cell cycle. Most information on the budding yeast cell cycle can be translated to other systems however, since there is a high level of conservation in the molecules concerned.

In budding yeast, G1 phase requires at least one of three cyclins: Cln1, Cln2 or Cln3. In the absence of all three, cells arrest in G1 (Richardson et al., 1989). Therefore, Cln1-3 are known as G1-cyclins. Six B-type cyclins are responsible for S and M phases. Clb5 and Clb6 are expressed earlier and trigger DNA replication, the main event of S phase. Clb1-4 drive mitosis. Clb3 and Clb4 increase during mid S phase, at the same time that the spindle pole bodies start to separate. Finally, Clb1 and Clb2 levels rise during spindle assembly (Fitch et al., 1992).

G1 and B-type cyclins do not share the same transcriptional machinery, which increases the specificity of their regulation. The CLN3 gene is transcribed throughout the cell cycle, although its transcription is accentuated during late M phase and early G1. The CLN1 and CLN2 genes are transcribed at the end of G1. This process is mediated by SBF, a heterodimeric transcription factor composed of Swi4 and Swi6. The CLB5 and CLB6 genes are transcribed during G1-S. This process is mediated by the transcription factor MBF, which is composed of Mbp1 and Swi6. Hence, MBF is closely related to

SBF. Indeed, recent evidence suggests there is a high degree of functional overlap between these two transcription factors (Bean et al., 2005).

Cln3 has an important role in activating the transcription of Cln1 and Cln2. The Cln3/CDK1 complex phosphorylates the SBF inhibitor, Whi5, and promotes its export from the nucleus. Consequently, SBF can be activated, and the CLN1 and CLN2 genes transcribed. Cln1,2/CDK1 complexes also phosphorylate Whi5, and therefore promote the activation of their own transcription factor, SBF. This positive feedback loop is crucial to enhance the upregulation of Cln/CDK1 complexes in G1 phase (Figure 4).

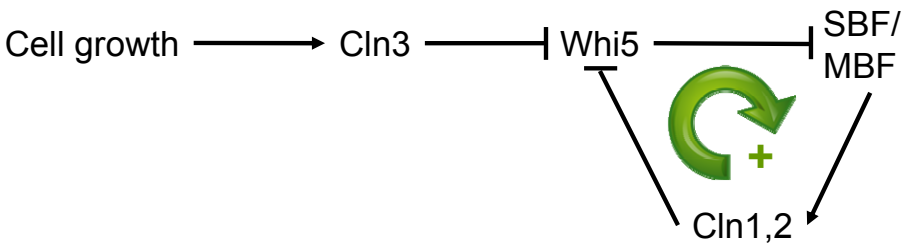


**Figure 4: With cell growth G1 cyclins (Cln1-3) are upregulated. Cln3 is responsible for triggering the positive feedback on Cln1,2 transcription. Pointed arrows represent positive interactions and blunt arrows represent negative interactions.**

Clb6 also plays a role in SBF/MBF regulation, since Clb6/CDK1 is known to phosphorylate Swi6. The phosphorylated form of Swi6 migrates to the cytoplasm and SBF is downregulated. In addition, Clb2 can specifically inhibit SBF transcriptional activity by binding to its subunit Swi4. At this stage, cells are entering mitosis and the levels of G1 cyclins decrease (Amon et al., 1993; Siegmund and Nasmyth, 1996).

Clb2 transcription is mediated by the transcription factor Mcm1, the forkhead transcription factor Fkh2, and the co-activator Ndd1; all three of them being directed to the CLB2 gene promoter. Ndd1 requires Clb2/CDK1 mediated phosphorylation to be recruited, which means that Clb2 enhances its own transcription (Pic-Taylor et al., 2004).

Specificity in cyclin regulation occurs not only at the transcriptional level, but also at the level of protein degradation. Cyclin degradation depends on previous ubiquitylation; the chain of ubiquitin molecules allows the 26S proteasome to target the cyclin and degrade it. Specificity arises from different cyclins being substrates of different ubiquitin ligases. Cln1, Cln2 and Clb6 are targets of the SCF complex, while the other B-type cyclins are ubiquitylated by the Anaphase Promoting Complex (APC). The SCF complex that targets Cln1 and Cln2 contains the F-box protein Grr1, while the SCF complex that targets Clb6 contains the F-box protein Cdc4 (Barral et al., 1995; Skowyra et al., 1997). The APC binds with two mutually exclusive activating subunits, Cdc20 and Cdh1, and exhibits a differential degradation of cyclins, depending on which subunit is bound to it. Cdc20 binds first and is responsible for targeting all B-type cyclins (with the exception of Clb6). However, degradation of Clb2 is only completed when Cdh1 binds to the APC (Shirayama et al., 1999; Wasch and Cross, 2002).

Despite the range of mechanisms conferring specificity to cyclin regulation, experimental results have shown that cells lacking any one cyclin are viable (Fitch et al., 1992). There is therefore redundancy in the system; although different cyclins peak at different times, their functions appear to overlap. In fact, one B-type cyclin in particular seems able to promote mitosis on its own: the triple mutant *clb1*Δ*clb3*Δ*clb4*Δ is viable, demonstrating the importance of Clb2 (Fitch et al., 1992).

### b. *Control of CDK1 activity*

Cyclin concentrations are not the only mechanism by which CDK1 activity is regulated; CDK1 can also be activated or inactivated by phosphorylation. The presence of CDK1 inhibitor proteins may also downregulate its activity.

For CDK1 to be active, its T169 residue must be phosphorylated. In budding yeast, the enzyme responsible belongs to the CDK1-activating kinases (CAKs) family, and is known as Cak1. Cak1 is maintained at a constant level throughout the cell cycle and phosphorylates CDK1 before cyclin binding (Harper and Elledge, 1998).

CDK1 can also be inhibited by phosphorylation. This inhibitory step mainly targets the Clb2/CDK1 complex and occurs during S and G2 phases. The kinase responsible is Swe1, an ortholog of the Wee1 kinase in Schizosaccharomyces pombe (fisson yeast), which targets the Y19 and T18 residues. Swe1-mediated phosphorylation specifically inhibits Clb1-4, while Cln1-3, Clb5 and Clb6 are unaffected. In addition, CDK1 reciprocally regulates Swe1. Phosphorylated Swe1 migrates to the bud neck, where it is degraded (McMillan et al., 2002; Sia et al., 1998). Swe1 is thought to prevent mitosis if there is a malformation in the bud. In this event, Swe1 cannot be degraded and instead will enhance Clb2/CDK1 inhibition. The counteracting phosphatase is Mih1, an ortholog of the Cdc25 phosphatase in fission yeast (Russell et al., 1989).

Cyclin-dependent Kinase Inhibitors (CKIs) are proteins that can bind to CDK1-cyclin complexes and inactivate their kinase activity. They are present in most, if not all, eukaryotic organisms. In budding yeast, the main CKI is Sic1 (Mendenhall, 1993). Sic1 expression is regulated by the transcription factor Swi5, and is limited to the M/G1 transition. Swi5 is downregulated by Clb/CDK1 complexes and upregulated by Cdc14, a phosphatase known to be present at the completion of mitosis (Toyn et al., 1997). In this way, Sic1 transcription is activated at the end of mitosis. Sic1 is a substrate of Cln/CDK1 complexes, and therefore, at the end of G1, Sic1 is phosphorylated and targeted for degradation by the SCF complex (Schwob et al., 1994; Verma et al., 1997).

Sic1 function is related to the prevention of premature S phase. Until Cln/CDK1 complexes have reached levels high enough to trigger bud initiation and spindle pole duplication, Sic1 levels remain high and inhibit Clb5- and Clb6/CDK1 complexes

(Schwob et al., 1994). Sic1 is also important in late anaphase, when it downregulates Clb2/CDK1 and thereby promotes an efficient exit from mitosis (Toyn et al., 1997).

Cdc6 also behaves like a CKI, although the Cdc6-Clb/CDK1 complex is less stable than the Sic1-Clb/CDK1 complex. While its main known function is related to the promotion of DNA replication, its overexpression may cause a G2 delay (Bueno and Russell, 1992). In this way, it is thought that Cdc6 is responsible for the fine-tuning of Clb5 and Clb6 activity at the origins of replication (Piatti et al., 1995). The regulation of Cdc6 is similar to that of Sic1; it is destroyed at the G1/S transition by an ubiquitination system analogous to the one that targets Sic1 (Basco et al., 1995; Drury et al., 1997).

### *c. Substrate Targeting by Cyclin/CDK1 complexes*

The different cyclin/CDK1 complexes have overlapping roles. Therefore, it is unlikely that cyclins confer essential target specificity to CDK1 activity. Nevertheless, evidence suggests that when the S phase cyclin Clb5 is substituted by the M phase cyclin Clb2, the initiation of DNA replication is less accurate (Cross et al., 1999). In addition, overexpression of Clb5 is unable to block cells in mitosis, as has been reported for Clb2 overexpression (Jacobson et al., 2000). This is clear evidence of cyclin target specificity.

Cyclin/CDK1 complexes possess an active T-loop site, which interacts with the phosphorylation sites on their substrates, enabling them to recognise their substrates (interaction occurs at the SPXK consensus sequence). S phase cyclins have a hydrophobic patch on their surface that recognises the RXL motives present on some substrates, conferring substrate-specificity to these cyclins (Loog and Morgan, 2005).

Subcellular localization is another mechanism that confers target specialization; quite clearly, the enzyme has to reach the substrate in order to act upon it. In this way, some cyclins present sequence information that regulates their localization inside the cell and

thus directs the cyclin/CDK1 complex to a specific location. A good example in budding yeast is the hydrophobic patch on S phase cyclins. This sequence directs Clb5 to the origins of DNA replication where it is required during S phase (Wilmes et al., 2004).

### *d. Protein Degradation in Cell Cycle Control*

Protein degradation is the main driving force of cell cycle progression. Cyclins, CDK1 inhibitor proteins, and other cell cycle regulators are degraded in timely fashion, so that the cell cycle engine moves from one state to the next in an orderly and conserved fashion. The degradation of proteins is generally regulated through poli-ubiquitination, the attachment of an ubiquitin tail to the target protein, making it recognizable to the proteasome. Ubiquitination involves the coordination of three enzymes, generically called E1, E2 and E3, and is carried out in three steps (Hershko and Ciechanover, 1998):

- Ubiquitin activation – ubiquitin is covalently attached to E1;
- Ubiquitin conjugation – ubiquitin is transferred to E2, the ubiquitin-conjugating enzyme;
- Ubiquitin-protein ligation – E3 catalyses the transfer of ubiquitin from E2 to the target protein.

At the G1/S transition, G1 cyclins and CKI are recognised by the ubiquitin protein ligase SCF (Orlicky et al., 2003). They are ubiquitinated and degraded before cells enter S phase. During mitosis, B-type cyclins are degraded by the ubiquitin ligase APC and its activating subunits Cdc20 and Cdh1 (Visintin et al., 1997).

These transitions separate two alternative states in the cell cycle. The first state corresponds to G1 where cells are small and the chromosomes unreplicated. In the cell

cycle engine, it corresponds to low levels of B-type cyclins and high levels of G1 cyclins and CDK1 inhibitors. Before cells initiate the replication-division process, G1 cyclins must target Sic1 for degradation by the SCF complex (Orlicky et al., 2003), allowing B-type cyclins to be upregulated. This transition is known as START, because, from this point onwards, cells are committed to replicating their DNA and dividing (Tyson and Novak, 2008). The second transition occurs at the metaphase-to-anaphase transition, and is marked by sister-chromatid segregation. At this point, the APC is activated and promotes B-type cyclin degradation, a crucial requirement for the completion of mitosis. This transition is known as EXIT (Tyson and Novak, 2008).

Both START and EXIT are irreversible transitions and proteolysis plays an important role in this irreversibility (Novak et al., 2007). Nevertheless, recent evidence suggests that proteolysis is not the sole requirement; feedback loops (e.g. double negative feedback loop between Sic1 and CDK1) in the network further ensure that the cell cycle works as a clock whereby events are irreversible (Lopez-Aviles et al., 2009).

### *e. Checkpoint Mechanisms*

The cell-cycle control system regulates transitions at very well-defined points in the cell cycle, known as checkpoints. When the cell reaches a checkpoint, the control system should stop cell cycle progression unless all of the conditions to proceed are fulfilled. The checkpoint control system can also drive cell death if the problem cannot be solved (Elledge, 1996; Hartwell and Weinert, 1989).

The first checkpoint regulates the START transition in budding yeast. DNA damage, nutrient depletion, and the presence of mating pheromone are by themselves conditions to block the cell in G1 phase. Another crucial factor is cell size. The cell is only allowed to divide if it has reached a critical size. The activation of this checkpoint depends on the

prevention of Cln/CDK1 activation, and consequently, on the stabilization of Sic1. This CDK1 inhibitor is a strong Clb/CDK1 antagonist, and thus the cell cannot enter S phase (Johnston et al., 1977).

The second checkpoint regulates G2 to M transition (G2/M checkpoint) and is thought to correspond to a morphogenetic checkpoint in budding yeast. If bud formation fails or cells lose their polarity, then progression to mitosis is prevented and cells arrest in G2. For this to happen, Swe1 level is kept high and CDK1 is inhibited by tyrosine phosphorylation. The absence of CDK1 activity prevents cells from entering mitosis (Lew and Reed, 1995; Sia et al., 1998).

The third checkpoint occurs in mitosis, during the metaphase-to-anaphase transition. This checkpoint is known as the spindle assembly checkpoint (SAC), since it is activated if the mitotic spindle is corrupted or if there is a problem with the bipolar attachment of the sister chromatids at the metaphase plate. Indeed, a single unattached sister chromatid is enough to trigger this checkpoint control, and the cell remains arrested in metaphase with sister chromatids bound together. The target of this checkpoint is the APC subunit Cdc20, which is indirectly responsible for sister chromatid segregation. While the checkpoint is active, Cdc20 is bound to an inactive complex, and thus, prevented from binding to and activating APC (De Antoni et al., 2005; Hwang et al., 1998).

The fourth checkpoint monitors the positioning of the mitotic spindle along the cell. In budding yeast, the accurate location of one set of chromosomes in the bud and another in the mother is crucial for proper cellular division. This is achieved by a correct orientation of the mitotic spindle along the mother-bud axis. Therefore, this checkpoint, known as the Spindle Orientation Checkpoint (SPOC), delays cell cycle progression if the two sets of chromosomes are not correctly located (e.g., both sets of chromosomes are located in the mother). The target of this checkpoint is the CDK1 counteracting

phosphatase, Cdc14. This phosphatase is crucial for cells to successfully conclude mitosis, and thus, when Cdc14 is inactive, the cell cycle is arrested (Lew and Burke, 2003; Pereira et al., 2000; Pereira et al., 2002; Pereira and Schiebel, 2005; Seshan et al., 2002).

## *4. Temporal Organization of the Cell Cycle*

Maintaining the correct order of events is essential to the success of the cell cycle. For instance, DNA replication and chromosome segregation must alternate so that, after cell division, each daughter cell has a single and complete copy of the mother cell's genome. To ensure the correct timing of each cellular event, the cell cycle control machinery is guided by the checkpoints (Elledge, 1996).

From a system's perspective, the checkpoints correspond to stable steady-states where the cell is arrested (Tyson and Novak, 2008). When the checkpoint conditions are satisfied, a signal is triggered and the steady-state disappears, allowing the cell cycle machinery to continue. These signals are transient, but once they are switched off, the cell cycle is already committed to proceed in one direction and cannot revert to the previous steady-state. This is known as an irreversible transition. In budding yeast, the two most important irreversible transitions are START and EXIT.

### *a. START transition*

The START transition occurs in G1 phase when the cell triggers a new round of DNA replication and mitosis. A crucial condition to trigger the START transition is for cells to reach a critical size. Until this condition is verified, cells remain in G1 to allow them to grow until they reach this size. This requirement is important to guarantee that the cycle

time (the period between two successive divisions) is equal to the cytoplasmic doubling time, and thus, that cells maintain the same average size across successive generations (Jorgensen and Tyers, 2004; Mitchison, 2003).

In G1, the START transition is triggered by the synthesis of the 'starter kinases' Cln1-3. These are required to downregulate the CDK1 stoichiometric inhibitor Sic1 in late G1 (Tyers, 1996). As Sic1 level decreases, S phase cyclins are activated (Clb5,6) and the cell becomes capable of synthesising DNA (DNA replication) (Zachariae et al., 1998). This step marks G1/S transition.

Subsequently, Clb5/CDK1 is responsible for Cdh1 phosphorylation and APC/Cdh1 inactivation (Zachariae et al., 1998). The level of Clb2/CDK1 increases and cells are able to enter mitosis. At this stage, the activator signal for START is no longer required, because, with Clb/CDK1 activation, the transition has become irreversible. Clb2/CDK1 phosphorylates SBF and the transcription factor is inactivated (Amon et al., 1993). As a result, the level of 'starter-kinases' in the cell decreases, turning off the activator signal for the START transition (Tyson and Novak, 2008).

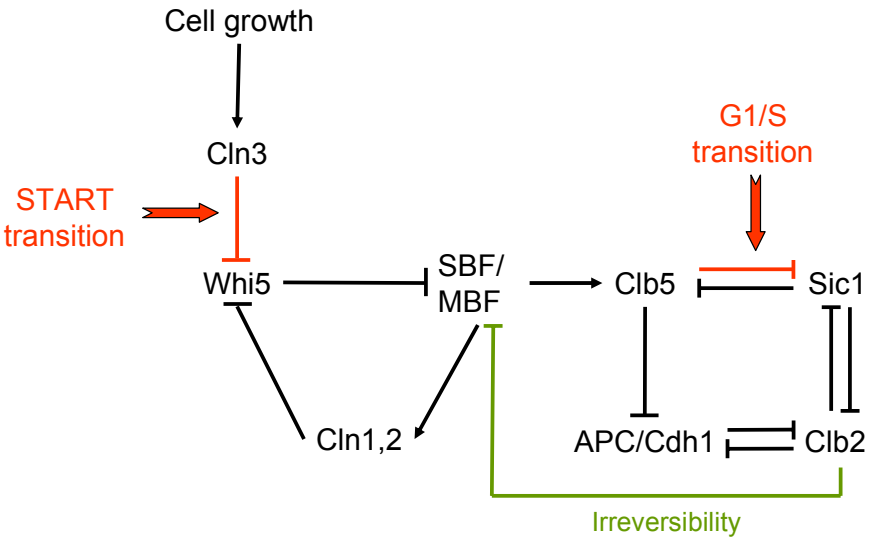


**Figure 5: Wiring diagram illustrating the molecular interactions responsible for START and G1/S transitions. The signal triggering these transitions is transient due to the activation of Clb2 (green arrow). Since the system does not revert, these transitions are irreversible.**

### *b. EXIT transition*

The EXIT transition is triggered after the metaphase-to-anaphase transition and ensures that the cell cycle progresses into the next G1. The triggering signal for the first transition is the activation of the APC/Cdc20 complex (Figure 6). This complex initiates the degradation of B-type cyclins, a fundamental step for cells to be reset to G1 phase (Morgan, 1999). In parallel, APC/Cdc20 triggers its own downregulation by promoting the activation of Cdh1 (a negative feedback loop). The APC/Cdh1 complex targets Cdc20 for degradation, and thus the activator signal for EXIT is transient. Once the signal is turned off, the EXIT transition cannot be reversed, because both Clb/CDK1 antagonists have been activated (i.e. APC/Cdh1 and Sic1) and they completely downregulate CDK1 activity (Figure 6). Hence, the EXIT transition is an irreversible transition (Tyson and Novak, 2008).

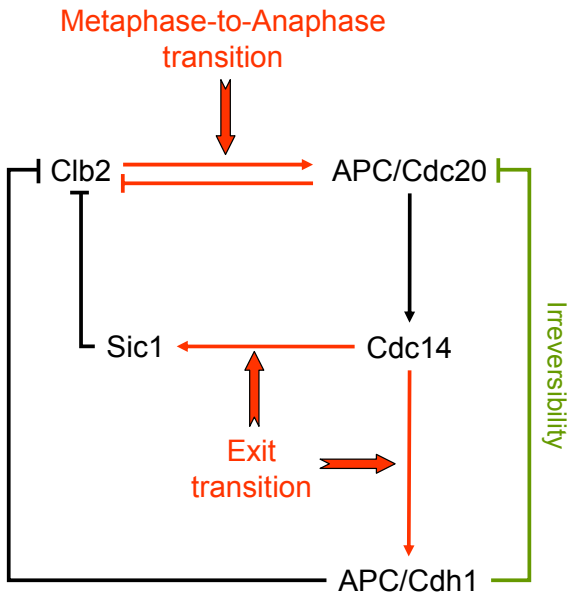


**Figure 6: Wiring diagram illustrating the molecular interactions responsible for metaphase-to-anaphase and EXIT transitions. The signal triggering these transitions is transient due to the inactivation of Cdc20 by Cdh1 (green arrow). Since the system does not revert, these transitions are irreversible.**

## 5. The Completion of Mitosis

### a. Activation of the APC

Anaphase initiation requires the activation of APC/Cdc20 to destroy 'anaphase inhibitors', which are responsible for keeping the sister chromatids bound tightly together. Cdc20 transcription factor (the Ndd1/Mcm1/Fkh2 complex) is upregulated by Clb2/CDK1 and therefore Cdc20 will be synthesised in late S phase until early mitosis. However, APC/Cdc20 activation is abrupt and should depend on another mechanism besides the increased level of Cdc20 in the cell (Fang et al., 1998). One proposed mechanism includes CDK1-dependent phosphorylation of Cdc20 and of several subunits of the APC core.

Besides anaphase inhibitors, the APC/Cdc20 complex targets S and M phase cyclins, forming a negative feedback loop (Schwab et al., 1997; Visintin et al., 1997). By promoting APC/Cdc20 activity, CDK1 triggers its own downregulation, which in turn results in decreased phosphorylation of APC and the dissociation of Cdc20. After anaphase, Cdc20 disappears completely, since APC/Cdh1 mediates its degradation (Prinz et al., 1998). This promotes a complete transition to APC/Cdh1 activity at the end of mitosis.

Cdh1 is known to downregulate CDK1 activity during G1 phase, when Cdc20 is no longer present to fulfil this role. The main difference between Cdh1 and Cdc20 concerns their regulation. While Cdc20 is upregulated by CDK1, Cdh1 and CDK1 are strong antagonists. CDK1 phosphorylates and inactivates Cdh1, and Cdh1 promotes the destruction of CDK1 M-phase cyclin partners. Hence, Cdh1 can only be activated once CDK1 activity is low. The double negative feedback loop switches the cell to a state of high APC/Cdh1 activity and low Clb2/CDK1 activity (G1 phase).

Cdh1 levels remain approximately constant during the cell cycle. Hence, its activity is regulated predominantly by its phosphorylation levels. Only the unphosphorylated form can bind to APC, and thus CDK1 mediated phosphorylation prevents APC/Cdh1 activity. After APC/Cdc20 degrades S and M phase cyclins, a phosphatase dephosphorylates and activates Cdh1. In budding yeast, the phosphatase responsible for this step is Cdc14. Cdc14 is itself activated at the metaphase-to-anaphase transition, enhancing the importance of APC/Cdc20 in the activation of Cdh1.

### *b. Control of sister chromatid separation*

Sister-chromatid segregation only occurs at the metaphase-to-anaphase transition, and, in the meantime, sister chromatids are held together through a phenomenon known as cohesion. Cohesion is fundamental to ensure the correct attachment and orientation of the chromosomes during metaphase. Essential to this phenomenon is a protein called cohesin, formed by a complex of four subunits: Smc1, Smc3, Scc1 and Scc3 (Nasmyth et al., 2000).

Smc1 and Smc3 are bound together at opposite ends, and with Scc1 bound at one end, they form a tripartite ring structure. Scc3 binds to this structure through interactions with Scc1 and the ATP domains of the Smc proteins. It has been shown that the molecular lock for the ring structure is particularly dependent on Scc1 binding, and that Scc1 proteolysis is responsible for the release of cohesin from chromosomes at the metaphase-to-anaphase transition (Hopfner, 2003; Ivanov and Nasmyth, 2005). Once cohesin is removed from the chromosomes, the sister chromatids are pulled towards opposite poles due to the polar ejection forces exerted by the mitotic spindle (Higuchi and Uhlmann, 2005; Maddox et al., 2000). At this point, the sister chromatids have been segregated and anaphase successfully completed.

The time at which cohesin is cleaved is very well-defined in the cell cycle. The spindle assembly checkpoint (SAC) ensures that the sister chromatids are bound tightly together until all of the chromosomes are correctly aligned and attached to opposite poles of the mitotic spindle. Only then is the SAC inactivated, and consequently, cohesin is cleaved in a highly synchronous manner in all chromosomes.

This process depends on the activity of a protease, kept inactive until the right moment. The protease in question is known as separase (Esp1 in budding yeast), and its substrate is the Scc1 subunit. Before anaphase, Esp1 is kept inactive in a complex with the protein securin (Pds1 in budding yeast). Pds1 is an 'anaphase inhibitor' and an APC/Cdc20 substrate, so when APC/Cdc20 is activated in metaphase, Pds1 is degraded and Esp1 is freed to cleave cohesin. This brings about sister chromatid segregation, and consequently, anaphase (CohenFix et al., 1996; Shou et al., 1999).

The SAC ensures the exact timing of this process by inhibiting Cdc20 and all subsequent events. With this mechanism, cells ensure that mitosis will only progress if metaphase is successfully completed (Hwang et al., 1998).

### c. Cdc14 release

The physiological events that occur in mitosis after anaphase are known as 'mitotic exit' and require the dephosphorylation of CDK1 substrates. This is achieved in part by CDK1 downregulation through APC activation and Sic1 synthesis. However, it is widely believed that phosphatases also contribute to the timely removal of phosphates from CDK1 targets. In budding yeast, the activation of a single phosphatase, Cdc14, is thought to drive the last mitotic events and promote the resetting of the cell for a new cycle. Indeed, the process by which Cdc14 is activated after metaphase has been extensively studied in recent years.

Cdc14 regulation is directly related to Cdc14 localization. During G1 phase, S phase and early mitosis, Cdc14 is found in the nucleolus, but after the start of nuclear division, it is delocalised to the nucleus and the cytoplasm. The protein responsible for Cdc14 localization is Net1. This nucleolar protein anchors to Cdc14, and together with Sir2, they form the RENT (*RE*gulator of *N*ucleolar silencing and *T*elophase) complex. Whilst part of RENT, Cdc14 is inactive (Traverso et al., 2001; Visintin et al., 1999).

The mechanism responsible for Cdc14 detachment from Net1 is still not well established. Nevertheless, it is believed that the phosphorylation of Net1 destabilises the RENT complex and promotes Cdc14 release (Azzam et al., 2004). Underlying this process are two regulatory pathways, employed in such way that Cdc14 activation occurs only when the cell is ready to exit mitosis (never before the onset of sister chromatid segregation).

Cdc14 is released in early anaphase through the FEAR (*C*dc14 *F*ourteen *E*arly *A*naphase *R*elease) network. This early release is not directly responsible for mitotic exit events, but for other events such as chromosome segregation, mitotic spindle dynamics, and the localization of chromosomal passenger proteins (Higuchi and Uhlmann, 2005; Ross and Cohen-Fix, 2004; Widlund et al., 2006), FEAR by itself is unable to maintain Cdc14 levels in the cytoplasm, and thus the activation of a second network, MEN (*M*itotic *E*xit *N*etwork), is required for sustained Cdc14 release. Hence, MEN is the main pathway that governs mitotic exit. Experimental results clearly show that cells are unable to exit mitosis when MEN is inactivated, even with a transient release of Cdc14 at anaphase onset (Pereira et al., 2002; Stegmeier et al., 2002). These results also indicate that cells require phosphatase activity from anaphase until the end of mitosis; transient phosphatase activity in early anaphase is insufficient to promote mitotic exit.

### *d. FEAR network*

Since the FEAR network is not essential for mitotic exit (nor cell viability), its discovery came after that of MEN. The existence of FEAR only became apparent during observations of cells lacking MEN activity. The fact that these cells still release Cdc14 from the nucleolus makes it clear that another pathway must be controlling Cdc14 activity. This pathway, FEAR, differs from MEN in three main aspects: (i) it is transient (Pereira et al., 2002; Stegmeier et al., 2002; Sullivan and Uhlmann, 2003; Yoshida and Toh-e, 2002); (ii) it is limited to the nucleus, Cdc14 is not exported to the cytoplasm; and (iii) it is insufficient to reduce Clb/CDK1 activity (Stegmeier et al., 2002).

Our knowledge of the FEAR network, its components, and how they relate to each other, is still limited. All available results are of a genetic nature, so it becomes difficult to determine exactly how they interrelate. Nonetheless, it has been established that nine proteins belong to the FEAR network; six engage in a positive role, while the other three engage in a negative role. A positive role is one that brings Cdc14 out of the nucleolus, and a negative role is one that prevents Cdc14 from being released. FEAR components with positive roles are CDK1, Esp1, Slk19, Spo12, Bns1 (Spo12 homolog) and Cdc5. Those with negative roles are Pds1, $PP2A^{Cdc55}$ and Fob1.

Net1 has three phosphorylation sites in its N-terminus that are important for Net1/Cdc14 association, and six CDK1 phosphorylation sites in the region where Net1 interacts with Cdc14. The CDK1 phosphorylation sites have been shown to regulate Cdc14 release, and thus CDK1 participates in the FEAR network by phosphorylating Net1 (Azzam et al., 2004). Another kinase that may be responsible for Net1/Cdc14 phosphorylation and its consequent complex dissociation is Cdc5 (Manzoni et al., 2010; Shou et al., 2002; Visintin et al., 2003; Yoshida and Toh-e, 2002). Nevertheless, Cdc5 is also involved in MEN, so disentangling its specific contribution to FEAR is not trivial.

Since CDK1 activity is high in mitosis, it might be expected to promote Net1 phosphorylation. However, Cdc14 is not released until after metaphase, so another factor must counteract Net1 phosphorylation. Queralt et al. (2006) showed that the phosphatase $PP2A^{Cdc55}$ is responsible for preventing premature Net1 phosphorylation and Cdc14 release. $PP2A^{Cdc55}$ is a type 2A phosphatase with Cdc55 as its regulatory subunit. It acts on Net1, promoting Net1 dephosphorylation, and thus, its binding to Cdc14 (Queralt et al., 2006).

At the end of metaphase, the SAC is silenced and APC/Cdc20 is activated. APC/Cdc20 degrades Pds1, and Esp1 becomes free and active. Esp1 is a FEAR component, but counterintuitively, its role in FEAR is independent of its role in cleaving cohesin. In fact, Esp1 activates FEAR by inhibiting $PP2A^{Cdc55}$. It has been reported that Esp1 can bind to Cdc55, so it is probable that the inhibition of $PP2A^{Cdc55}$ is tightly connected to the nature of this interaction (Queralt et al., 2006).

Slk19 was identified as a FEAR component because MEN mutant cells with a Slk19 deletion do not show a transient release of Cdc14 (Stegmeier et al., 2002). Moreover, it has been reported that the mutant *slk19*Δ*mad1*Δ has about a 50% reduction in Cdc14 release in anaphase and telophase. Esp1 cleaves Slk19 during anaphase, but this cleavage has proven to be irrelevant to Cdc14 early release, indicating that the relationship between Esp1 and Slk19 is non-proteolytic in nature (Sullivan and Uhlmann, 2003). Since Slk19 is a kinetochore/spindle protein that can form a complex with Esp1, Slk19 might be responsible for directing Esp1 to the spindle midzone when these two proteins bind to each other (Sullivan et al., 2001; Sullivan and Uhlmann, 2003). On the other hand, overexpression of Esp1 does not restore the early Cdc14 release in *slk19*Δ*mad1*Δ cells, suggesting that Slk19 role in FEAR is downstream of Esp1 (Visintin et al., 2003).

Besides Pds1 and $PP2A^{Cdc55}$, the FEAR network includes another negative factor called Fob1. Fob1 is a nucleolar protein that binds to Net1 and stabilises the RENT complex (Stegmeier et al., 2004). During mitotic exit, the phosphoproteins Spo12 and Bns1 bind to Fob1 and the formation of this complex is thought to be responsible for Fob1 inhibition (Stegmeier et al., 2004).

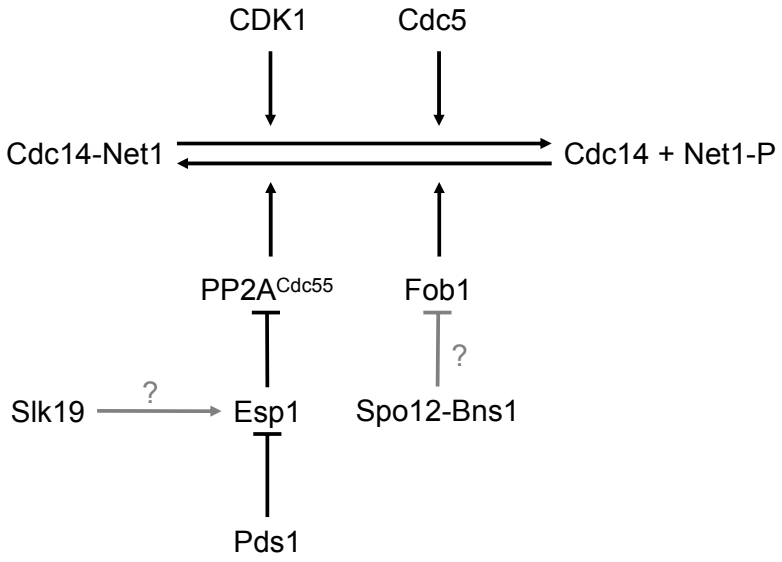


**Figure 7: Wiring Diagram of the FEAR network. Pointed arrows represent positive interactions and blunt arrows represent negative interactions. Molecular interactions still under debate are represented in grey (with an interrogation mark).**

As one can see, the relationships between the FEAR network components are still poorly understood at a molecular level. The contribution of single components to FEAR activation is all that has been clearly determined thus far, and from these results, several hypotheses have been proposed as to how the network might function. Nonetheless, the role of the FEAR network in mitotic exit is well established. FEAR network mutants show a delay in Cdc14 release and in mitotic exit, which clearly indicates that FEAR is important for a timely exit from mitosis.

The FEAR network promotes mitotic exit by activating MEN. Cdc14 released by FEAR directly dephosphorylates and activates the MEN kinase Cdc15 (Jaspersen and

Morgan, 2000). It has been shown that FEAR is important to trigger an amplification signal for Cdc14 release due to the existence of a positive feedback loop between Cdc14 and MEN. In accordance with this idea, FEAR mutants do not show Cdc15 dephosphorylation during early anaphase, which has consequences for the activity of a downstream MEN component, Dbf2 (Stegmeier et al., 2002). Other MEN components are likely to be Cdc14 targets; for instance, Bfa1 and Lte1 can also be dephosphorylated by Cdc14, and this could affect their role in MEN (Jensen et al., 2002; Pereira et al., 2000; Pereira et al., 2002; Seshan et al., 2002).

FEAR-mediated release of Cdc14 has also been shown to regulate other anaphase events besides MEN activation. The Ipl1-Sli15-Bir1 complex is important for the stabilization of the anaphase spindle midzone, and because Sli15 is a substrate of Cdc14, Cdc14 is responsible for directing Ipl1-Sli15-Bir1 to the spindle midzone (Mirchenko and Uhlmann, 2010; Pereira and Schiebel, 2003). Cdc14 also acts on the condensin complex, and although the details of this mechanism are presently unknown, Cdc14 is responsible for the localization of the condensin complex in the nucleolus (D'Amours et al., 2004; Wang et al., 2004). Finally, Cdc14 is thought to regulate the positioning of the nucleus in the daughter cell by dephosphorylating Kar9, a protein required for correct positioning of the mitotic spindle and for orienting cytoplasmic microtubules (Liakopoulos et al., 2003; Maekawa et al., 2003).

### *e. MEN*

The signalling pathway known as MEN was initially outlined by identifying genes required for mitotic exit and by establishing several genetic interactions between these genes (Jaspersen et al., 1998).

One of the main regulatory points in the MEN network is the regulation of the GTPase Tem1 (Shirayama et al., 1994). This control is extremely important to ensure that MEN is activated only if the nucleus is correctly localised at the mother-bud axis. Tem1 is negatively regulated by the GTPase-activating protein (GAP) Bub2-Bfa1 complex. Both proteins are bound to the scaffold protein Nud1, and localise mainly to the daughter-bound spindle pole body (SPB) (Bardin et al., 2000; Fesquet et al., 1999; Geymonat et al., 2003; Gruneberg et al., 2000; Pereira et al., 2000). The guanine nucleotide exchange factor (GEF) that positively regulates Tem1 is thought to be Lte1, a protein that resides in the bud cortex (Bardin et al., 2000; Jensen et al., 2002). In this way, Tem1 is kept inactive by Bub2-Bfa1 until anaphase. At anaphase onset, the spindle elongates and the daughter-bound SPB migrates into the bud, carrying both Tem1 and Bub2-Bfa1 with it. Once at the bud, Tem1 is activated and this signal promotes MEN activation. In addition, Bub2-Bfa1 activity is regulated by the spindle positioning checkpoint through the kinase Kin4, which phosphorylates and activates Bub2-Bfa1. Kin4 is predominantly present in the mother cell, and thus its positive effect on Bub2-Bfa1 is strongly reduced when Bub2-Bfa1 migrates to the bud during anaphase (D'Aquino et al., 2005; Pereira and Schiebel, 2005). At the bud, Bub2-Bfa1 is inhibited by the kinase Cdc5 (Hu et al., 2001; Pereira and Schiebel, 2005). This layer of regulation further promotes Tem1 activation at anaphase onset.

The MEN kinase Cdc15 is also bound to the scaffold protein Nud1 (Gruneberg et al., 2000). Once Tem1 is activated, it sends a signal to Cdc15 that triggers Cdc15 activation. In turn, Cdc15 kinase activity is required to activate another protein kinase, Dbf2, in complex with the regulatory factor Mob1. The Dbf2-Mob1 kinase complex is the MEN component most likely to phosphorylate Net1 and to bring about Cdc14 release (Komarnitsky et al., 1998; Luca and Winey, 1998; Mah et al., 2001; Visintin and Amon, 2001).

Cdc15 is further regulated through phosphorylation. This kinase contains seven CDK1-consensus sites and is highly phosphorylated during G1 and S phases. At anaphase onset, Cdc15 is dephosphorylated by Cdc14. It is unclear how this dephosphorylation enhances Cdc15 role in mitotic exit, as experimental evidence indicates that Cdc15 kinase activity remains the same whether Cdc15 is phosphorylated or not. Having said this, cellular viability is restored in several MEN mutant situations by the expression of Cdc15-7A, a Cdc15 protein immune to phosphorylation. For instance, viability is restored to *cdc5-1*, *dbf2-2* and *tem1-2* mutant cells when Cdc15-7A is expressed (Jaspersen and Morgan, 2000). One possible explanation is that the dephosphorylation of Cdc15 promotes its localization to the SPB rather than its activity, although this has yet to be confirmed.

The early release of Cdc14 by the FEAR network has a positive effect on Cdc15 mitotic function; this effect represents a connection between the FEAR and MEN networks. Moreover, there is a clear positive feedback loop between Cdc14 and Cdc15: not only does Cdc14 have a positive effect on Cdc15, but Cdc15 is also responsible for Cdc14 activation through its role in MEN (Jaspersen and Morgan, 2000).

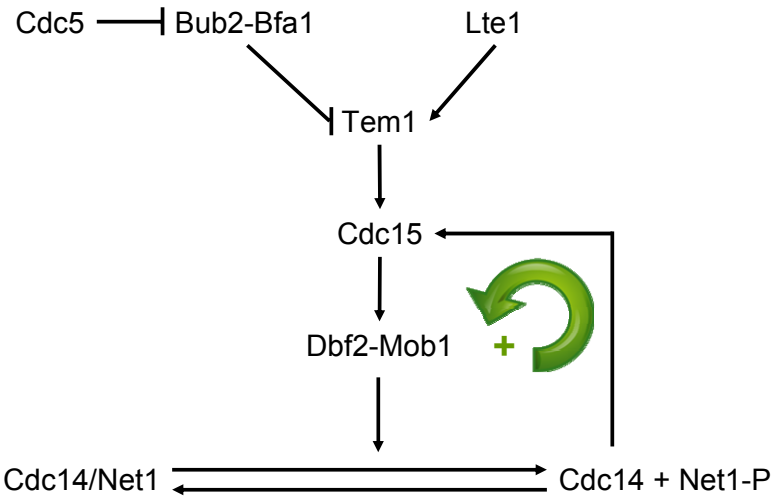


**Figure 8: Wiring Diagram of MEN. Pointed arrows represent positive interactions and blunt arrows represent negative interactions. The positive feedback between Cdc15 and Cdc14 is highlighted by a green arrow.**

In contrast with the FEAR network, which promotes a transient release of Cdc14, MEN is capable of promoting a complete and sustained release of Cdc14, which is necessary for cells to exit mitosis. In addition, Cdc14 released through FEAR remains mainly in the nucleus, while Cdc14 released through MEN reaches the cytoplasm. As a consequence, Cdc14 released by each of the networks interacts with different substrates. The Cdc14 substrates active during mid anaphase (FEAR substrates; e.g. Sli15, the condensin complex, etc) are found mainly in the nucleus, while the Cdc14 substrates active in late anaphase/telophase (MEN substrates; e.g. Cdh1 and Swi5) are found mainly in the cytoplasm (Higuchi and Uhlmann, 2005; Jaquenoud et al., 2002; Moll et al., 1991; Pereira and Schiebel, 2003). In this way, the MEN pathway regulates not only the dissociation of Cdc14 from Net1, but also the presence of Cdc14 in the cytoplasm. The MEN component Dbf2, together with its regulatory factor Mob1, phosphorylates Cdc14 on several sites close to the C-terminal nuclear localization signal (NLS), and thus, the NLS is inhibited. As a result, the phosphorylated Cdc14 molecules that migrate to the cytoplasm do not return to the nucleus (Mohl et al., 2009). Therefore,

Dbf2-Mob1-mediated phosphorylation of Cdc14 is responsible for Cdc14 lodging in the cytoplasm where it can dephosphorylate substrates such as Cdh1 and Swi5 (Jaquenoud et al., 2002; Mohl et al., 2009; Moll et al., 1991).

### *f. Dephosphorylation of CDK1 targets governs the final steps of mitosis*

The final steps of mitosis are driven by a downregulation of CDK1 activity. If CDK1 activity remains high, the cell arrests in mitosis (Irniger, 2002; Wasch and Cross, 2002). In budding yeast, this downregulation is achieved in two different ways: through Clb degradation by the APC/C, and through CDK1 inhibition by Sic1 (King et al., 1996; Mendenhall et al., 1995; Sudakin et al., 1995). Both mechanisms are controlled by MEN-mediated Cdc14 release (Visintin et al., 1998).

Cdh1 and Sic1 are both CDK1 substrates (Amon et al., 1994; Skowyra et al., 1997; Verma et al., 1997): CDK1 phosphorylation inactivates Cdh1, and targets Sic1 for degradation. When CDK1 activity is high, Cdh1 activity and Sic1 level are low. However, this state is reversed when Cdc14 is released, because active Cdc14 counteracts CDK1-mediated phosphorylation of Cdh1 and Sic1 in late anaphase (Visintin et al., 1998).

Cdc14 promotes Sic1 accumulation not only by stabilising this protein, but also by promoting its transcription. Phosphorylated Swi5 is retained in the cytoplasm, and Cdc14 dephosphorylation promotes the migration of Swi5 to the nucleus where it enhances the transcription of Sic1 (Visintin et al., 1998).

In this way, Cdc14 triggers mitotic exit by dephosphorylating three CDK1 substrates: Cdh1, Sic1 and Swi5. The dephosphorylation of these proteins is crucial for switching the double negative feedback loop to a state where CDK1 activity is low.

The major events of late anaphase and telophase (e.g. spindle disassembly and chromosome decondensation) only occur if CDK1 activity is reduced. Therefore, it is expected that the CDK1 substrates are also Cdc14 targets, and that Cdc14 dephosphorylates them at the end of mitosis. This assumption has yet to be verified however.

### *g. Cdc14 inactivation after mitosis*

Cdc14 activation in anaphase is crucial for cell cycle progression. However, Cdc14 inactivation at the end of mitosis is of no less importance. Cells showing Cdc14 activity after the completion of mitosis present major growth defects (Shou et al., 1999; Visintin et al., 1998; Visintin et al., 1999). This situation is prevented by a negative feedback loop mechanism, whereby Cdc14 triggers its own recapture to the nucleolus. When Cdc14 dephosphorylates Cdh1, Cdh1 activates the APC, and the active complex targets Cdc5 for degradation (Visintin et al., 2008). Cdc5 destruction promotes FEAR and MEN shutdown, and consequently, Cdc14 recapture. Other less important contributions of Cdc14 are the dephosphorylation of Bfa1, which activates the Bub2-Bfa1 complex (Hu et al., 2001; Pereira et al., 2002), and a possible role in Lte1 regulation (Jensen et al., 2002; Seshan et al., 2002).

### *h. Mathematical Modelling of Mitotic Exit*

Considering the amount of information available on mitotic exit, intuitive reasoning is by itself insufficient to understand the key interactions governing the dynamical behaviour of the network. Using biochemical kinetics, several mathematical models have been designed to systematise the upcoming experimental knowledge. The model

present in Novak et al (1999) clearly states the importance of a protein phosphatase to upregulate APC/Cdh1 and Sic1 at the end of mitosis, and the model present in Ciliberto et al. (2005) establishes a connection between the SAC and mitotic exit.

A detailed model focusing mainly on the events of mitotic exit was published in 2006 (Queralt et al., 2006). Queralt's model (QM) is restricted to the time window from metaphase to G1, and centres on the reversible phosphorylation/dephosphorylation of Net1. The proteins acting on Net1 fall into two categories; on one side are the CDK1 and MEN kinases, and on the other side are the $PP2A^{Cdc55}$ and Cdc14 phosphatases. In QM, Esp1 acts on both the MEN and FEAR networks through the downregulation of $PP2A^{Cdc55}$, and thus the proteolytic function of this enzyme is not explicit. Once released, Cdc14 participates in two feedback loops: a negative feedback loop involving FEAR (Cdc14 dephosphorylates Net1), and a positive feedback loop involving MEN (Cdc14 activates Cdc15 and therefore MEN). Clb2 also has a dual effect; it phosphorylates Net1, promoting Cdc14 release, but inactivates Tem1, inhibiting MEN activation.

QM is based on 13 differential equations, the parameters of which were estimated by fitting numerical simulations to experimental data. QM can faithfully reproduce 13 mutant situations besides the wild-type situation. However, since 2006, new experimental results have been published (e.g.; Lu and Cross, 2010; Manzoni et al., 2010; Visintin et al., 2008), and QM has proved insufficient to explain this new data. There is therefore a need for a new, more comprehensive model of mitotic exit.

This thesis describes the development of a new model, which was built to analyse a broader set of experiments (from single to quintuple mutants). QM was used as a starting point, and various changes were implemented to improve our current understanding of mitotic exit. At each stage of the model's development, the addition of novel features proved essential, as will be explained in the following chapters.

# Methods

## *1. Basic Principles for cell cycle modelling*

Biological systems are composed of a large number of proteins which interact through a large number of biochemical reactions. These systems exhibit complex dynamics which determine the physiological changes that a cell undergoes in both space and time (e.g. growth, reproduction, differentiation, etc.). Due to the high level of complexity in these systems, it has become increasingly necessary to develop theoretical approaches that can be used to predict and understand system dynamics using the available biological information (Christopher P. Fall, 2002).

The first step in a theoretical study of a biological system is to identify its components and to recognise how are they 'wired together'. At this stage, relevant information from the literature is laid out as a wiring diagram of the system's molecular interactions (very similar to the wiring diagram of a modern electronic gadget) (Figure 9).

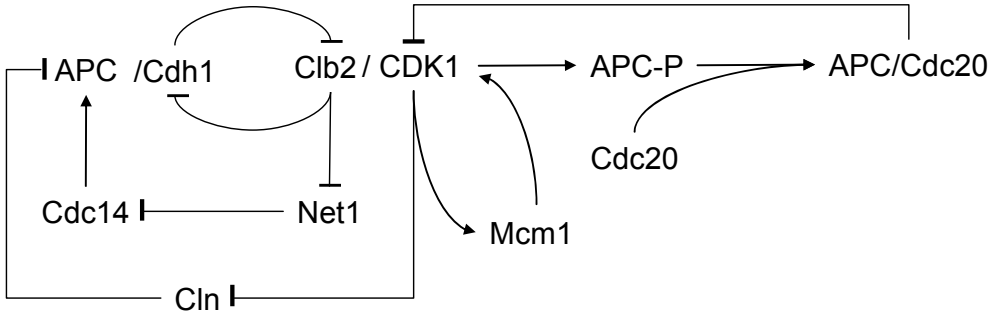


**Figure 9: Wiring diagram of the molecular network regulating Clb2/CDK1 activity during cell cycle. Pointed arrows represent protein activation and blunt arrows represent protein inhibition.**

The wiring diagram depicts the molecular interactions present in the network, but the picture is static; it does not contain any information on when each of the interactions takes place. As a result, the wiring diagram cannot offer insights into the dynamical

properties of the system, so this information has to be converted into a set of mathematical equations, which describe how the system evolves in both time and space. Thus, after obtaining the wiring diagram, the next step is to choose an appropriate modelling technique that can be used to study the system's dynamics (Tyson, 2007).

The cell cycle control system is commonly described using Ordinary Differential Equations (ODEs) (Tyson et al., 2001). This deterministic method only captures the temporal dynamics of cell cycle components. The spatial dynamics can also be described by using partial differential equations (PDEs). However, since membrane transport and molecular diffusion are faster processes (in the order of seconds) than the cell cycle (in the order of hours), ODE based modelling is considered appropriate.

The mathematical equations are written based on chemical reaction kinetics, since the components of the system are mainly enzymes and other proteins. These equations should describe how a protein is synthesised, degraded, activated and inactivated (e.g. phosphorylation/dephosphorylation and complex formation). One of the main challenges is to specify the values of the rate constants for the kinetic reactions. Since most have not yet been determined experimentally, the choice of parameter values (rate constants) depends on a different kind of experimental data, both qualitative and quantitative, that can be used to optimise or constrain the choice of values (Tyson et al., 2001). Qualitative data can come from many different sources such as cellular microscopy, western blot and FACS (Fluorescent Activated Cell Sorting). Quantitative data may come from analyses of messenger RNA expression or protein expression in cells. In addition, live cell imaging provides exact information on the temporal dynamics of cell cycle events.

The model simulations result from the standing parameter set, and are compared with all the available experimental findings. This comparison indicates whether the choice of parameter values was adequate or if changes should be made. Moreover, the

nature of the differences between the simulations and the experiments points towards which parameters should be changed. It is important to identify the source of the discrepancy so to identify which parameter values need to be manually optimized. At times, intuitive trial and error approach can be sufficient. However, for a more formal approach, bifurcation theory is an appropriate tool to understand how the system's dynamical behaviour depends on parameter values.

A system of ODEs describes how the variables change with time, so to describe the temporal evolution of the variables, the solution of the system also depends on the choice of initial conditions. For modelling biological systems, the initial conditions can be obtained based on an experimental setting. For example, when modelling cell cycle, the common choice of initial condition is based on the cell cycle arrest used to synchronise cells (i.e. G1 arrest, metaphase arrest).

The combination of the wiring diagram, the set of equations, the set of parameter values and the set of initial conditions forms the mathematical model of the biological system. The model is a useful tool to study the system's dynamic properties and to make predictions about future experimental results. The developed model can be further refined with the appearance of newer experimental results, and the established iterative flow of information between experimentalists and modellers increases the understanding of the biological system.

## *2. Ordinary Differential Equations*

An ODE depicts how fast the state of a component (e.g. concentration, number of proteins, activity) changes with time. To obtain the function that shows how the component varies with time, one must integrate the ODE. Since most biological systems are best modelled by nonlinear ODEs, these ODEs can very rarely be solved

analytically. In most cases, computer simulations are required to find approximate numerical solutions.

As a general example, let us consider the dynamics of a generic protein X, and use the same notation X to refer to its concentration. The ODE for X can be described as follows:

$$\frac{dX}{dt} = V_{synthesis} + V_{activation} - V_{degradation} - V_{inactivation} \quad (1)$$

where each V represents the reaction rate for the synthesis, degradation, activation and inactivation of protein X.

The reaction rates can be described with two commonly used kinetics: (i) the law of mass action (mostly for synthesis and degradation rates); and (ii) Michaelis-Menten kinetics (mostly for activation and inactivation rates).

The law of mass action states that the reaction rate (V) at which a chemical (X) is produced is proportional to the product of the reactants (A and B).

$$A + B \rightarrow X \quad (2)$$

$$V = \frac{dX}{dt} = k \times [A] \times [B], \text{ where k is the reaction rate constant} \quad (3)$$

If the reactants are in excess and their concentration is approximately constant during the production of X, $k \times [A] \times [B]$ can be treated as a single constant. This is commonly the case for protein synthesis where amino-acids are largely available:

$$V_{synthesis} = k_{sX}, \text{ where } k_{sX} \text{ is the synthesis rate constant} \quad (4)$$

To describe protein degradation with the law of mass action, one has to think of the reverse, where X is the reactant:

$$V_{degradation} = k_{dX} X, \text{ where } k_{dX} \text{ is the degradation rate constant} \quad (5)$$

As an example, consider a simple situation whereby X is only regulated by synthesis and degradation ($V_{activation} = V_{inactivation} = 0$). If these two terms follow the law of mass action, then the reaction rates are the following:

$$\frac{dX}{dt} = k_{sX} - k_{dX}X \tag{6}$$

This biochemical system is represented in Figure 10A.

Michaelis-Menten kinetics is used to describe the rate of enzymatic reactions where the reaction rate (V) depends on the concentration of substrate and on an intermediate step in which the enzyme and the substrate form a complex before the substrate is converted into product. Assuming the concentration of substrate largely exceeds the concentration of enzyme, the reaction rate is given by:

$$V = k_{max}\frac{[Substrate]}{J + [Substrate]} \tag{7}$$

where $k_{max}$ is the maximum rate of conversion and J is known as the Michaelis constant. A more detailed description can be found in (Johnson and Goody, 2011), which is a new translation of the original paper by (Menten and Michaelis, 1913).

In a situation where the activity of X is regulated according to Michaelis-Menten kinetics and the concentration of X is constant ($X_T$), the activation and inactivation reaction rates are:

$$V_{activation} = k_{aX}\frac{X_T - X_a}{J_a + X_T - X_a} \tag{8}$$

$$V_{inactivation} = k_{iX}\frac{X_a}{J_i + X_a} \tag{9}$$

where $k_{aX}$ and $k_{iX}$ are activation and inactivation rate constants, respectively, and $J_a$ and $J_i$ are Michaelis constants for the activation and inactivation terms, respectively. Because $X_T$ is constant, the inactive form of X ($X_i$) can be calculated by the relation $X_T = X_a + X_i$. The biochemical system referring to X activation/inactivation is represented in Figure 10B, and has been carefully studied by Goldbeter and Koshland (1981). The Goldbeter-Koshland equation for the equilibrium solution of X is the following:

$$X_a = \frac{2k_{aX}J_i}{k_{iX} - k_{aX} + k_{iX}J_a + k_{aX}J_i + \sqrt{(k_{iX} - k_{aX} + k_{iX}J_a + k_{aX}J_i)^2 - 4(k_{iX} - k_{aX})k_{aX}J_i}} \quad (10)$$

An important feature of the Goldbeter-Koshland function is the sigmoidal response curve obtained for very small values of J (<<1). This mechanism is commonly used in modelling biological systems because it creates a switch-like response in protein activity (known as zero-order ultrasensitivity) (Goldbeter and Koshland, 1981).

The previous examples focused on the kinetics of one protein; however, a real biochemical network usually involves more than one molecule. Therefore, to illustrate how a system of ODEs can describe the chemical interactions between different molecular species, a simple example involving just two components (X and Y) is shown. In this case, let us suppose that X and Y are in a situation of homeostasis, whereby X and Y regulate each other in a counteractive manner. X activates Y, and Y enhances the degradation of X. The resulting system of ODEs can be written as follows:

$$\frac{dX}{dt} = k_{sX} - k_{dX}\,X - k_{dX}'\,Y\,X \quad (11)$$

$$\frac{dY_a}{dt} = k_{aY}\frac{Y_T - Y_a}{J_a + Y_T - Y_a}X - k_{iY}\frac{Y_a}{J_i + Y_a} \quad (12)$$

where $k_{dX}$' is the rate constant of the degradation of X mediated by Y. This biochemical system is represented in Figure 10C.

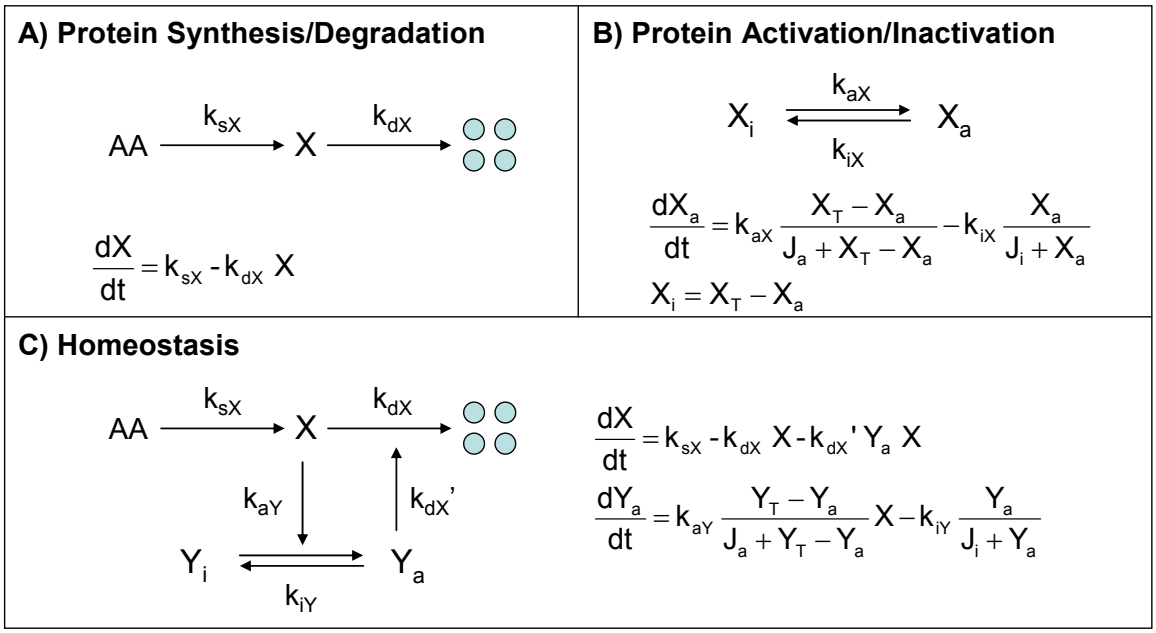


**Figure 10: Wiring diagrams and corresponding ODEs for three different examples of protein regulation. A) X is synthesised and degraded according to the law of mass action: zero-order synthesis and first order degradation. B) X activity is regulated through Michaelis-Menten kinetics. C) X and Y regulate each other according to a homeostatic system. X is synthesised and degraded according to the law of mass action, and Y activity is regulated through Michaelis-Menten kinetics. AA stands for amino-acids.**

The temporal evolution of each protein (X and Y) can be calculated using a numerical approximation (e.g. the Euler method) when an exact solution cannot be found. It is important to choose an appropriate numerical method so that the approximate solution does not diverge from the exact solution. Most numerical methods are already implemented in different software packages. The numerical solutions presented in this thesis were computed by the software packages XPPAUT, and its Windows-based equivalent, WINPP. Both programs are freely available from G. Bard Ermentrout at the Department of Mathematics, University of Pittsburgh (http://www.mathematics.pitt.edu/) (Ermentrout et al., 2003). In this thesis, the simulations were performed using the numerical method 'Stiff', which assigns a flexible or variable step size depending on the curvature of the solution at every time step. Due to the oscillatory features of cell cycle control, this numerical method is the most

appropriate to simulate the equations. The time courses of X and Y were calculated in XPPAUT and the solution is shown in Figure 11A.

## 3. Analysis of Dynamical Systems

Most dynamical systems are nonlinear, which means that they cannot be separated into different parts and described as the sum of these parts. As a consequence, nonlinear dynamical systems have been widely studied in the past century, resulting in well-established theories (Strogatz, 1994; Tyson et al., 2003). These theories avoid analytical solutions and focus instead on the qualitative behaviour of the system. Two of the most common methodologies are phase plane analysis and bifurcation analysis.

### a. Phase Plane Analysis

A phase plane is a 2-dimensional picture of the system where the two state variables (X and Y) are represented by the axes, and a trajectory starting at ($x_1$, $y_1$) represents the evolution of the system with respect to time.

Two important curves in a phase plane are the nullclines of the system. These are defined by the ODEs when the corresponding time rate of change is zero (dX/dt = 0 or dY/dt = 0). The nullclines are also important to define the steady-states of the system since the intersect of both solutions is a steady-state (dX/dt = dY/dt = 0).

Figure 11B depicts the phase plane portrait of the homeostatic system presented in Equations (11) and (12). The nullclines for X and Y are given by the red and the green lines, respectively. The dashed curve represents the trajectory of the system when the initial conditions are null (X = 0; Y = 0). As one can see, the trajectory line ends at the

steady-state of the system (exactly where the two nullclines intersect), inferring that this steady-state must be stable (an attractor for nearby trajectories).

### b. *Bifurcation Theory*

The qualitative behaviour of a system of ODEs may change depending on its parameter set. Therefore, it is important to analyse how the system responds to changes in parameter values. The theory that determines how the qualitative nature of the system's solution varies with respect to its parameters is called bifurcation theory. A bifurcation occurs when a small, 'smooth' change to a parameter value (the bifurcation parameter) causes a sudden, qualitative change in the behaviour of the system. Bifurcations are therefore connected to changes in stability of equilibrium points, and the creation or destruction of steady-states. There are different types of bifurcations (four examples are illustrated in Figure 12), and a thorough description of their characteristics can be found in (Strogatz, 1994). A bifurcation diagram is a graphical representation of the equilibrium solutions and their associated stability as a function of a parameter. In general, stable steady-states are represented by a solid line, and unstable steady-states are represented by a dashed line. A good description of different cell cycle bifurcations can be found in Csikasz-Nagy et al. (2006).

Figure 11C depicts the associated bifurcation diagram of the homeostatic system presented in Equations (11) and (12). Here, the steady-state solution for protein X is plotted against different values of $k_{dx}$', the chosen bifurcation parameter, and the solid line represents a stable steady-state.

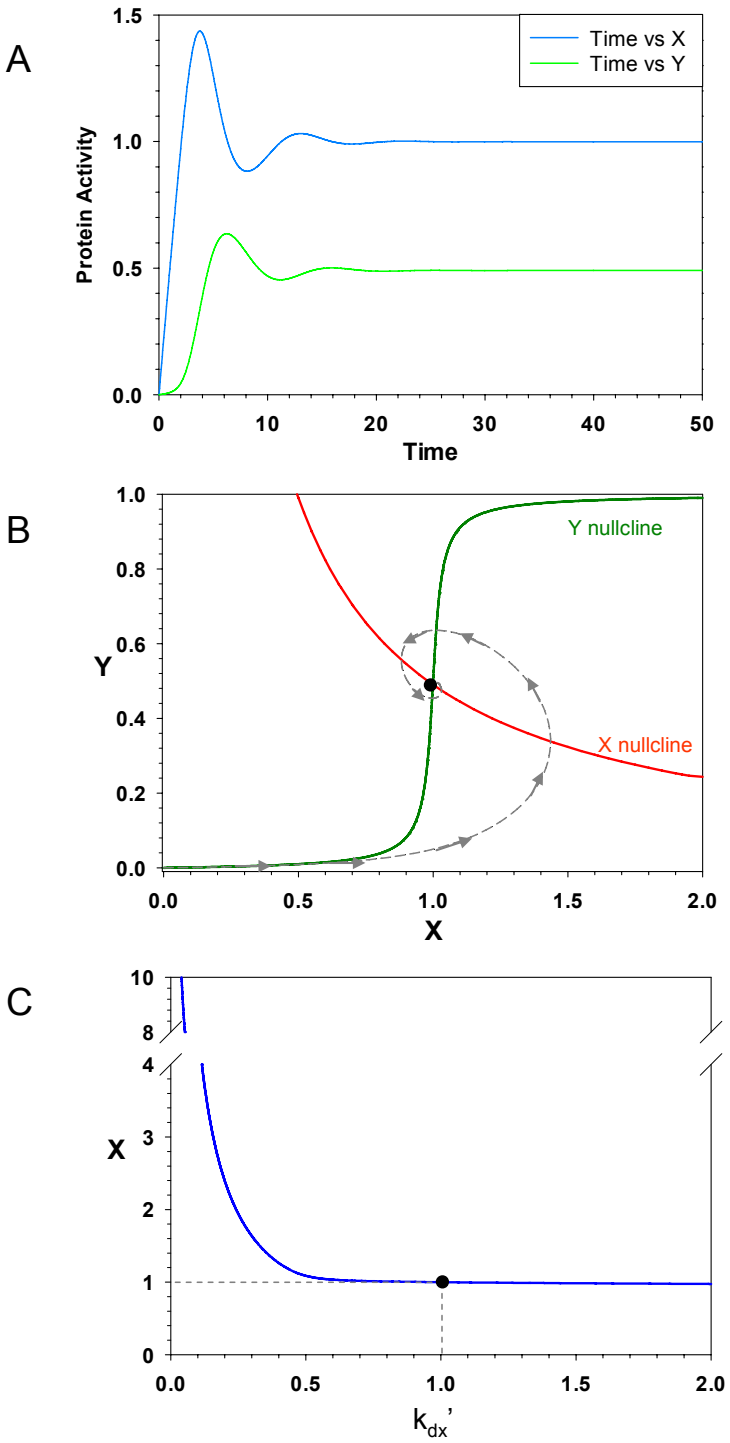


**Figure 11: Homeostatic system where two proteins (X and Y) counterbalance each other. The ODEs governing this systems are presented in (11) and (12), with parameters $k_{sX} = 0.5$, $k_{dX} = 0.01$, $k_{dX}' = 1$, $Y_T = 1$, $k_{aY} = 0.5$, $k_{iY} = 0.5$, $J_a = 0.01$, $J_i = 0.01$. (A) Time course of X and Y with initial conditions X = 0 and Y = 0. (B) Phase Plane of X vs Y. The X and Y nullclines are shown in red and green respectively. The trajectory is shown in a dashed grey line and arrows indicate its direction. The black dot shows the system's stable steady-state. (C) Bifurcation diagram of X with $k_{dx}$' as the bifurcation parameter. Black dot shows the steady-state of X when $k_{dX}' = 1$, the same value chosen to run the time course in (A) and to draw the phase plane in (B).**

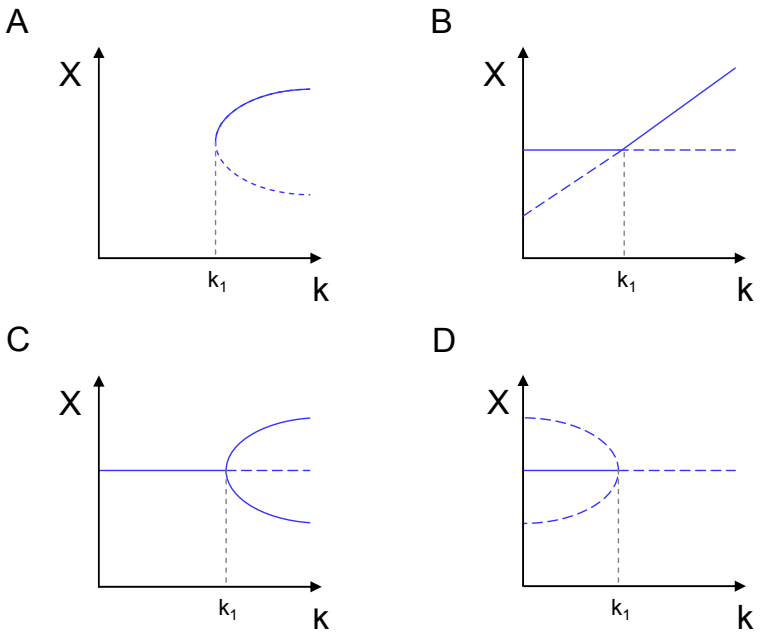


**Figure 12: Bifurcation diagrams for four different types of bifurcations. Stable steady-states are represented by solid lines while unstable steady-states are represented by dashed lines. (A) Saddle-node bifurcation, at $k_1$ one steady-state is created, and for k values larger than $k_1$, two steady-states are generated, one stable (solid line) and one unstable (dashed line). (B) Transcritical bifurcation, at $k_1$, the steady-states interchange stability (the solid line becomes dashed and the dashed line becomes solid). (C) Supercritical pitchfork bifurcation, at $k_1$, the stable steady-state becomes unstable (solid horizontal line becomes dashed after $k_1$) and two other symmetric stable steady-states are generated. (D) Subcritical pitchfork bifurcation, at $k_1$, the stable steady-state becomes unstable (solid horizontal line becomes dashed after $k_1$) and the two unstable steady-states (symmetric dashed lines) collide and disappear.**

## *4. Basic Regulatory Motifs*

Thus far, a single basic regulatory motif (homeostasis) has been described in order to illustrate the different methodologies used to analyse nonlinear systems of ODEs. Homeostasis is a very important motif because it allows the network to fine tune the signal-response behaviour. X triggers its own degradation by activating a second protein Y, and thus, the level of X is tightly coupled to the activity of Y and will never rise above a certain threshold (determined by the activity of Y). This type of regulation is known as a negative feedback loop, because X promotes its own downregulation.

In biology however, there are a wide variety of regulatory motifs that determine different systems' behaviours. For instance, mutual activation and mutual inhibition create irreversible switches in the system, and other feedback loops might trigger oscillatory responses.

Mutual activation (or a positive feedback loop) is the regulatory motif by which two proteins upregulate each other. For instance, a protein X activates a protein Y, and the activated form of Y enhances the synthesis of X. A positive feedback loop may create a discontinuous switch-like response if one of the components has a nonlinear behaviour (e.g. if Y is described by Goldbeter-Koshland kinetics). This feature, also known as bistability, is very important because it is a source of irreversibility (e.g. if X reaches a certain value, Y is activated and cannot be inactivated even if X decreases).

Mutual inhibition (or a double negative feedback loop) is the regulatory motif by which two proteins downregulate each other. For instance, a protein X inhibits the activation of a protein Y, while protein Y promotes the degradation of protein X. As such, this mechanism works like a positive feedback loop, because inhibiting one's inhibitor has the effect of promoting one's own activity. Therefore, mutual inhibition shares characteristics with mutual activation. In both cases, the system may create a discontinuous switch-like response, as long as one of the components has a nonlinear behaviour.

A negative feedback loop can be a source of oscillatory behaviour. However, a two-component negative feedback loop without time-delay (e.g. system depicted in Figure 10C) is unable to sustain oscillations, and the result is damped oscillations terminating in the stable steady-state. To sustain oscillation, the system requires a minimum of three components because the third component enables the time-delay necessary to make the system overshoot and undershoot repeatedly around the steady-state solution. This can be clearly observed in a hypothetical system with X, Y and Z, whereby X promotes Y

which promotes Z, but Z inhibits X. Other regulatory motifs can generate oscillatory behaviour in a system; these have been reviewed in (Novak and Tyson, 2008).

Figure 13 summarises the wiring diagrams and corresponding equations for the regulatory motifs of mutual activation, mutual inhibition and the three component negative feedback loop.

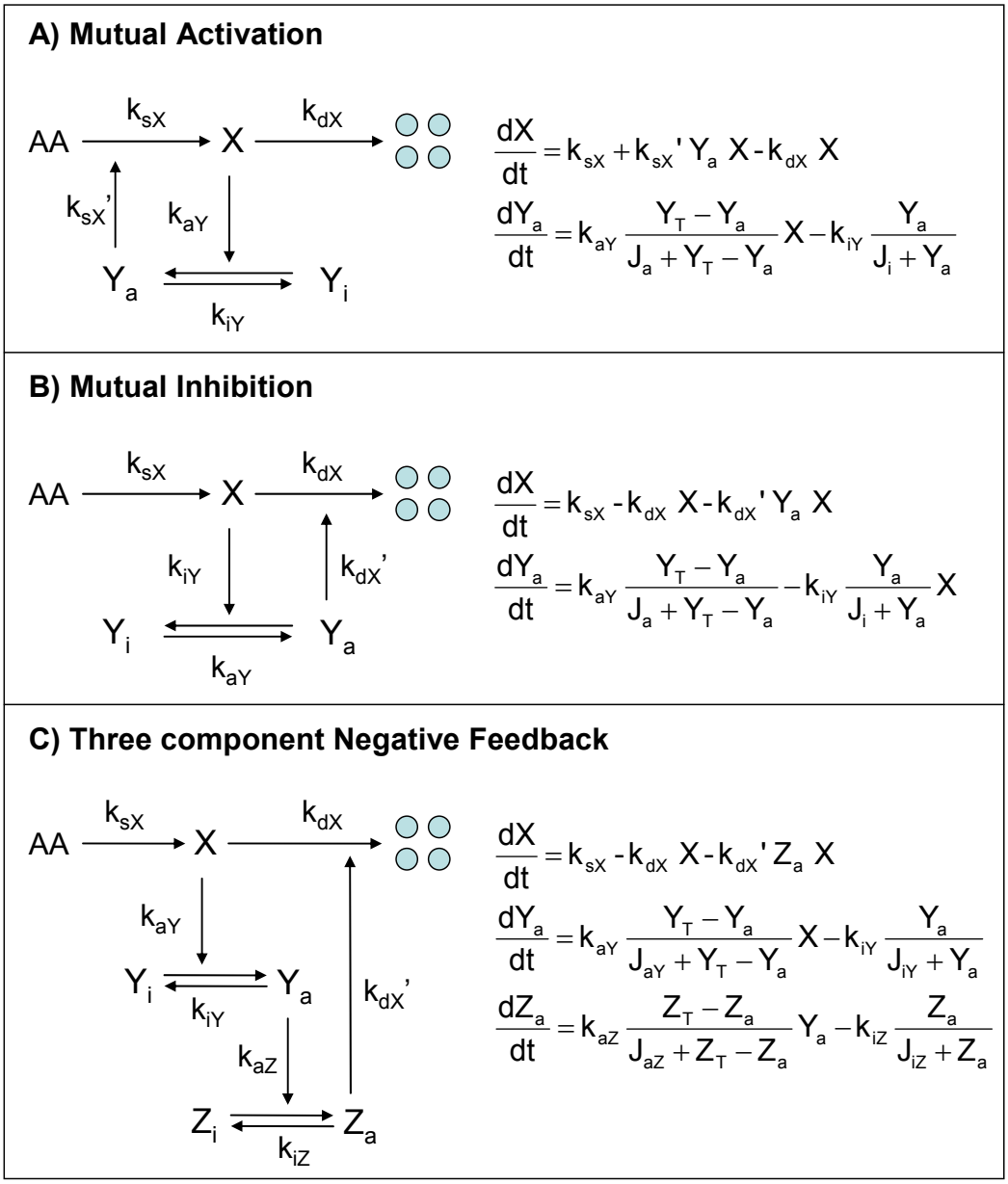


**Figure 13: Wiring diagrams and corresponding ODEs for three different basic regulatory motifs. A) Mutual activation, X activates Y and Y promotes the synthesis of X. B) Mutual inhibition, X inactivates Y and Y promotes X degradation. C) Three component negative feedback loop, X activates Y, Y activates Z and Z promotes the degradation of X.**

The feedforward loop motif is also common in biology and increases the system's sensitivity to an input signal. The minimum number of components in a feedforward loop (FFL) is three, and these components are linked through three interactions. For instance, a protein X interacts with protein Y, and both X and Y interact with protein Z. This sort of molecular system can have eight different structures, because each of these interactions can be either activatory or inhibitory (see Figure 14). Four of these structures are termed coherent FFL when Z is subjected to signals with the same sign; the other four structures are termed incoherent FFL because Z is subjected to signals of opposite sign. As a result, coherent FFL have a distinct effect than incoherent FFL. Coherent FFL have noise filtering properties so that Z is very sensitive to X. On the other hand, incoherent FFL have a transient signal response so that Z initially receives a signal from X which is then turned off by Y.

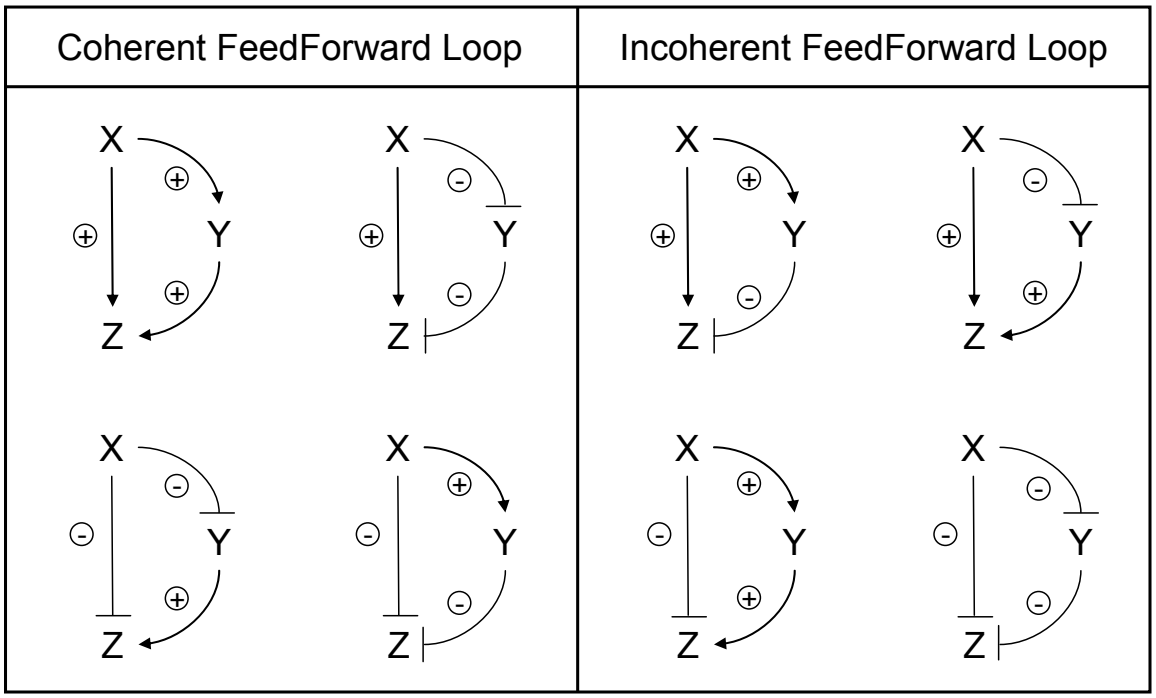


**Figure 14: Wiring diagram representing the eight different structural types that a three component feedforward loop might exhibit.**

## 5. Theoretical Descriptions of Mitotic Exit

### a. Queralt's model

Queralt's model (QM), published in 2006, summarises the molecular network and dynamics responsible for cell cycle progression from metaphase to G1 in budding yeast (Queralt et al., 2006). The aim of QM was to provide a system's perspective on the mitotic exit phenomenon, and to explain the phenotypes observed in a number of specific experimental (i.e. mutant) situations.

In this model, the molecular network is converted into a system of ODEs using the basic principles of biochemical reaction kinetics. Some components are present with a constant concentration and thus algebraic equations for the conservation of mass are also included. The number of equations (algebraic or differential) is equal to the number of components present in the wiring diagram. The rate of change of a particular component depends on the number of biochemical processes that the component is involved in. Since absolute protein levels have not been measured experimentally, all variables are dimensionless and refer instead to relative intracellular protein concentrations. QM's wiring diagram is depicted in Figure 15.

Biochemical reactions such as reversible phosphorylation/dephosphorylation (of Cdh1, Net1, Cdc15 and Cdc5) and activation/inactivation (of Tem1) follow Michaelis-Menten kinetics. Reactions such as synthesis, degradation, complex formation and dissociation are described by the law of mass action. Synthesis rates are of zero-order, unregulated degradation and dissociations are of first order, while associations and regulated degradations are of second order. All kinetic parameters have a dimension of $min^{-1}$, with the exception of the Michaelis constants and total concentrations which are dimensionless.

The system of ODEs does not include CDK1 or APC because the level of these components remains constant throughout the cell cycle. Their activity is fully regulated by the binding of their activatory subunits, and thus only these are considered in the equations (e.g. Clb2, Cdc20 and Cdh1).

Some proteins are considered to be present in the system with a constant total concentration. These include Cdh1, Net1, Cdc14, Tem1 and Cdc15. Other proteins do not fit into this description; instead their total concentration varies with time. These include Clb2, Cdc20, Securin (Pds1), Separase (Esp1) and Cdc5.

MEN activation corresponds to the association of the active forms of Tem1 and Cdc15. Because this association is reversible, MEN is inactivated by the dissociation of the complex, which can be triggered by the inactivation of either Tem1 or Cdc15.

Net1 phosphorylation and Net1 association with Cdc14 are core reactions in the system. In QM, there are two equations for unphosphorylated Net1; one for free Net1 and one for Net1 bound to Cdc14. It is considered that the phosphorylated form of Net1 is unable to bind to Cdc14 (phosphorylated Net1:Cdc14 complexes should dissociate quickly), and thus only one equation is necessary to describe this species.

Net1 is present in a larger amount than Cdc14 (its concentration is twice as much). This assumption is justified by the idea that noise in gene expression could bring fragility to a system where the stoichiometric inhibitor (such as Net1) would be at the same level of the molecule it is inhibiting (such a Cdc14). In this way, it is likely that the inhibitor would be in excess, and thus, provide the system with increased robustness to fluctuations in gene expression and protein levels. This assumption was experimentally verified few years after the QM was published (Kaizu et al., 2010).

QM is fully described in the paper (Queralt et al., 2006), including the system of ODEs and corresponding parameter set.

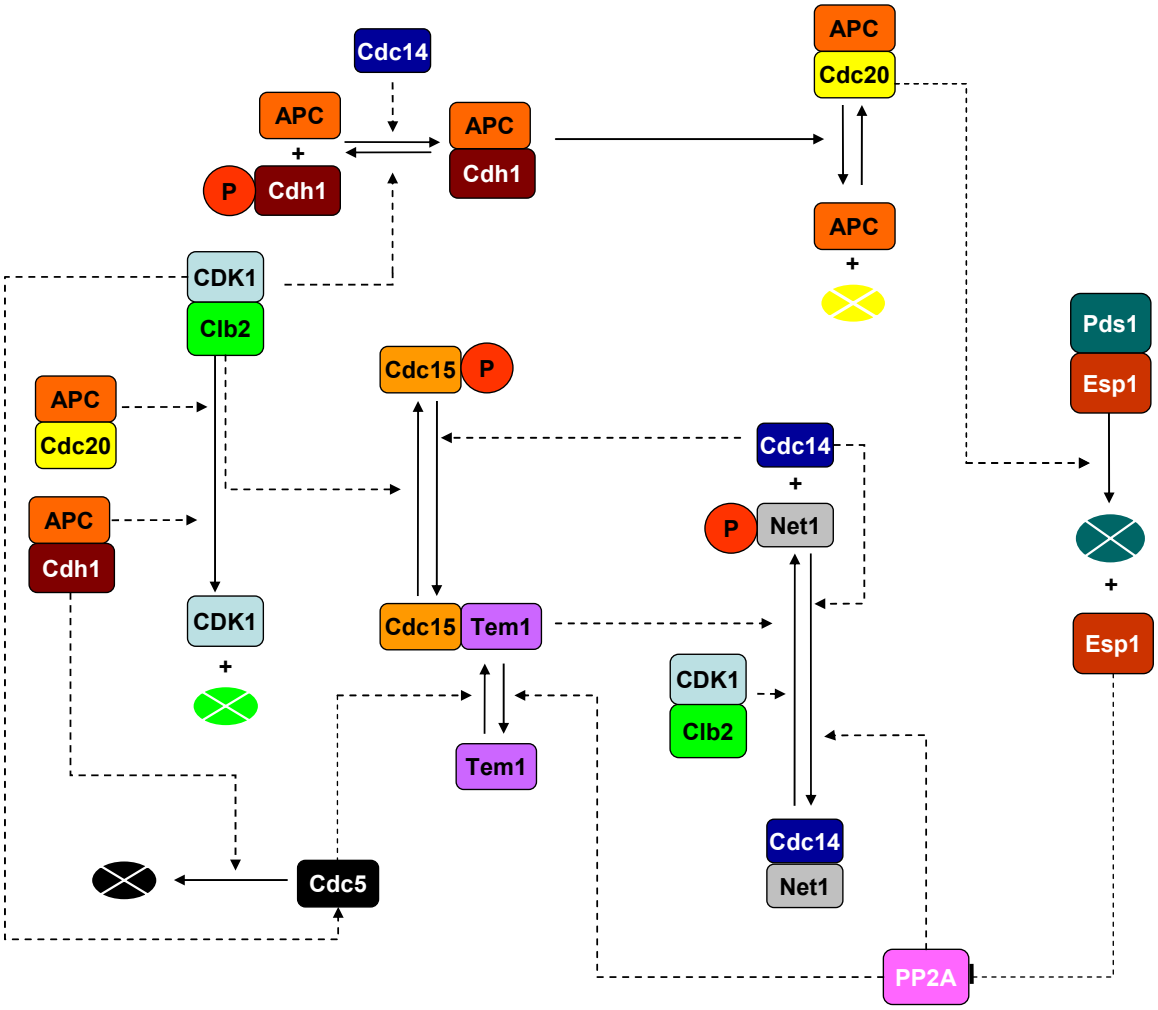


**Figure 15: Wiring diagram representing the molecular network used to build the Queralt's model. Solid arrows leading to or from a component indicate biochemical reactions (e.g. phosphorylation/dephosphorylation, degradation) while dashed arrows indicate the regulation of these biochemical reactions by other components. To simplify the diagram, all unregulated protein synthesis is not represented in this diagram. Components which are synthesised from amino acids are Clb2, Cdc20, Pds1, Esp1 and Cdc5. All other components are present with constant concentrations.**

### *b. New Mathematical Model*

In this thesis, QM was used as the basis for modelling a more comprehensive understanding of the mitotic exit phenomenon. Each chapter of this thesis describes how different mutants can be described by updating the model, following the incorporation of new components and altered assumptions. At the end of this work, a finalised model is presented, which is no longer restricted to the time window between metaphase and G1, but includes all of the phases of budding yeast cell cycle. From Chapter I to Chapter IV, there are four different sets of ODEs; each of which corresponds to a different version of the model. Therefore, each set of ODEs was written in XPPAUT and can be found in Appendix 1.

As all the modifications made to the QM are thoroughly described in the first four chapters of this thesis; this section outlines only the main considerations of the model's design.

The system of ODEs was written using the same assumptions made for QM. Transcription factors (e.g. Swi5, MBF) were incorporated into the model with the assumption that they are present in the cell at a constant total concentration, and that their activity varies according to a Michaelis-Menten kinetics. Endogenous Sic1 has a regulated synthesis term dependent on the transcription factor Swi5 (first order reaction), and different degradation terms depending on which cyclin-CDK1 complex mediates its degradation (second order reactions). Sic1 also forms inactive trimers with Clb2/CDK1 and Clb5/CDK1 (Trim2 and Trim5, respectively).

From MV3 onwards, a distinction between nuclear free Cdc14 and cytoplasmic free Cdc14 was introduced. Since there is a difference in volume between these two cellular compartments, normalisation with volume was required.

Conservation of number of molecules:

$$Cdc14T = Cdc14_{nuc} + RENT + Cdc14_{cyt} \quad (13)$$

where, Cdc14T is the total number of Cdc14 molecules in the cell (constant during the cell cycle), and RENT is the notation for the complex Net1-Cdc14 (RENT – REgulator of Nucleolar silencing and Telophase) .

Let us divide Equation (13) by the total volume of the nucleus ($V_{nuc}$):

$$\frac{Cdc14T}{V_{nuc}} = \frac{Cdc14_{nuc}}{V_{nuc}} + \frac{RENT}{V_{nuc}} + \frac{Cdc14_{cyt}}{V_{nuc}}$$

$$[Cdc14T]_{nuc} = [Cdc14_{nuc}] + [RENT] + \frac{Cdc14_{cyt}}{V_{nuc}}$$

$$\frac{Cdc14_{cyt}}{V_{nuc}} = [Cdc14T]_{nuc} - [Cdc14_{nuc}] - [RENT] \quad (14)$$

where $[Cdc14T]_{nuc}$ represents the ratio between the total number of Cdc14 molecules in the cell and the nuclear volume of the cell. $[Cdc14_{nuc}]$ and [RENT] are simply the nuclear concentrations of Cdc14 and RENT, respectively.

Let us divide Equation (14) by the total volume of the cytoplasm ($V_{cyt}$):

$$\frac{Cdc14_{cyt}}{V_{nuc}} \times \frac{1}{V_{cyt}} = ([Cdc14T]_{nuc} - [Cdc14_{nuc}] - [RENT]) \times \frac{1}{V_{cyt}}$$

$$\frac{Cdc14_{cyt}}{V_{cyt}} \times \frac{V_{cyt}}{V_{nuc}} = [Cdc14T]_{nuc} - [Cdc14_{nuc}] - [RENT]$$

$$[Cdc14_{cyt}]\frac{V_{cyt}}{V_{nuc}} = [Cdc14T]_{nuc} - [Cdc14_{nuc}] - [RENT] \quad (15)$$

where $[Cdc14_{cyt}]$ is the concentration of Cdc14 present in the cytoplasm.

As a result, from MV3 onwards, $Cdc14_{cyt}$ plotted in all the figures, represents the cytoplasmic concentration normalised to the nuclear volume, as shown in equation (15).

This normalisation also affects the rate constants dependent on cytoplasmic Cdc14, as is the case for Cdh1 and Swi5 dephosphorylation. Therefore, $k_{dcdh}$' and $k_{dswi}$' implicitly include the ratio $V_{nuc}/V_{cyt}$.

Despite the fact that a different set of ODEs was used to run simulations in each chapter, the procedure used to simulate mutant situations was overall unchanged. This procedure can be summarised as follows:

- Gene deletions were simulated by setting the synthesis rate of the particular protein to zero, except in the case of Clb5, where both the regulated and unregulated rates were halved, because of the back-up S phase cyclin (Clb6).

*cdc20Δ*: $k_{s20}' = k_{s20} = 0$

*sic1Δ*: $k_{ssic}' = k_{ssic} = 0$

*pds1Δ*: $k_{spds}' = k_{spds} = 0$ and $Pds1_T = 0$, $Esp1_b = 0$ initial conditions

*cdc5Δ*: $k_{spolo} = k_{spolo}' = 0$ and $Polo_T = 0$, Polo=0 initial conditions

- In the case of proteins with a constant level (no synthesis or degradation), the rate constants for their activation step were set to zero to simulate gene deletions.

*cdh1Δ*: $k_{dcdh} = k_{dcdh}' = 0$

*cdc15Δ*: $k_{ac15} = k_{ac15}' = 0$

- Since Bub2 is not represented in our model, *bub2Δ* was simulated by setting the Tem1 inhibition terms to zero.

*bub2Δ*: $k_{item}=0$, $k_{item}'=0$

- Proteins with destruction box deletions (or mutations) were simulated by setting the APC-dependent destruction rate constants to zero.

*PDS1-mdb*: $k_{dpds}' =0$

*CDC5-nd*: $k_{dpolo}' = 0$

*CLB5-nd*: $k_{dclb5}' = 0$

- The incorporation of a non-degradable Clb2 protein (lacking D- and KEN-boxes) was modelled as the parameter Clb2nd. Clb2nd can bind to Sic1 to form an inactive trimer. The sum of degradable and non-degradable Clb2 is equal to the free plus the inactive Sic1-bound Clb2 (Trim2):

Clb2T + Clb2nd = Clb2 + Trim2

- Separase overexpression was simulated by a 10-fold increase in the rate of separase synthesis ($k_{sesp}=0.01\ min^{-1}$).

- Two types of Sic1 overexpression were simulated. For the simulation of Thornton and Toczyski's experiments (2003a), in which 10 copies of the *Sic1* gene were integrated at the *TRP1* locus, Swi5-dependent synthesis was increased 10-fold. For the simulation of Lu and Cross experiments (2009b), in which non-degradable Sic1 was expressed by the Gal promoter, the unregulated

Sic1 synthesis term was increased 5-fold, while the CDK1-dependent rate constants were set to zero and the background degradation rate was halved.

- TEV protease is used in some experimental situations. This protease allows cells to cleave the SCC1 subunit of an engineered cohesin which possesses a TEV site (Uhlmann et al., 2000). As a consequence, this protease can mimic the proteolytic activity of Esp1. In the model, the TEV protease was not incorporated through the addition of an extra equation; instead, the separase differential equation ($Esp1_T$) was used to describe TEV overexpression experiments (besides describing separase experiments). The parameters describing PP2A inhibition ($k_i$) and securin binding ($I_{apds}$) were set to zero, because TEV does not share the non-proteolytic function of separase, and does not bind to securin. The initial conditions for $Esp1_T$ and $Esp1_b$ were also set to zero, because TEV is not present in the system before its overexpression begins at the start of the simulation.

## *6. Model Robustness to Parameter Perturbation*

Biochemical regulatory networks exhibit different levels of behavioural robustness, depending on the variations to which they are exposed. For instance, biological systems tend to be robust when exposed to frequently occurring variations, but highly fragile when confronted with rare perturbations (Morohashi et al., 2002).

The robustness of a biochemical regulatory network is determined by its system's proprieties. Therefore, a mathematical model of a biological system should be as robust to variation as the biological system it describes. Analysing a model's robustness provides an understanding of how the biological system can maintain its function in the

face of perturbations. In this thesis, a robustness analysis was performed on the final model, MV4 (see equations in Appendix 1d), with the aim of identifying the features most responsible for the behavioural robustness of the system.

Firstly, the model was subjected to a global parameter perturbation, in order to estimate the range in which all of the parameters can be varied without losing the observed phenotype (control phenotype). The study was then extended from this estimate, so to identify the parameter subsets for which the model is most sensitive to fluctuation.

The method adopted was the same as that used by (Mirsky et al., 2009) to analyse a model of the circadian clock. This method is based on a Monte Carlo simulation, the structure of which is described below:

1. Define a base for possible inputs (e.g. nominal parameter set);
2. Randomly generate new inputs from a probability distribution over the original base;
3. Perform a deterministic computation of the inputs (e.g. use the system of ODEs to compute new results)
4. Interpret the results of the computation.

To perform a large set of simulations with different parameter sets, and to compute the results, a MATLAB-based code was developed for the final model, MV4. This code can be found in Appendix 5e. All of the MATLAB files used in the robustness analysis can also be found in Appendix 5.

### *a. Generation of new parameter sets*

To generate a new parameter set from the nominal set, each new parameter value was randomly drawn from a normal probability distribution with a mean equal to the

nominal parameter value (see Equation (13)). The standard deviation (SD) of this normal probability distribution determines the variation allowed between the nominal value and the new value. To allow the same proportional variation for all parameters in the set, it was established that the SD would be determined from a percentage of the nominal value (x). For each chosen value of x, 10,000 parameter sets were generated.

$$new\_p = (nom\_p + randn * SD) \; ; \; SD = x * nom\_p / 100 \qquad (16)$$

where:

new_p – new parameter value

nom_p – nominal parameter value

randn – random number drawn from a standard normal distribution (mean=0, SD=1)

x – percentage of variation allowed

The nominal parameter set was implemented in the MATLAB file 'ALLParameters.m' (Appendix 5a). This file creates a data file containing all nominal parameter values, and thus, by modifying, 'ALLParameters.m', one can change the nominal parameter set.

The file that generates 10,000 different parameter sets from a single nominal set is 'ParameterDistributions.m'. This file reads the data file created by 'ALLParameters.m' and applies Equation (16) to each parameter value in the nominal set, which produces a new parameter set (Appendix 5b). This process is repeated 10,000 times to produce 10,000 new parameter sets. In the process of creating new parameter sets, two important factors were taken into consideration: (i) for large values of SD, there was a small chance that the newly created parameters could be negative. Since this is unrealistic, 'ParameterDistributions.m' prevents it from happening by replacing any negative value by zero; (ii) to avoid numerical errors, Michaelis constants should never

be equal to zero. For this reason, 'ParameterDistributions.m' replaces all null-valued Michaelis constants with a value very close to zero (0.00001).

### *b. Generation of new initial conditions (IC)*

New parameter sets need new initial conditions. This is especially true if the total concentrations of proteins have been changed, because, in this case, the mass balance equations have to be satisfied for the new total concentrations. For this reason, a new set of initial conditions was created for each parameter set.

The initial conditions of our model were generated from a Cdc20 block (cdc20Δ) situation, which is a steady-state condition. To generate new initial conditions, steady-state values were obtained by running a simulation for each of the newly generated parameter sets in the absence of Cdc20 for 1000 min. The last concentration values were recorded in a new data file.

The MATLAB file responsible for this computation is 'InitialConditions.m' (Appendix 5d). For this to run a Cdc20 block simulation, parameters sets for a cdc20Δ mutation are required (i.e. $k_{s20} = 0$ and $k_{s20}' = 0$). These parameter sets are generated by the file 'MB_set.m' (Appendix 5c).

### *c. How the model tracks viability*

Once the new parameter sets and corresponding initial conditions were created, simulations were run for 600min, to test whether the results retained a number of essential features of the control simulation. To aid this search, two generic substrates, $X_S$ and $X_M$, are used to represent proteins that are typically active in S or M phases. $X_S$ represents any protein that must be activated in S phase and remain active during M

phase ($X_S$ is any substrate of Clb2, Clb5 and Cdc14). $X_M$ represents any protein that must be activated only in M phase ($X_M$ is any substrate of Clb2 and Cdc14). The notations '$X_S$-P' and '$X_M$-P' indicate the phosphorylated forms of the generic substrates $X_S$ and $X_M$, respectively.

For a simulation to pass the viability test, all the following essential features must be retained:

1) The simulation shows oscillations in Clb2. The period of these oscillations must be constant with a 5% relative error.

2) The period cannot be smaller than 30min or larger than 100min.

3) The value of Esp1 must be larger than 0.1 when Clb2 curve reaches its maximum.

4) The generic substrate $X_S$-P must decrease below 0.4 (mark of mitotic exit) before the generic substrate $X_M$-P rises above 0.6 (mark of mitotic entry). The algebraic equations for $X_S$-P and $X_M$-P are the following:

$$X_S - P = \frac{[Clb2] + [Clb5]}{[Clb2] + [Clb5] + K([Cdc14_{cyt}] + 0.2 \times [Cdc14_{nuc}])} X_T \quad (14)$$

$$X_M - P = \frac{[Clb2]}{[Clb2] + K([Cdc14_{cyt}] + 0.2 \times [Cdc14_{nuc}])} X_T \quad (15)$$

Where:

$$K = \frac{\text{dephosphorylation rate constant}}{\text{phosphorylation rate constant}} = 2 \quad (16)$$

$X_T = 1$

$Cdc14_{cyt}$ – Cdc14 that is free in the cytoplasm

$Cdc14_{nuc}$ – Cdc14 that is free in the nucleus

The Net1-free form of nuclear Cdc14 makes less contact with the substrates $X_S$ and $X_M$, and thus its contribution is multiplied by a factor.

These essential features are more thoroughly described within the biological context of this study in Chapter V, where they are referred to as the 'viability criteria'.

The MATLAB file responsible for this computation is 'MitoticExit.m' (Appendix 5f). This file uses the function 'checkviability.m' to decide whether each simulation satisfied the viability criteria, and only saves simulations that do so. (Appendix 5g)

### *d. Calculate Period of Oscillations*

A very important feature of the simulations is whether they exhibit oscillatory behaviour; and in particular, how the period of these oscillations fluctuates between simulations. For this reason, a separate file was created to calculate and store the period values of all simulations that exhibited oscillatory behaviour with a constant period. This file was named 'Calc_Period_Ampl.m' (Appendix 5h).

### *e. Mitotic Exit Models depleted of Regulatory Layers*

The robustness analysis was extended beyond the final mitotic exit model (MV4), to compare robustness across different conditions. Two additional models were created by depriving MV4 of two different layers of protein regulation: regulated transcription and regulated degradation. The model deprived of regulated transcription is conveniently referred to as No Regulated Transcription model (NRT model), while, the model deprived of regulated degradation is called the No Regulated Degradation model (NRD model).

Each of these models has a nominal parameter set, contained in the MATLAB files 'Parameters_noTransc.m' and 'Parameters_noDeg.m', for the NRT and NRD models, respectively (Appendixes 6i and 6j). The robustness analysis was performed on these

models by repeating the procedure applied to the original model (MV4), as described above.

To remove transcriptional regulation from the model, all parameters referring to regulated synthesis (through transcription factors) were set to zero. In addition, the non-regulated synthesis rates of Cdc20 and Cdc5 were increased, in order to prevent cell cycle blocks in the absence of these essential cell cycle regulators.

Likewise, to remove proteolytic regulation from MV4, all parameters referring to regulated protein degradation were set to zero, and, in three cases (Clb2, Sic1 and Pds1), non-regulated parameter values were increased. This was done to prevent the rise of these proteins to unrealistic levels during the cell cycle.

The nominal parameter sets for the NRT and NRD models can be found in Table 1. The highlighted boxes indicate parameter changes from the nominal set.

**Table 1: Nominal Parameters for the Wild-type, NRT and NRD models**

| Parameter | Parameter Values | | |
|---|---|---|---|
| | Wild-type model | NRT model | NRD model |
| Clb2nd | 0 | 0 | 0 |
| ksclb2 | 0.015 | 0.015 | 0.015 |
| ksclb2' | 0.005 | 0 | 0.005 |
| kdclb2 | 0.02 | 0.02 | 0.05 |
| kdclb2' | 0.1 | 0.1 | 0 |
| kdclb2'' | 0.4 | 0.4 | 0 |
| kasic2 | 40 | 40 | 40 |
| kdisic2 | 0.1 | 0.1 | 0.1 |
| kasic5 | 10 | 10 | 10 |
| kdsic5 | 0.1 | 0.1 | 0.1 |
| kssic | 0.004 | 0.004 | 0.004 |
| kssic' | 0.2 | 0 | 0.2 |
| kdsic | 0.04 | 0.04 | 0.2 |
| kdsic' | 2 | 2 | 0 |
| kdsic'' | 2 | 2 | 0 |
| kdsic''' | 1.5 | 1.5 | 0 |
| ksmcm | 0.01 | 0.01 | 0.01 |
| ksmcm' | 1 | 1 | 1 |
| kdmcm | 0.25 | 0.25 | 0.25 |
| Jmcm | 0.01 | 0.01 | 0.01 |
| ksclb5 | 0.002 | 0.002 | 0.002 |
| ksclb5' | 0.01 | 0 | 0.01 |
| kdclb5 | 0.01 | 0.01 | 0.01 |
| kdclb5' | 1 | 1 | 0 |
| kscln | 0.01 | 0.01 | 0.01 |
| kscln' | 0.1 | 0 | 0.1 |
| kdcln | 0.25 | 0.25 | 0.25 |
| ks20 | 0.001 | 0.01 | 0.001 |
| ks20' | 0.05 | 0 | 0.05 |
| kd20 | 0.1 | 0.1 | 0.1 |
| kd20' | 1 | 1 | 0 |
| kdcdh | 0.03 | 0.03 | 0.03 |
| kdcdh' | 0.3 | 0.3 | 0.3 |
| kpcdh | 0.001 | 0.001 | 0.001 |
| kpcdh' | 0.04 | 0.04 | 0.04 |
| kpcdh'' | 0.75 | 0.75 | 0.75 |
| Jcdh | 0.01 | 0.01 | 0.01 |
| kaswi | 0.2 | 0.2 | 0.2 |
| kaswi' | 1 | 1 | 1 |
| Jswi | 0.1 | 0.1 | 0.1 |
| kiswi | 0.01 | 0.01 | 0.01 |
| kiswi' | 0.5 | 0.5 | 0.5 |
| kiswi'' | 0.75 | 0.75 | 0.75 |
| Swi5t | 1 | 1 | 1 |
| kspds | 0.006 | 0.006 | 0.006 |

**Table 1: Nominal Parameters for the Wild-type, NRT and NRD models (continuation).**

| Parameter | Parameter Values | | |
|---|---|---|---|
| | Wild-type model | NRT model | NRD model |
| kdpds | 0.01 | 0.01 | 0.1 |
| kdpds’ | 2 | 2 | 0 |
| ksesp | 0.001 | 0.001 | 0.001 |
| kdesp | 0.004 | 0.004 | 0.004 |
| lapds | 500 | 500 | 500 |
| ldpds | 1 | 1 | 1 |
| Net1T | 1 | 1 | 1 |
| kd’ | 0.1 | 0.1 | 0.1 |
| kd | 0.45 | 0.45 | 0.45 |
| kp | 0 | 0 | 0 |
| kp’ | 2 | 2 | 2 |
| kp’’ | 0.2 | 0.2 | 0.2 |
| kp’’’ | 3 | 3 | 3 |
| Jnet | 0.05 | 0.05 | 0.05 |
| Cdc14T | 0.5 | 0.5 | 0.5 |
| lanet | 500 | 500 | 500 |
| ldnet | 1 | 1 | 1 |
| kexp | 0.01 | 0.01 | 0.01 |
| kexp’ | 20 | 20 | 20 |
| kexp’’ | 0 | 0 | 0 |
| kimp | 1 | 1 | 1 |
| kspolo | 0.001 | 0.05 | 0.001 |
| kspolo’ | 0.05 | 0 | 0.05 |
| kdpolo | 0.05 | 0.05 | 0.05 |
| kdpolo’ | 0.5 | 0.5 | 0 |
| kdpolo’’ | 0 | 0 | 0 |
| kapolo | 0 | 0 | 0 |
| kapolo’ | 1 | 1 | 1 |
| kipolo | 0.1 | 0.1 | 0.1 |
| Jpolo | 0.1 | 0.1 | 0.1 |
| katem | 0 | 0 | 0 |
| katem’ | 0.6 | 0.6 | 0.6 |
| kitem | 0.1 | 0.1 | 0.1 |
| kitem’ | 1 | 1 | 1 |
| kitem’’ | 20 | 20 | 20 |
| Jtem1 | 0.005 | 0.005 | 0.005 |
| kac15 | 0.03 | 0.03 | 0.03 |
| kac15’ | 0 | 0 | 0 |
| kac15’’ | 0.5 | 0.5 | 0.5 |
| kic15 | 0.03 | 0.03 | 0.03 |
| kic15’ | 0.2 | 0.2 | 0.2 |
| Jcdc15 | 1 | 1 | 1 |
| lamen | 100 | 100 | 100 |
| ldmen | 0.1 | 0.1 | 0.1 |
| kambf | 0.1 | 0.1 | 0.1 |
| kimbf | 0 | 0 | 0 |

**Table 1: Nominal Parameters for the Wild-type, NRT and NRD models (continuation).**

| Parameter | Parameter Values | | |
|---|---|---|---|
| | Wild-type model | NRT model | NRD model |
| kimbf' | 0.5 | 0.5 | 0.5 |
| kimbf'' | 0.5 | 0.5 | 0.5 |
| Jmbf | 0.01 | 0.01 | 0.01 |
| PPT | 1 | 1 | 1 |
| kpp | 0.1 | 0.1 | 0.1 |
| ki | 40 | 40 | 40 |
| kdcdh'' | 0 | 0 | 0 |
| kaswi'' | 0 | 0 | 0 |
| Cdh1T | 1 | 1 | 1 |
| Tem1T | 1 | 1 | 1 |
| Cdc15T | 1 | 1 | 1 |
| MBFT | 1 | 1 | 1 |

# Chapter I – The role of Separase in Mitotic Exit

This Chapter describes the implementation of the first improvements to QM. These modifications enable the model to address the role of separase in mitotic exit. The new version of the model is referred to as MV1 (Model Version 1).

It is well established that separase is required for sister chromatid separation in anaphase, and for Cdc14 release. However, the magnitude of its contribution to mitotic exit is still a matter of debate. QM assumes that separase influences mitotic exit through both the FEAR and MEN networks, via the separase-dependent downregulation of $PP2A^{CDC55}$. Recently, Lu and Cross (Lu and Cross, 2009a) have questioned this idea, arguing that this non-proteolytic function of separase is not required for cells to exit mitosis. $PP2A^{CDC55}$ is a component of the FEAR network, but as outlined in the introduction, FEAR is not essential for mitotic exit, as it only promotes a transient release of Cdc14. Thus, on the basis of its influence on FEAR, $PP2A^{CDC55}$ cannot be considered fundamental to mitotic exit. MEN, on the other hand, promotes a complete and sustained release of Cdc14, and is considered essential for mitotic exit. Therefore, if MEN can be activated independently of $PP2A^{CDC55}$ downregulation, it would appear that the non-proteolytic function of separase is not required for mitotic exit. Consistent with this, the MEN component Tem1 is activated when the spindle elongates, a direct consequence of separase proteolytic activity (Bardin et al., 2000).

In light of these results, we modified QM so that Esp1 promotes Tem1 activity independently of $PP2A^{CDC55}$ (henceforth referred to as PP2A) (compare Figure 15 and Figure I - 1). The idea was to mimic Tem1 activation when Tem1 co-localises with its activator Lte1 at the bud only after anaphase. In MV1, Esp1 directly inhibits the inhibition of Tem1, since Tem1 and Lte1 co-localization can only occur after spindle elongation

(see Tem1 equation in Appendix 1a). To confirm that this modification does not affect the results already achieved by QM, MV1 was tested against all mutant situations studied with QM.

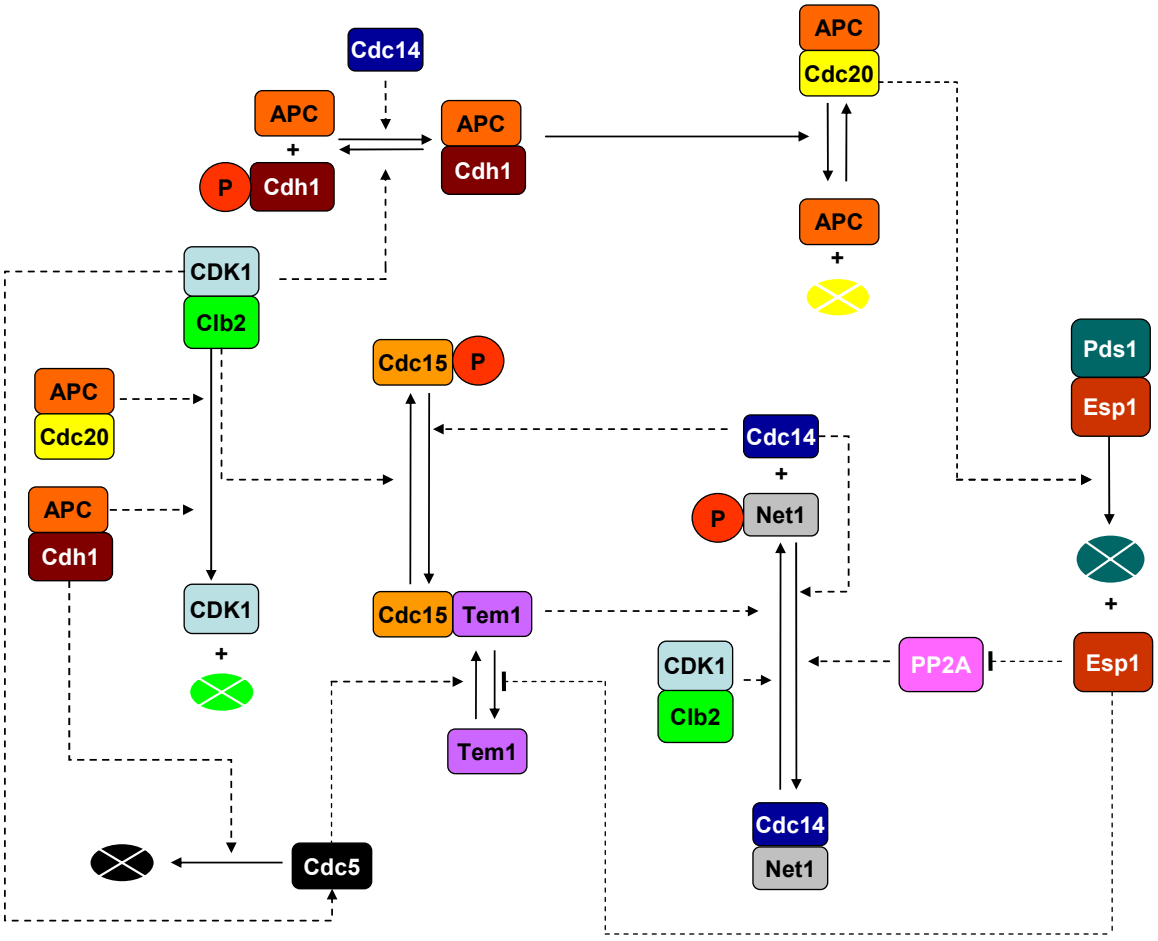


**Figure I - 1: Wiring Diagram of the molecular network present in MV1. QM was modified so that Esp1 promotes Tem1 activity independently of PP2A.**

## *1. Cdc20 block and release experiment*

A common experimental procedure is to arrest cells in metaphase through the depletion of Cdc20 (Sullivan and Uhlmann, 2003). This is achieved by using the methionine-repressible MET3-CDC20 construct and growing cells in a medium rich with methionine. Once all cells are blocked in metaphase, they can be released by switching them to a medium without methionine. In this way, cells are synchronised and can

proceed to anaphase. This situation is designated as a ‘Cdc20 block and release’, since cells are blocked by Cdc20 depletion but can exit mitosis once Cdc20 is re-synthesised ($Cdc20^{b/r}$). This situation is simulated in Figure I - 2B, and will be used as a control for efficient mitotic exit.

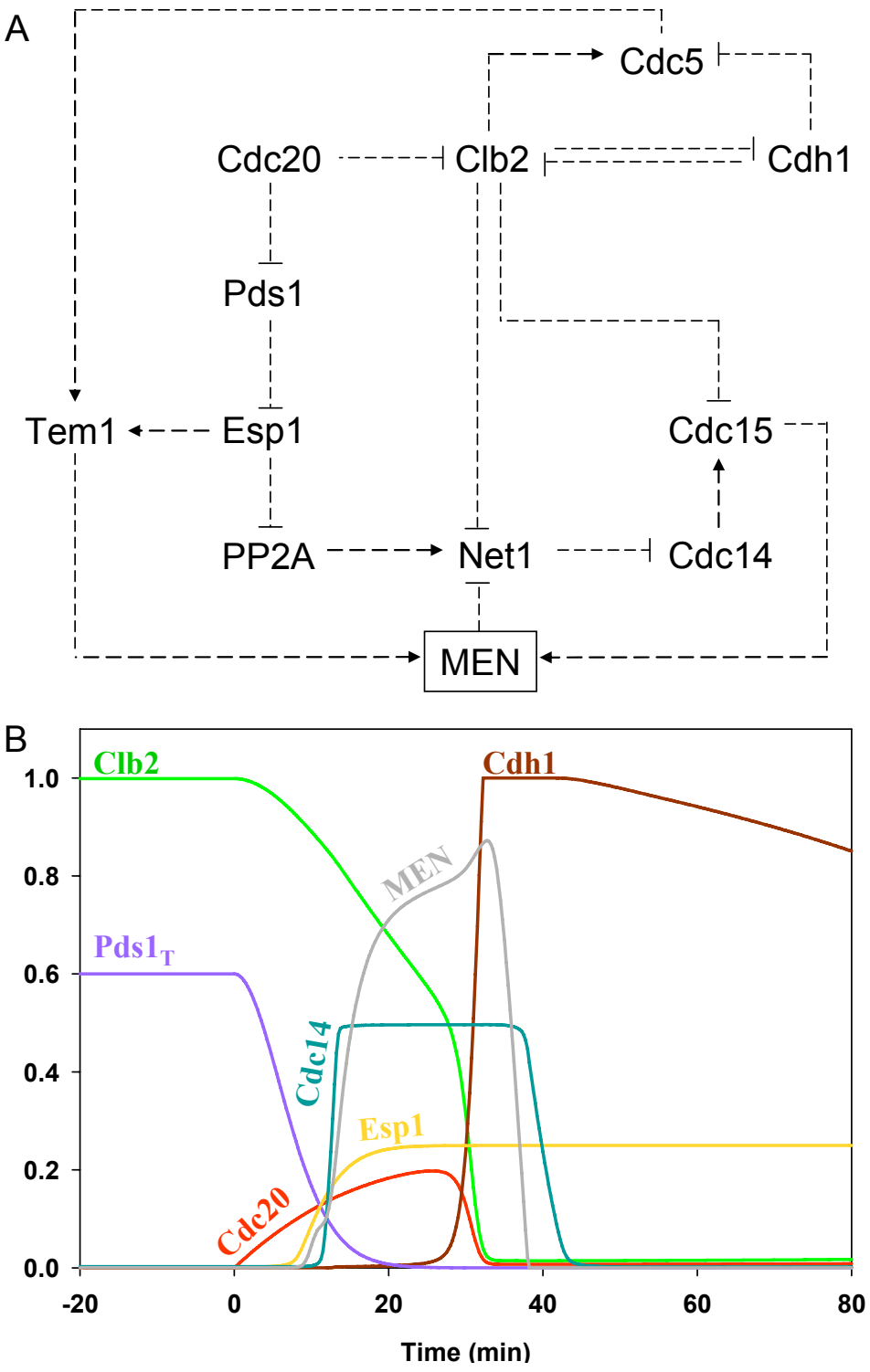


**Figure I - 2: Main features of the mitotic exit model for budding yeast. A) Simplified wiring diagram showing the main biochemical and genetic interactions present in the model. Pointed arrows represent protein activation and blunt arrows represent protein inhibition. B) Numerical simulation of mitotic exit in a Cdc20 block and release situation. The model was simulated for 20min (until t=0) without Cdc20 synthesis ($k_{s20}$=0) which defines a stable steady-state corresponding to metaphase block. At t=0, Cdc20 synthesis is induced ($k_{s20}$ = 0.015min$^{-1}$) and the simulation is run for 80 minutes. Cells exit mitosis 30min after Cdc20 release.**

## 2. MEN inactive

MEN is known to be crucial for mitotic exit, and, if one of its components is inactivated, cells are blocked in telophase with reduced CDK1 activity (Yeong et al., 2000). Cdc14 release in these cells is transient and observed only in early anaphase (Stegmeier et al., 2002). To faithfully reproduce this phenotype, the model has to balance the rate of Net1 phosphorylation by Clb2 with the rate of Net1 dephosphorylation by PP2A. This is achieved by assuming that high Clb2 activity is required for Clb2-mediated Net1 phosphorylation, and that Cdc20-mediated degradation of Clb2 restricts it. On the other hand, Cdc20-mediated degradation of Pds1 activates Esp1, which inhibits PP2A through its non-proteolytic function and thereby increases Net1 phosphorylation. Pds1 is degraded faster than Clb2, promoting Esp1 activation and PP2A inhibition. Clb2 degradation is slower, and thus Clb2 levels are high enough to drive Cdc14 release. However, when Clb2 reaches its steady-state value, it is unable to keep Net1 phosphorylated, and thus Cdc14 is re-sequestered into the nucleolus (Figure I - 3). In principle, Cdc20's regulation of its substrates resembles an incoherent feedforward loop, whereby Cdc20 promotes Net1 phosphorylation through Pds1 degradation and then inhibits it through Clb2 degradation. Such network motifs produce a transient response, and this is how MV1 explains why this mutant goes from a metaphase block to a telophase block (separase release marks anaphase).

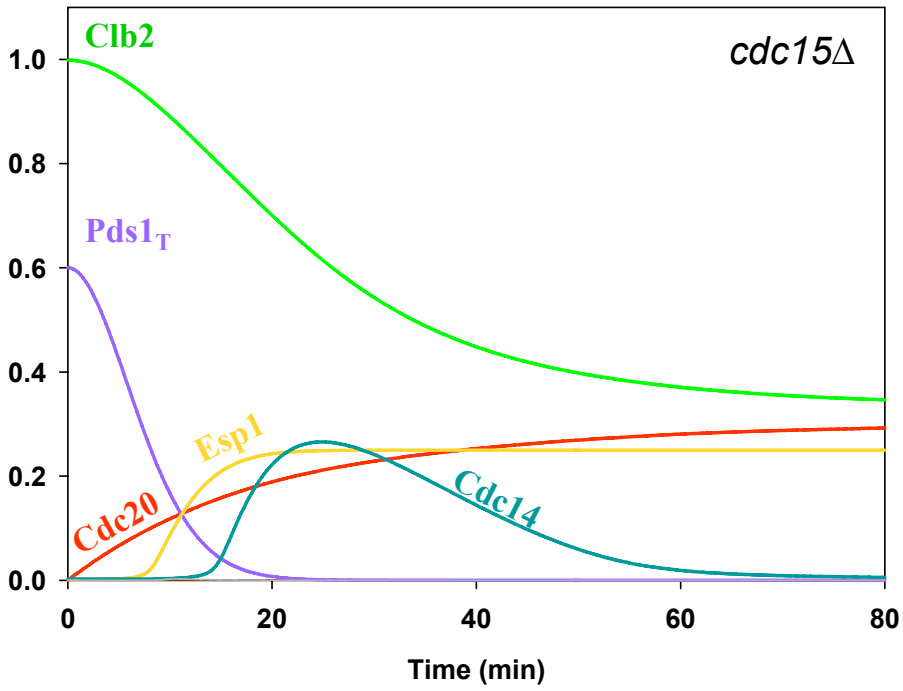


**Figure I - 3: Cdc20 block and release in the absence of MEN (Cdc15) activity. Simulations were done like on Figure I - 2B except that the Cdc15 activation rate constants were set to zero ($k_{ac15} = k_{ac15}' = 0$).**

## 3. *Activation of Separase in a Cdc20 block condition*

In a Cdc20 block condition, cells remain arrested in metaphase because Pds1 cannot be degraded and thus Esp1 remains inhibited. It has been hypothesised that under these conditions, an activation of separase could overcome this mitotic arrest.

It has been shown by (Shirayama et al., 1999) that the deletion of Pds1 on top of a Cdc20 deletion (*cdc20*Δ*pds1*Δ) results in an activation of Esp1. However, these cells are unable to exit mitosis; instead they remain arrested in telophase. This result shows that separase activation is necessary but not sufficient to complete mitotic exit. In support of this evidence, Sullivan and Uhlmann (Sullivan and Uhlmann, 2003) overexpressed separase in cells under a Cdc20 block, and observed that only a very small fraction of cells underwent mitotic exit.

These experiments were simulated with MV1 and the results can be seen in Figure I - 4A and Figure I - 4B. From a modeller's perspective, the deletion of Pds1 has a similar effect to the overexpression of Esp1. In both simulations, Esp1 is activated and Cdc14 is fully released; however, cells do not exit mitosis. The main difference between these two simulations is the timing of Cdc14 release. In *a cdc20*Δ*pds1*Δ mutant, separase is fully active from t=0 and Cdc14 is immediately released, while in a *cdc20*Δ*ESP1*$^{OP}$ mutant, there is a delay caused by the titration of Esp1 by endogenous Pds1.

Sullivan and Uhlmann (2003) showed that Esp1 can promote Cdc14 release independently of MEN. The authors inactivated MEN by using a temperature sensitive Cdc15 (cdc15-1 allele) in cells depleted of Cdc20 and overexpressing Esp1. These cells show a release of Cdc14 independent of MEN.

According to MV1, these results are explained through the separase-mediated inhibition of PP2A. This downregulation, together with high levels of Clb2, promotes Net1 phosphorylation and consequent Cdc14 release. In this situation, MEN is not required for Cdc14 release from the nucleolus (Figure I - 4C).

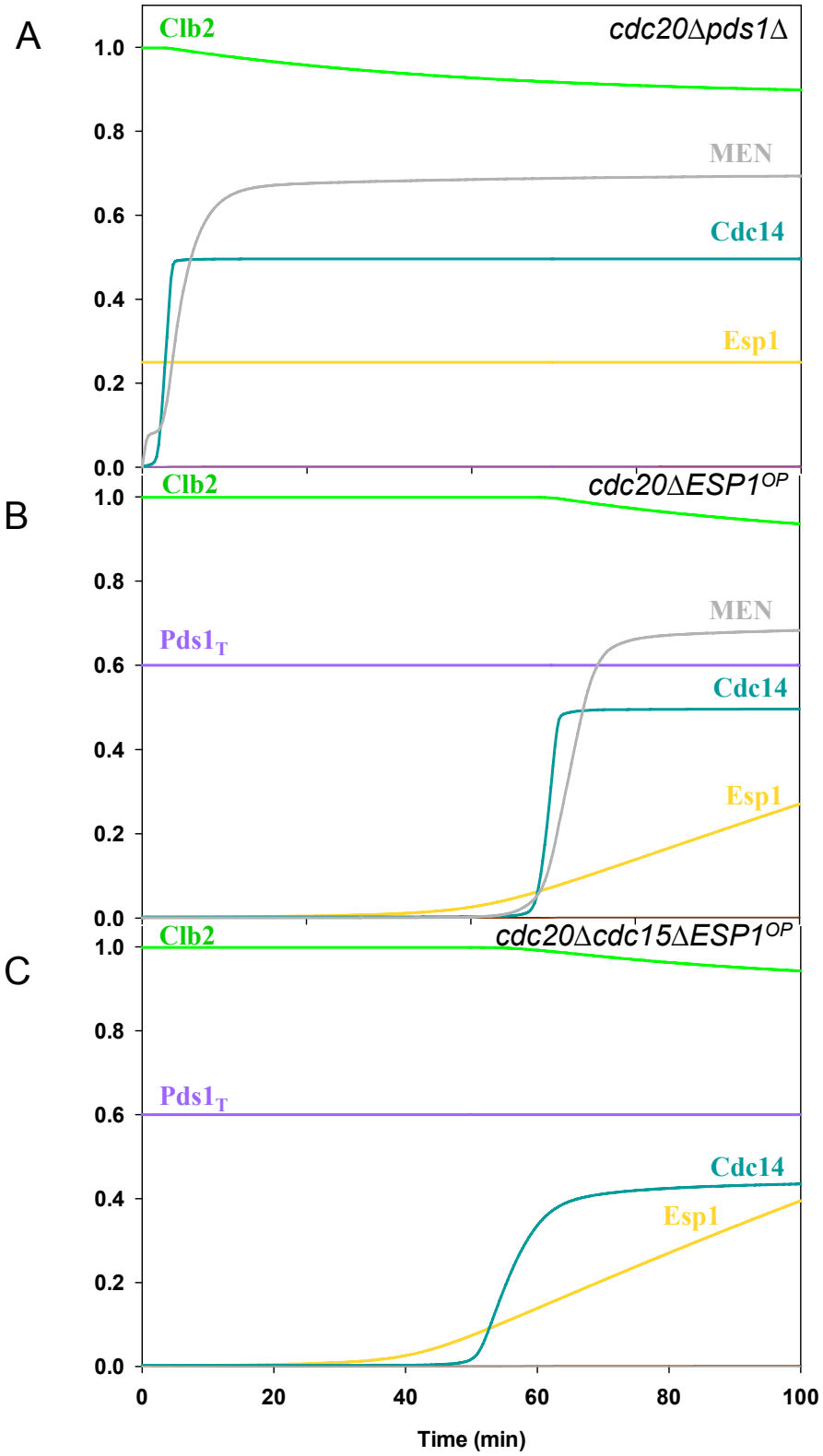


**Figure I - 4: Numerical simulations of mitotic progression in metaphase-blocked cells ($k_{s20}$=0) (A) with a Pds1 deletion (Initial Conditions: [$Pds1_T$] = 0, [$Esp1_B$] = 0]), (B) overexpressing separase ($k_{sesp}$ = 0.01 $min^{-1}$), and (C) overexpressing separase with Cdc15 deletion ($k_{ac15}$ = $k_{ac15}$' =0 $min^{-1}$).**

## *4. The role of Separase in Cdc14 activation*

All the simulations presented above are in agreement with the results published by Queralt et al. (2006).The next step was to test whether MV1 could describe more recent results, namely results by Lu and Cross (2009). The authors propose that CDK1 inactivation and separase proteolytic function are the main factors responsible for mitotic exit. Their aim was to determine which of the two is the most critical for the timing and efficiency of mitotic exit.

In Lu and Cross (2009) figure 1, cells were depleted of Cdc20 using a methionine-repressible MET3-CDC20 construct (Sullivan and Uhlmann, 2003), and thus, cells were arrested in a metaphase block. To overcome the absence of Esp1 (inhibited by endogenous Pds1), they used the GAL1-TEV/SCC1-TEV system. This system allows cells to express the Tobacco etch virus (TEV) protease, that will cleave the SCC1 subunit of cohesin which possesses an engineered TEV site (Uhlmann et al., 2000). Note that TEV only mimics the proteolytic activity of Esp1; it cannot inhibit PP2A. To induce the downregulation of Clb/CDK1 activity, the authors used a stable version of the CDK1 inhibitor, Sic1 (GAL1-SIC1-4A). This allowed them to inactivate Clb/CDK1 activity in the absence of Cdc20-driven Clb proteolysis (Verma et al., 1997). These manipulations provide the means to examine independently the importance of each factor (cohesion cleavage and Clb/CDK1 downregulation) in mitotic progression, from a metaphase block.

Their results show that:

- Cells overexpressing non-degradable Sic1 (GAL1-SIC1-4A) are forced to exit mitosis without going through anaphase, although there is a delay;
- Cells overexpressing TEV elongate their spindle but do not exit mitosis;

- Cells overexpressing both Sic1 and TEV are able to exit mitosis efficiently; the timing is very similar to the timing obtained when Cdc20 is re-induced and the metaphase block is released.

Because cells overexpressing non-degradable Sic1 can exit mitosis while cells overexpressing TEV are arrested in telophase, Lu and Cross argue that CDK1 inactivation is essential for mitotic exit, whereas cohesin cleavage is important for its efficiency but not absolutely essential.

These experiments cannot be tested using QM, because the model only includes Cdh1 as a CDK1 antagonist, and not Sic1. To overcome this drawback, MV1 was supplemented with an additional equation that is used only where it is necessary to induce the expression of the non-degradable CDK1 inhibitor, Sic1. Overexpressed Sic1 binds to Clb2 and forms an inactive trimer with it (see Sic1 equation in Appendix 1a).

In this way, the MV1 model can be used to test the experiments from figure 1 in Lu and Cross (2009). This makes it possible to quantify the relative importance of Clb/CDK1 downregulation and separase function (Figure I - 5).

In the *cdc20*Δ*SIC1*$^{OP}$ mutant, Clb2/CDK1 activity has to be completely downregulated for cells to exit mitosis. Since there is no Esp1 in the system, Cdc14 is not released and cannot dephosphorylate CDK1 substrates. Therefore, all CDK1 activity has to be inhibited in order for the cell to enter G1 phase (illustrated by activity of Cdh1 in MV1). In the simulations, it is considered that cells have exited mitosis when Cdh1 level rises to 50% of its maximum value. This occurs after 130 min in the *cdc20*Δ*SIC1*$^{OP}$ mutant (Figure I - 5A). Furthermore, TEV overexpression in MV1 does not induce mitotic exit, in accordance with experimental observations (Lu and Cross, 2009a). However, these cells can recover their ability to exit mitosis efficiently if Clb2 levels are decreased. This can be seen in *cdc20*Δ*TEV*$^{OP}$*SIC1*$^{OP}$ cells (Figure I - 5C); these cells are not only able to exit mitosis (60 min after release), but also to activate Cdc14 release.

These results confirm that the non-proteolytic function of Esp1 is not an essential requirement for mitotic exit; however, this does not mean that this function is completely not required. In this regard, I compared the mutants *cdc20*Δ*ESP1*$^{OP}$ and *cdc20*Δ*TEV*$^{OP}$ mutants, of which the only genetic difference is the overexpression of TEV instead of separase. In the *cdc20*Δ*ESP1*$^{OP}$ mutant situation, cells are arrested in a post-anaphase state with Cdc14 released. In the *cdc20*Δ*TEV*$^{OP}$ mutant situation, cells are arrested with no Cdc14 release (Sullivan and Uhlmann, 2003). Clearly, in a *cdc20*Δ background situation, TEV overexpression is not able to fully recover the function of separase, demonstrating that the Esp1 non-proteolytic function is crucial for Cdc14 release.

MV1 provides an explanation for these observations based on the structure of the molecular network. The MEN kinase Cdc15 is inhibited by Clb2 but activated by Cdc14 which forms a positive feedback loop in MEN activation. Thus, in a *cdc20*Δ background where Clb2 level is high, Cdc15 is strongly inhibited. When TEV is overexpressed, it cleaves cohesin and the mitotic spindle is elongated. This event is responsible for Tem1, activation but has no observable effect on Cdc15 activation. Since both components are needed to promote Net1 phosphorylation, the absence of Cdc15 activation prevents any Cdc14 release. However, when Esp1 is overexpressed, PP2A is inhibited, which promotes Cdc14 release through FEAR network. This release promotes Cdc15 activation (which counterbalances Clb2-mediated inhibition), and, together with active Tem1, activates MEN. In this case, the non-proteolytic activity of Esp1 plays a role in MEN activation and Cdc14 release.

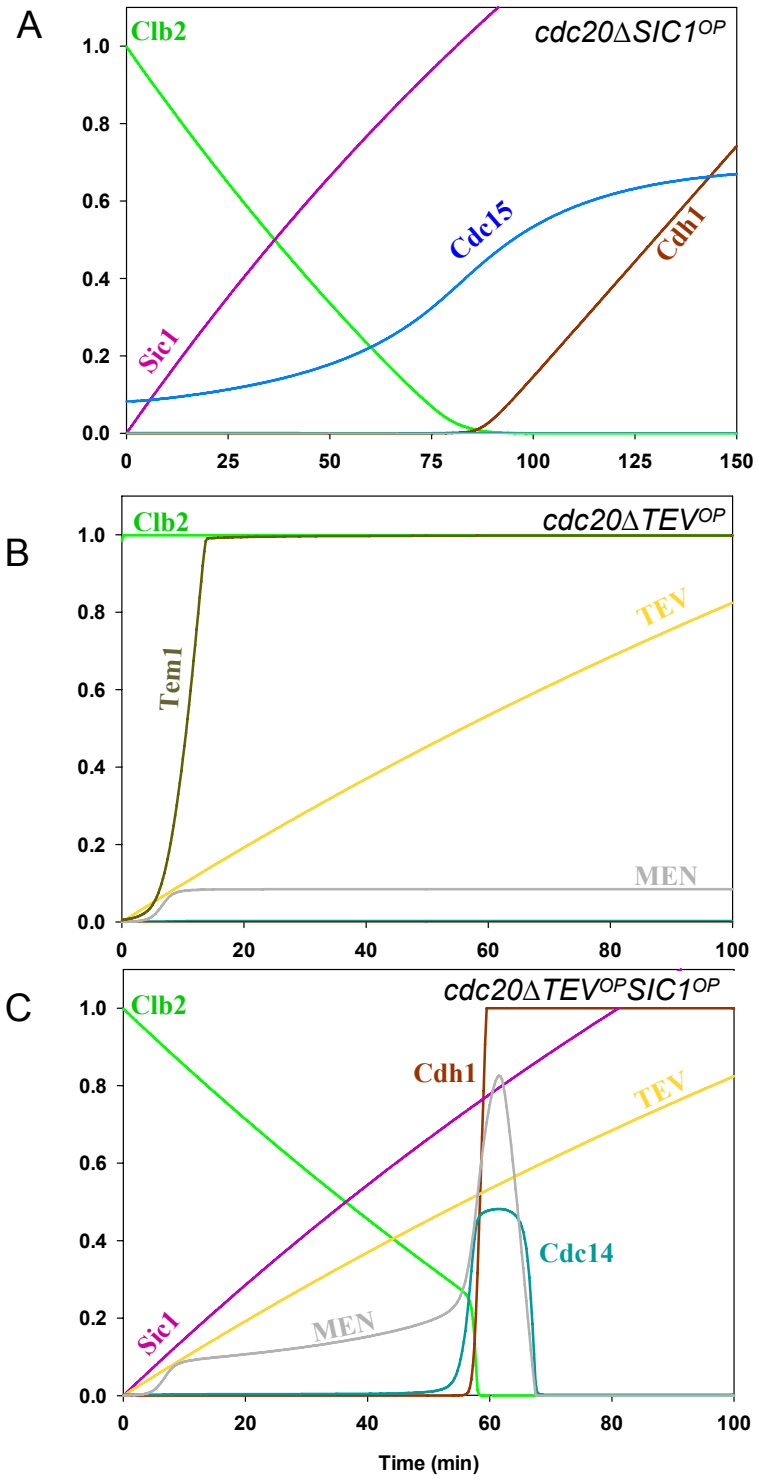


**Figure I - 5: Efficient exit from the *cdc20*Δ stable mitotic state requires both inhibition of CDK1 and activation of Cdc14. (A) Non-degradable Sic1 overexpressed ($k_{ssic}$ = 0.015 $min^{-1}$) in a Cdc20 block brings about mitotic exit after a long time because Cdc14 is not activated. (B) A ten-fold TEV expression over separase level ($k_{sesp}$ = 0.01 $min^{-1}$, $k_i$ = 0, $l_{apds}$ = 0 ; Initial Conditions: $[Esp1_T]$ = 0; $[Esp1_B]$ = 0) in a Cdc20 block can only induce partial MEN activation but no Cdc14 release nor mitotic exit. (C) Overexpression of TEV and non-degradable Sic1 in a Cdc20 block activates Cdc14 release and mitotic exit.**

Lu and Cross (2009) also conducted experiments on the inhibition of Esp1 in a $Cdc20^{b/r}$ situation. They expressed endogenous levels of non-degradable Pds1 (Pds1-mdb – which carries a mutated destruction box, resistant to Cdc20-mediated degradation), in order to keep Esp1 inactive throughout cell cycle progression. These cells are inviable, arresting in mitosis with no nuclear division. It was also demonstrated that the overexpression of either Esp1 or TEV protease can rescue their ability to exit mitosis. Figure I - 6 depicts the simulations involving these mutants (Lu and Cross, 2009a).

It is interesting to compare *cdc20*Δ*TEV*$^{OP}$ and *PDS1-mdb TEV*$^{OP}$ mutants (Figure I - 5B and Figure I - 6C). In the first case, cells remain arrested in telophase, while in the second, cells exit mitosis efficiently. In both situations, Esp1 is inhibited by Pds1 and TEV only recovers the proteolytic function of separase, so the basis of this phenotypic difference is unclear. MV1 provides a logical explanation for this discrepancy.

As outlined previously, high levels of Clb2 present in *cdc20*Δ*TEV*$^{OP}$ mutant prevent the activation of MEN and Cdc14 release. However, in a $Cdc20^{b/r}$ situation where cells express Pds1-mdb, Cdc20 is activated and degrades Clb2 partially. This degradation is sufficient to weaken Clb2 inhibition on Cdc15 and, aided by a basal dephosphorylation (independent of Cdc14), is sufficient to activate Cdc15. Active Cdc15, together with active Tem1 (activated by spindle elongation), fully promotes MEN activation and Cdc14 release. These events alter the ratio of Clb2/Cdc14 (the ratio is decreased), which is sufficient to activate Cdh1 through Cdc14-mediated dephosphorylation. Activated Cdh1 promotes the complete degradation of Clb2 and promotes mitotic exit. This explanation predicts that Cdc14 release is by itself insufficient to promote mitotic exit, and that Cdc20-mediated degradation of Clb2 is required to activate Cdh1. Such a difference in the ratio of kinase/phosphatase explains the phenotypic differences between *cdc20*Δ*TEV*$^{OP}$ and *PDS1-mdb TEV*$^{OP}$ mutants.

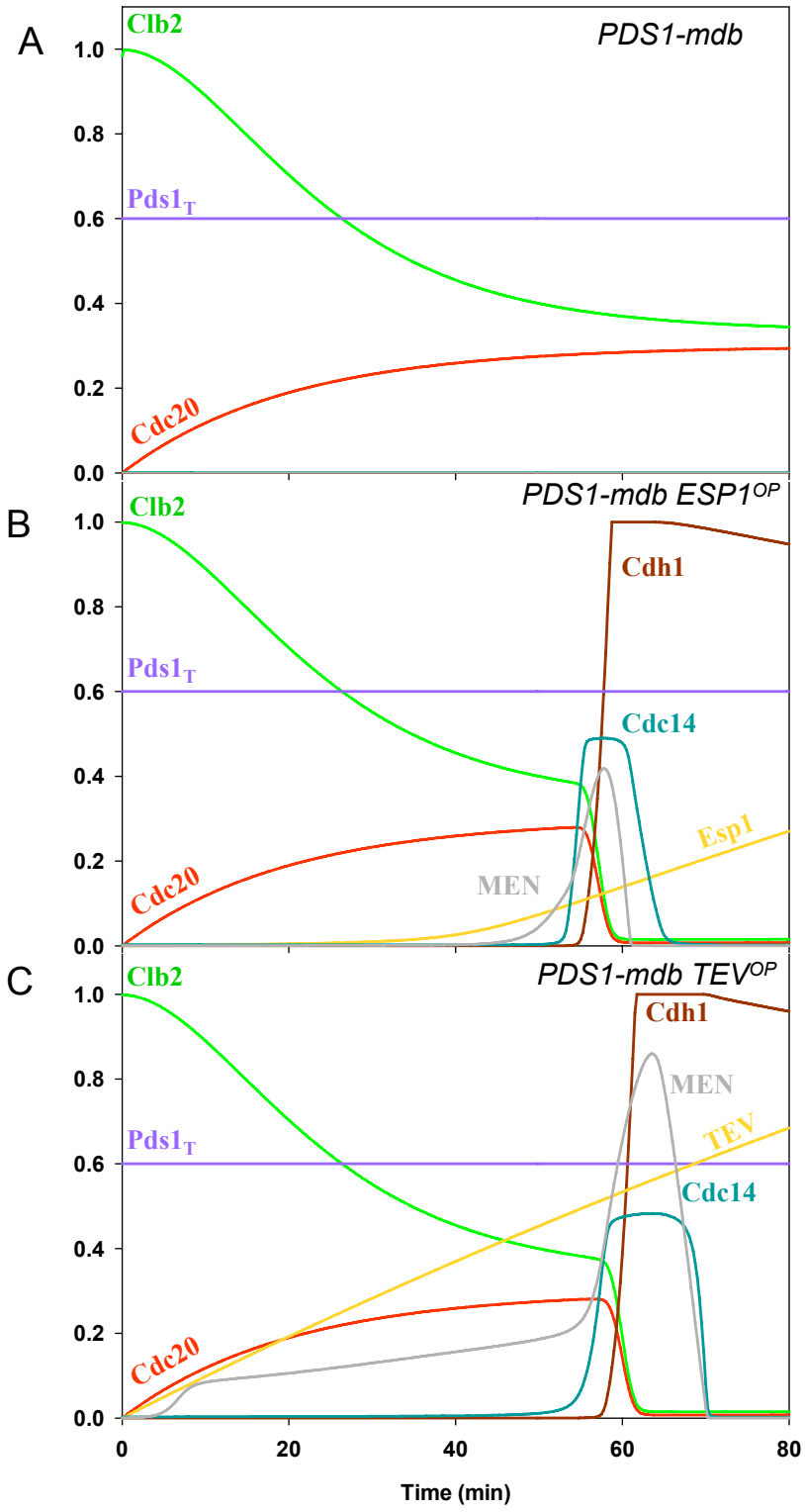


**Figure I - 6: Numerical simulations of mitotic progression after Cdc20 release in cells (A) expressing endogenous levels of non-degradable Pds1 ($k_{dpds}$' = 0), and (B) overexpressing separase ($k_{sesp}$ = 0.01 $min^{-1}$) or (C) TEV ($k_{sesp}$ = 0.01 $min^{-1}$, $k_i$ = 0, $l_{apds}$ = 0 ; Initial Conditions: [$Esp1_T$] = 0; [$Esp1_B$] = 0).**

### *a. The role of spindle elongation in Mitotic Exit and Cdc14 release*

It is believed that the proteolytic function of Esp1 activates MEN by promoting the migration of the spindle pole body and Tem1 to the bud cortex, where Tem1 can be activated by Lte1 (Bardin et al., 2000). This happens when cohesin is cleaved and the spindle is elongated. In a situation where the spindle cannot be elongated, (e.g. in the presence of nocodazole), Tem1 cannot be activated by Esp1 and thus the phenotype should be similar to that of a MEN mutant. In MV1, the simulation of a *cdc20*Δ*ESP1*$^{OP}$ mutant in the presence of nocodazole results in a mutant similar to the one depicted in Figure I - 4C (*cdc20*Δ*cdc15*Δ*ESP1*$^{OP}$mutant), where MEN is inactivated. This mutant shows a constitutive release of Cdc14 caused by FEAR activation. In contrast, Lu and Cross (2009) have reported findings whereby the release of Cdc14 is strongly reduced under these conditions.

This contradicts the previous results obtained by Sullivan and Uhlmann (2003) and Visintin et al. (2003), in which a release of Cdc14 was observed. The research groups used different experimental techniques, which may explain the discrepancy in their results. Sullivan and Uhlmann (2003) and Visintin et al. (2003) both used immunofluorescence to detect Cdc14, and did not track Net1 nor any other nucleolar marker. Lu and Cross (2009) argue that this approach is insufficient to make a full assessment of Cdc14 nucleolar localization. Hence, they developed a quantitative measure of Cdc14 nucleolar localization, whereby the co-localization of Net1 and Cdc14 can be measured during mitotic progression.

Based on these results, Lu and Cross (2009) argue that spindle elongation plays a crucial role in Cdc14 release, and that Esp1 function in mitotic exit is tightly connected with this phenomenon. With MV1, it is possible to control the proteolytic and non-

proteolytic actions of Esp1 separately, although Cdc14 release can be triggered by both. This is why the simulation of the *cdc20*Δ*ESP1*$^{OP}$ mutant shows full Cdc14 release in the presence of nocodazole, triggered by the FEAR network (high Clb2 phosphorylates Net1, and active Esp1 inhibits PP2A$^{CDC55}$). According to Lu and Cross (2009), this simulation cannot be accurate, as spindle elongation is necessary for a full release of Cdc14, and this cannot happen in the presence of nocodazole.

At this point, MV1 is unable to explain the available experimental results, and hence, the role of MEN in the model will be revised in future chapters (see Chapter III, section 2a 'Spindle elongation and MEN activation').

### *b. Non-degradable Clb2 (Clb2-kd)*

Esp1 is not the only component that has a dual role in mitotic exit. Clb2, for instance, is a key regulator of both FEAR and MEN. On one hand, Clb2 promotes FEAR by phosphorylating Net1, and on the other, it inhibits MEN by phosphorylating Cdc15. In order to better understand the role of Clb2 in Cdc14 release and subsequent mitotic exit, Lu and Cross (2009) quantified the release kinetics of Cdc14 in the presence of non-degradable Clb2 (Clb2-kd, lacking KEN and destruction boxes). However, since Clb2-kd is lethal at its endogenous locus (it results in a mitotic exit block – cells arrest in telophase), the authors rescued these cells by overexpressing Sic1 using the GAL1 promoter.

Cells were synchronised with α-factor and released into a glucose medium to inactivate the GAL1-SIC1 gene. Cdc14 localization was quantified, and the results show full release followed by recapture. This was much unexpected, since, at first glance, there appears to be no reason why Cdc14 should be recaptured once it is released. MV1 is able to reproduce Cdc14 release and telophase block, although it cannot explain why

Cdc14 goes back to the nucleolus. In the simulation, Cdc14 is kept constitutively active by the high level of Clb2 combined with free Esp1 (Figure I - 7A).

Lu and Cross (2009) employed a different approach to address the importance of constitutively high Clb2, by studying mutants with a Cdc20 and Cdh1 double deletion. Then, the authors overexpressed Esp1 to bypass Pds1 inhibition. Results show that these cells did not recapture Cdc14 once it is released, in agreement with the computed MV1 simulation (the phenotype is very similar to a *cdc20*Δ*ESP1*$^{OP}$ mutant – see Figure I - 4B and Figure I - 7C). These results violated the authors' expectations, that this phenotype would mirror the Clb2-kd situation. MV1 was also unable to provide immediate insights, but this subject will be revisited in the chapters that follow.

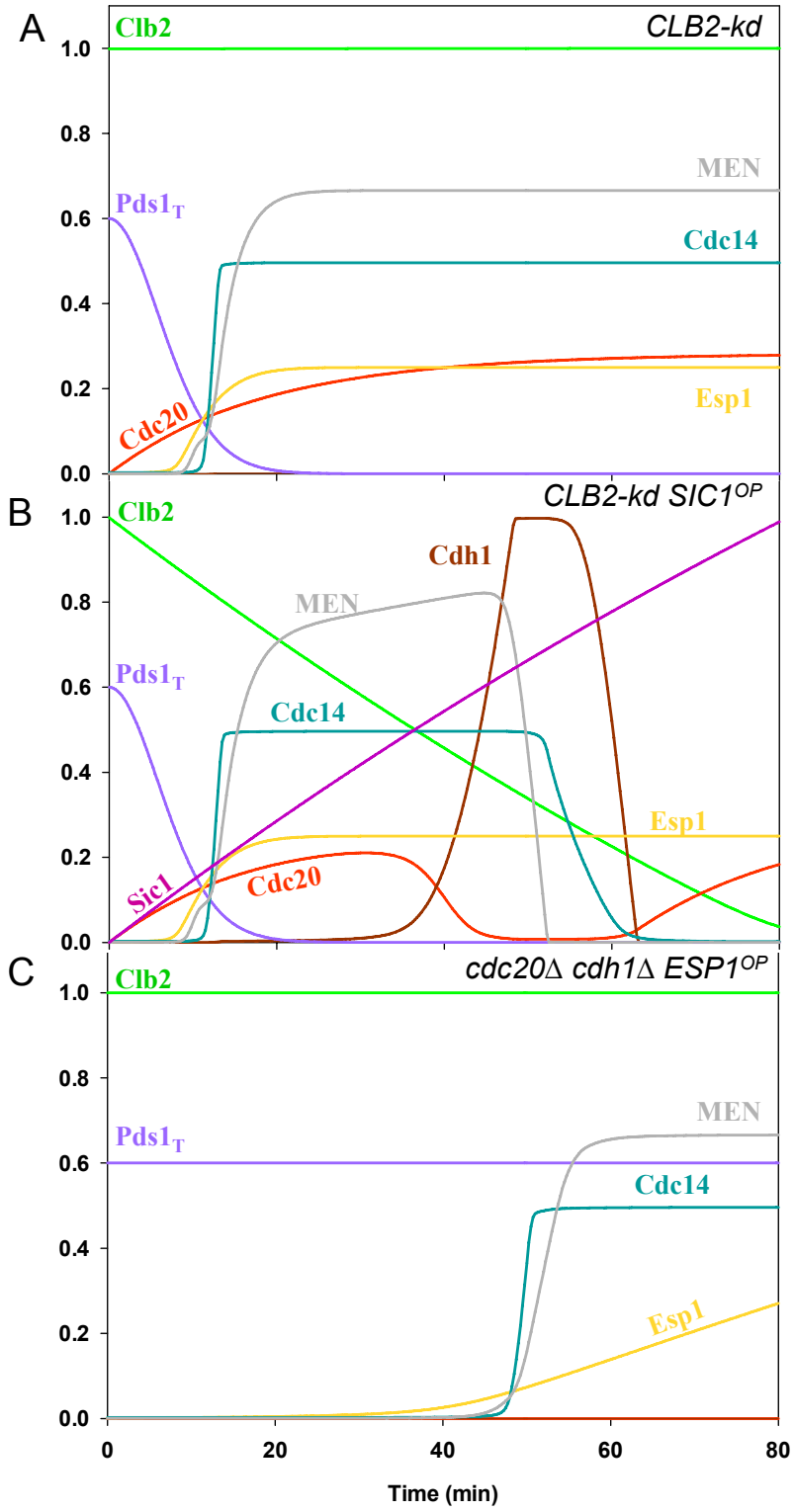


**Figure I - 7: Effect of constitutively active Clb2. Numerical simulations of mitotic progression: (A) after Cdc20 release in cells expressing Clb2-kd (non-degradable Clb2 lacking KEN and destruction boxes) ($k_{dclb2}$' = 0 and $k_{dclb2}$" = 0); (B) after Cdc20 release in cells expressing Clb2-kd and overexpressing Sic1 ($k_{ssic}$ = 0.015 $min^{-1}$); (C) in cells depleted of Cdc20 ($k_{s20}$=0), overexpressing separase ($k_{sesp}$ = 0.01 $min^{-1}$) and with a Cdh1 deletion ($k_{dcdh}$ = $k_{dcdh}$' = 0).**

### *c. Cdc14 nuclear export and MEN*

It is well known that Cdc14 localization is regulated by Net1, which sequesters it to the nucleolus. Hence, in MV1, it is considered that Cdc14 is released into the nucleus and cytoplasm as soon as it is freed from Net1. Thus, in any mutant situation involving Net1 depletion, one would expect to observe a constitutive release of Cdc14 to the cytoplasm (Figure I - 8). Lu and Cross (2009) tested exactly this hypothesis in cells with a Net1 deletion (*net1*Δ cells), but unexpectedly, Cdc14 remained in the nucleus for most of the cell cycle, only spread to the cytoplasm during mitotic exit. This suggests that there is another mechanism, besides the one involving Net1, which controls the timing of Cdc14 to the cytoplasm. To test whether this pathway involves the MEN network, Lu and Cross inactivated MEN in a *net1*Δ strain, using the temperature sensitive allele *cdc15-2*. Cdc14 remained in the nucleus throughout the cell cycle, suggesting that MEN is indeed required for timely Cdc14 release to the cytoplasm.

Clearly, MV1 cannot reproduce these results. In order to improve the model, Cdc14 compartmentalisation was added as a further factor regulating Cdc14. This adjustment is described in chapters III and IV.

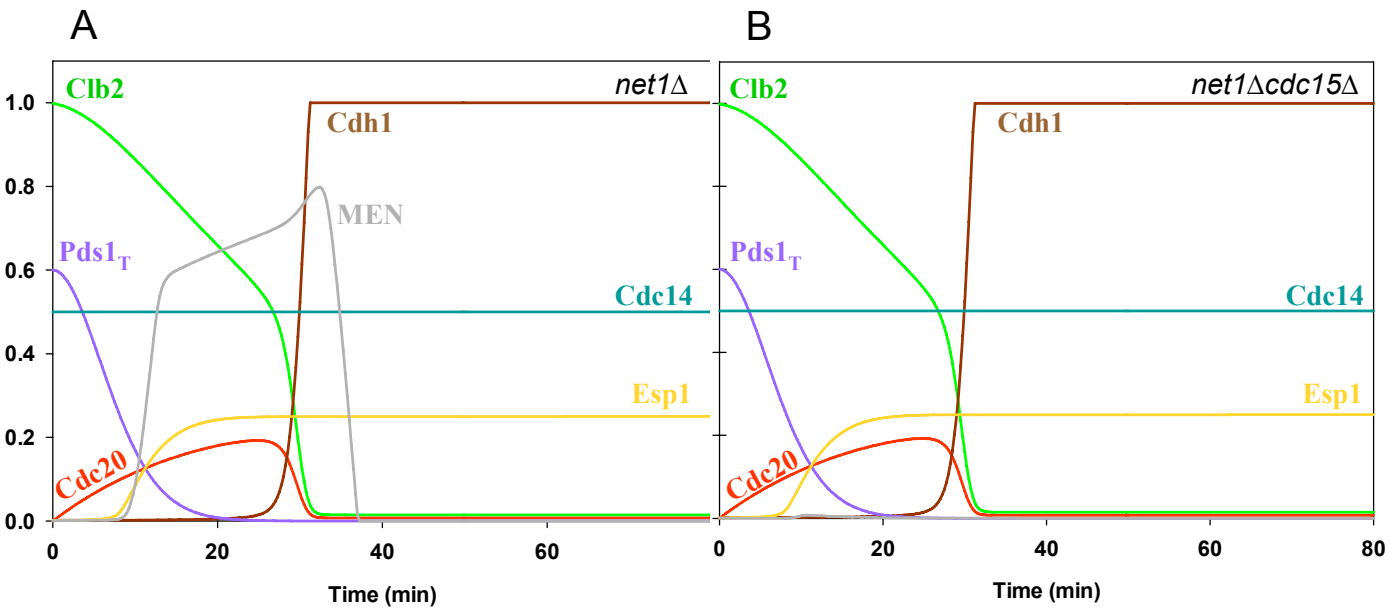


**Figure I - 8: Numerical simulations of mitotic progression after Cdc20 release in cells depleted of (A) Net1 ($l_{anet}$ = 0, Initial Conditions: [Net1] = [RENT] = 0) and (B) Cdc15 as well ($k_{ac15} = k_{ac15}' = 0$).**

### *d. The role of Polo kinase (Cdc5) in Cdc14 release*

The role of Polo kinase (Cdc5) in the promotion of Cdc14 release still requires clarification. MV1 considers that Cdc5 promotes Cdc14 release through Tem1 activation alone (Hu and Elledge, 2002; Hu et al., 2001; Pereira et al., 2002), and therefore assumes that Cdc5 belongs only to the MEN network. By this view, Cdc5 depletion should not affect the FEAR network, and hence, a transient release of Cdc14 should still be observed in Cdc5 depleted cells (Figure I - 9). Contrary to this prediction, Amon and others have shown that Cdc5 depletion results in complete prevention of Cdc14 release (Stegmeier et al., 2002). A similar outcome was observed in Esp1-overexpressing cells depleted of Cdc5 (Visintin et al., 2008). Therefore, Cdc5 must also be part of the FEAR network. MV1 cannot reproduce these results because it considers Cdc5 inactivation equivalent to MEN inactivation only. Cdc5's role in Net1 phosphorylation and Cdc14 release will be revisited in the chapters that follow (Chapter II and Chapter IV).

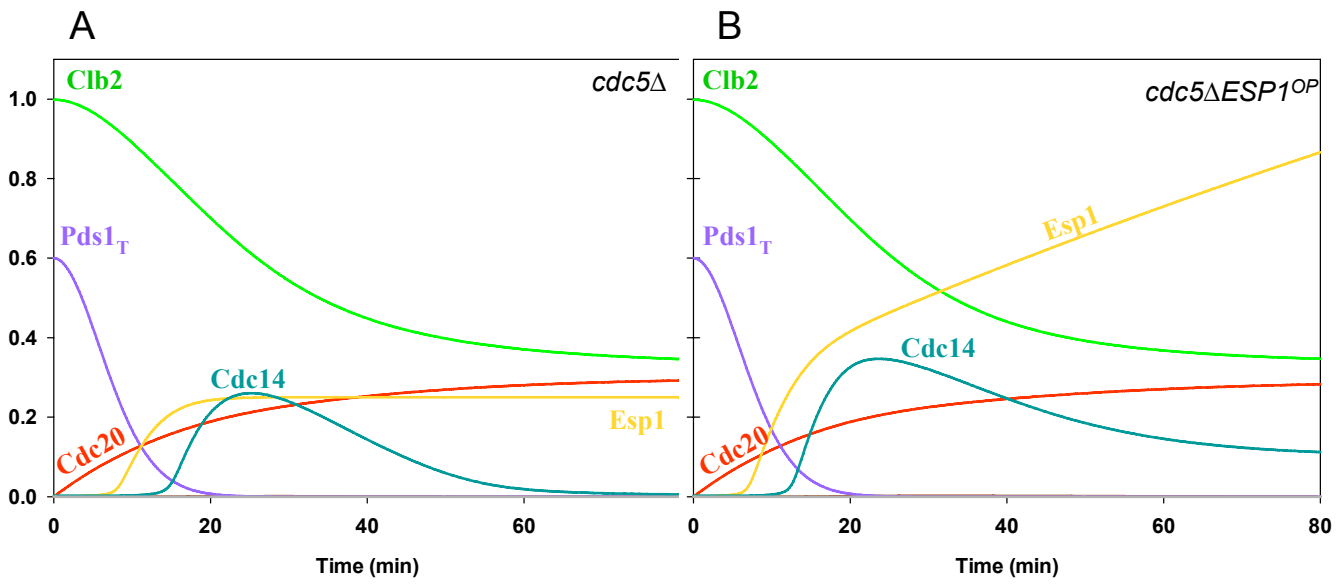


**Figure I - 9: Numerical simulations of mitotic progression after Cdc20 block and release in cells with (A) Cdc5 deletion ($k_{apolo}$ = 0; Initial Conditions: [PoloT] = [Polo]= 0) and (B) with Esp1 overexpression ($k_{sesp}$ = 0.01 $min^{-1}$).**

# Chapter II – The role of Cdc20 in Mitotic Exit

Cdc20 is a key component in mitotic progression. In its absence (e.g. in the *cdc20*Δ mutant), cells arrest in metaphase with high Clb/CDK1 activity and unseparated sister chromatids. The simultaneous deletion of Pds1 and Clb5 in *cdc20*Δ cells overcomes the Cdc20 requirement for mitotic exit; restoring viability to these cells (Shirayama et al., 1999). These results suggest that the major roles of Cdc20 in mitosis are the release of Esp1 and the downregulation of Clb5/CDK1 activity. In Chapter I, this idea is implicit but not clearly addressed. In MV1, Clb2 is the only Clb subunit that regulates CDK1 activity, and consequently, the manipulation of CDK1 is restricted.

Cdc20 synthesis is promoted by the transcriptional complex Fkh2/Mcm1/Ndd1, which is upregulated by Clb2/CDK1. This generates a negative feedback loop in the system, whereby Clb2/CDK1 promotes the synthesis of its own inhibitor (Cdc20). Interestingly, the Fkh2/Mcm1/Ndd1 complex is also part of a positive feedback loop, since it is also the transcriptional activator of the Clb2 subunit. A third mitotic component, Cdc5 (polo kinase), also has its transcription activated by the Fkh2/Mcm1/Ndd1 complex. These additional regulatory components may influence the dynamics of the mitotic exit, and should therefore be added to MV1.

Sic1 is an important Clb/CDK1 antagonist which functions redundantly with Cdh1 during mitotic exit; a Cdh1 deletion is not lethal, since Sic1 can substitute its role (Schwab et al., 1997). Sic1 transcription is regulated by the transcription factor Swi5, which is upregulated by Cdc14 and downregulated by Clb2. Thus, Sic1 is indirectly upregulated by Cdc14 and downregulated by Clb2. Moreover, Sic1 is directly phosphorylated by Clb/CDK1, which promotes Sic1 degradation. Since Sic1 acts as a stoichiometric inhibitor of CDK1, this forms a double-negative feedback loop in the

system. MV1 does not model Sic1 regulation in detail; it only includes an equation for non-degradable Sic1 overexpression. Thus, as will be described in this chapter, the regulation of endogenous Sic1 through Swi5 was added to MV1.

As mentioned in Chapter I, Cdc5's role in MV1 should also be reviewed. There is evidence that Cdc5 promotes Net1 phosphorylation independently of MEN (Stegmeier et al., 2002; Visintin et al., 2008) which is not considered in MV1. To take this into account, Net1 phosphorylation by Cdc5 was incorporated into the model, supplementing Net1 phosphorylation by Clb2 and MEN kinases. Thus Cdc5 now has a role in the FEAR network, in addition to its role in MEN (activating Tem1).

This chapter describes the incorporation of the following components into MV1: the S phase cyclins (Clb5/6), the Fkh2/Mcm1/Ndd1 complex, Sic1 and Swi5 (Figure II - 1). For simplicity, S phase cyclins are referred to simply as Clb5, and the Fkh2/Mcm1/Ndd1 complex is referred to as Mcm1. This version of the model is named MV2 and is able to address a larger set of mutant situations without losing any information from MV1 (all previous mutant situations can still be simulated using MV2).

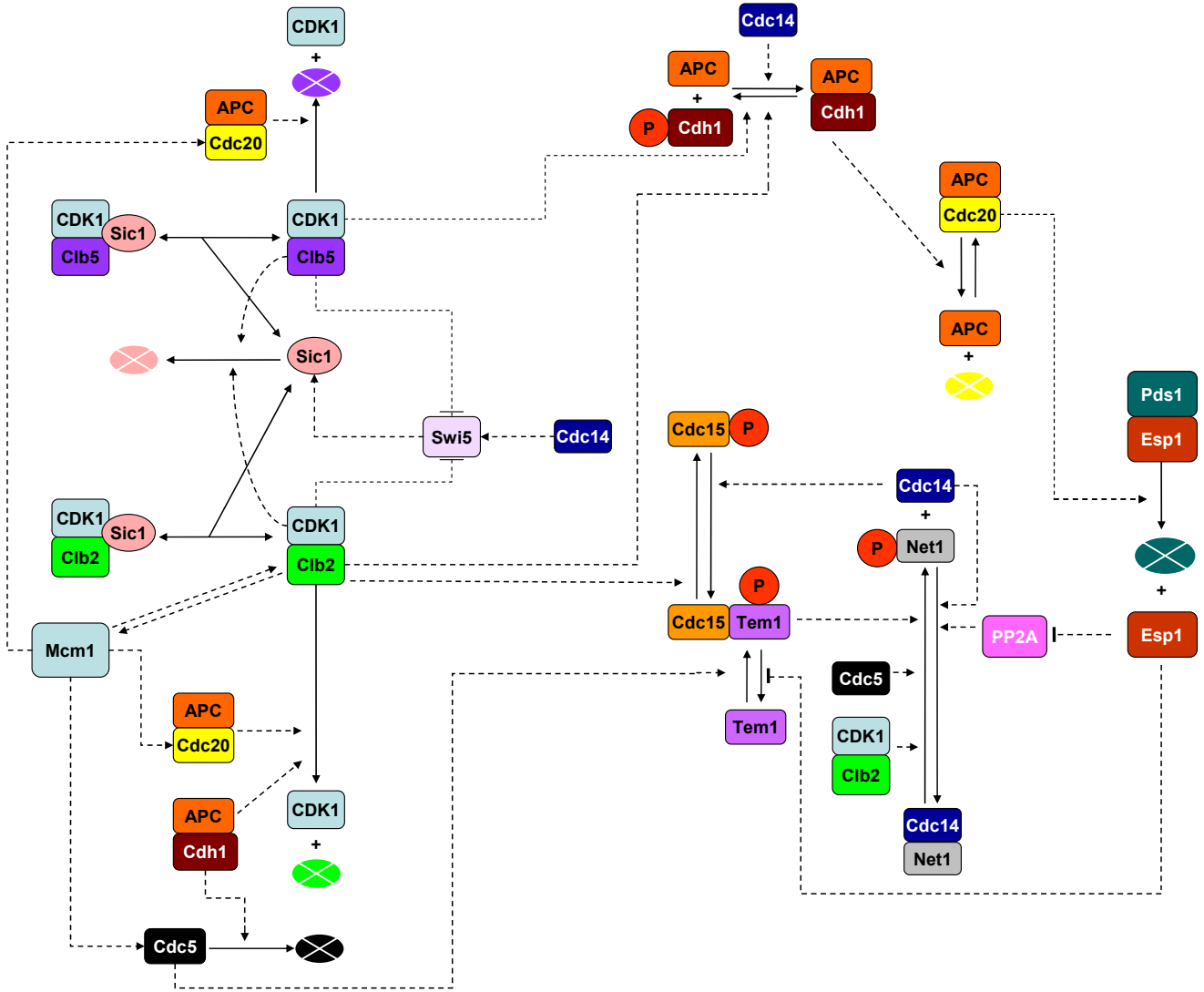


**Figure II - 1: Wiring Diagram of the molecular network present in MV2. The following components have been incorporated to MV1: Clb5, Sic1, Swi5 and Mcm1.**

## *1. Cdc20 Block and Release experiment*

As in Chapter I, the $Cdc20^{b/r}$ situation is used as a control for efficient mitotic exit. Here, Cdc20 now has two rate constants for synthesis: an unregulated term ($k_{s20}$) and a Mcm1-regulated term ($k_{s20}$') (see equation for Cdc20 in Appendix 1b). To simulate the release from the metaphase block, both of these terms were set to non-zero values ($k_{s20}$ = 0.001 $min^{-1}$ and $k_{s20}$'=0.01 $min^{-1}$) at t=0. The choice of these parameter values is strongly restricted by the previous parameter set. In order to maintain the same set of mutants that MV1 could reproduce, MV2 parameter set must be close to MV1 parameter set. In this way, the new values attributed to the synthesis rate constants of Cdc20 must provide Cdc20 with a similar dynamical behaviour that was observed in MV1 (compare Figure I - 1B and Figure II - 2).

In experiments, a constitutive MET3-Cdc20 allele has a constant rate of transcription, while MV2 includes regulated and unregulated (constant) synthesis of Cdc20 (Figure II - 2). However, this difference does not affect the results of the simulation; the model still works both with and without regulated Cdc20 synthesis.

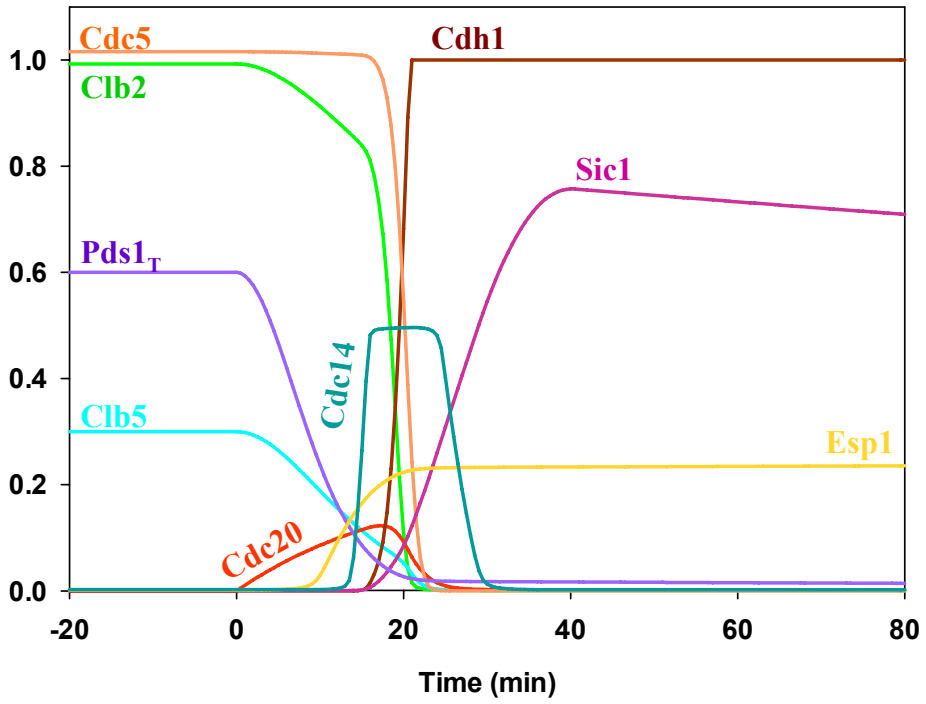


**Figure II - 2: Numerical simulation of mitotic exit in a Cdc20$^{b/r}$ situation. The model was simulated for 20min (until t=0) without Cdc20 synthesis ($k_{s20}$= $k_{s20}$'=0) which defines a stable steady-state corresponding to a metaphase block. At t=0, Cdc20 synthesis is induced ($k_{s20}$ = 0.001 min$^{-1}$ and $k_{s20}$'=0.01 min$^{-1}$) and the simulation is run for 80 minutes.**

## *2. Suppression of Cdc20 requirement*

Once cells are in metaphase, APC/Cdc20 targets three proteins for degradation: Pds1, Clb5 and Clb2. The degradation of each of these substrates initiates a pathway important for mitotic exit; MV2 is able to describe how these pathways progress and converge on mitotic exit, and can quantify their relative importance. To better understand each pathway, each Cdc20 substrate was deleted in turn, to see which, if any, could overcome the metaphase block caused by Cdc20 deletion.

As seen in Chapter I, the deletion of Pds1 on a *cdc20Δ* background triggers Cdc14 release, but cells remain blocked in mitosis. This mutant is only one step further in mitotic progression than the Cdc20 block, since it is blocked after anaphase in another stable steady-state (Lim et al., 1998). This shows that Pds1 is not the only Cdc20-target

that must be degraded to enable mitotic exit. The other two targets are Clb2 and Clb5. Since Clb2 is essential for mitotic progression, the model was challenged further by deleting Clb5. Cells of the *cdc20Δpds1Δclb5Δ* triple mutant overcome the Cdc20 block and exit mitosis, as shown experimentally by (Shirayama et al., 1999). This suggests that the combined deletion Clb5 and Pds1 is sufficient to release the mitotic block.

According to MV2, Clb5 deletion can release the mitotic block present in *cdc20Δpds1Δ* double mutant cells, because the absence of Clb5 allows the activation of the CDK1 antagonist APC/Cdh1 (Figure II - 3A). Clb5/CDK1 is a strong inhibitor of APC/Cdh1, and, as its level is high in *cdc20Δpds1Δ* mutants, APC/Cdh1 remains inactive. However, when Clb5 is deleted, the inhibition on Cdh1 is weakened and APC/Cdh1 can be activated. Consequently, Clb2 and Polo are degraded and the cell cycle can progress.

The role of APC in mitotic progression has been thoroughly studied experimentally in (Thornton et al., 2004; Thornton and Toczyski, 2003b). In these papers, the authors inactivated APC by deleting different APC subunits, and showed that a lack of APC activity can be overcome by the simultaneous inactivation of Pds1 and Clb/CDK1. Their experiments show that Cdh1 is essential for cell cycle progression in *cdc20Δpds1Δclb5Δ* cells, since *cdc20Δpds1Δclb5Δcdh1Δ* cells are inviable. MV2 explains this loss of viability by demonstrating that, without Cdh1, Clb2/CDK1 cannot be inactivated and its high activity prevents cell cycle progression (Figure II - 3B).

The downregulation of Clb/CDK1 activity can be achieved in different ways: through Clb5 deletion, and through overexpression of the CDK1 stoichiometric inhibitor, Sic1. Thornton and Toczyski (2003) rescued *cdc20Δ pds1Δ* cells by integrating 10 copies of the Sic1 gene into the genome. MV2 can simulate this experiment and overcome the telophase block (Figure II - 3C). Moreover, MV2 shows that in *cdc20Δ pds1Δ* cells, Sic1

cannot accumulate in the presence of Clb5. This can be explained by the fact that Sic1 is one of the major substrates of Clb/CDK1-mediated degradation. Therefore, there is a need to overexpress Sic1 so that it can overcome its inhibition and promote the inhibition of Clb/CDK1. *cdc20Δpds1ΔSIC1$^{10x}$* cells are still dependent on Cdh1 for exit (Figure II - 3D), in accordance with the experimental results (Thornton and Toczyski, 2003b).

The combined effect of Clb5 deletion and Sic1 overexpression on a *cdc20Δpds1Δ* background also produces viable cells (Thornton and Toczyski, 2003b). MV2 shows that this quadruple mutant has new emergent properties, which do not characterise any of the triple mutants mentioned previously (*cdc20 Δpds1Δclb5ΔSIC1$^{10x}$*, see Figure II - 3E). Moreover, Cdh1 becomes dispensable for mitotic exit and the cell cycle in this scenario, because *cdc20Δpds1Δclb5Δcdh1ΔSIC1$^{10x}$* cells can only downregulate their Clb2 kinase activity via Sic1 (see Figure II - 3F). This is how MV2 explains the underlying dynamics which make the quintuple mutant viable experimentally (Thornton and Toczyski, 2003b). Indeed, the essential core subunits of the APC, which are major regulators of cell cycle protein stability, become dispensable in this setting.

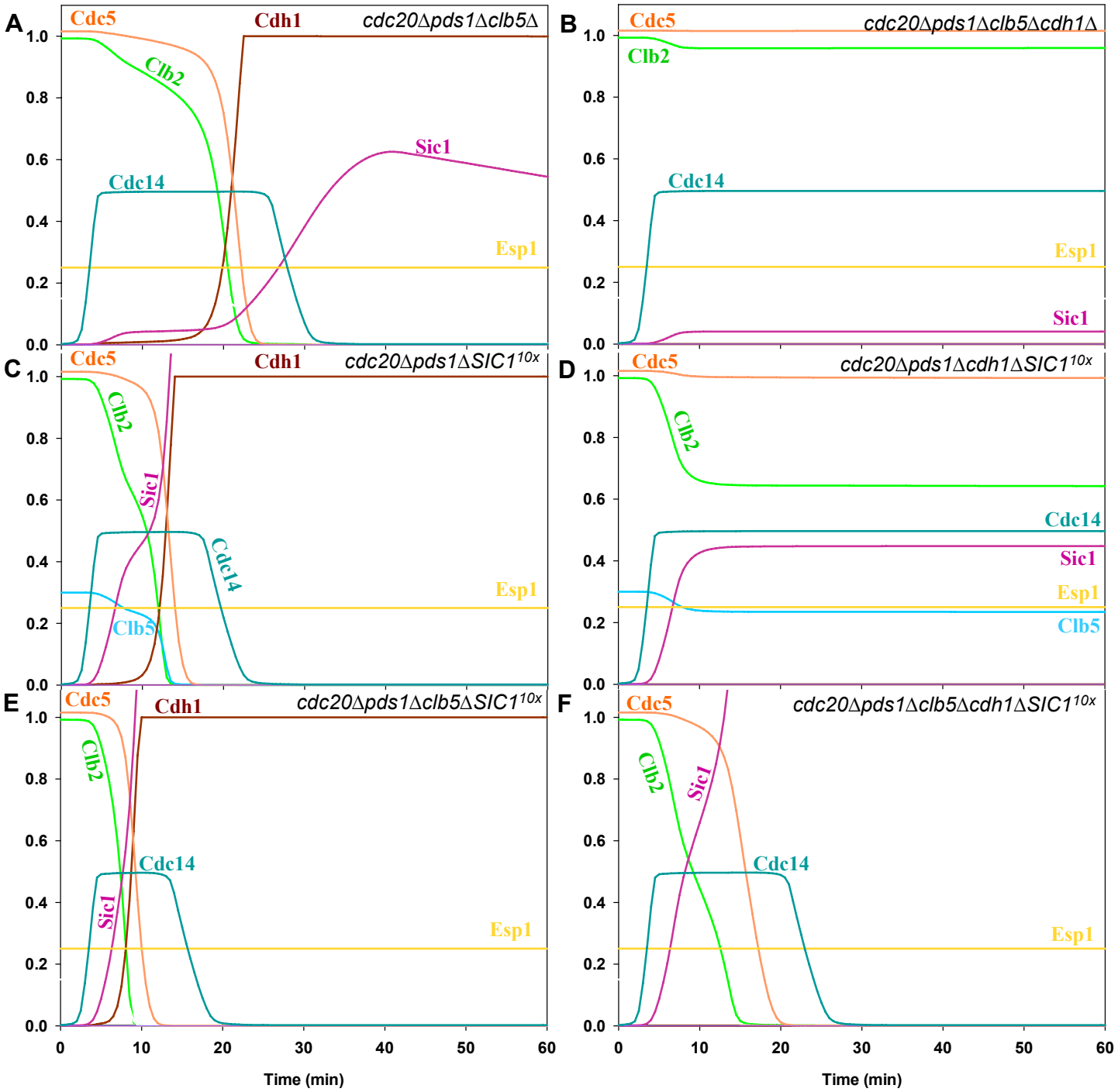


**Figure II - 3: Numerical simulations of mitotic progression in metaphase-blocked cells with different Cdc20 substrates deleted: (A) *cdc20Δpds1Δclb5Δ* mutant; (B) *cdc20Δpds1Δclb5Δcdh1Δ* mutant; (C) *cdc20Δpds1ΔSIC1*$^{10x}$ mutant; (D) *cdc20Δpds1Δcdh1ΔSIC1*$^{10x}$ mutant; (E) *cdc20Δpds1Δclb5ΔSIC1*$^{10x}$ mutant; (F) *cdc20Δpds1Δ clb5Δcdh1ΔSIC1*$^{10x}$ mutant.**

**Each deletion is simulated in the following way: $k_{s20}$=0 for *cdc20Δ*; Initial Conditions: $[Pds1_T] = 0$ and $[Esp1_B] = 0$ for *pds1Δ*; Initial Conditions: $[Clb5_T] = 0.15$ for *clb5Δ* considering the presence of Clb6, the other S phase cyclin still present in the system; $k_{dcdh} = k_{dcdh}' = 0$ for *cdh1Δ*; $k_{ssic} = 0.5\ min^{-1}$ for SIC1$^{10x}$.**

## 3. MEN and CDK1 activity

In MV1, Clb2 is the only cyclin that controls CDK1 activity. MV2 incorporates Clb5, making it possible to simulate experimental situations in which Clb5 is inhibited. This is useful, since the contribution of Clb5/CDK1 to the control of MEN activity is unclear. MV1 considered that Clb/CDK1 activity promotes Cdc15 phosphorylation, and as a consequence, MEN inhibition. Thus, MV1 predicted that MEN should remain inactive in *cdc20*Δ*TEV*$^{OP}$ mutant, due to high CDK1 activity. In this situation, both Clb2/CDK1 and Clb5/CDK1 levels are high and could potentially inhibit MEN. However, it has been shown experimentally that the *cdc20*Δ*clb5*Δ*TEV*$^{OP}$ mutant does not exit mitosis or release Cdc14 (Sullivan and Uhlmann, 2003). Therefore, Clb5 deletion does not release CDK1's inhibition on MEN. These observations suggest that the inhibitory effect of CDK1 on MEN comes from Clb2/CDK1 rather than Clb5/CDK1. Thus, to accurately simulate the phenotype of *cdc20*Δ*clb5*Δ*TEV*$^{OP}$, MV2 considers that Clb5/CDK1 does not inhibit MEN. As a direct consequence, the mutant *cdc20*Δ*clb5*Δ*TEV*$^{OP}$ is much more similar to the mutant *cdc20*Δ*TEV*$^{OP}$ than the mutant *cdc20*Δ*SIC1*$^{OP}$*TEV*$^{OP}$, which releases the mitotic block because the overexpression of Sic1 strongly inhibits both Clb2 and Clb5 (compare Figure II - 4A, 3B and 3C). These observations suggest that the inhibitory effect of CDK1 on MEN comes from Clb2/CDK1 rather than Clb5/CDK1.

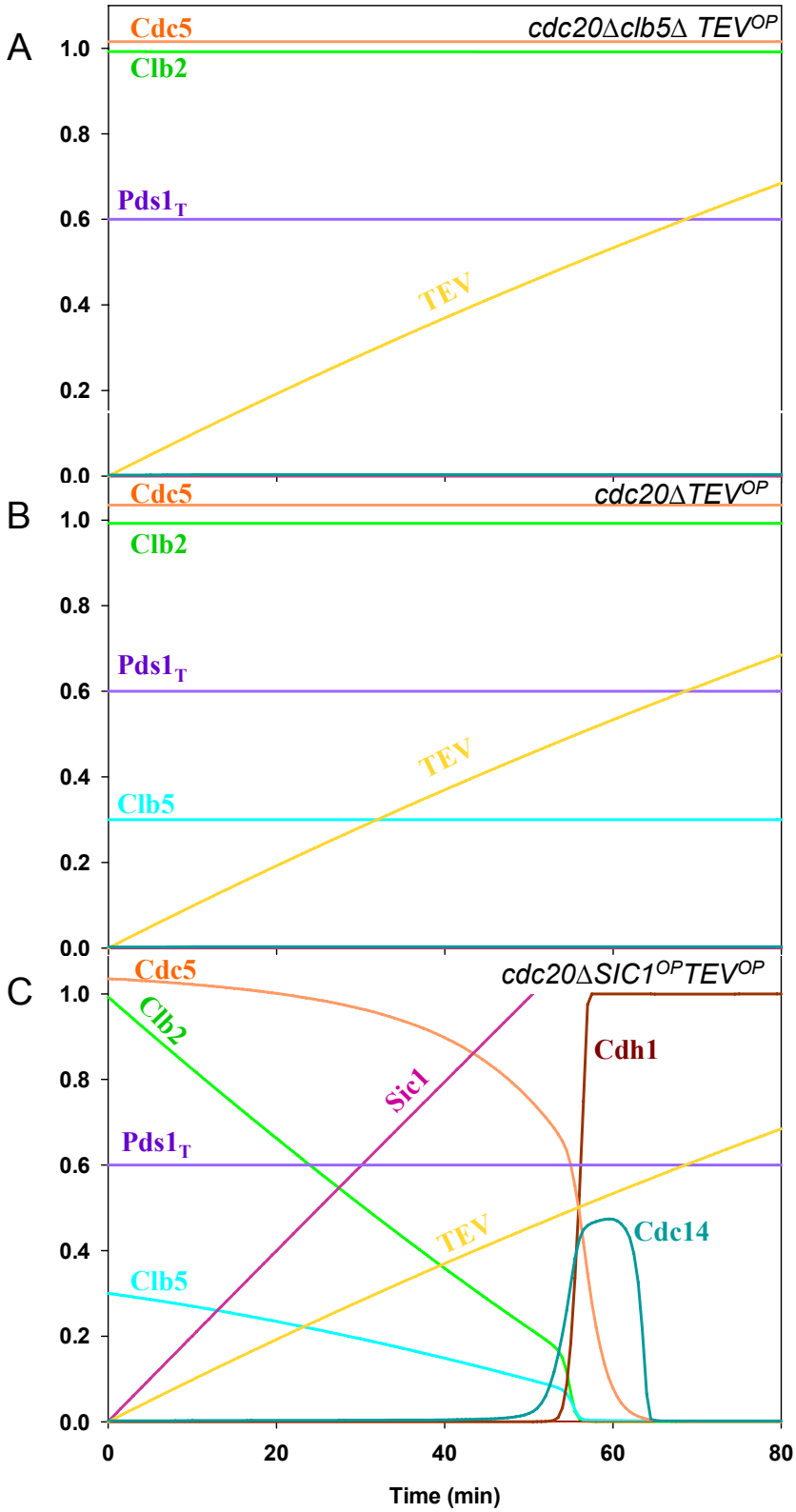


**Figure II - 4: Numerical simulations of mitotic progression in: (A) *cdc20Δclb5Δ* cells with TEV overexpression ($k_{s20}$=0; Initial Conditions: $[Clb5_T]$ = 0.15; $[Esp1_T]$ = $[Esp1_B]$ = 0; $k_{ssep}$ = 0.01 $min^{-1}$, $k_i$ = 0, $l_{apds}$=0); (B) *cdc20Δ* cells with TEV overexpression; (C) *cdc20Δ* cells with TEV overexpression and non-degradable SIC1 overexpression ($k_{dsic}$'=0.0005 $min^{-1}$; $k_{dsic}$=$k_{dsic}$"=0; $k_{ssic}$=0.015 $min^{-1}$) .**

## 4. The logic of the mitotic exit process in budding yeast

The results simulated until this point allow us to outline the existence of a hierarchy in the network controlling mitotic exit (Figure II - 5). At the top of this hierarchy is Cdc20 because its depletion causes an early mitotic block in metaphase. Clearly, APC/Cdc20-dependent poli-ubiquitylation of proteins, which targets them for degradation by the proteasome, is required for mitotic progression and mitotic exit. MV2 indicates that the three crucial substrates of APC/Cdc20 are Pds1, the S phase cyclins (Clb5) and the M phase cyclins (Clb2) (Morgan, 2007a), which are conceptualised as three different pathways. In the first pathway, Pds1 degradation activates Esp1, which brings about anaphase (Nasmyth et al., 2000) and Cdc14 release through two different networks (FEAR and MEN) (Bardin et al., 2000; Sullivan and Uhlmann, 2003). This pathway is called the Cdc14 pathway. The other two pathways are triggered by the degradation of the B-type cyclins: the S phase cyclins (Clb5) and the M phase cyclins (Clb2); and are named accordingly. Both of these cyclins activate CDK1, which keeps their target proteins phosphorylated, and prevents mitotic exit. Thus, in order to exit mitosis, the B-type cyclins must be degraded, allowing the CDK1 substrates to be dephosphorylated by Cdc14 (Visintin et al., 1998). In this way, it is evident that the three pathways (Cdc14, Clb5 and Clb2) converge at the level of their substrates to bring about mitotic exit. Among these substrates, are Sic1 and Cdh1, whose activation is crucial to conclude the exit process. These components are responsible for the creation of two double-negative feedback loops:

- APC/Cdh1 promotes Clb2 degradation, while Clb2/CDK1 promotes Cdh1 degradation;
- Sic1 inhibits both Clb2/CDK1 and Clb5/CDK1, which in turn inhibit Sic1 transcription factor (Swi5) and phosphorylate Sic1.

The known outcome of a double-negative feedback loop is a switch-like behaviour of the system, and thus, these antagonistic relationships result in an abrupt activation of Sic1 and Cdh1 in G1 phase, and in their abrupt inactivation during S/G2/M phases. Accordingly, the reverse behaviour is observed for Clb/CDK1 activity (Chen et al., 2004; Chen et al., 2000).

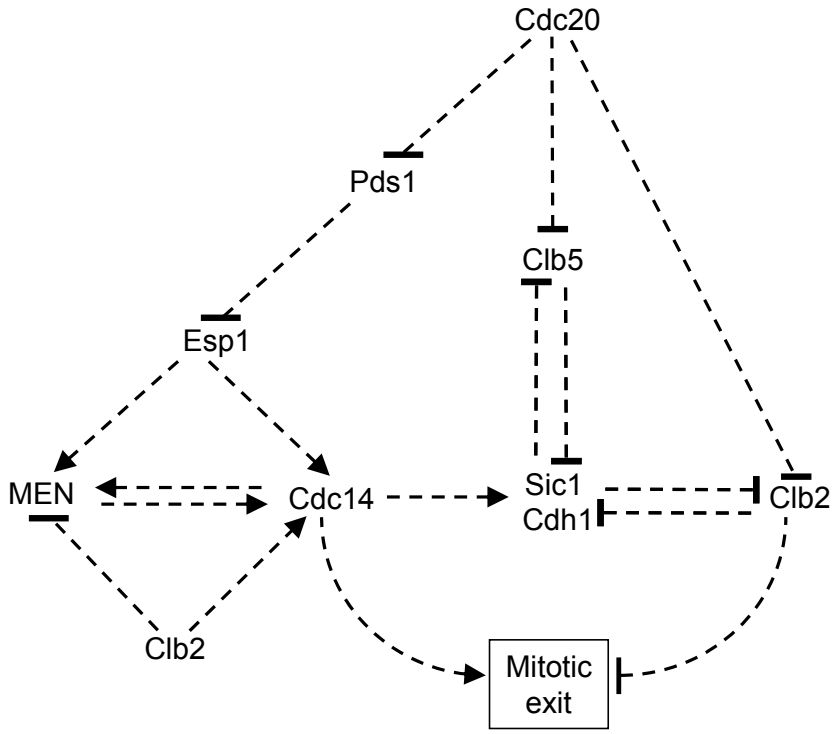


**Figure II - 5: The hierarchy of the mitotic exit controlling network. APC/Cdc20, at the top of the hierarchy, promotes mitotic exit via three different pathways directed by its substrates Pds1, Clb5 and Clb2. The mitotic exit process is amplified by Cdc14-MEN positive feedback loop and the double-negative feedback loops between Clb-kinases and their negative regulators (Sic1 and Cdh1).**

## *5. Non-degradable Clb5*

Previously, it was shown how cells progress in the absence of Cdc20 when different APC/Cdc20 substrates were deleted. In this section, the focus is on a single APC/Cdc20 substrate, Clb5, and on how cells progress when this substrate becomes resistant to degradation.

The Cdc20 block and release experiment synchronises the mitotic exit process by triggering the degradation of three substrates (Pds1, Clb5 and Clb2) and thus activating three exit pathways (Figure II - 5). Therefore, the use of a Cdc20 substrate resistant to degradation reveals the individual contribution of the corresponding pathway in mitotic exit. Previously, MV1 addressed the situation of a non-degradable securin (PDS1-mdb) of which the phenotype is a metaphase arrest (Figure I - 6A). Clearly, the Pds1 pathway makes a crucial contribution to mitotic exit.

Here, MV2 was used to test the importance of the Clb5 pathway, by simulating a mutant situation involving non-degradable Clb5. Figure II - 6 shows that Sic1 synthesis and Cdh1 activation are compromised by the constant level of Clb5. This slows down Clb2 downregulation but is not sufficient to block mitotic exit completely; cells can still exit mitosis after a delay. Apparently, cells can exit mitosis with only the activation of the Pds1 and Clb2 pathways; in these circumstances, the Clb5 pathway can be neglected.

Hence, MV2 is able to simulate experimental results demonstrating that cells expressing a stable version of Clb5 have no problem in exiting mitosis (Sullivan et al., 2008; Wasch and Cross, 2002). Nevertheless, it has been reported that persistent Clb5/CDK1 activity causes replication-licensing problems in S phase, leading to a loss of viability (Wasch and Cross, 2002).

The inactivation of the Clb2 pathway, using a non-degradable Clb2 (Clb2-kd), was shown to prevent mitotic exit by MV1, as described in Chapter I (Figure I - 7). Similar to the Pds1 pathway, the Clb2 pathway has to be activated in order for cells to exit mitosis. However, MV2 is as limited as MV1 in reproducing the phenotype of Clb2-kd cells. These two models fail to explain experimental results showing Cdc14 recapture into the nucleus after its release during anaphase (Lu and Cross, 2009a). This issue will be addressed in Chapters III and IV.

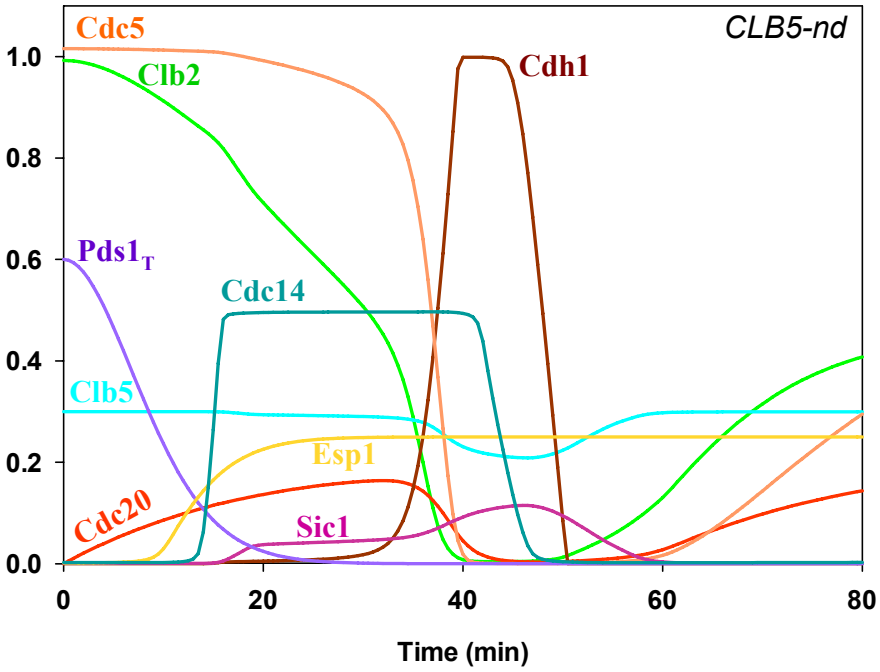


**Figure II - 6: Numerical simulation of a Cdc20 block and release situation in cells with non-degradable Clb5 ($k_{dclb5}$=$k_{dclb5}$'=0).**

## 6. *The role of Polo kinase Cdc5 in Cdc14 release*

In MV2, the FEAR network is controlled by the combined impact of Cdc5, Clb2 and Esp1 on Cdc14 release (see equation for Net1 in Appendix 1b). This change was made in order to reproduce the mutant situations of *cdc5*Δ and *cdc5*Δ*ESP1*$^{OP}$ cells, which could not be explained with MV1.

As depicted in Figure II - 7, both *cdc5*Δ and *cdc5*Δ*ESP1*$^{OP}$ mutants fail to release Cdc14, consistent with experimental results (Stegmeier et al., 2002; Visintin et al., 2008). In the updated model, where Cdc5 is now required to phosphorylate Net1, Cdc5 inactivation prevents Cdc14 release. This is because Clb2 by itself is no longer strong enough to phosphorylate Net1, even whilst PP2A is being downregulated by overexpression of Esp1 (Figure II - 7B).

MV2 is able to capture the phenotypes of the *cdc5*Δ and *cdc5*Δ*ESP1*$^{OP}$ mutants; however, the outcome of these simulations is strongly dependent on the choice of

appropriate parameter values for Net1 phosphorylation. For example, a slight increase in the rate of Net1 phosphorylation by Clb2 kinase is sufficient to trigger a transient release of Cdc14. Overall, MV2 provides us with accurate results, and its sensitivity to parameter changes will be addressed further in Chapter IV.

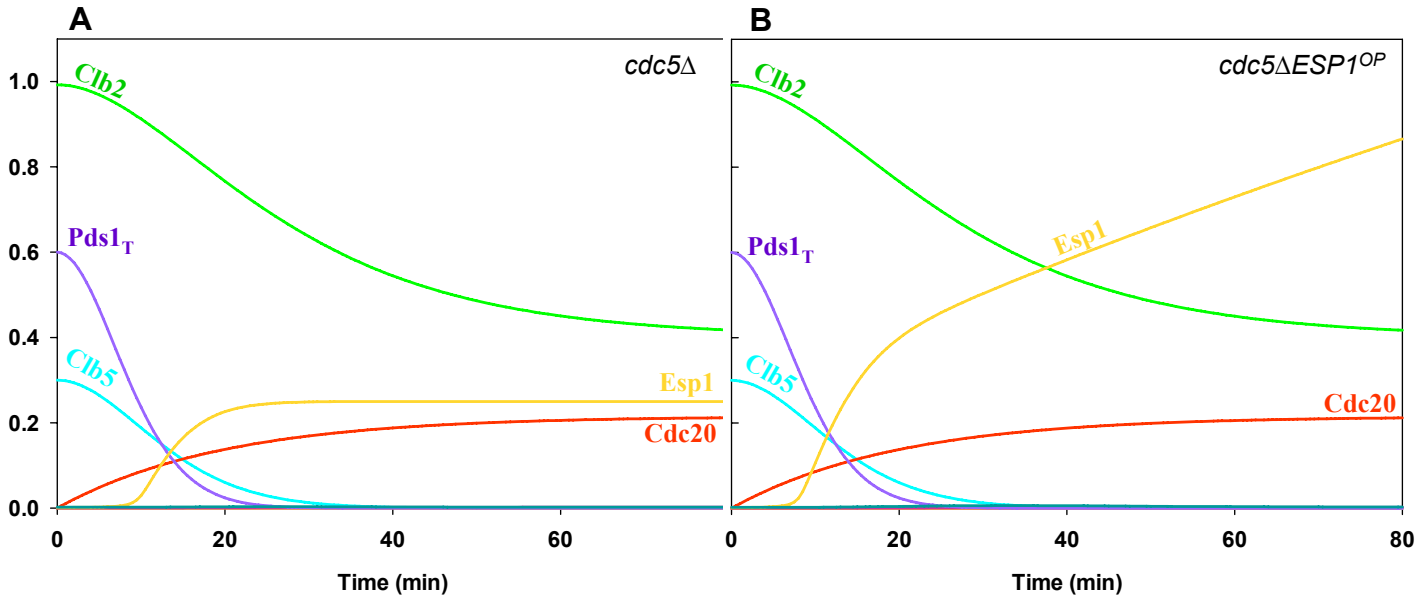


**Figure II - 7: Numerical simulations of mitotic progression after Cdc20 release in cells (A) depleted of Cdc5 activity ($k_{apolo}$ = $k_{apolo}$' = 0, Initial Conditions: [$Polo_T$] = [Polo]= 0) (B) and with Esp1 overexpression ($k_{sesp}$ = 0.01 $min^{-1}$).**

# Chapter III – Cdc14 Activity in Mitotic Exit

Despite the alterations made to QM in Chapters I and II, there are still a number of experimental results that none of the models can address, such as the *cdc20*Δ*ESP1*$^{OP}$ cells in nocodazole, *Clb2-kd* cells and *cdc15*Δ*net1*Δ cells. In this chapter, MV2 is further developed in order to explain these different mutant situations. The new model is referred to as MV3 (Model Version 3) and maintains the ability to simulate all of the experimental situations already explained by MV1 and MV2.

## *1. Oscillatory Dynamics of the model*

MV1 and MV2 both simulate a tightly defined window of the cell cycle; they start with a metaphase block and finish when cells exit mitosis and enter G1. This restricts the number of experimental situations that can be studied using these models. Synthesis terms for Pds1 and Clb5 were incorporated into MV3, allowing these components to be re-synthesised and cells to enter a new cycle (see Figure III - 1B and the parameter set in Appendix 1c, together with equations for Pds1 and Clb5).

The characteristics of cycling cells are distinct from those in the Cdc20$^{b/r}$ situation. These differences are caused mainly by the regulation of Clb2 levels. When cells are arrested in metaphase, Clb2 accumulates to a high degree due to the lack of APC activity. This level is not achieved in cells that progress normally in the cell cycle, because APC/Cdc20 is activated before Clb2 can reach its steady-state level. Indeed, it has been shown experimentally that arrested cells can accumulate twice as much Clb2 as cycling cells (Drapkin et al., 2009; Yeong et al., 2000). MV3 was parameterised in

order to be consistent with these observations, and thus, Clb2 levels reach 1.0 in metaphase arrested cells, and over 0.4 in cycling cells.

In MV3, a release from the metaphase block results in a limit cycle oscillation. The characteristics of this limit cycle depend on the Clb5 unregulated synthesis term, which allows Clb5 to be re-synthesised after Cdc20 is degraded by APC/Cdh1. The increased level of Clb5 promotes the inactivation of Cdh1 and the degradation of Sic1. This effect turns the antagonistic switch towards Clb2 activation. The negative feedback loop (whereby Clb2 promotes Cdc20 synthesis) is then triggered, leading not only to Clb2 degradation but also to Clb5 degradation. Cdc20 also activates Cdc14 (through Pds1 degradation), which helps to activate Cdh1 and Sic1. In this way, the observed oscillations are driven by the combination of negative feedback loops and double negative feedback loops present in the network (Figure III - 1A).

However, it must be noted that the limit cycle oscillations present in MV3 lack proper G1 control, and thus they do not represent a plausible budding yeast cell cycle. Cdh1 and Sic1 are used as G1 indicators, but their regulation is controlled solely by S and M phase cyclins.

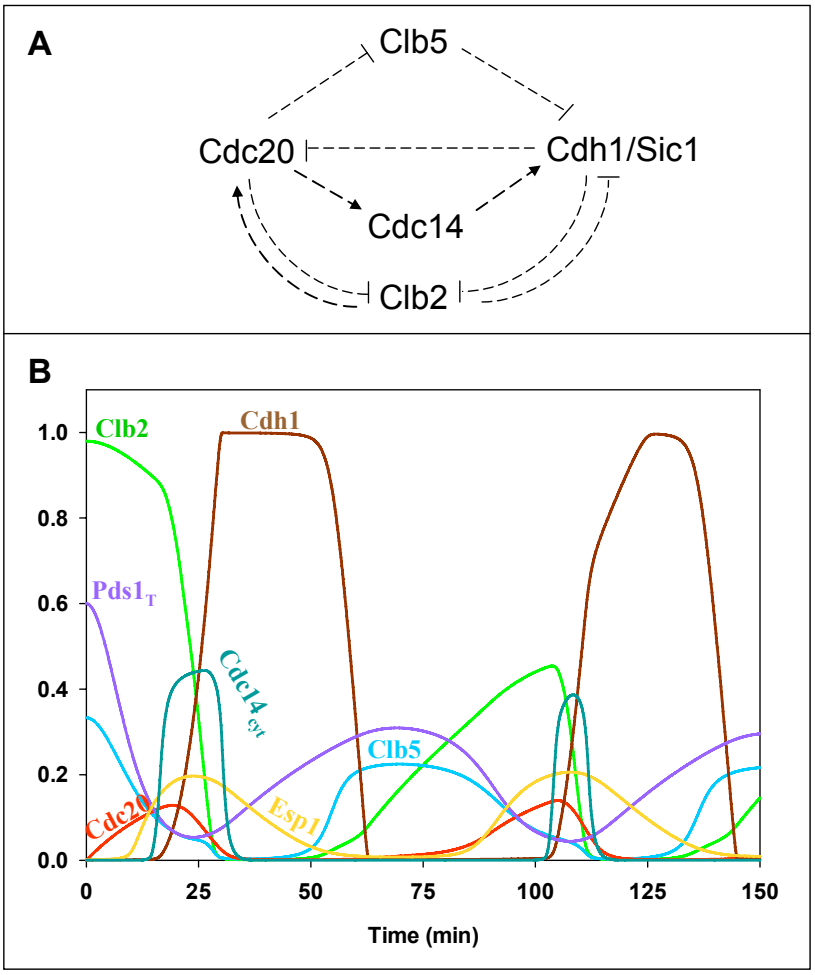


**Figure III - 1: Limit Cycle Oscillations. (A) Network motif responsible for driving oscillations in the model. (B) Numerical simulation of wild-type cells. The initial conditions were set from a Cdc20 block ($k_{s20}$= $k_{s20}$'=0). At time zero, Cdc20 synthesis is induced (t = 0, $k_{s20}$ = 0.001 $min^{-1}$, $k_{s20}$' = 0.01$min^{-1}$) and the simulation is run for 150 minutes.**

## 2. *Cdc14 Nuclear Export*

Cdc14 localization depends on many factors, although Net1-mediated Cdc14 inhibition was commonly thought to be the most important. For most of the cell cycle, Cdc14 is sequestered in the nucleolus by Net1, and only when Net1 is phosphorylated during mitosis, Cdc14 is released into the nucleus. Recent results show that other factors also contribute for Cdc14 localization (Lu and Cross, 2009a; Mohl et al., 2009). After being released from the nucleolus, Cdc14 must migrate from the nucleus to the

cytoplasm to trigger mitotic exit. Lu and Cross (2009) have demonstrated that MEN is essential for this process, whereas Net1 is not (provided Net1 is phosphorylated and cannot bind to Cdc14). A detailed description of these experiments is included in Chapter I. Although the migration process is fairly independent of Net1, it is particularly dependent on Dbf2-Mob1, a MEN kinase. This kinase phosphorylates Cdc14 on residues adjacent to a nuclear localization signal (NLS), and thus, inhibits its NLS activity (Mohl et al., 2009). In other words, MEN promotes the retention of Cdc14 in the cytoplasm once Cdc14 leaves the nucleus.

In MV3, there are two distinct forms of released Cdc14: nuclear and cytoplasmic. It is considered that Cdc14 can be released into the nucleus and then into the cytoplasm, in a regulated fashion. The Net1:Cdc14 complex is restricted to the nucleolus and Net1 phosphorylation releases Cdc14 into the nucleus. The shuttle of Cdc14 between the nucleus and the cytoplasm is solely regulated by MEN (Figure III - 2). This could have been done in two ways: by considering that MEN inhibits Cdc14 import to the nucleus, or by considering that MEN promotes Cdc14 export to the cytoplasm. In this analysis, MEN promotes the cytoplasmic migration of Cdc14 to the cytoplasm by increasing the export rate of Cdc14 from the nucleus (see Methods section and equations for cytoplasmic Cdc14, Cdc14c, and for nuclear Cdc14, Cdc14n, in Appendix 1c).

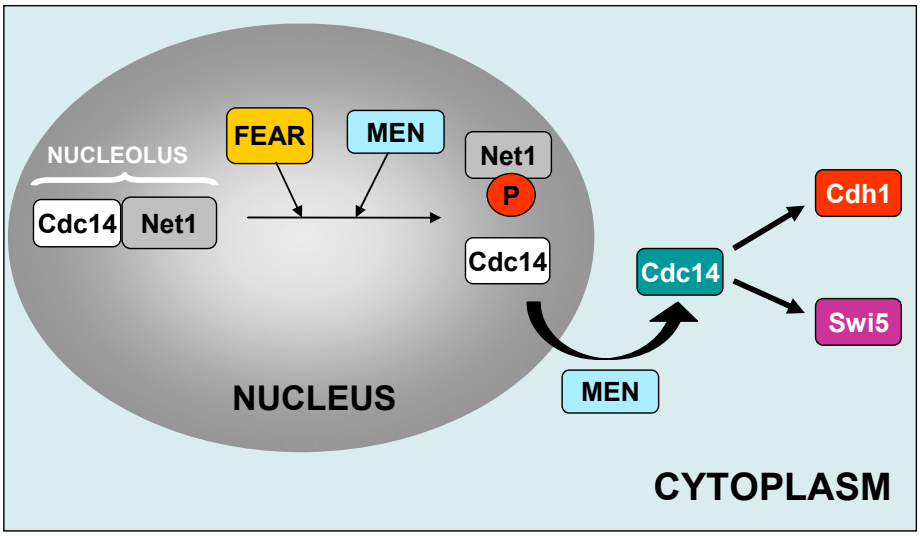


**Figure III - 2: Cdc14 cellular compartmentalisation. Cdc14 bound to Net1 is inactivated and localises in the nucleolus: nucleolar Cdc14. FEAR and MEN kinases promote Net1 phosphorylation and Cdc14 is released from the complex and goes into the nucleus: nuclear Cdc14. MEN kinases phosphorylate Cdc14 on residues adjacent to a nuclear localization signal and thus promote Cdc14 export to the cytoplasm: cytoplasmic Cdc14.**

### *a. Spindle elongation and MEN activation*

This new level of Cdc14 compartmentalisation has proven very helpful in explaining some of the experimental results that the previous models (QM, MV1 and MV2) could not. For example, Cdc14 compartmentalisation can provide insights into the contradictory phenotypes of *cdc20ΔESP1*$^{OP}$ cells in nocodazole (no spindle elongation).

According to MV1 and MV2, Cdc14 cannot be released through MEN in this scenario, because MEN is not activated in the presence of nocodazole. However, Cdc14 can be released through FEAR network activation.

According to MV3, FEAR is responsible for nuclear Cdc14 release, but cannot promote a full release to the cytoplasm (Figure III - 3). MEN would normally fulfil this role, but with MEN activity blocked by nocodazole, there can be no Cdc14 migration to the cytoplasm. Thus, MV3 predicts that Cdc14 should be released from the nucleolus into the nucleus, but not from the nucleus into the cytoplasm. This is consistent with Lu

and Cross (2009) findings that Cdc14 was not visible in the cytoplasm, but was scattered in the nucleus.

Surprisingly, two other experimental studies did report the detection of Cdc14 release in the same genetic setting (Sullivan and Uhlmann, 2003; Visintin et al., 2003). Although this would appear to contradict the findings of Lu and Cross (2009), it could be explained by a difference in the interpretation of their experimental observations. It is possible that, in both studies, the authors quantified only the nuclear release of Cdc14. In contrast, Lu and Cross (2009) probably neglected the nuclear release, and concluded that there was no Cdc14 release because they did not observe Cdc14 in the cytoplasm. Thus, according to MV3, these experimental results are not contradictory; in fact they are perfectly consistent.

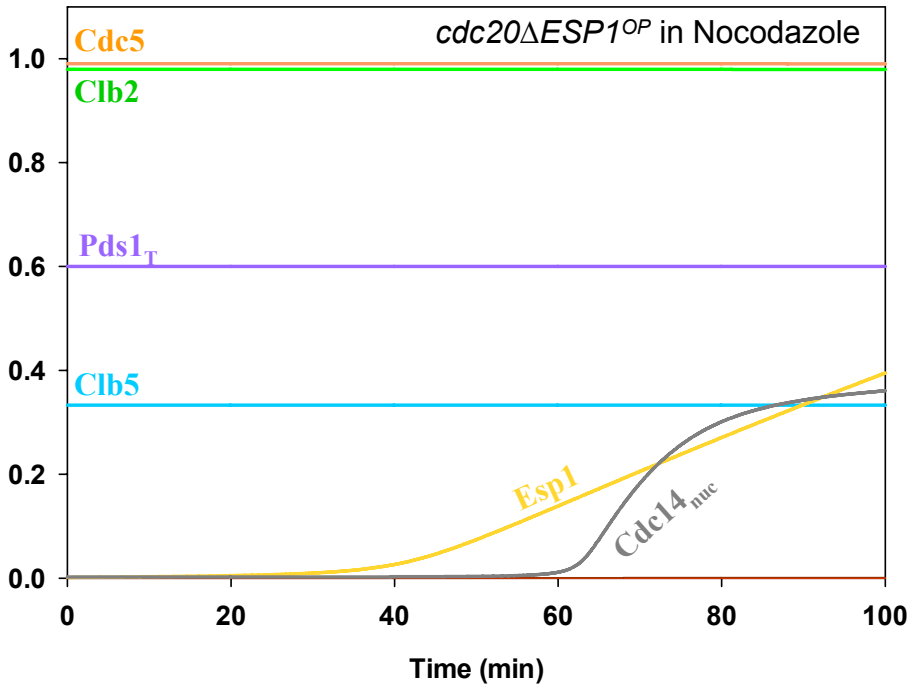


**Figure III - 3: Effect of nocodazole in cells depleted of Cdc20 ($k_{s20} = k_{s20}' = 0$) and overexpressing separase ($k_{sesp} = 0.01\ min^{-1}$). Nocodazole inhibits spindle elongation which is a requirement for Tem1 activation. In these cells, Tem1 is inactive ($k_{atem} = k_{atem}' = 0$).**

### *b. Cdc14 endocycles with non-degradable Clb2*

Lu and Cross (2009) have demonstrated that Cdc14 is released and recaptured in cells expressing a non-degradable version of Clb2 (Clb2-kd). Studying this phenomenon further, they showed that Cdc14 localization oscillates from released to recaptured, despite the mitotic block caused by high activity of CDK1 (Lu and Cross, 2010). These results have been confirmed by another research group (Manzoni et al., 2010).

To address this phenomenon, MV3 was parameterised according to the experimental procedure used by Lu and Cross (2010). The authors blocked cells in metaphase by methionine repressible Cdc20 (MET3-Cdc20), and transiently induced a non-degradable Clb2 (Clb2-kd, lacking both destruction and KEN boxes) to various levels. The expression level of non-degradable Clb2 was estimated by the GFP signal attached to Clb2, and its value was related to the Clb2 peak value during the wild-type cycle[1]. The expression of non-degradable Clb2 was terminated at the point of Cdc20 re-induction, and the effect of different levels of Clb2-kd on mitotic progression was analysed in single cells. Figure III - 4A depicts these simulations, with Clb2-kd expression (Clb2nd = 0.5) roughly equal to the peak value during the normal mitotic cycle. After Cdc20 induction, Cdc14 is activated, while Cdc5 and endogenous Clb2 are degraded by activated APC/Cdh1. Observe that the active Clb2 level (the sum of non-degradable and endogenous Clb2, without the inactive complex Clb2/CDK1/Sic1) drops to the value of Clb2-kd (0.5). Despite of the mitotic block caused by high CDK1 activity, Cdc14 continues to oscillate, a phenomenon called Cdc14 endocycles by Lu and Cross (2010). Notice that the Clb2 curve shows oscillations of small amplitude around the value of Clb2-kd, because Sic1 is periodically activated by Cdc14 and forms an inactive trimer with Clb2/CDK1.

[1] Clb2 mitotic peak value is assigned to one by Lu & Cross (2010) and it corresponds to 0.5 in the model.

Cdc14 endocycles are an abnormality that arises from the underlying properties of cell cycle control. A clear explanation of this phenomenon is important to better understand the molecular network controlling the cell cycle engine. For this reason, a detailed analysis of the Cdc14 endocycles was conducted, involving the simulation of different mutant situations that have been reported in the literature (Lu and Cross, 2010; Manzoni et al., 2010).

According to MV3, the cell cycle regulators responsible for Cdc14 endocycles can fall into one of two categories: components that create the right conditions for the oscillatory behaviour, and components intrinsic to the mechanism itself. For instance, Cdc20 and Esp1 have important roles in initiating Cdc14 endocycles, but after the initiation, they become independent of both Cdc20 and Esp1 (Manzoni et al., 2010). Figure III - 4B shows that once Pds1 and Clb5 are degraded, Cdc20 is no longer required to maintain the endocycles. Similarly, a non-degradable version of Cdc20 does not disrupt the endocycles (Figure III - 4C).

Cdc20-mediated degradation of Pds1 and Clb5 are important for the generation of the endocycles, while Cdc20-mediated degradation of Clb2 is not. Expression of a non-degradable version of Pds1 in a *CLB2-kd* background arrests the endocycles, with Cdc14 captured in the nucleolus (Figure III - 4D). Hence, Cdc20-mediated degradation of Pds1 is crucial to promote Esp1 activation and the subsequent activation of FEAR and MEN, the two networks responsible for Cdc14 release and therefore the endocycles. Clb5 degradation is no less important since a non-degradable Clb5 also disrupts the endocycles (Figure III - 4E). Although Cdc14 is released in this scenario, Cdh1 is kept inactive due to the high level of Clb5. This suggests that Cdh1 is necessary for Cdc14 recapture rather than its release during the endocycles. Finally, the Cdc20-mediated degradation of endogenous Clb2 proves to be irrelevant to the endocycles. As depicted

in Figure III - 4F, Cdc14 activity oscillates perfectly without endogenous Clb2. Rather, it is the high level of non-degradable Clb2 that promotes the Cdc14 endocycles.

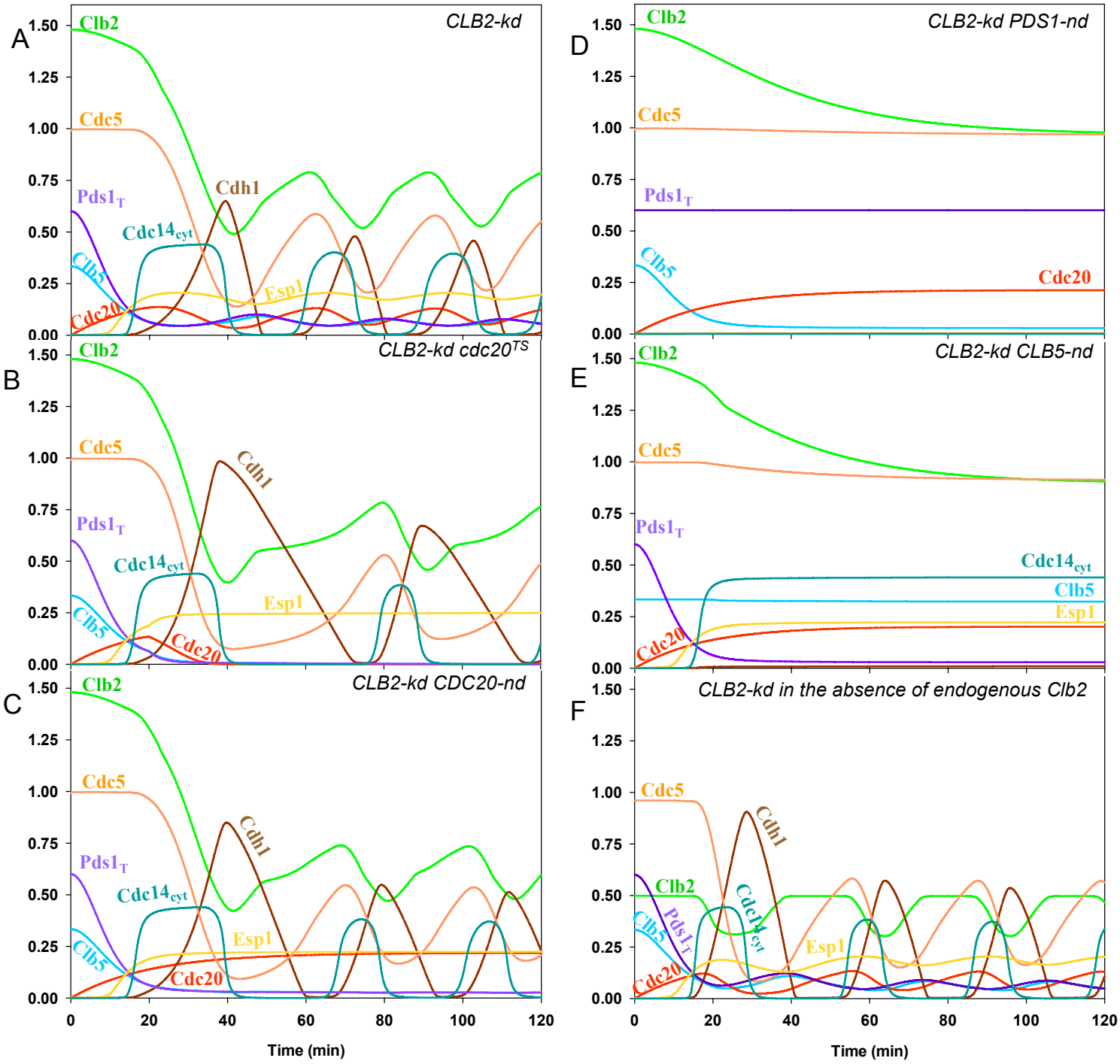


**Figure III - 4: Numerical simulations of mitotic progression after Cdc20 release in cells with non-degradable Clb2 (Clb2nd = 0.5). (A) The parameter Clb2nd is set to 0.5 to simulate the effect of KEN- and destruction box deficient (dbΔ) Clb2 on mitotic progression. (B) and (C) Cdc20 role in the Cdc14 endocycles is connected with Pds1 and Clb5 degradation. (B) Simulation was run for 20min as in (A) after that Cdc20 was inactivated (temperature sensitive allele – $k_{s20} = k_{s20}' = 0$) and Pds1 and Clb5 were not allowed to be re-synthesised ($k_{sclb5} = 0$, $k_{spds} = 0$). (C) Cells with non-degradable Cdc20 ($k_{d20}' = 0$). (D), (E) and (F) Cdc20 targets immune to degradation and Cdc14 endocycles. (D) Cells with non-degradable Pds1 ($k_{dpds}' = 0$); (E) Cells with non-degradable Clb5 ($k_{dclb5} = 0$); (F) Cells with no endogenous Clb2 ($k_{sclb2} = k_{sclb2}' = 0$; Initial Conditions $[Clb2_T] = 0$).**

Cdh1 falls within the category of components intrinsic to the mechanism of Cdc14 endocycles. MV3 shows that in the absence of Cdh1, cells are blocked in a stable steady-state with Cdc14 released in the cytoplasm. The resulting phenotype is similar to the *CLB5-nd* block (compare Figure III - 4E with Figure III - 6A).

Since the degradation of Cdc20 and endogenous Clb2 is not important for the endocycles, Cdc5 must be the Cdh1 substrate most crucial for the oscillatory behaviour. Indeed, Cdc5 deletion prevents Cdc14 release in Clb2-kd cells. Thus, Cdc5 must be a core component of the endocycle mechanism (Figure III - 6B).

The proactive contribution of Cdc14 to the endocycle phenomenon can also be tested. Manzoni et al. (2010) used a temperature sensitive Cdc14-1 mutant protein in cells overexpressing stable Clb2, to test if an inactive form of Cdc14 would still oscillate. The experiment was conducted so as to inactivate Cdc14 only after cells had entered anaphase and released Cdc14. It was shown that after the temperature shift, these cells did not exhibit Cdc14 endocycles. This is a consequence of the fundamental role Cdc14 plays in phosphorylating and activating Cdh1, despite the high level of Clb2. Without Cdc14 activity, Cdh1 is strongly inhibited and the endocycles cannot take place (Figure III - 6C).

Together with Cdc14, Cdh1 and Cdc5 define the negative feedback loop (Cdc14 $\rightarrow$ Cdh1 $\dashv$ Cdc5 $\rightarrow$ Cdc14, see Figure III - 5) that is responsible for driving Cdc14 endocycles (Lu and Cross, 2010; Manzoni et al., 2010). Another negative feedback loop involving Cdh1 and Cdc5 is present in the system, this time through Cdc20 (Cdc20 $\dashv$ Clb5 $\dashv$ Cdh1 $\dashv$ Cdc20, see Figure III - 5). However this loop is not required for the endocycle phenomenon. As depicted in Figure III - 4C, Cdc14 activity maintains its periodic oscillations even if Cdc20 is not degraded by Cdh1 and stays at a constant value in the system.

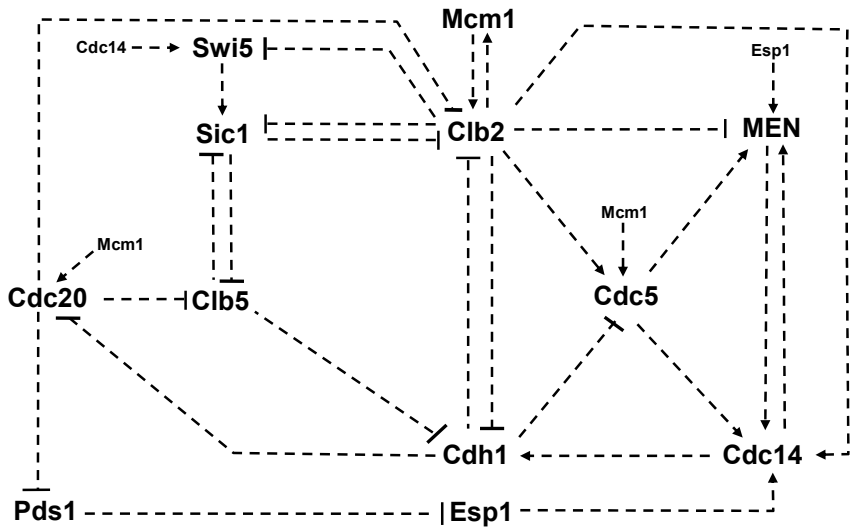


**Figure III - 5: Positive and negative interactions among the main cell cycle regulators present in MV3.**

The MEN kinase Cdc15 is another component that contributes to the Cdc14 endocycles. As shown in Figure III - 6D, the deletion of Cdc15 blocks the endocycles. According to MV3, MEN has a dual role in this phenomenon. On one hand, MEN and Cdc14 are part of a positive feedback loop whereby MEN activates the phosphatase and Cdc14 activates Cdc15 by promoting its dephosphorylation. This positive feedback loop is important to overcome the high level of inhibition on Cdc15 from non-degradable Clb2. On the other hand, MEN is essential for promoting Cdc14 cytoplasmic localization; without this, the endocycles cannot take place.

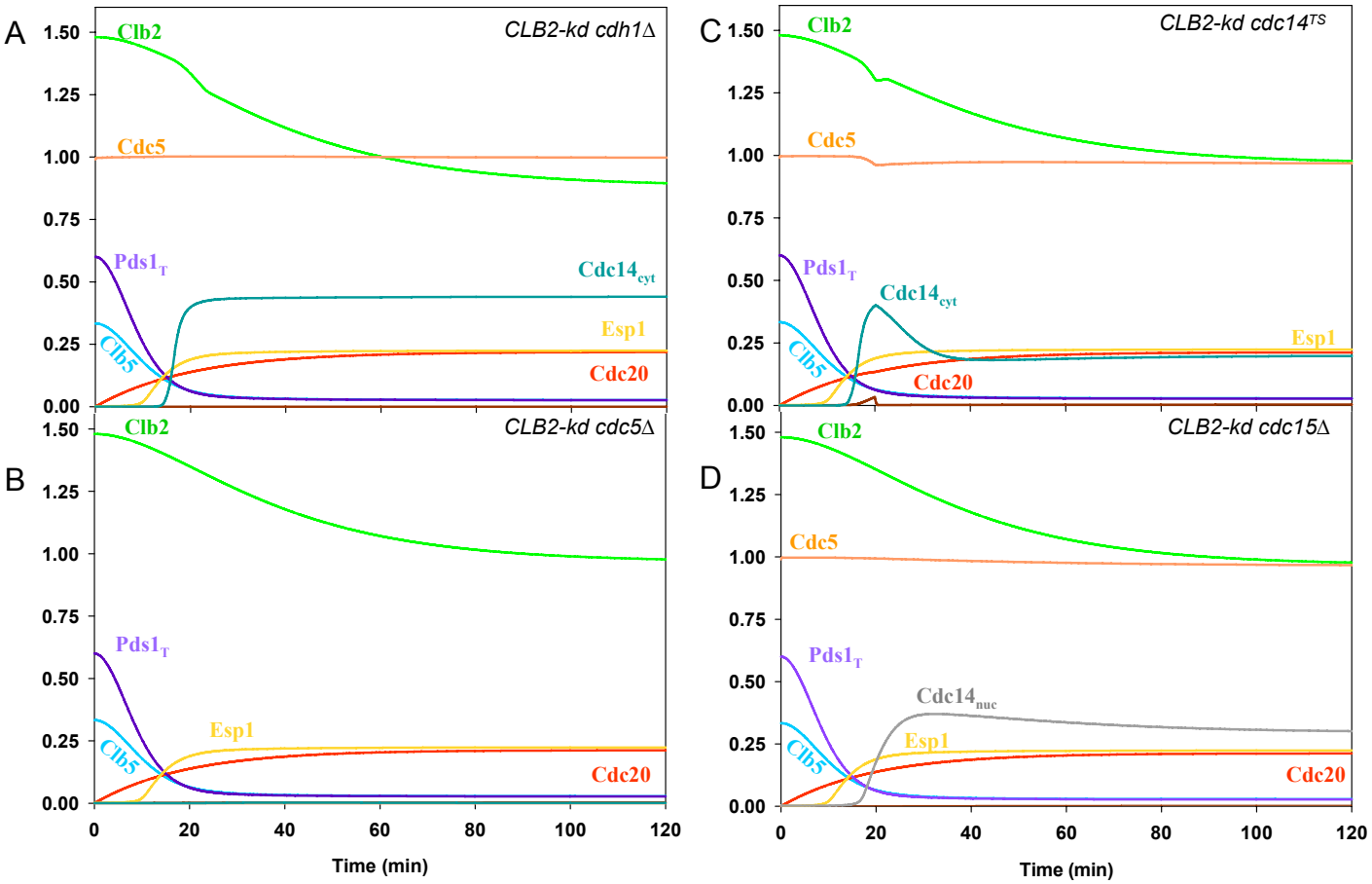


**Figure III - 6: Cdh1 activity, Cdc5 degradation and MEN activity are required for Cdc14 endocycles. Numerical simulations of mitotic progression in cells with non-degradable Clb2 (Clb2nd = 0.5) (A) lacking Cdh1 activity ($k_{dcdh} = k_{dcdh}' = 0$); (B) depleted of Cdc5 ($k_{dpolo} = k_{dpolo}' = 0$; Initial Conditions: $[Polo_T] = [Polo] = 0$ ); (C) with Cdc14 inactivated after 20min from Cdc20 release (temperature sensitive allele – $k_{dcdh}'=0$, $k_{aswi}'=0$, $k_d'=0$, $k_{ac15}'=k_{ac15}''=0$); (D) lacking MEN activity ($k_{ac15} = k_{ac15}'=0$).**

## 3. *Nuclear Cdc14 versus Cytoplasmic Cdc14*

The distinction between the nuclear and cytoplasmic forms of Cdc14 is a very important addition to MV3, since it allows the model to explain the contradictory phenotypes of *cdc20ΔESP1*$^{OP}$ cells exposed to nocodazole, and the newly discovered phenomenon of Cdc14 endocycles. In MV3, it is assumed that Cdc14 released in the nucleus cannot dephosphorylate its substrates (e.g. Cdh1, Swi5, etc.) in the cytoplasm. This assumption can be questioned however, as will be explained.

MV3 predicts that in the *net1*Δ*cdc15*Δ mutant, Cdc14 is released into the nucleus but not the cytoplasm, so cells should be unable to exit mitosis (see Figure III - 7B). According to experimental results however, Net1 deletion is able to restore the viability of the *cdc15*Δ mutant (Lu and Cross, 2009a; Shou et al., 1999). Hence, the assumption that nuclear Cdc14 is unable to act on its substrates cannot be true. In *net1*Δ cells, Cdc14 is released into the nucleus and MEN promotes its migration to the cytoplasm during mitosis. In *net1*Δ*cdc15*Δ cells, this full-scale migration of Cdc14 to the cytoplasm does not take place. Thus, it is probable that a small proportion of Cdc14 substrates are constantly migrating from the cytoplasm to the nucleus and vice versa, making this mutant viable. The inconsistency between MV3 and these experimental results will be addressed in the next chapter.

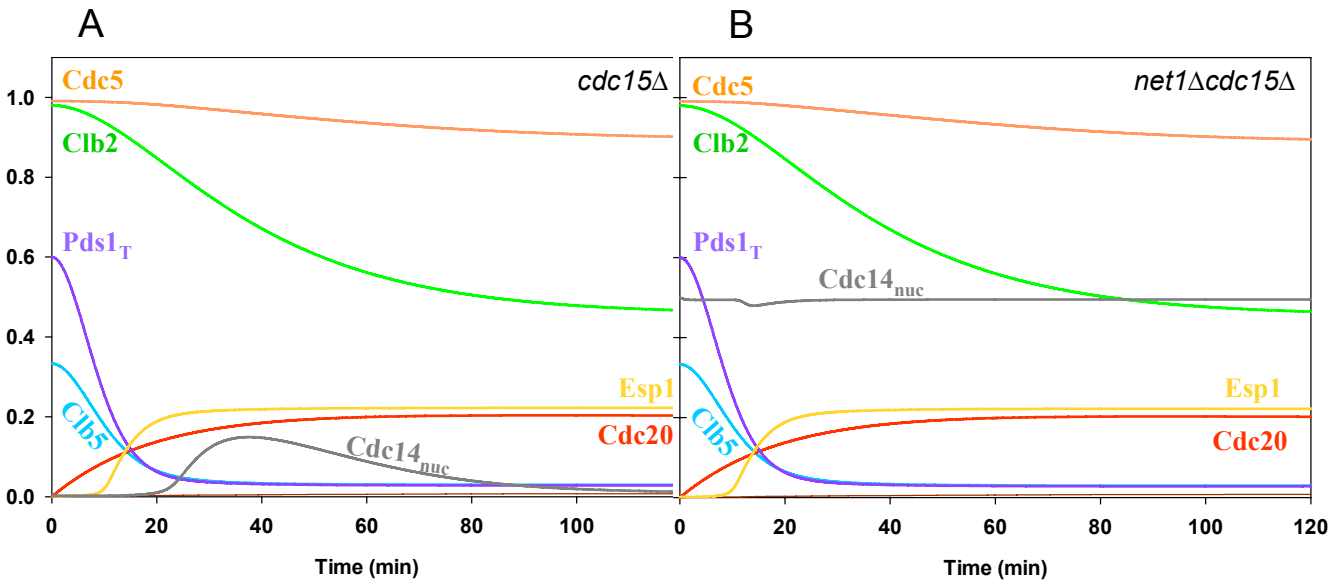


**Figure III - 7: Numerical simulations of mitotic progression after Cdc20 release in cells depleted of MEN activity (Cdc15 deletion) and Net1. (A) Cells with Cdc15 deletion ($k_{ac15} = k_{ac15}' = 0$). (B) Cells with Cdc15 deletion and Net1 deletion ($Net1_T$=0; Initial Conditions [Net1] = [RENT] = 0; [Cdc14n] = 0.5).**

# Chapter IV – Comprehensive Characterization of Cdc14 Endocycles

In this chapter, the model is improved to overcome the limitations of MV3. The new model, MV4 (model version 4), is consistent with all mutant phenotypes analysed with the previous models (see Appendix 3) and provides a more a comprehensive view of the dynamical control of mitotic exit.

## *1. G1 phase*

MV3 is not restricted to the time window from metaphase to G1 phase, as is the case for MV1 and MV2. As is shown in Figure III - 1B, MV3 can describe cell cycle progression after the exit from mitosis. However, the oscillatory behaviour present in MV3 lacks any clear G1 regulation. Cdh1 and Sic1 are used to indicate when the cell has entered the next G1 phase; however, their regulation depends on the S and M phase cyclins, which are Clb5 and Clb2, respectively.

In order to improve the description of G1 phase in MV4, the G1 phase cyclins were incorporated, (i.e., the Cln-kinases Cln1, Cln2 and Cln3). Like the Clb-kinases, the Cln-kinases are responsible for degrading Sic1; however, they do not bind to Sic1, and thus escape its inhibitory effect. As a result, the Cln-kinases are important to promote the START transition before the S-phase cyclins are activated.

Cln regulation depends on the transcription factor SBF, while S-phase Clb regulation depends on the transcription factor MBF (Dirick et al., 1995). These two transcription factors have a very similar regulation, and thus they were incorporated into the model as a single component called MBF (see complete molecular network in Figure 2). In

budding yeast cells, MBF activation is controlled by size; the transcription factor can only be activated once cells have reached a critical size. Because MV4 does not consider cell size control, MBF regulation by cell size has been ignored. Therefore, MBF is solely regulated by the inhibitory action of Clb/CDK1 activity, and can only be activated during G1 phase (Dirick et al., 1995).

The absence of cell size control is a valid assumption for a large budding yeast cell, because the cell has already achieved the critical size to undergo the START transition. Since budding yeast cells undergo asymmetric cell division, the mother cell is large while the daughter cell is small and fails to satisfy the critical cell size. Hence, size only becomes a rate-limiting factor (for the START transition and MBF activation) in the small daughter cell.

By incorporating MBF and Cln, MV4 describes a complete cell cycle; however, by ignoring the cell size-dependent regulation of MBF activation, this description is restricted to a cell cycle occurring in a large mother cell. Figure IV - 1 depicts mitotic exit after the cell is released from a Cdc20 block, and also the subsequent cell cycle.

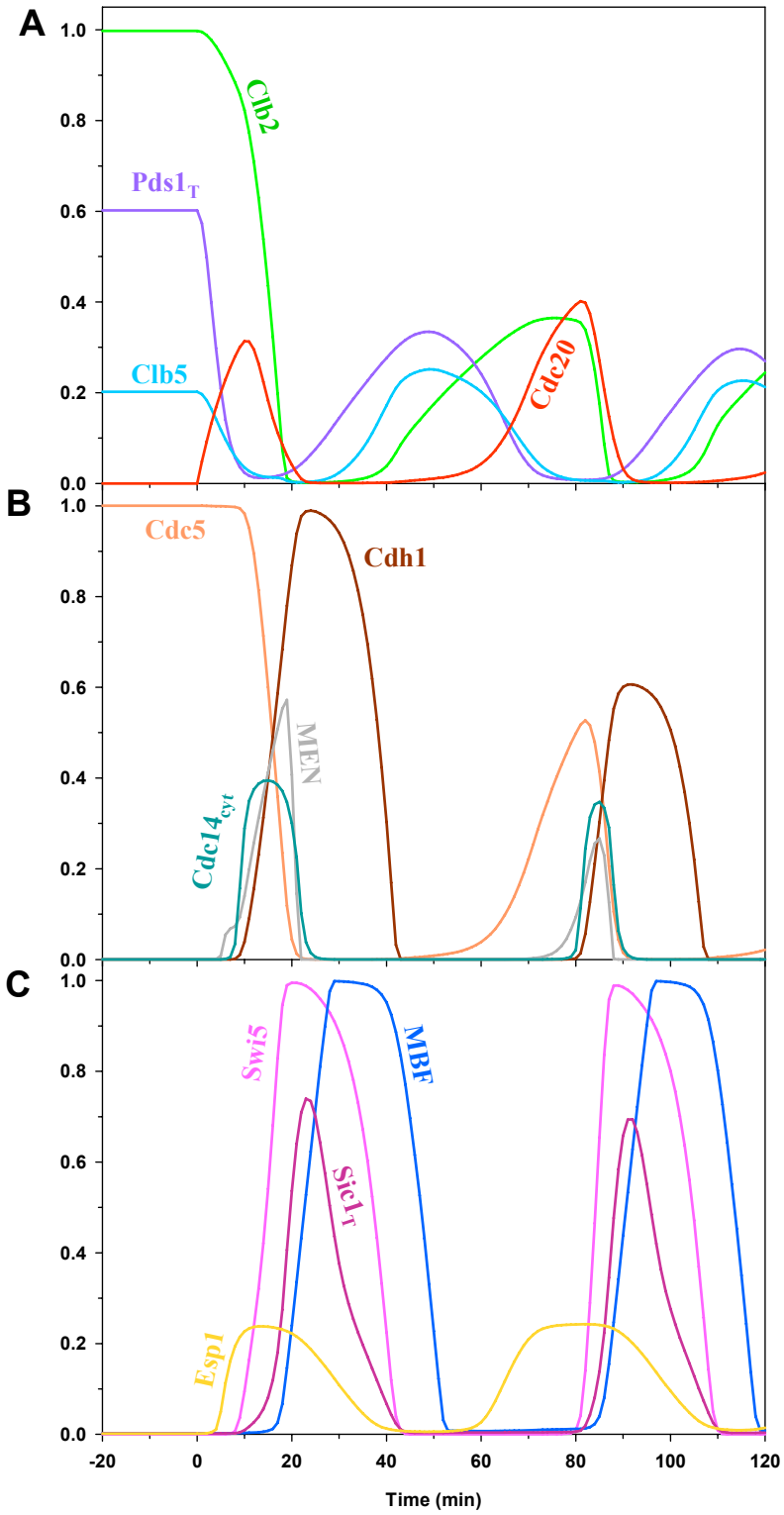


**Figure IV - 1: Simulation of Cdc20 block and release experiment. The model was simulated without Cdc20 synthesis ($k_{s20}$'= $k_{s20}$=0) which defines a stable steady-state corresponding to metaphase block. The metaphase state is shown for 20 min, after which Cdc20 synthesis is induced and the simulation of mitotic cycles are continued for 120 min. The three panels show the fluctuation of different cell cycle regulators during Cdc20 block and release.**

## 2. Different levels of Clb2-kd and their influence on the Cdc14 endocycles

With the incorporation of Cln and MBF, the model is able to differentiate between the events happening after mitotic exit and before the next S phase. This becomes particularly important for distinguishing normal cell cycle oscillations from the mitotic block with Cdc14 endocycles. Simulations with MV3 did not make a clear distinction; the main assumption was that high levels of Clb2/CDK1 activity (above the mitotic peak of cycling cells) would prevent the cell from exiting mitosis. In MV4 however, MBF is a clear indicator of G1 phase, since this transcription factor is inhibited during S-G2-M phases.

The experiments in (Lu and Cross, 2010) report that, at Clb2-kd values higher than the mitotic Clb2 peak values, cells stop dividing but some cell cycle components keep oscillating, creating the previously described Cdc14 endocycles (see Chapter III). With the incorporation of MBF, one can clearly see that cells do not exit mitosis when Clb2-kd assumes values above the mitotic threshold (Figure IV - 2B). In fact, MBF activity remains low, inhibited by high Clb2 activity. Lu and Cross (2010) also show that, for Clb2-kd values lower than the mitotic Clb2 peak value, cells retain their ability to exit mitosis and divide. MV4 can make this distinction, since, in these conditions, MBF is able to rise. Thus it is clear when the cell has progressed to G1, and therefore, has successfully exited mitosis.

Since Clb2-kd can only induce mitotic block with Cdc14 endocycles once it reaches a value larger than the mitotic peak, this phenomenon depends strongly on the Clb2-kd levels within the cell. Increasing this value has a strong influence on the period of the endocycles: higher Clb2-kd levels induce endocycles with shorter periods. The

amplitude of the Cdc14 oscillations remains unchanged, however ((Lu and Cross, 2010). MV4 provides a molecular explanation for these observations.

The high level of Clb2-kd strongly inhibits the activity of certain cell cycle regulators, namely Swi5 and MBF. As a result, levels of the cell cycle components dependent on these transcription factors are reduced in the endocycles. For instance, Sic1 cannot accumulate during the oscillations at high Clb2-kd; the same happens to Cln, Pds1 and Clb5. This downregulation is crucial because components such as Sic1 and Clb5 counteract the endocycles. Sic1 inhibits Clb2/CDK1 activity, and when overexpressed at a high level, promotes mitotic exit in cells expressing Clb2-kd (mutant situation *CLB2-kd Sic1$^{OP}$*, Figure I - 7) (Lu and Cross, 2009a). Clb5 phosphorylates Cdh1 and indirectly prevents recapture of Cdc14 into the nucleolus (mutant situation *CLB2-kd CLB5-nd*, Figure III - 4E). Consequently, the Clb2/CDK1-mediated inhibition of Sic1 and Clb5 promotes the endocycles, while Sic1 and Clb5 tend to oppose them. The period of the endocycles is determined by the balance of these antagonistic effects. The higher the Clb2-kd expression in cells, the lower the Sic1 and Clb5 activity, and thus the shorter the endocycles become. The other cell cycle regulators (e.g. Cdc20, Cdc14, Cdc5 and MEN) are not strongly inhibited by Clb2-kd, so when Clb2-kd levels are very high, the amplitude of the oscillations remains almost unchanged even if their period is shortened (Figure IV - 2C and 2D).

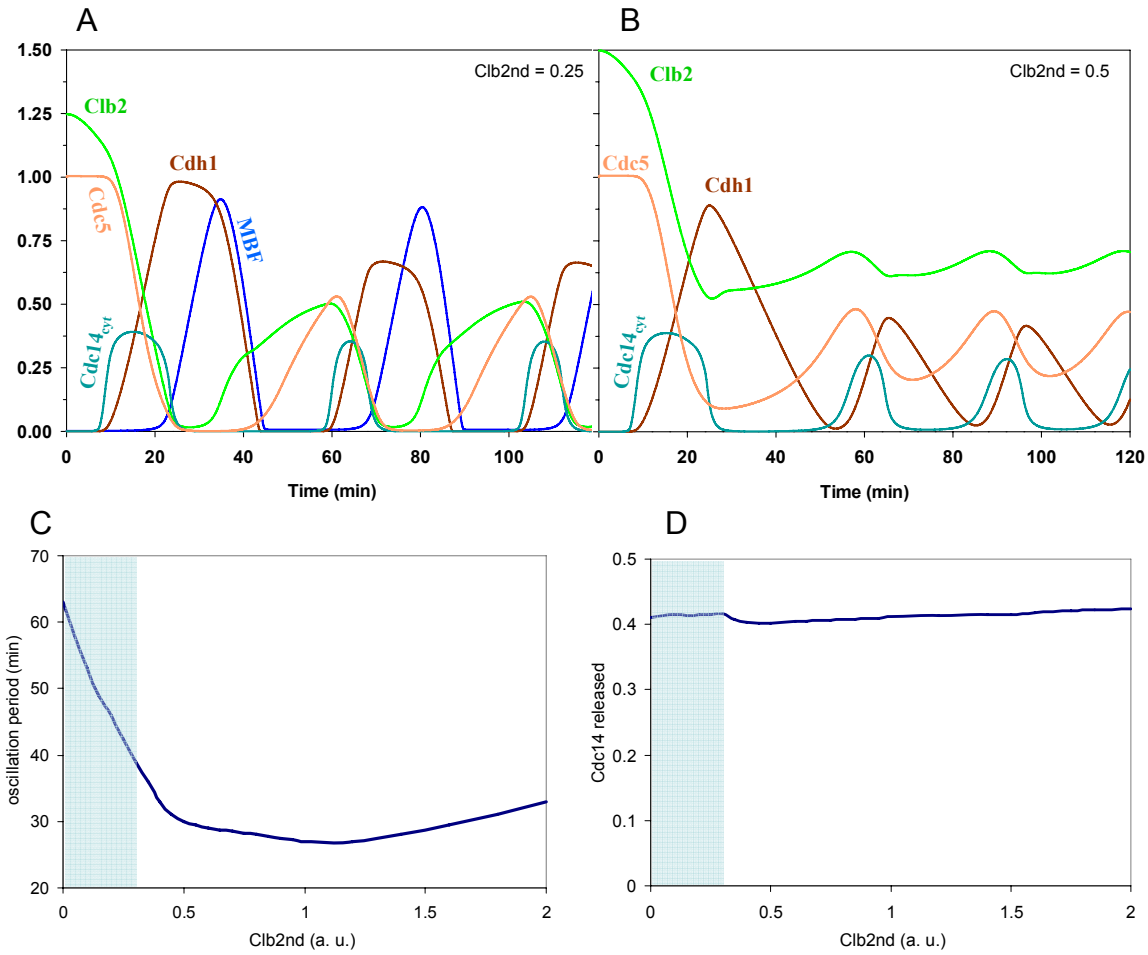


**Figure IV - 2: Different levels of Clb2-kd. (A) Clb2-kd levels smaller than peak value during normal mitosis (Clb2nd=0.25); (B) Numerical simulation of a Cdc20 block and release with Clb2-kd level about the mitotic peak (Clb2nd=0.5); (C) Period of Cdc14 oscillations versus Clb2nd values; (D) Amplitude of Cdc14 oscillations versus Clb2nd values. Cdc14 endocycles are only observed for values of Clb2nd above 0.3, this corresponds to the white background in (C) and (D).**

## *3. Net1 Phosphorylation – The two-hit Model*

The role of Cdc5 in Net1 phosphorylation is also reviewed in this chapter. In MV2 and MV3, Cdc5 acts on Net1 in parallel with Clb2 and MEN kinases. This simple description is enough to faithfully reproduce the mutants *cdc5*Δ and *cdc5*Δ*ESP1*$^{OP}$ (Figure II - 7). However, this description is highly dependent on the choice of parameters; a small increase in Clb2-mediated phosphorylation of Net1 ($k_p$") is all that is required to promote a transient release of Cdc14.

The paper (Manzoni et al., 2010) challenges this previous description by stating that while Cdc5 is absolutely necessary for Cdc14 release, MEN and Clb2 have partially overlapping roles. Moreover, it is believed that Cdc5 (Polo kinase) contains a conserved sequence motif which mediates the interaction between Cdc5 and its substrates. The conserved sequence motif is called the polo box domain (PBD), and requires a priming phosphorylation by another kinase to aid its activity. The priming kinases are believed to be Clb2 (Azzam et al., 2004) and the MEN component Dbf2 (Manzoni et al., 2010).

Based on this evidence, the description of Net1 phosphorylation was modified in MV4. Now, Cdc5-mediated Net1 phosphorylation is dependent on a priming phosphorylation by Clb2/CDK1 or MEN kinases. In addition, only the double phosphorylated form of Net1 (phosphorylated by Clb2 or MEN, and then by Cdc5) can dissociate from Cdc14. The reverse process is controlled by the counteracting phosphatases PP2A and Cdc14. These enzymes can dephosphorylate Net1 when it is singly or doubly phosphorylated. Figure IV - 3 illustrates the mechanism by which Net1 is phosphorylated and Cdc14 is released. Hence, MV4 contains a formal description of the mechanism described by Manzoni et al. (2010), which they named the two-hit model.

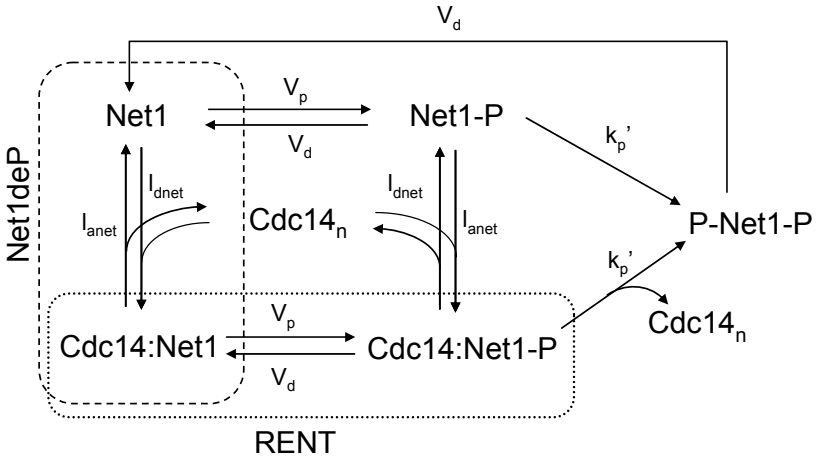


**Figure IV - 3: Schematic representation of the mechanism by which Net1 is phosphorylated and Cdc14 released. Net1 is distributed among five forms different in phosphorylation states and Cdc14 binding. Clb2 and MEN kinases phosphorylate ($V_p$) Net1 and its complex with Cdc14 (Net1deP). Both of these phosphorylated forms of Net1 (free and Cdc14 bound) are further phosphorylated by Polo kinase ($k_p$'). Polo phosphorylation of Net1 in the Net1P:Cdc14 complex causes the dissociation of Cdc14 and Net1PP (Net1 double phosphorlyted form). These phosphorylation steps are reverted by phosphatases, $PP2A^{Cdc55}$ and Cdc14 ($V_d$). $Cdc14_n$ stands for the free Cdc14 present in the nucleus.**

The two-hit model makes two key predictions. Firstly, Cdc5 is a crucial component in the release of Cdc14, and thus, in the generation of Cdc14 endocycles. Secondly, the contributions of Clb2 and MEN kinases to endocycle generation are partially redundant. In (Manzoni et al., 2010), the authors present several experiments that support these predictions. To assess the importance of Clb2 phosphorylation on Net1, they constructed a Net1 allele lacking six Clb2/CDK1 phosphorylation sites (*Net1-6CDK1*), and expressed it in cells with high levels of non-degradable Clb2. Cdc14 was still released in this scenario, and the endocycles still occurred.

MEN activity was then inactivated in the same mutant, using the cdc15-as1 allele (easily inactivated by the analogue-sensitive inhibitor). In this situation, the endocycles did not occur, and depending on the time point at which Cdc15 was inactivated, Cdc14 recapture was observed.

A further experiment involved the sole inactivation of Cdc5. For this purpose, they used a temperature sensitive allele (Cdc5-1), and shifted cells to a restrictive

temperature only after Cdc14 was released. The result was immediate Cdc14 recapture, and the prevention of further endocycles.

From these experiments, it is clear that oscillations can still persist without Clb2 activity, as long as MEN activity is present. However, if both Clb2 and MEN activities are abolished, the endocycles will disappear. Furthermore, Cdc5 was confirmed as a crucial contributor to endocycles; it must be activated for Cdc14 to be released in each endocycle.

MV4 is consistent with these experimental results. As depicted in Figure IV - 4, the mutants *CLB2-kd Net1-6CDK1*, *CLB2-kd Net1-6CDK1 cdc15-as1* and *CLB2-kd cdc5-1* faithfully reproduce the findings described above. According to these simulations, the two-hit model provides the most adequate description of Net1 phosphorylation and subsequent Cdc14 release.

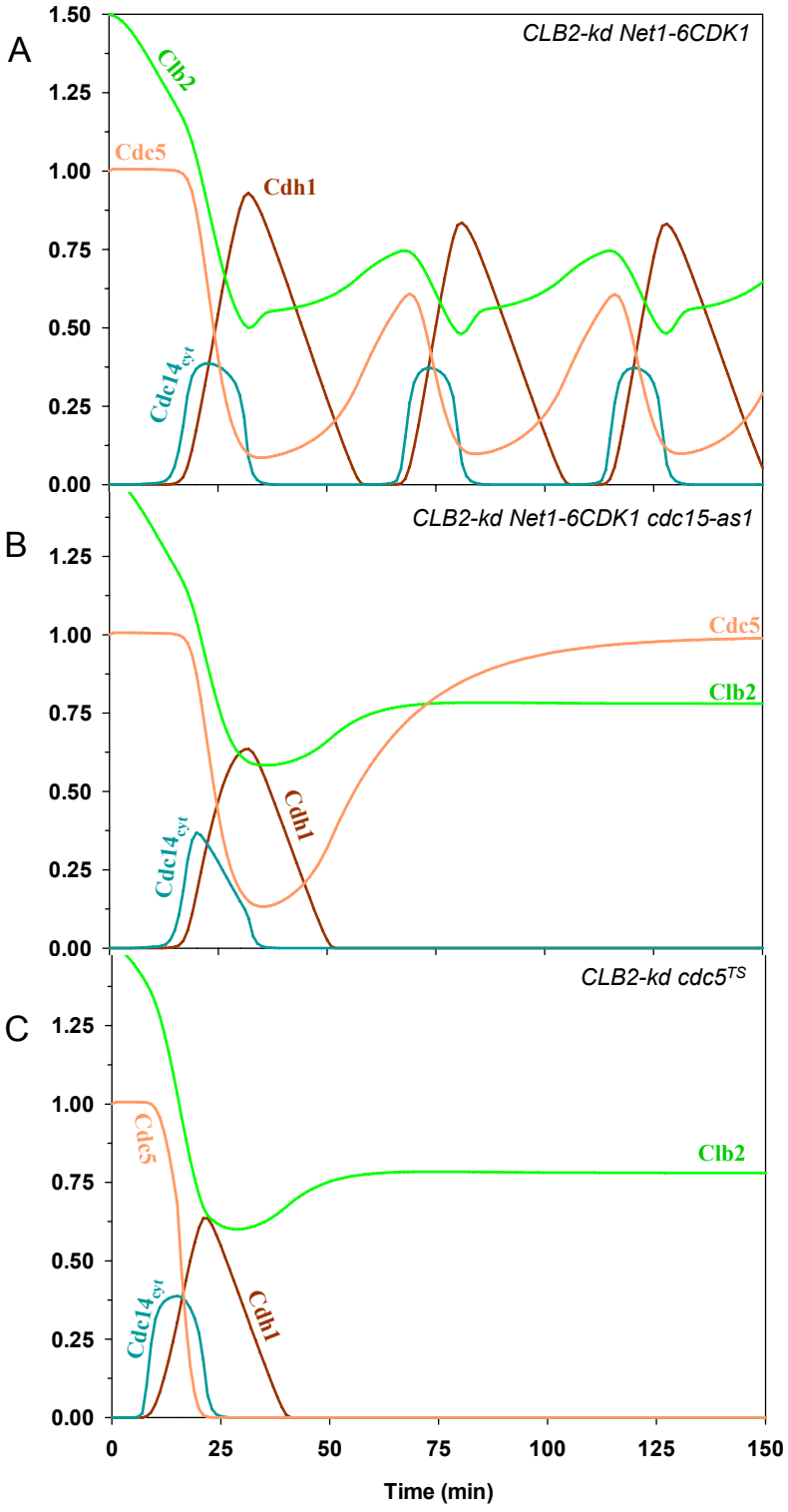


**Figure IV - 4: The two-hit model is in agreement with the Cdc14 endocycles. Numerical simulations of mitotic progression after Cdc20 relesease in cells with non-degradable Clb2 (Clb2nd = 0.5) and three different mutations: (A) Net1 is not phosphorylated by Clb2 ($k_p$"=0); (B) Net1 is not phosphorylated by Clb2 and after 20min Cdc15 is inactivated (use of analogue sensitive inhibitor – $k_{ac15} = k_{ac15}' = 0$); (C) after 15min Cdc5 is inactivated (temperature sensitive allele – $k_{apolo}=k_{apolo}'=0$).**

## *4. Antagonism between CDK1 and APC*

The cell cycle has been described as a sequence of events tightly regulated by the CDK1 activity: it is high when cells enter mitosis, and low when cells exit mitosis. The main component responsible for this variation is the APC, together with its two subunits, Cdc20 and Cdh1. Indeed, CDK1 and APC are antagonists: APC destroys S and M cyclins, while CDK1 phosphorylates and inactivates Cdh1 (Novak et al., 1998). This double-negative feedback loop creates a switch-like behaviour similar to a positive feedback loop, suggesting that the cell cycle results from the alternation between two-self-maintaining states (Nasmyth, 1996; Tyson and Novak, 2001).

It would be interesting to know just how important this antagonism is to the generation of Cdc14 endocycles. One can immediately see that one leg of the double negative feedback loop is not essential for endocycle generation, since endocycles are observed in the *Clb2-kd* mutant in which Cdh1-mediated Clb2 degradation is blocked. But what about the other leg of the feedback loop? How important is the Clb2/CDK1-mediated Cdh1 phosphorylation to the generation of endocycles? This question can be answered by simulating conditions in which Cdh1 can no longer be inactivated by Clb2/CDK1 ($k_{pcdh}$'=0). MV4 clearly shows that the endocycles are interrupted (Figure IV - 5A). During Cdc14 endocycles, Clb5 has been completely degraded by APC/Cdc20, and only Clb2 is present to inhibit Cdh1. As seen previously, Cdh1 synthesis and degradation are essential for these endocycles, and thus, this crucial contribution of Clb2/CDK1 is not unexpected. Further analysis led to the conclusion that Clb2-mediated Cdh1 inhibition is a major determinant of the Cdc14 oscillation period: the stronger this inhibition, the shorter the period of the endocycles. Eventually, if Clb2-mediated Cdh1 inhibition becomes too strong, then the oscillations are blocked completely (Figure IV - 5B).

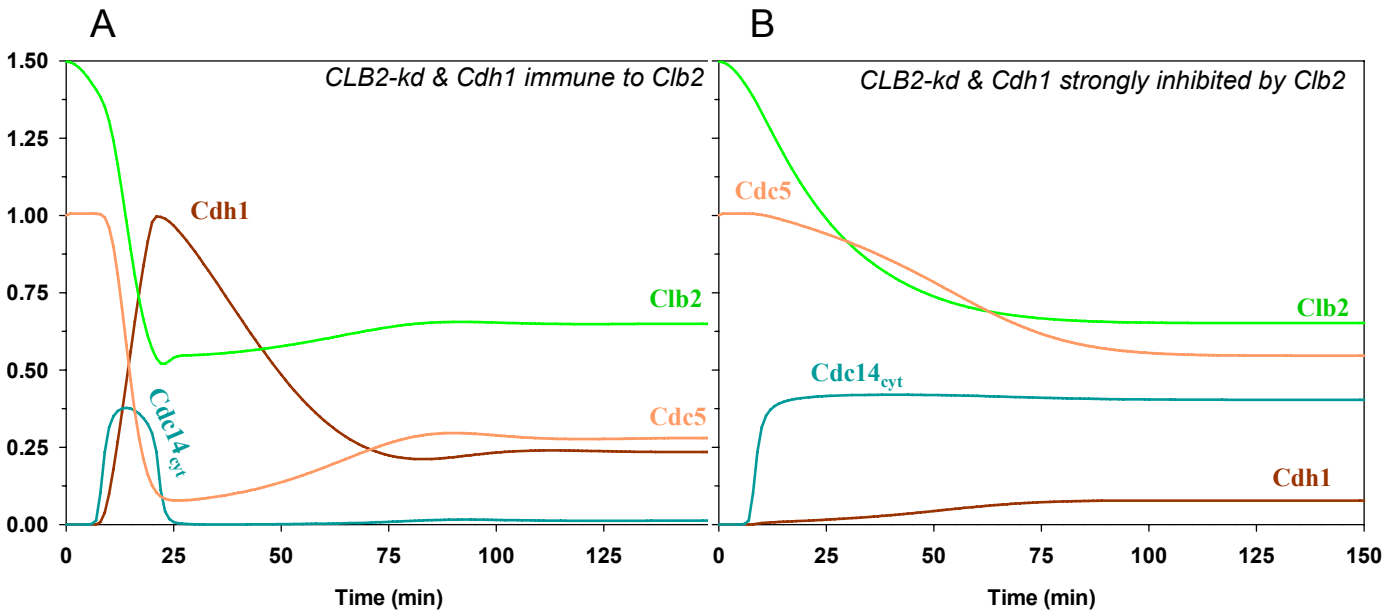


**Figure IV - 5: Cdh1 inhibition by Clb2 is crucial for the Cdc14 endocycles despite the opposite being not true. Numerical simulations of mitotic progression after Cdc20 relesease in cells with non-degradable Clb2 (Clb2nd = 0.5) and: (A) Cdh1 is immune to Clb2 activity ($k_{pcdh}$'=0); (C) Cdh1 is strongly inhibited by Clb2 ($k_{pcdh}$'=0.2 $min^{-1}$; 5-fold more than the original value).**

## 5. *FEAR component PP2A inhibits Cdc14 endocycles*

The contribution of MEN to endocycle generation has now been thoroughly reviewed; however, the role of the FEAR network must still be addressed. The FEAR components in MV4 are Clb2, Esp1 and PP2A. Clb2/CDK1 phosphorylates Net1 directly, which promotes Cdc14 release. Moreover, Clb2/CDK1 promotes Cdc20 (through Mcm1 activation), which in turn results in Esp1 activation. Esp1 then inhibits PP2A, the phosphatase that dephosphorylates Net1, so that Cdc14 is sequestered by Net1 in the nucleolus.

Disentangling the role of the FEAR network in endocycle generation is not straightforward. Clb2 and Esp1 also participate in MEN (Clb2 inhibits Cdc15, and Esp1 promotes Tem1 activation by triggering spindle elongation), and thus, manipulating any of these components might disrupt MEN activation. To avoid this, only PP2A was

considered in this analysis, since PP2A is the only component that belongs solely to the FEAR network. The effect of constitutively active PP2A on the endocycles proved to be strongly dependent on levels of Clb2-kd. When Clb2-kd levels were low, the period of the endocycles was increased (Figure IV - 6A). In this scenario, PP2A keeps a large portion of Net1 dephosphorylated, which prevents a full release of Cdc14. Partial release of Cdc14 is responsible for a delay in Cdh1 activation, and consequently, for the increase in endocycle period. When Clb2-kd levels are high, the outcome is the complete inhibition of the endocycles. According to MV4, partial release of Cdc14 becomes insufficient to dephosphorylate Cdh1 in the presence of very high Clb2 activity.

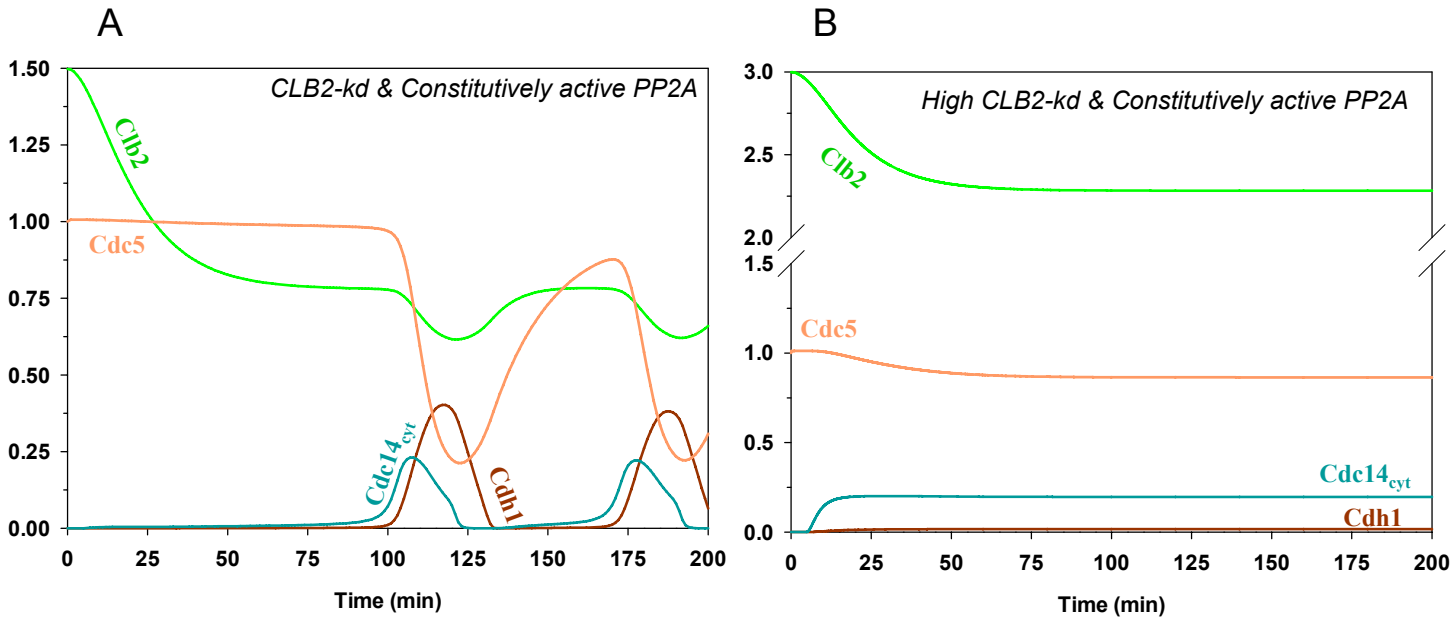


**Figure IV - 6: PP2A inhibits Cdc14 endocycles. Numerical simulations of mitotic progression after Cdc20 relesease in cells with non-degradable Clb2 and constitutively active PP2A ($k_i$=0). (A) Mitotic level of Clb2-kd (Clb2nd=0.5); (B) High level of Clb2-kd (Clb2nd=2).**

## *6. Essential Requirements for Cdc14 endocycles*

A systematic analysis of the essential requirements for Cdc14 endocycle generation was performed by disrupting each different molecular interaction in the network, and verifying whether the system could still generate endocycles. Figure IV - 7 depicts the

system's framework for Cdc14 endocycle generation by representing mitotic exit components as nodes and their interactions as edges. The essential components and interactions are represented in black, while the non-essential ones are in grey.

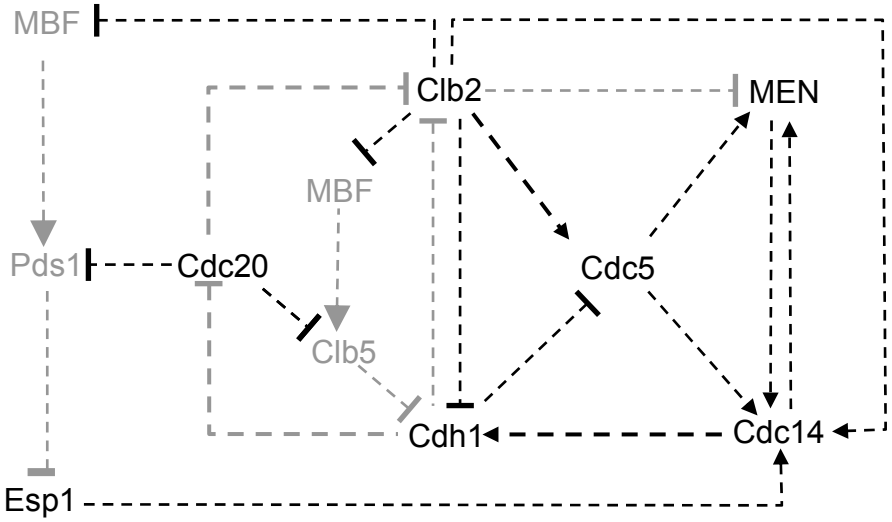


**Figure IV - 7: The positive and negative interaction among cell cycle regulators create positive and negative feedback loops which drive cell cycle oscillations. The cell cycle regulators and interactions labelled by black colours are required for Cdc14 endocycles at high Clb2-kd levels. In contrast the components and interactions labelled by grey colours are dispensable.**

## *7. Nuclear Cdc14 versus Cytoplasmic Cdc14*

Chapter III showed how Cdc14 cellular localization controls mitotic exit and Cdc14 endocycle generation. It is also shown that, despite its main substrates being localised in the cytoplasm (e.g. Swi5 and Cdh1), the contribution of nuclear Cdc14 cannot be neglected. Indeed, by considering that nuclear Cdc14 can act on its substrates, one is able to explain why *cdc15*Δ*net1*Δ cells are viable, though *cdc15*Δ cells are inviable (Lu and Cross, 2009a). The comparison of these two mutants clearly indicates that, even if the cytoplasmic form of Cdc14 is more liable to dephosphorylate targets in the cytoplasm, the nuclear form is still playing a role, presumably because its substrates can shuttle from the cytoplasm to the nucleus.

In this chapter, the model was adapted to incorporate the influence of nuclear Cdc14 on Swi5 and Cdh1. The equations for these two components have activating terms dependent on nuclear Cdc14, besides the ones dependent on cytoplasmic Cdc14 (see equations for Swi5 and Cdh1 in Appendix 1d). Nevertheless, compartmentalisation is still important to define different mutational situations, and thus, the new parameters were set at lower values compared with the cytoplasmic form. This change proved sufficient for the model to simulate the viability of the *cdc15Δnet1Δ* mutant, as depicted in Figure IV - 8.

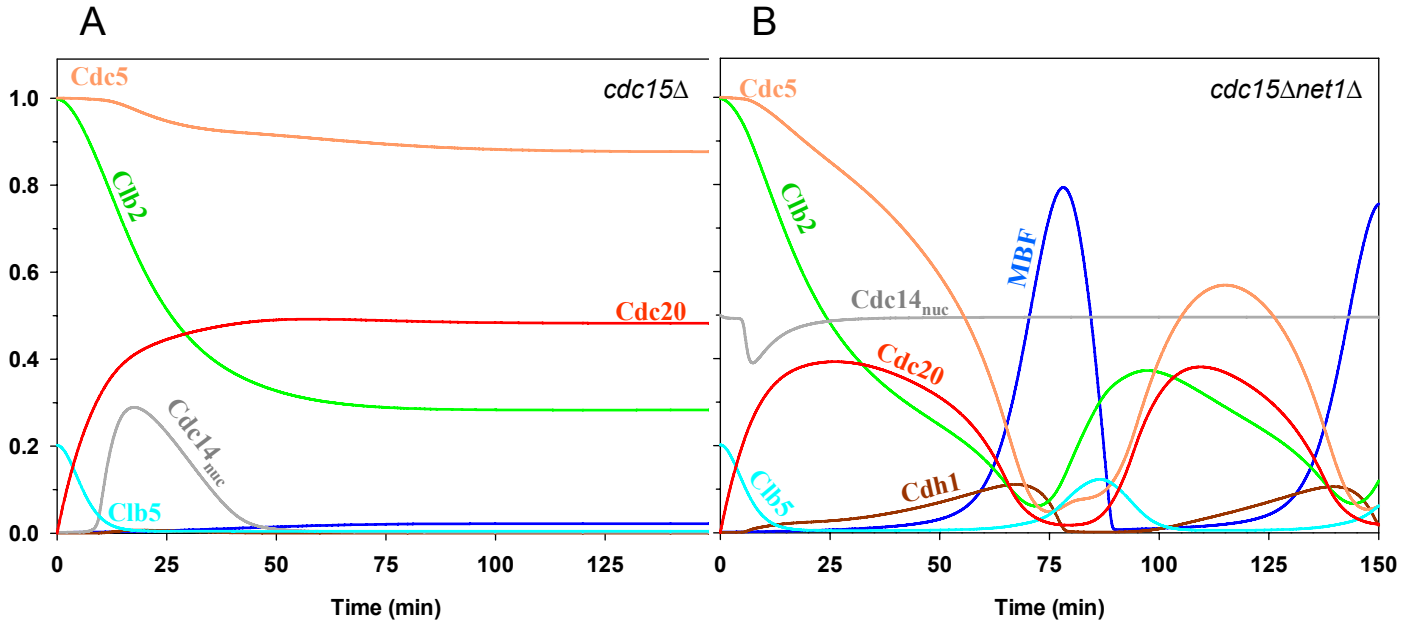


**Figure IV - 8: Cdc20 block and release in the absence of MEN (Cdc15) activity and Net1. Numerical simulations of mitotic progression after Cdc20 release in cells (A) with Cdc15 deleted ($k_{ac15} = k_{ac15}' = 0$) and (B) with both Cdc15 and Net1 deleted ($Net1_T=0$; Initial Conditions [Net1deP] = [Net1PP] = [RENT] = [RENTP] = 0; [Cdc14n] = 0.5).**

# Chapter V – Characterisation of the Model MV4

In Chapter IV, a comprehensive description of budding yeast cell cycle was developed. The resulting model, MV4, can be used as an appropriate theoretical tool for further studies on the budding yeast cell cycle. In this chapter, the capabilities of the model were explored in more detail, phase plane analysis was performed to understand the trajectories of the system, and the model's robustness to global parameter variation was tested.

## *1. Viability versus Mitotic Exit*

MV4 is capable of simulating all of the mutants that were tested using MV1, MV2 and MV3. MV4 provides more quantitative information on these mutants than the previous models, due to its more complete description of the cell cycle. To illustrate this point, MV4 was used to simulate the classic experiments performed by (Thornton and Toczyski, 2003b), which, using different mutational backgrounds, showed that cells remain viable without APC proteolytic activity. In MV4 simulations, cells retained viability in four different mutants in which APC core subunits were deleted:

- *cdc20*Δ*pds1*Δ*clb5*Δ (Figure II - 3A);
- *cdc20*Δ*pds1*Δ*SIC1*$^{10x}$ (Figure II - 3C);
- *cdc20*Δ*pds1*Δ*clb5*Δ *SIC1*$^{10x}$ (Figure II - 3E);
- *cdc20*Δ*pds1*Δ*clb5*Δ*cdh1*Δ*SIC1*$^{10x}$ (Figure II - 3F);

MV2 can only assess whether cells are able to exit mitosis (Figure II - 3), but with MV4, one can also assess whether cells are able to start a new cell cycle. In Figure V - 1, it is shown that the four mutant situations yield cell cycle oscillations, which means

that cells are able to exit mitosis and progress to the next cell cycle. These results are in agreement with (Thornton and Toczyski, 2003b).

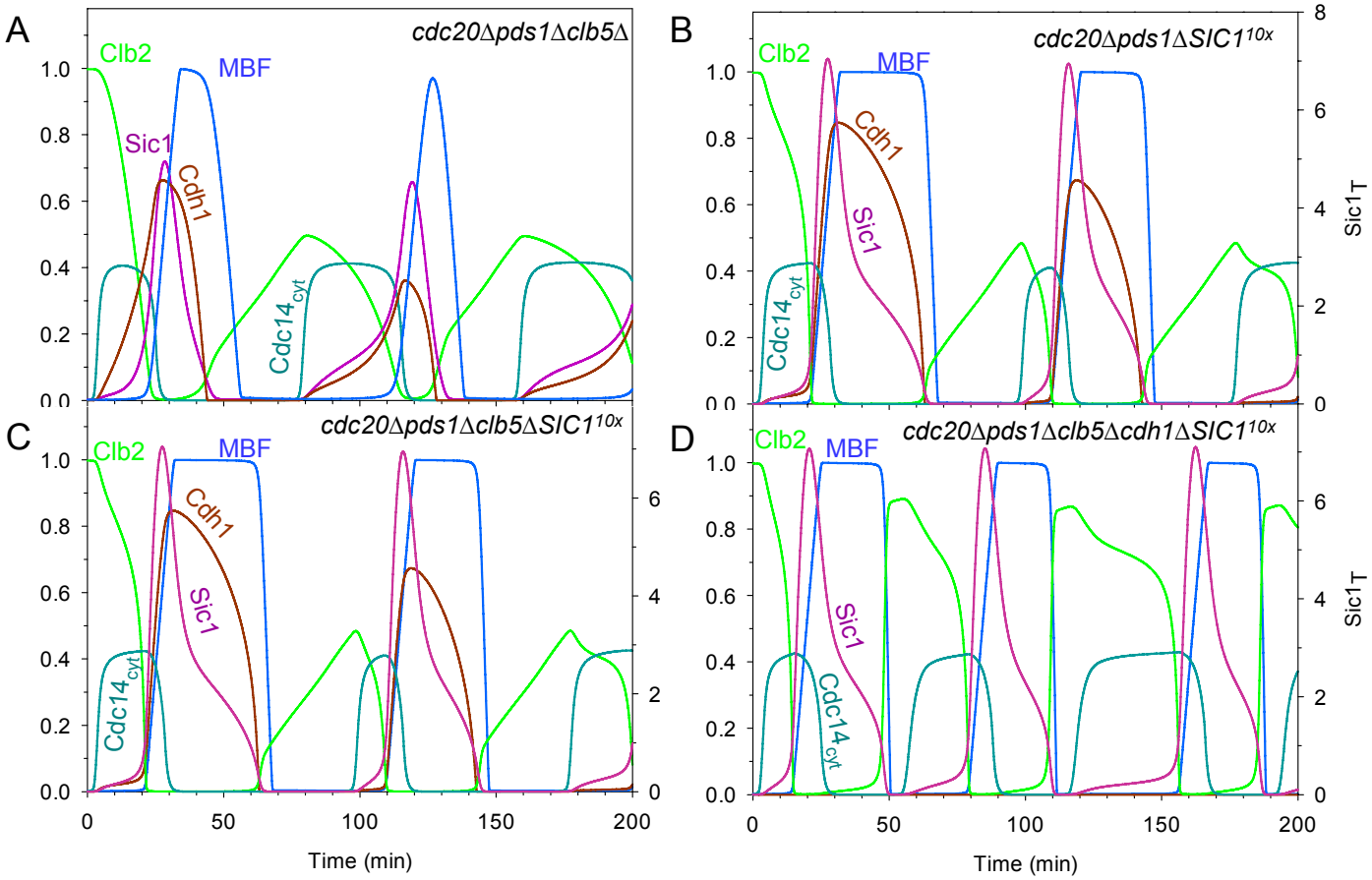


**Figure V - 1: Suppression of lack of Cdc20 activity by different genetic backgrounds: (A) *cdc20Δ pds1Δ clb5Δ*, (B) *cdc20Δ pds1Δ SIC1$^{10x}$*, (C) *cdc20Δ pds1Δ clb5Δ SIC1$^{10x}$*, (D)*cdc20Δ pds1Δ clb5Δ cdh1Δ SIC1$^{10x}$*. All simulations were started from *cdc20Δ* steady-state as initial conditions (metaphase block). Details of the simulations:**
***cdc20Δ*: $k_{s20} = k_{s20}' = 0$;**
***pds1Δ*: $k_{spds} = k_{spds}' = 0$; Initial Conditions: $[Pds1_T]=0$, $[Esp1_b]=0$;**
***clb5Δ*: $k_{sclb5} = 0.001\ min^{-1}$; $k_{sclb5}' = 0.005\ min^{-1}$; Initial Conditions: $[Clb5_T] = 0.1$**
**SIC1$^{10x}$: $k_{ssic}' = 2\ min^{-1}$.**

## 2. Initial Conditions

All of the simulations described in the preceding chapters were initiated from a metaphase arrest caused by Cdc20 depletion. In this steady-state, all the APC substrates (Pds1, Clb5, Clb2 and Cdc5) are high, whereas Cdc14, Cdh1, Sic1, Esp1,

MBF, Swi5 and the MEN components are inactive. Clb2 levels are particularly high; about twice the peak level seen in cycling cells. This is consistent with the experimental data (Drapkin et al., 2009; Yeong et al., 2000), which demonstrates that cells arrested in metaphase are able to synthesise more Clb2 then cycling cells. In cycling cells, Clb2 cannot reach such a high level because Cdc20 is turned on earlier.

Taking this into consideration, the model was tested using a different set of initial conditions. In many experiments, cells are synchronised using α-factor, which causes a temporary cell cycle arrest in G1 phase (the arrest is released when the cells are switched to a medium lacking α-factor). Thus, simulations were run with a set of initial conditions that mimicked G1 instead of metaphase.

In MV4, there is no stable steady-state in G1 phase (unlike metaphase). When cells exit mitosis, they immediately synthesise Cln, and undergo the START transition. Therefore, when defining a set of initial conditions that characterise G1, it is considered that only G1 regulators are present while all other components must be downregulated (see Table 2). This set of initial conditions proved adequate to simulate a wild-type cell cycle phenotype (Figure V - 2).

**Table 2: Initial Conditions assumed when starting simulations from G1 phase.**

| Initial Conditions for G1 phase | | | | | | | |
|---|---|---|---|---|---|---|---|
| CLB2T | 0 | | SIC1T | 0.83 | | RENTP | 0 |
| TRIM2 | 0 | | SWI5 | 1 | | CDC14N | 0 |
| MCM | 0 | | PDS1T | 0 | | POLOT | 0 |
| CLB5T | 0 | | ESP1T | 0.25 | | POLO | 0 |
| CLN | 0.44 | | ESP1B | 0 | | TEM1 | 0 |
| TRIM5 | 0 | | NET1DEP | 1 | | CDC15 | 0 |
| CDC20 | 0 | | NET1PP | 0 | | MEN | 0 |
| CDH1 | 0.63 | | RENT | 0.5 | | MBF | 1 |

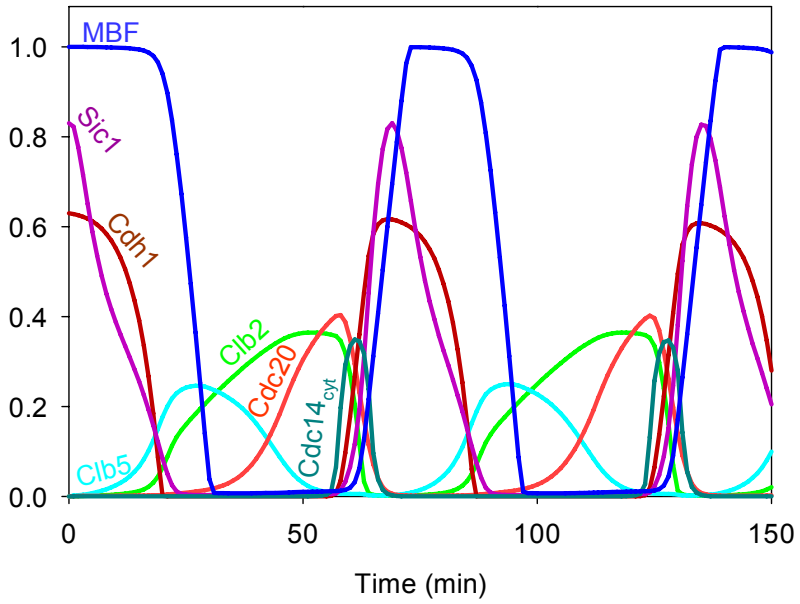


**Figure V - 2: Numerical simulation of a wild-type budding yeast cell cycle, starting from G1 initial conditions (Set for Initial Conditions shown in Table 2).**

Experiments in which cells were synchronised with α-factor – namely the mutant conditions *cdh1*Δ and *sic1*Δ, which are viable cells (Mendenhall et al., 1995; Schwab et al., 1997) – were simulated with this new set of initial conditions.

When simulating *cdh1*Δ and *sic1*Δ mutants from a metaphase block, the high initial level of Clb2 affects the results, since both Cdh1 and Sic1 are Clb2/CDK1 antagonists. Therefore, a new set of initial conditions – starting from G1 phase – seems more appropriate to study these mutant situations. The results that follow show that these mutants are viable because the compromise of one antagonistic component is compensated for by the presence of the other. MV4 captures these dynamics; at least one of the two genes is required under these mutant situations (Figure V - 3A and 3B). The antagonism between Sic1 and CDK1 drives cell cycle progression in *cdh1*Δ cells, and the antagonism between Cdh1 and CDK1 drives cell cycle progression in *sic1*Δ cells. As additional evidence, the double mutant *cdh1*Δ*sic1*Δ is completely inviable (Schwab et al., 1997; Wasch and Cross, 2002) (Figure V - 3C), which clearly indicates

that at least one of the antagonistic components must be present to drive the cell cycle forward.

According to MV4, Cdc20 is the only inhibitor of Clb2 in *cdh1*Δ*sic1*Δ cells, and this component is not sufficient to degrade Clb2 completely. As a consequence, Clb2 levels remain high, around the peak level seen in cycling cells. Cdc14 is released into the cytoplasm, but the absence of Cdh1 prevents its recapture. Presumably, this phenotype reflects a cellular arrest in late mitosis, as observed by (Schwab et al., 1997). It could also reflect an early G1 block, as was reported by (Wasch and Cross, 2002) in *cdh1*Δ*sic1*Δ mutant, a possibility that the model cannot eliminate.

Recently, it was reported that a number of *cdh1*Δ*sic1*Δ cells were able to undergo multiple cell cycles before ultimately becoming inviable (Lu and Cross, 2010). According to MV4, this mutant phenotype is very sensitive to a single parameter: the Cdc20-dependent Clb2 degradation rate constant ($k_{dclb2}$'). If this parameter is increased (i.e. if Cdc20 promotes Clb2 degradation more strongly), the mutant can approximate the experimentally observed phenotype whereby cells undergo successive cycles (Figure V - 3D). In this way, MV4 suggests that the results published in (Lu and Cross, 2010) could have resulted from the stochasticity inherent in Cdc20 expression in a population of cells.

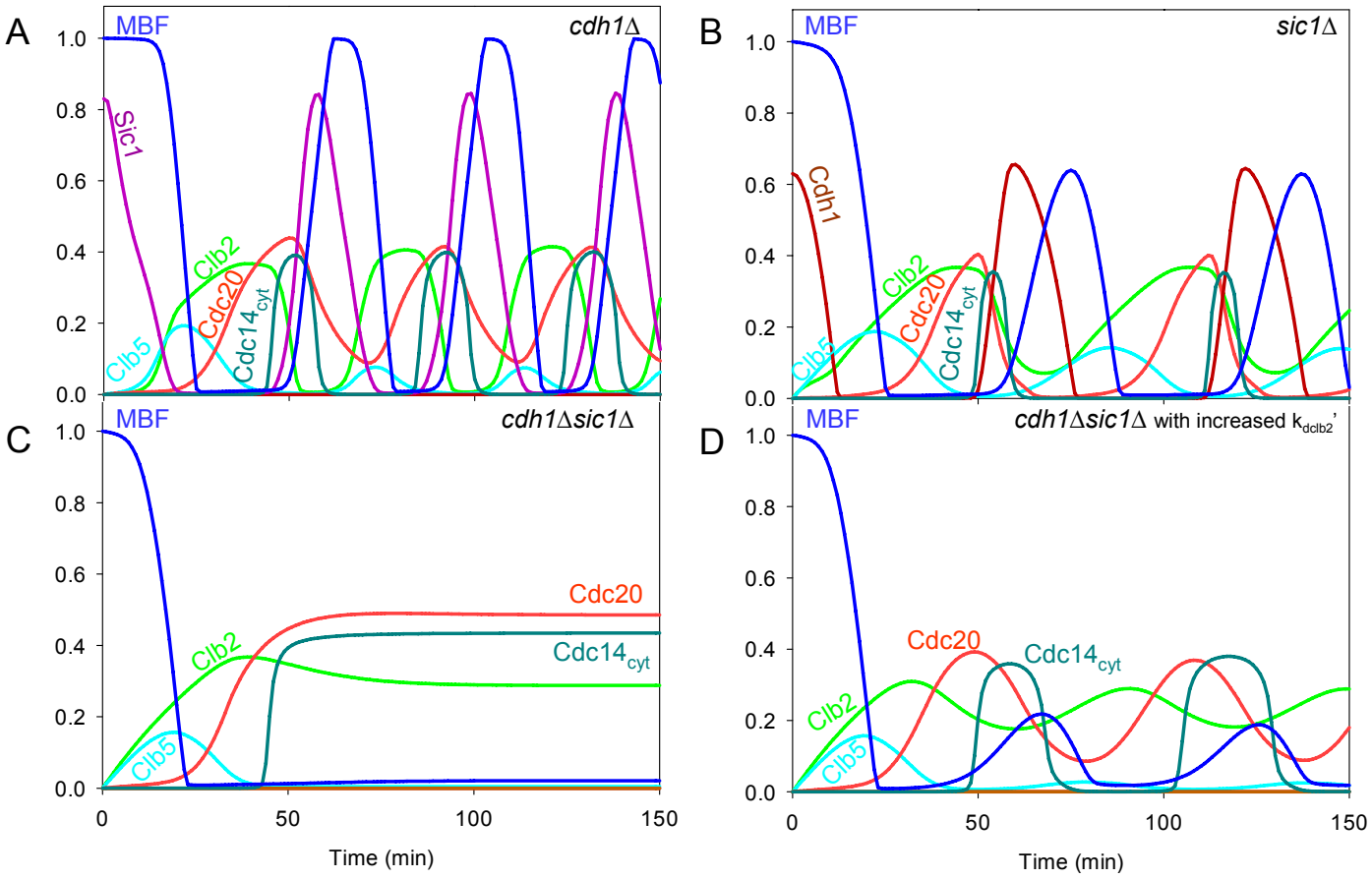


**Figure V - 3: The effect of Cdh1 and Sic1 on mitotic exit. Simulations were started from a low CDK1 activity G1 like state: (A) Cells with Cdh1 deletion ($k_{dcdh} = k_{dcdh}' = 0$; Initial Conditions: [Cdh1] = 0); (B) Cells with Sic1 deletion ($k_{ssic} = k_{ssic}' = 0$; Initial Conditions: $[Sic1_T] = 0$); (C) Cells with both Cdh1 and Sic1 deletions; (D) Simulation similar to (C) with the exception that the Cdc20-mediated degradation of Clb2 is increased ($k_{dclb2}' = 0.25$). These cells can exit mitosis and reproduce mitotic cell cycles.**

## 3. *Cell Cycle Progression*

### a. *Mother and daughter cells*

From the analysis of the mutant situations *cdh1*Δ, *sic1*Δ and *cdh1*Δ*sic1*Δ, it is evident that cell cycle progression depends on the antagonistic interactions between CDK1 and both of its negative regulators, Cdh1 and Sic1. In this section, it is demonstrated that these double-negative feedback loops are responsible for creating one-way switches. The cell progresses from one state to the next due to the presence of additional negative

feedback loops. In order to better understand how cell cycle progression relies on these feedback loops, a phase plane analysis of MV4 was conducted and is described here.

Cdc14 is fundamental for mitotic progression; without Cdc14 activation, cells remain arrested in a late mitotic state. According to MV4, Cdc14 is part of important negative feedback loops:

i. Cdc14 → Cdh1 —| Cdc5 → Cdc14

ii. Cdc14 → Cdh1 —| Clb2 → Cdc14

iii. Cdc14 → Swi5 → Sic1T —| Clb2 → Cdc14

Because Cdh1 is included in two of these feedback loops, Cdc14 and Cdh1 were used as variables in the phase plane analysis (Figure V - 4). The Cdh1 nullcline (red curve) exhibits an S shape, because in addition to participating in negative feedback loops with Cdc14, Cdh1 is also involved in a double-negative feedback loop with Clb2/CDK1. The Cdc14 nullcline (green curve) has a sigmoidal shape, due to the negative effect of Cdh1 on Cdc14 activation.

According to the phase plane analysis, cell cycle progression depends on the intersections between the two nullclines; that is, the steady-states of the system. In a mother cell (Figure V - 4A), the two nullclines intersect only once, and the resulting steady-state is unstable. This generates a limit-cycle solution around the unstable steady -state (open circle), and cell cycle progression is driven by a relaxation oscillator. It should be noted that this phase plane only applies for a mother cell that has bypassed the growth requirement for Cln synthesis, and therefore, does not show a stable G1 steady-state. This is why Cdh1 activity in MV4 is high after mitotic exit (point α in Figure V - 4A), and MBF is immediately activated promoting Cln and Clb5 synthesis. Clb5 is a strong antagonist of Cdh1, and thus its activity is reduced (point β in Figure V - 4A). Clb2 level increases when Cdh1 is downregulated. This rise in Clb2/CDK1 activity triggers the

negative feedback loop responsible for Cdc20 activation that ultimately initiates mitotic exit. Aided by Cdc20, Cdc14 is activated (point γ in Figure V - 4A), and in turn, activates Cdh1 (point δ in Figure V - 4A). The activation of Cdh1 drives Clb2 downregulation and mitotic exit. In addition, Cdh1 inhibits Cdc14, and thus Cdc14 is completely inactivated when cells start the next G1 (point α in Figure V - 4A). As an alternative to using Cdh1 as a variable, one can use Sic1 and obtain a very similar phase plane portrait. This is due to redundancy in the roles of Cdh1 and Sic1 in the cell cycle; both can bring about CDK1 downregulation on their own. In the case of Sic1 control, MBF activates Cln, which degrades Sic1, promoting Clb2 activation and Cdc14 release. In turn, Cdc14 dephosphorylates Swi5, and Sic1 synthesis is re-induced. Finally, the high level of Sic1 inactivates Clb2 and drives mitotic exit.

In a small daughter cell, the phase plane portrait is different. To draw such a diagram using MV4, certain parameter values were set to zero, in order to prevent the cell from progressing into S phase. All components responsible for the progression to S phase were kept at a low level; that is, Cln and Clb5 ($k_{scln} = 0$, $k_{scln}'=0$, $k_{sclb5} = 0$, $k_{sclb5}' = 0$). Clb/CDK1 antagonists were kept at a high level; that is, Sic1 and Cdh1 ($k_{iswi} = 0$, $k_{pcdh} = 0$). The resulting phase plane diagram shows that, besides the unstable steady-state (open circle), there is a stable steady-state (filled circle) with high Cdh1 and low Cdc14 activity (Figure V - 4B). This steady-state clearly reflects a stable G1 phase steady-state, and results from a leftward shift of the Cdh1 nullcline. This means that in a small daughter cell, Cdh1 cannot be inactivated, and the cell remains arrested in G1. The only way for the cell cycle to progress is to shift the Cdh1 nullcline back to the right, in order to lose this stable steady-state. This happens when the daughter cell has reached the critical size necessary to trigger the START transition, which results into the activation of MBF/SBF transcription. At this point, the phase plane resembles that of a large mother cell.

Finally, this phase plane analysis supports the idea that cell cycle progression is a combination of clock-like periodicity and switch-like 'checkpoint' transitions.

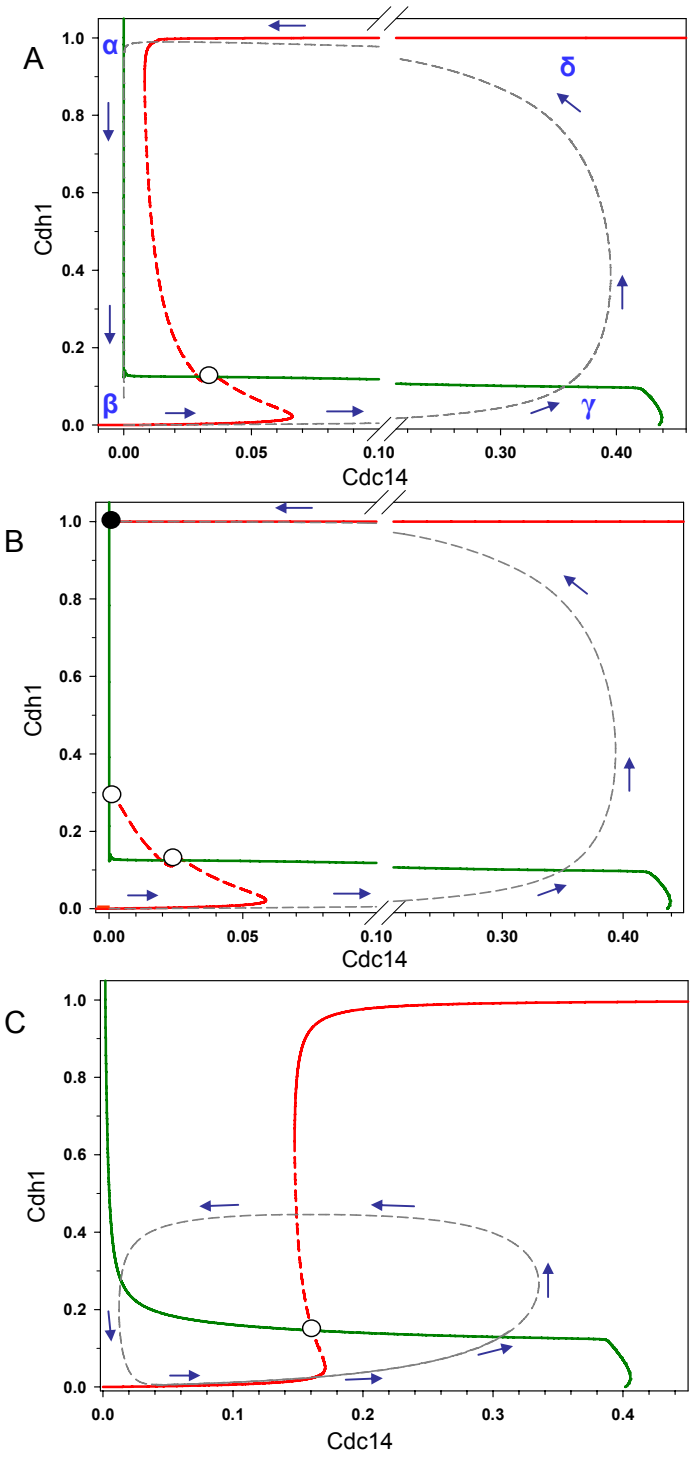


**Figure V - 4: Phase plane analysis of the budding yeast cell cycle and Cdc14 endocycles. The Cdc14 (green) and Cdh1 (red) nullclines were calculated as one-parameter bifurcation diagrams with the model using XPPAUT and combined to create a pseudo-phase plane portrait. All phase planes were calculated in anaphase when APC/Cdc20 has completely degraded Pds1 and Clb5. To generate the Cdc14 curve, Cdh1 is taken as the bifurcation parameter, and Cdc20, Sic1, Swi5, MBF, Cln, Clb5, Pds1 and Esp1 were considered to be in equilibrium. To generate the Cdh1 curve, Cdc14 is taken as the bifurcation parameter, and Cdc20, Clb5, Pds1, Esp1, Cdc15 and Tem1 were considered to be in equilibrium. Highlighted with small circles are marked the steady-states of the system, white circles show unstable steady states and dark circles show stable steady states. The black dashed curve represents the system's trajectory and its direction is indicated by the black arrows. The Cdh1 nullcline shows a dashed branch to highlight the unstable steady state. (A) Mother cell. (B) Small daughter cell ($k_{scln}$ = $k_{scln}$' = $k_{sclb5}$ = $k_{sclb5}$' = $k_{iswi}$ = $k_{pcdh}$ =0). (C) Cdc14 endocycles (Clb2nd=1).**

### *b. Cdc14 endocycles versus cell cycle progression*

Phase plane analysis can also be used to study the difference between normal cell cycle progression and abnormal cyclic behaviours, such as the Cdc14 endocycles. As previously described, the cell suffers a mitotic block at constitutively high values of Clb2/CDK1 (e.g. in *Clb2-kd* cells), even if many cell cycle components retain their oscillatory behaviour. The phase plane portraying this situation shows that the main difference here is a large rightward shift of the Cdh1 nullcline (compare Figure V - 4A and Figure V - 4C). The constitutively high level of Clb2/CDK1 activity strongly inhibits Cdh1, and thus, a higher level of phosphatase activity is required to activate Cdh1.

The Cdh1 and Cdc14 nullclines intersect only once, in an unstable steady-state. As a consequence, the Cdc14 endocycles are driven by a limit cycle oscillator. Following this observation, further analyses were carried out to clearly distinguish these Cdc14 oscillations from the limit cycles characteristic of mother cells. One-parameter bifurcation diagrams were computed for several cell cycle components, using Cdc14 as a parameter. To differentiate the two situations, each diagram was computed twice; first in a wild-type situation (Clb2nd=0), and then in the presence of non-degradable Clb2 (Clb2nd=1) (Figure V - 6). The comparison of diagrams from the two situations revealed that high activity of Clb2/CDK1 represses many cell cycle regulators, including Swi5, MBF, Cln and Sic1. As a result, Cdc14 endocycles become uncoupled from normal cell cycle events (e.g. DNA replication-division cycle), and can take place even if cell cycle progression is blocked.

To summarise, the bifurcation analysis of the Cdc14 endocycles showed that this uncharacteristic cell cycle behaviour arises from the redundancy of Clb2 and Cdc5 in driving Cdc14 release and recapture. On one hand, Net1 is phosphorylated by both Clb2 and Cdc5 (two-hit model), and on the other hand, both of these kinases are subjected to

Cdh1-mediated degradation. Thus, in cells expressing non-degradable Clb2, Cdc5 becomes the crucial agent for driving the Cdc14 endocycles (Figure V - 5).

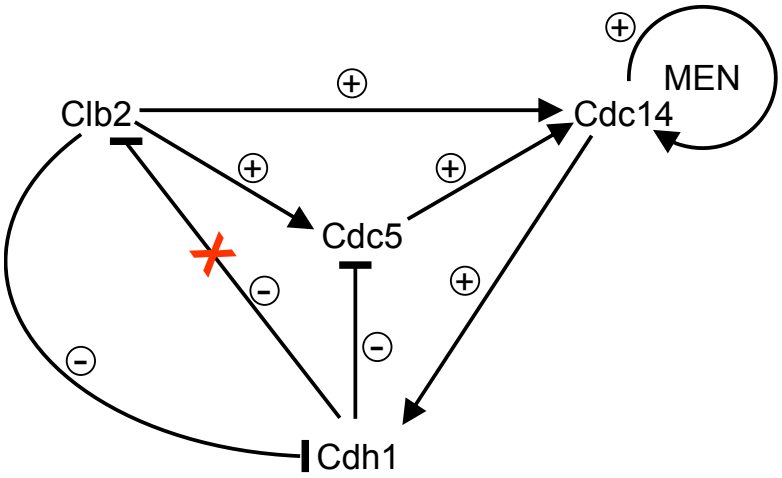


**Figure V - 5: Cdc14 endocycles are the consequence of the 'two-hit' mechanism controlling Cdc14 release. Since both Clb2 and Cdc5 are required for Cdc14 release, there are two negative feedback loops. If Clb2 is made non-degradable (Clb2-kd), the outside negative feedback loop (Clb2 → Cdc14 → Cdh1 ⊣ Clb2) is broken, but the inside one with Polo-kinase (Cdc5 → Cdc14 → Cdh1 ⊣ Cdc5) is still functional.**

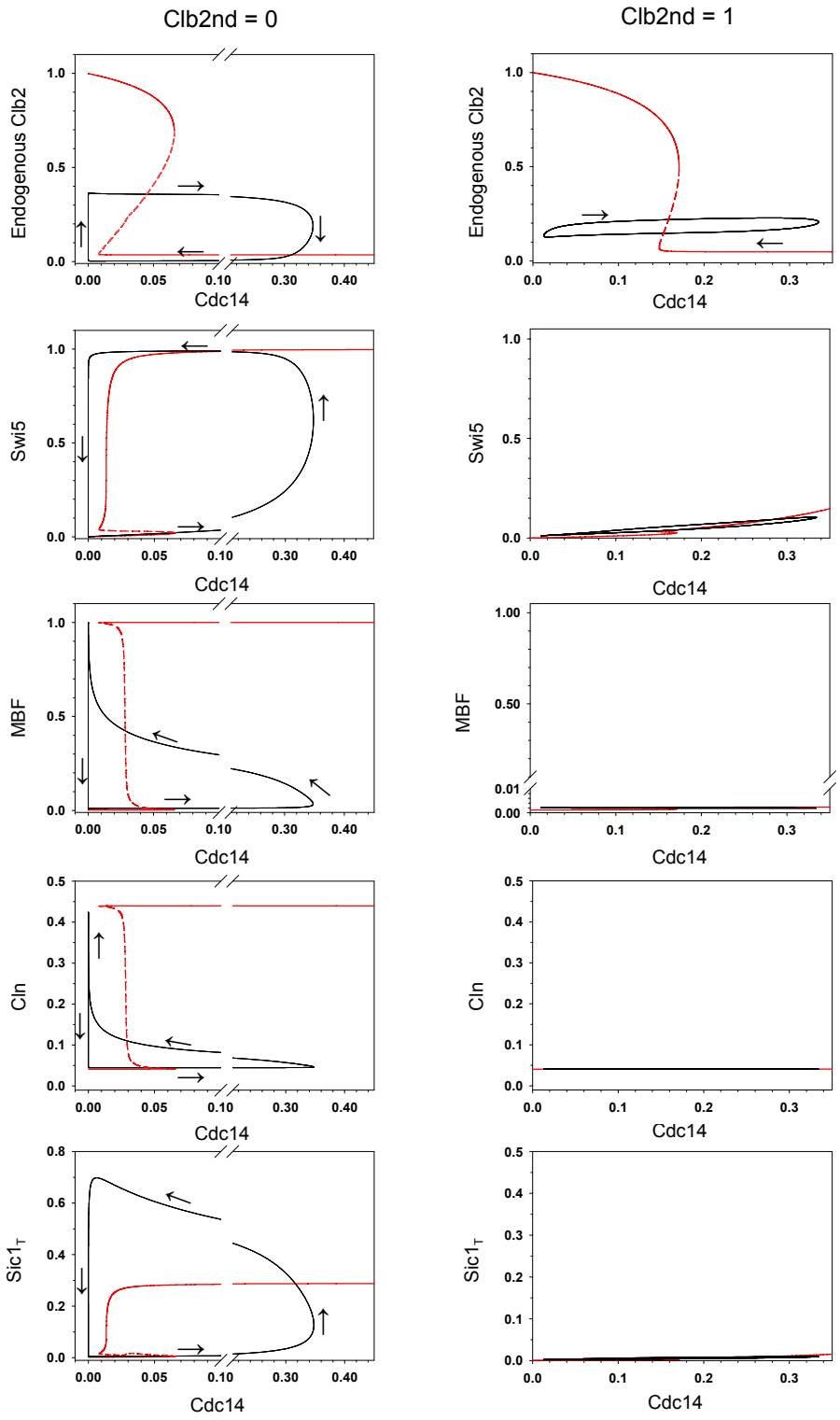


**Figure V - 6: One parameter bifurcation diagrams using Cdc14 as the bifurcation parameter in the absence (left panel) and in the presence (right panel) of Clb2-kd. The red curve shows the equilibrium solutions of the system; the solid line represents stable steady-states while the dashed line represents unstable steady-states. The black curve shows the system's trajectory and the arrows indicate the direction.**

## 4. Robustness Analysis

In this section, the model was subjected to global parameter perturbation, to investigate MV4's dependence on its parameter set. Before this robustness analysis could be performed on the model, the characteristics of successful cell cycle progression first had to be defined. According to common knowledge, both general and specifically to the budding yeast cell cycle, the following characteristics are observed in a successful cell cycle:

(i) The cell cycle control network oscillates with a constant period under constant environmental conditions.

(ii) During these oscillations, a high kinase/phosphatase ratio (CDK1/Cdc14 in budding yeast) promotes mitosis, while a low ratio permits mitotic exit and allows DNA replication origin re-licensing.

(iii) Chromosome segregation is triggered by separase during the high mitotic kinase (Clb2/CDK1) activity stage.

Computational analysis was used to check whether the cell cycle control network oscillates with a constant period (condition (i)). The period of the oscillations must be between reasonable upper and lower limits. During one oscillation period, DNA replication and mitosis must occur in an orderly fashion, and the execution of these processes requires a certain amount of time. Therefore, a lower limit of 30 min was set for the period of oscillation.

The coordination of cell growth and division requires that the length of the cell cycle is equal to the time it takes for the cell's mass to double. Because the division of budding yeast cells is asymmetric (small daughter and large mother cell), this coordination is different in a mother and a daughter cell. Since MV4 describes a mother cell, the model only addresses the coordination of cell growth and division in a large mother cell. As

mentioned previously, large mother cells are born above the critical size, and follow a minimal cycle time driven by a limit cycle oscillator with a period shorter than the mass-doubling time. Therefore, balanced growth and division sets an upper limit for the period of the limit cycle oscillation; it should be shorter than the shortest mass-doubling time obtained at the maximum growth rate. Since yeast cells can grow with a generation time of less than two hours, this threshold was set to 100 min.

To test whether the simulated dynamics follow an ordered cell cycle progression (S-M-S-M- etc), an analysis of CDK1/Cdc14 activity ratio was performed (condition (ii)). The model was supplemented with generic substrates for both the S and M phases, $X_S$ and $X_M$, respectively. $X_S$ is phosphorylated by both the Clb5/CDK1 and Clb2/CDK1 kinases, while $X_M$ is only targeted by Clb2/CDK1. The phosphorylated forms of both CDK1 substrates ($X_S$-P and $X_M$-P) are dephosphorylated by the CDK1-counteracting phosphatase Cdc14. At the end of mitosis, all CDK1 targets must be dephosphorylated so that the cells can start a new cycle (e.g. the spindle must be disassembled and the DNA replication origins licensed). In MV4, this event is determined by the drop in the concentration of the phosphorylated form of $X_S$ ($X_S$-P) below a threshold level. To enter mitosis on the other hand, Clb2/CDK1 targets must be phosphorylated, which is determined by an increase in the concentration of the phosphorylated form of $X_M$ ($X_M$-P) above a threshold level. The threshold for mitotic exit is $X_S$-P decreasing below 0.4. For mitotic entry, the threshold is $X_M$-P increasing above 0.6. Besides these thresholds in CDK1/Cdc14 activity ratio, Esp1 should be activated during mitosis (condition (iii)) when Clb2/CDK1 activity is maximal (the value of Esp1 must be larger than 0.1).

This set of conditions was used to establish the viability criteria for the budding yeast cell cycle model. These criteria determine whether simulations with different parameter sets reflect viable or inviable phenotypes. It should be added that these viability criteria

were formulated to be consistent with the phenotypes of all the mutant situations analysed previously.

Once the viability criteria were defined, MV4 was subjected to global parameter perturbation, to evaluate MV4's robustness in maintaining these viability criteria. This study employed the same Monte-Carlo method used by (Mirsky et al., 2009) to analyse a circadian clock model. Random parameter sets were generated by selecting new values for each parameter from a normal probability distribution. The mean value of this probability distribution was equal to the nominal parameter value identified in the original model, and the standard deviation (SD) was set according to the desired variation between the nominal value and the new value. 10,000 parameter sets were generated in this way. This approach was repeated several times; in each case, the SD was varied to determine how the model responds to different ranges of parameter perturbations. The simulations with each parameter set were analysed for both oscillatory behaviour and the viability criteria.

MV4 was challenged for parameter sets generated with SD values between 10% and 30% (Figure V - 7). The percentage of simulations satisfying the viability criteria decreased linearly with increasing standard deviation (Figure V - 7). Observe that at 10% SD, 99% of simulations satisfy the viability criteria. Only at a 30% SD does the percentage of simulations satisfying the viability criteria drop below 50% (Figure V - 7).

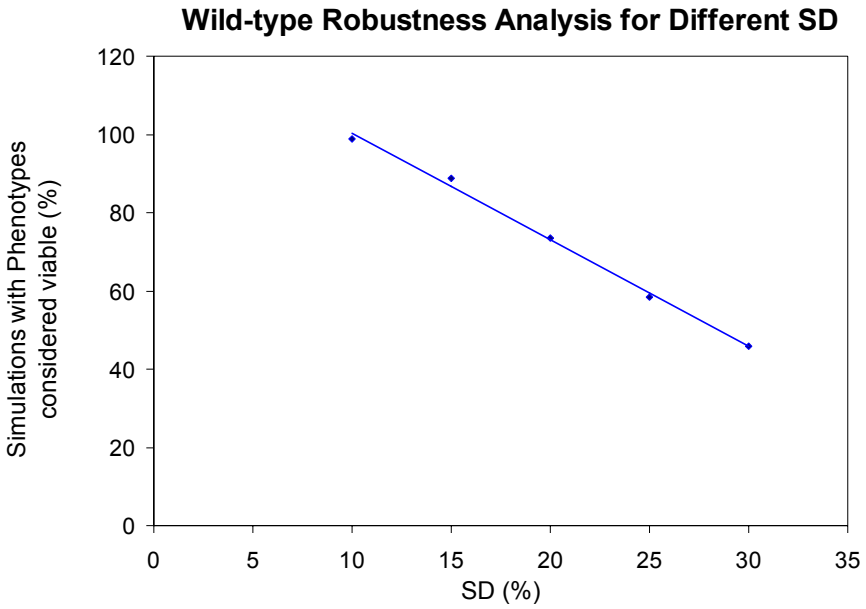


**Figure V - 7: Performance of MV4 to yield cell cycle oscillations that satisfy the viability criteria in face of parameter perturbation. MV4 was challenged for five groups of 10,000 parameter sets with different SD values: 10%, 15%, 20%, 25%, and 30%.**

# Chapter VI – Transcriptional and Proteolytic Regulation Contribute to Robust Cell Cycle Progression

To guarantee survival, a complex biological system – such as the cell cycle control network – must be robust against environmental and genetic perturbations. In Chapter V, the robustness of MV4 was evaluated by varying its nominal parameter set. The source of the model's robustness was not investigated however.

This chapter sought to reveal the molecular mechanism responsible for the robustness demonstrated in Chapter V. Two of the system's regulatory modules – transcriptional and proteolytic – were analysed further so as to quantify their relative contribution.

## *1. Regulated Transcription versus Regulated Degradation*

Different mechanisms have been proposed to enhance the robustness of complex biological systems (Kitano, 2004). One such mechanism that might be relevant to the cell cycle network is redundant control. Redundancy refers to any situation where there are multiple means to perform the same function. Thus, if one of the redundant pathways or mechanisms fails, the function is still guaranteed by another one (Kitano, 2004).

The vast majority of the cell cycle proteins are subjected to three different, but redundant, layers of control, each of which is represented in MV4:

-regulated synthesis via cell cycle-regulated transcription factors;

-regulated protein degradation via different cell cycle-regulated ubiquitin ligases;

-regulated enzymatic activity via post-translational modifications (e.g. phosphorylation/dephosphorylation, stoichiometric inhibitor binding, etc.).

Regulated transcription and protein degradation collaborate in controlling the level of many cell cycle proteins. For instance, MV4 shows that the accumulation of cell cycle proteins, such as Cdc20 and Cdc5, is achieved by a concomitant increase in their transcriptional synthesis and a decrease in their degradation. The accumulation of both proteins depends on the Clb2/CDK1-dependent activation of the Mcm1/Fkh2/Ndd1 transcriptional complex, and the Clb/CDK1-mediated inhibition of APC/Cdh1. Conversely, Cdc20 and Cdc5 levels are kept low in G1 phase by an increased rate of degradation and reduced rate of synthesis. This is achieved by the activation of APC/Cdh1 at the end of mitosis, which not only degrades Cdc20 and Cdc5, but also inhibits the transcription of these proteins via Mcm1 transcriptional complex (APC/Cdh1 degrades Clb2, and thus inhibits Mcm1). This and many other examples testify to the redundancy in regulating protein levels through transcription and degradation. The relative contribution of these different layers of regulation to robust cell cycle oscillations has yet to be quantified experimentally. Here, this was tested *in silico* by performing a comparative robustness analysis.

Besides the original parameter set for MV4 (i.e. the 'wild-type' parameter set), two other nominal parameter sets were generated, in which one of the aforementioned regulatory layers were eliminated from MV4. In one parameter set, regulated transcription of cell cycle regulators was removed, while in the other, regulated protein degradation was eliminated. It was decided that the regulatory modules should not be manipulated through post-translational modifications, since these mechanisms are inextricably linked in MV4, and cannot be separated in a straightforward way.

To remove transcriptional regulation from MV4, all of the rate constant values for regulated synthesis through transcription factors were set to zero. The values of the

basal rate constants for Cdc20 and Cdc5 synthesis were increased however, in order to prevent cell cycle block in the absence of these essential cell cycle regulators (Table 1). This version of the model is referred to as the NRT ('No Regulated Transcription') model. In another set of parameters, the rate constant values for the regulated protein degradation were set to zero. In three exceptional cases (Clb2, Sic1 and Pds1), the basal rate constant values were increased to prevent the accumulation of proteins to unrealistically high levels (Table 1). This version of the model is referred to as the NRD ('No Regulated Degradation') model.

The simulation of both the NRT and NRD models resulted in cell cycle oscillations that were able to satisfy the viability criteria (Figure VI - 1A and B). These results indicate that the cell cycle oscillations can persist in yeast, even if the regulated transcription or degradation of major cell cycle regulators is compromised. This is a consequence of redundancy in the feedback loops responsible for the cell cycle oscillations, at the level of both transcription and proteolysis. Experimental data support this notion, for the case of regulated degradation at least. As seen in chapters II and V, the role of APC ubiquitin-ligase in budding yeast can be bypassed by the simultaneous deletion of its two substrates (Pds1 and Clb5) and by the overexpression of Sic1 (Thornton and Toczyski, 2003b). In the absence of APC-dependent degradation of the Clb2 mitotic cyclins, the oscillation of Clb2/CDK1 kinase activity is driven by the following transcriptional feedback loops:

- Clb2/CDK1 $\rightarrow$ Cdc5 $\rightarrow$ Cdc14 $\rightarrow$ Swi5 $\rightarrow$ Sic1 $\dashv$ Clb2/CDK1 (negative feedback loop);
- Clb2/CDK1 $\rightarrow$ Mcm1 $\rightarrow$ Clb2/CDK1 (positive feedback loop);
- the post-translational double-negative feedback loop between Clb2/CDK1 and its stoichiometric inhibitor (Sic1).

Interestingly, cell cycle oscillations cannot be supported by post-translational mechanisms alone; that is, in the absence of both regulated transcription and protein degradation. Instead, they produce a steady-state solution of the cell cycle control system (see the combination of the NRT and NRD models in Figure VI - 1C).

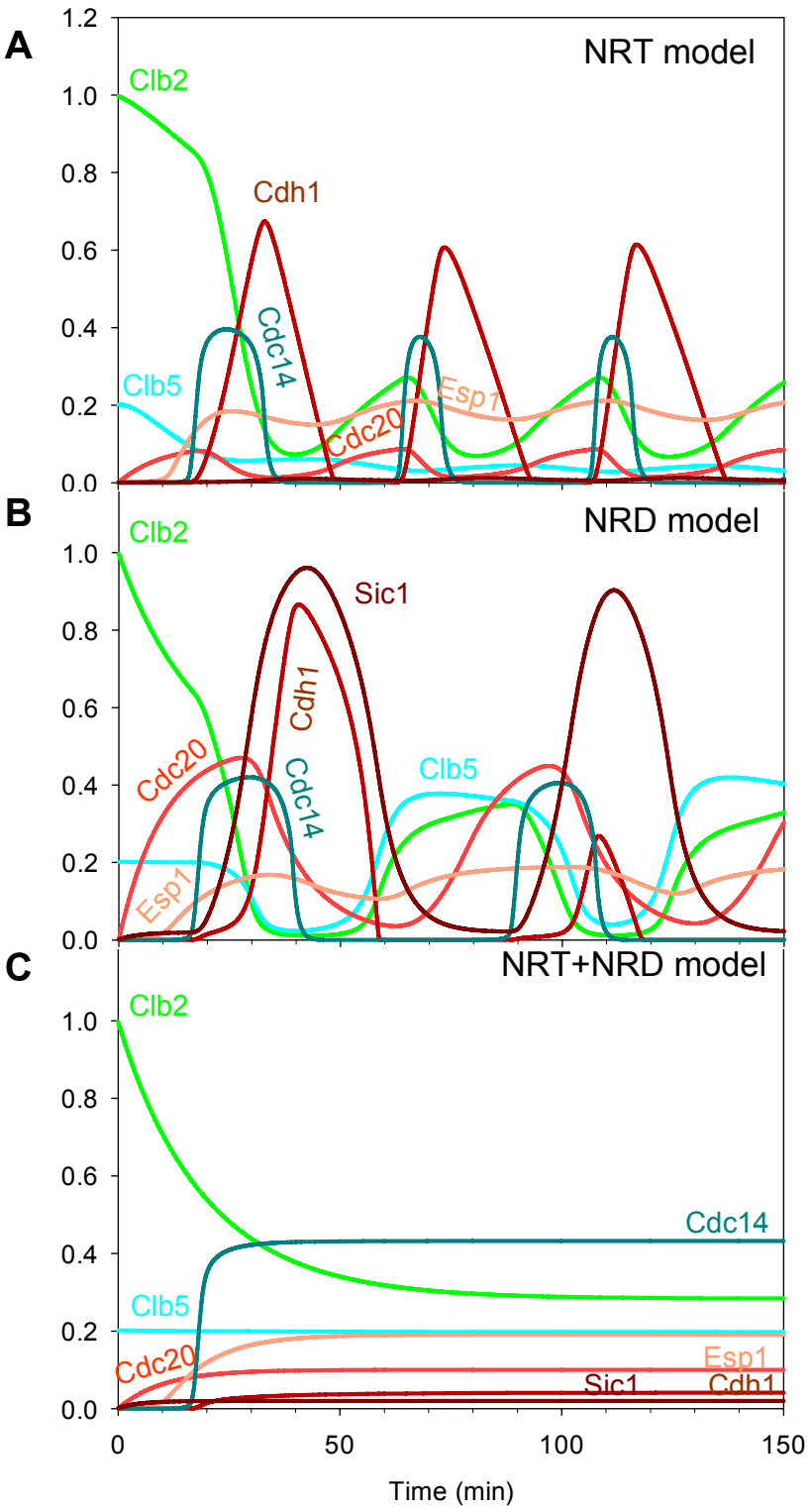


**Figure VI - 1: Simulations of modified versions of the wild-type model (MV4). The simulations were run from a Cdc20 block and release situation for the models (A) NRT, (B) NRD and (C) a combined version of the NRT and the NRD models.**

The next question addressed was how the loss of transcriptional or proteolytic control influenced the robustness of the NRT and NRD models. If the redundancy of these controls confers robustness to cell cycle behaviour, then the perturbation of kinetic parameters should reveal increased fragility in models lacking one of the control layers. Both models were analysed at three different SD values: 10%, 15% and 20%. A decrease in the percentage of oscillatory solutions and viable phenotypes was observed in the NRD model compared to the wild-type MV4 (Figure VI - 2A and 2C). The oscillatory solution is a fundamental viability criterion, and thus, in the NRD model, a drop in the number of oscillatory solutions explains the reduction in viable phenotypes. At 20% SD for example, 80% of the inviable simulations failed to oscillate. This indicates that regulated protein degradation has a fundamental role in maintaining robust cell cycle oscillations in face of parameter perturbation.

Interestingly, the NRT model did not show any noticeable differences in terms of oscillatory solutions or viability compared to the wild-type MV4 (Figure VI - 2A and 2B). This suggests that regulated transcription makes little contribution to the maintenance of robust cell cycle oscillations.

To further clarify the role of regulated transcription and protein degradation in cell cycle control, the period of oscillations during parameter perturbations was compared between the three models (wild-type MV4, NRT and NRD models).

In the absence of regulated proteolysis (NRD model), the mean oscillatory period was noticeably greater than in the wild-type (Figure VI - 3C). Moreover, the distribution of the period values became wider (see CV values in Figure VI - 3), with increasing SD values. This indicates that regulated protein degradation is also important for controlling the period of cell cycle oscillations.

In the case of the NRT model, the mean oscillatory period was significantly shorter than in wild-type model (44-45 min compared to 65min, Figure VI - 3). The period of the

oscillation is shorter because the regulation of the G1 transcription factors is compromised. In the wild-type MV4, the MBF and Swi5 transcription factors promote Cln, Clb5 and Sic1 synthesis in G1. By removing the regulated synthesis of these proteins and maintaining only small constant values, their production rate is severely affected. Thus, the NRT model resembles the *cln1-3Δ sic1Δ* quadruple mutant, which cycles with a very short G1 phase (Tyers, 1996). This suggests that the length of G1 and the period of the oscillation in the NRT model are highly sensitive to the level of Sic1.

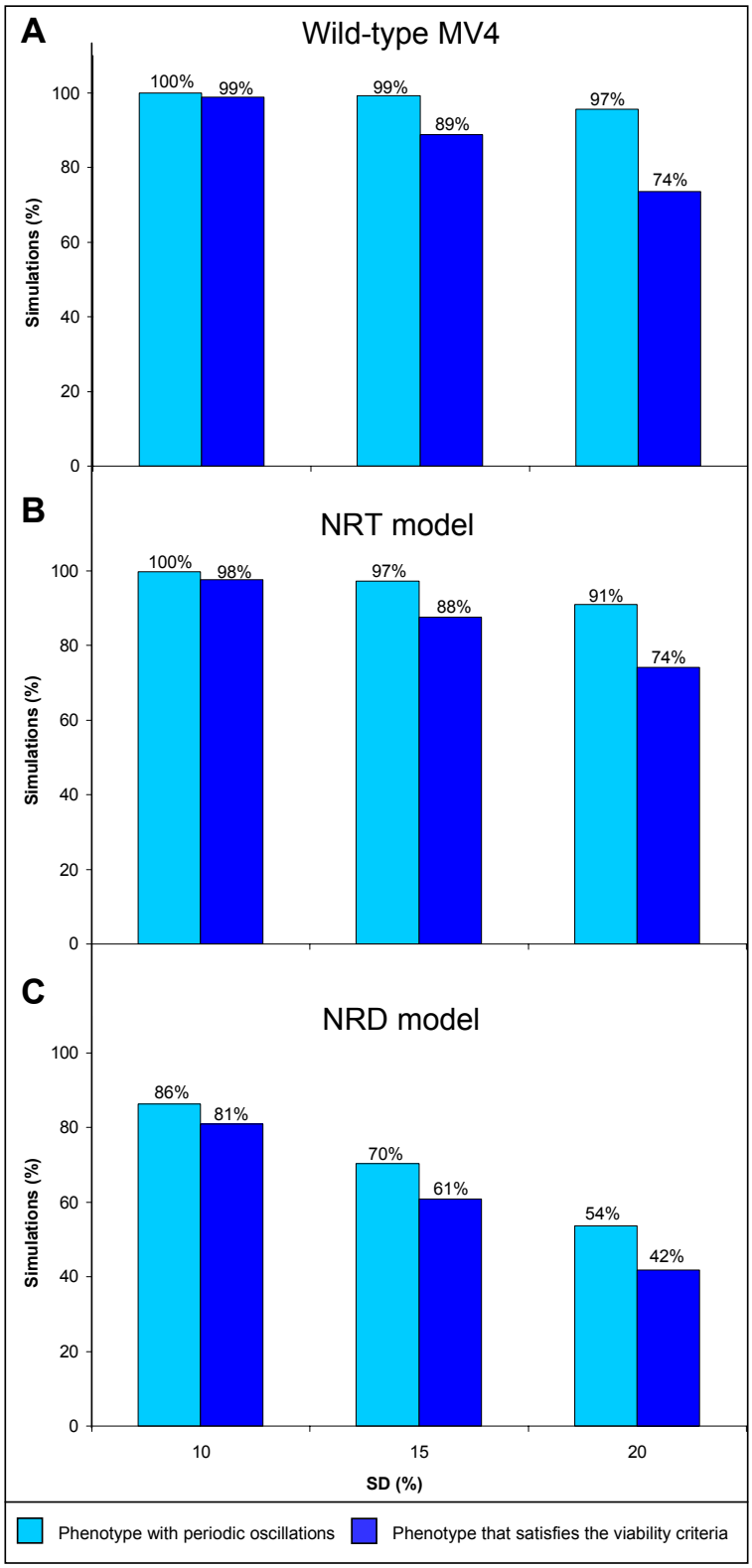


**Figure VI - 2: Bar Diagrams showing the percentage of simulations with a phenotype showing periodic oscillations (light blue) and satisfying the viability criteria (dark blue). (A) Wild-type MV4; (B) NRT model; (C) NRD model. The results are shown for three groups of 10,000 parameter sets with different SD values: 10%, 15% and 20%.**

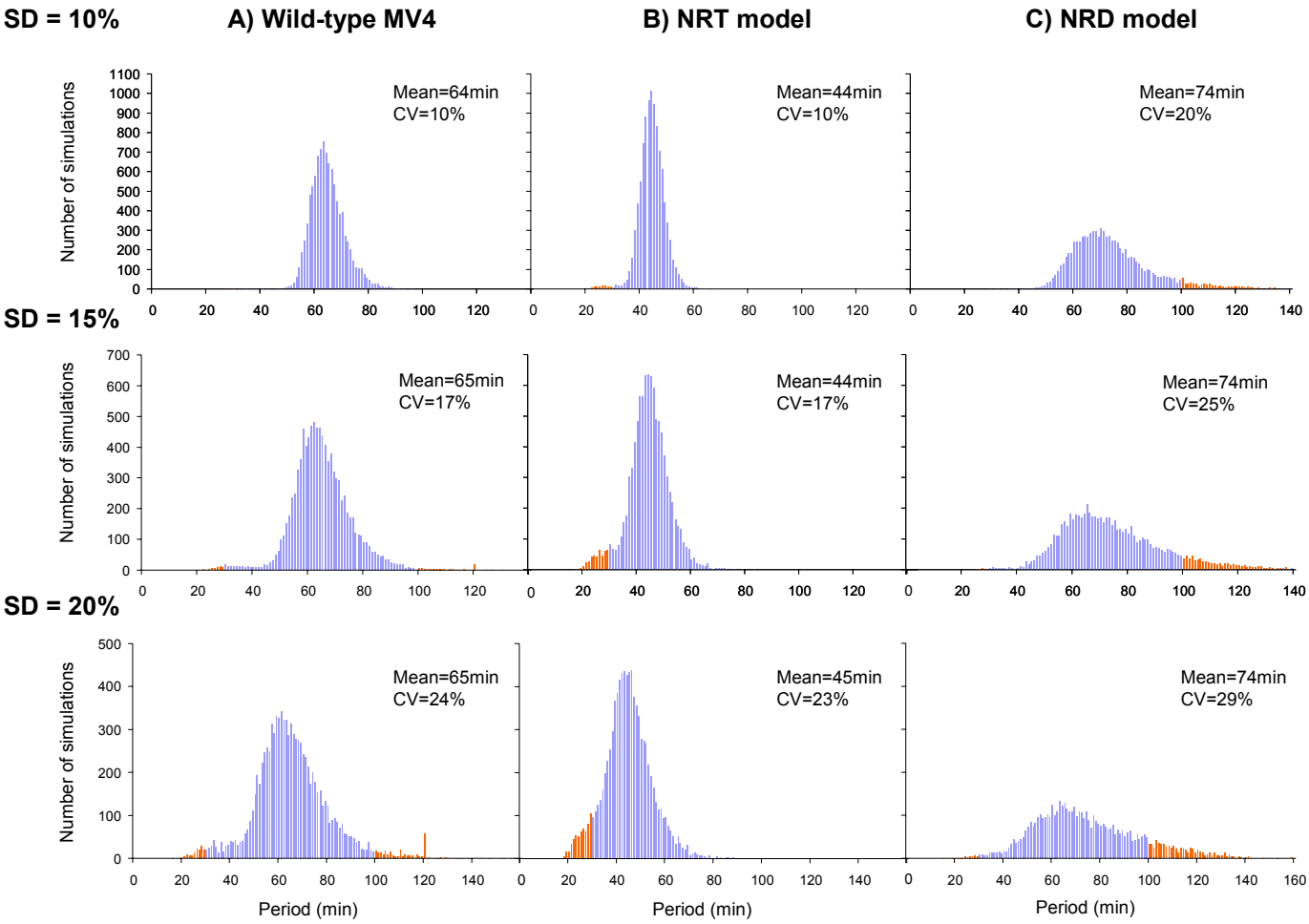


**Figure VI - 3: Histograms showing the distribution of period values in (A) the wild-type MV4, (B) the NRT model and (C) the NRD model. The results are shown for three groups of 10,000 parameter sets with different SD values: 10%, 15% and 20%. The blue bars correspond to period values between 30 and 100 min, while red bars correspond to period values outside this interval.**

In response to these results, the effect of increasing the basal synthesis rate constant value of Sic1 (originally $k_{ssic}$ = 0.004 $min^{-1}$) on the performance of the NRT model was also studied (Figure VI - 4 and Figure VI - 5). A robustness analysis was carried out for two different values of $k_{ssic}$, 0.02 $min^{-1}$ and 0.03 $min^{-1}$, in an attempt to completely recover the wild-type period distribution. The mean values of the period distributions increased to 55 min and 65 min, for $k_{ssic}$ = 0.02 $min^{-1}$ and $k_{ssic}$ = 0.03 $min^{-1}$ (at SD = 20%), respectively (Figure VI - 4). This confirms that Sic1 levels have a considerable influence on the period of cell cycle oscillations. Moreover, the period

distributions became considerably wider than both those of the wild-type model and the original NRT model with $k_{ssic}$=0.004 $min^{-1}$ (Figure VI - 3B and Figure VI - 5). However, the number of simulations exhibiting oscillations was not drastically decreased; both NRT analyses ($k_{ssic}$ = 0.02 $min^{-1}$ and $k_{ssic}$ = 0.03 $min^{-1}$) yielded more simulations displaying oscillations than the NRD model (Figure VI - 2C and Figure VI - 4). Instead, the major effect was the large number of simulations with period values that exceeded the interval established in the viability criteria.

To summarise, the analysis of the NRT model revealed that regulated transcription has a strong influence on the period of cell cycle oscillations, and contributes to period consistency in the face of perturbations.

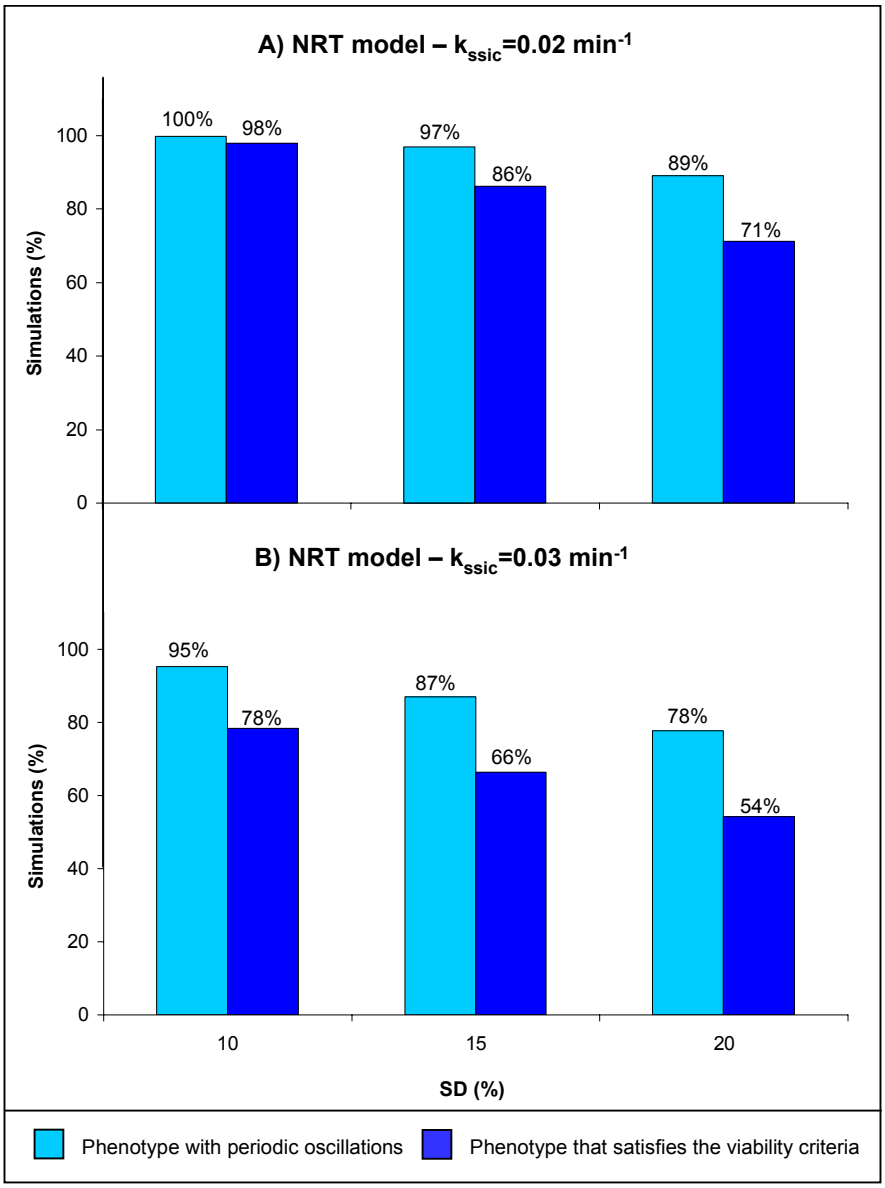


**Figure VI - 4: Bar Diagrams showing the percentage of simulations with a phenotype showing periodic oscillations (light blue) and satisfying the viability criteria (dark blue). (A) NRT model with $k_{ssic}$ increased to 0.02 $min^{-1}$; (B) NRT model with $k_{ssic}$ increased to 0.03 $min^{-1}$. The results are shown for three groups of 10,000 parameter sets with different SD values: 10%, 15% and 20%.**

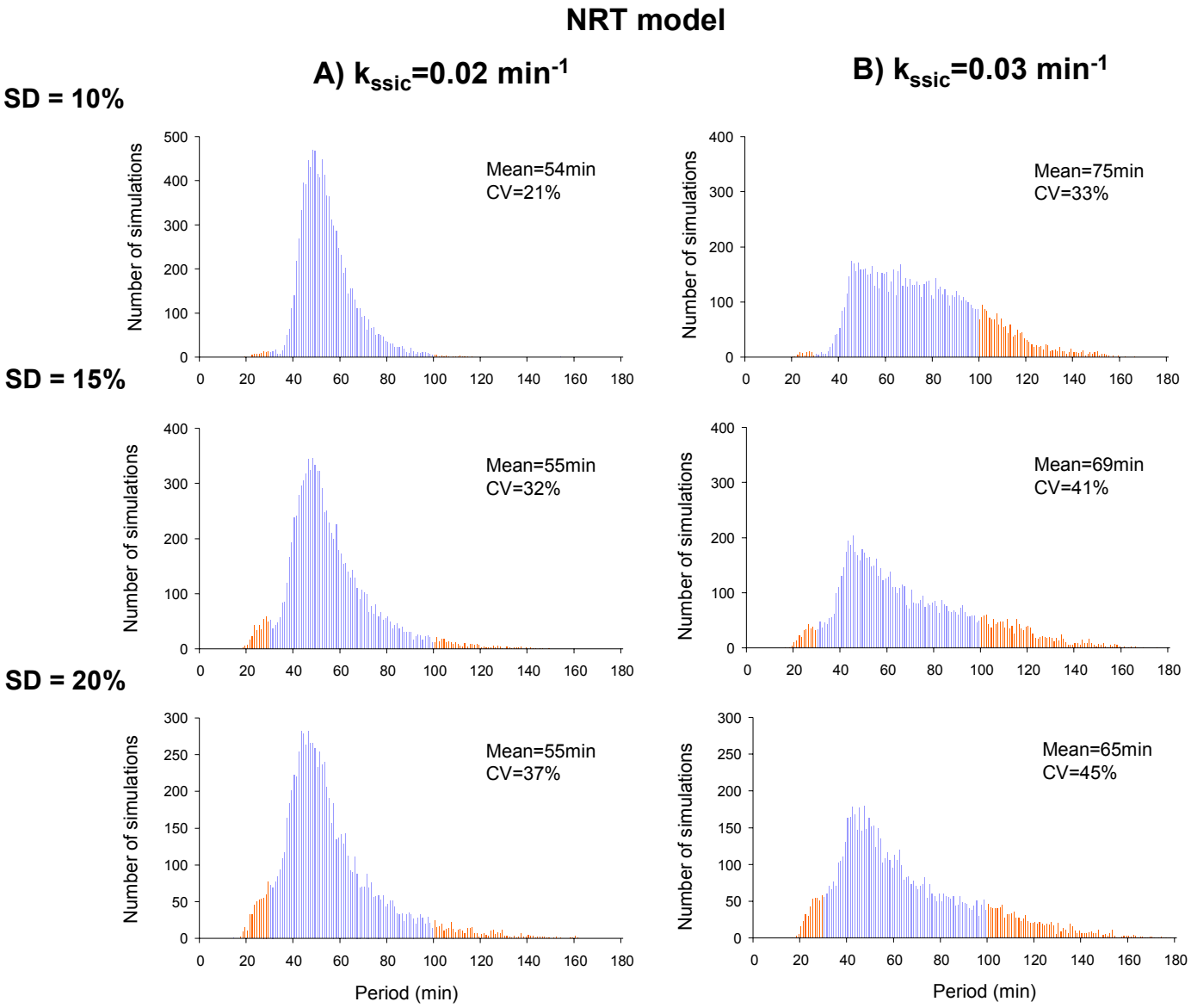


**Figure VI - 5: Histograms showing the distribution of period values in the NRT model with $k_{ssic}$ increased to (A) 0.02 min$^{-1}$, and (B) to 0.03 min$^{-1}$. The results are shown for three groups of 10,000 parameter sets with different SD values: 10%, 15% and 20%. Blue bars correspond to period values between 30 and 100 min, while red bars correspond to period values outside this interval.**

## *2. Phase Plane Analysis of the NRT and NRD models*

In Figure VI - 1, the simulated dynamic profiles of the NRD and the NRT models show cell cycle oscillations similar to the wild-type MV4, despite the major disruptions to

the cell cycle molecular network. This indicates that both the NRD and the NRT models have feedback loops that give rise to limit cycle oscillators.

The molecular network of the models was inspected closely to identify feedback loops that could potentially be driving the oscillations. In both cases, there is a negative feedback loop involving Clb2/CDK1 and Cdc14, which is coupled to a double negative feedback loop between Clb2/CDK1 and one of its antagonists (Figure VI - 6A and 6B). In the NRT model, this antagonist is Cdh1, while in the NRD model, the antagonist is Sic1. This was confirmed by performing a phase plane analysis on both the NRT and NRD models.

For the NRT model, the Cdh1 and Cdc14 nullclines were plotted (Figure VI - 6C). The phase plane shows that the two curves intersect in an unstable steady-state. The Cdh1 nullcline is S-shaped, because Cdh1 is involved in a double-negative loop with Clb2/CDK1 that generates a bistable region, and thus the Cdh1 nullcline exhibits an S-shape. The Cdc14 nullcline has a sigmoidal shape due to the negative feedback loop between Cdh1 and Cdc14; Cdc14 can only be activated once Cdh1 drops below a threshold.

For the NRD model, the Sic1 and Cdc14 nullclines were plotted (Figure VI - 6D). In this case, plotting the Cdh1 nullcline does not make sense, since Cdh1-mediated degradation of Clb2 and Cdc5 has been disrupted. The phase plane for the NRD model is very similar to the phase plane for the NRT model, despite the fact that Sic1 is plotted instead of Cdh1. This is not unexpected, considering that Sic1 is also involved in a double-negative feedback loop with Clb2/CDK1, and in a negative feedback loop with Cdc14. The Sic1 nullcline includes a bistable region, and the Cdc14 nullcline displays a switch-like behaviour. These two curves intersect in an unstable steady-state.

The NRD and NRT models show very similar phase plane portraits, which therefore shows that cell cycle progression in both these models is driven by limit cycle oscillators.

Despite this similarity, the robustness analyses performed on the two models produced considerably different results; the NRT model proved to be more robust in face of parameter variation than the NRD model. A closer look at the phase plane portraits reveals a possible reason for this difference. In the NRD model, the unstable steady-state responsible for the cell cycle oscillations is very close to the saddle node of the bistable curve. Therefore, a relatively small variation in the parameter set could easily shift this steady-state to the stable branch of the Sic1 nullcline, and switch its stability from unstable to stable. This would disrupt the cell cycle oscillations and promote an inviable phenotype. On the other hand, the steady-state in the NRT model is further away from the saddle node of the bistable curve. A larger variation in the parameter set would therefore be needed to switch the stability of the steady-state, making the NRT model more robust to parameter fluctuation.

Finally, comparing the phase plane portraits of the NRT model with the wild-type MV4 (Figure V - 4A and Figure VI - 6C), one can see that they are very similar. This could explain why the two models produce such similar results in generating robust oscillatory behaviour.

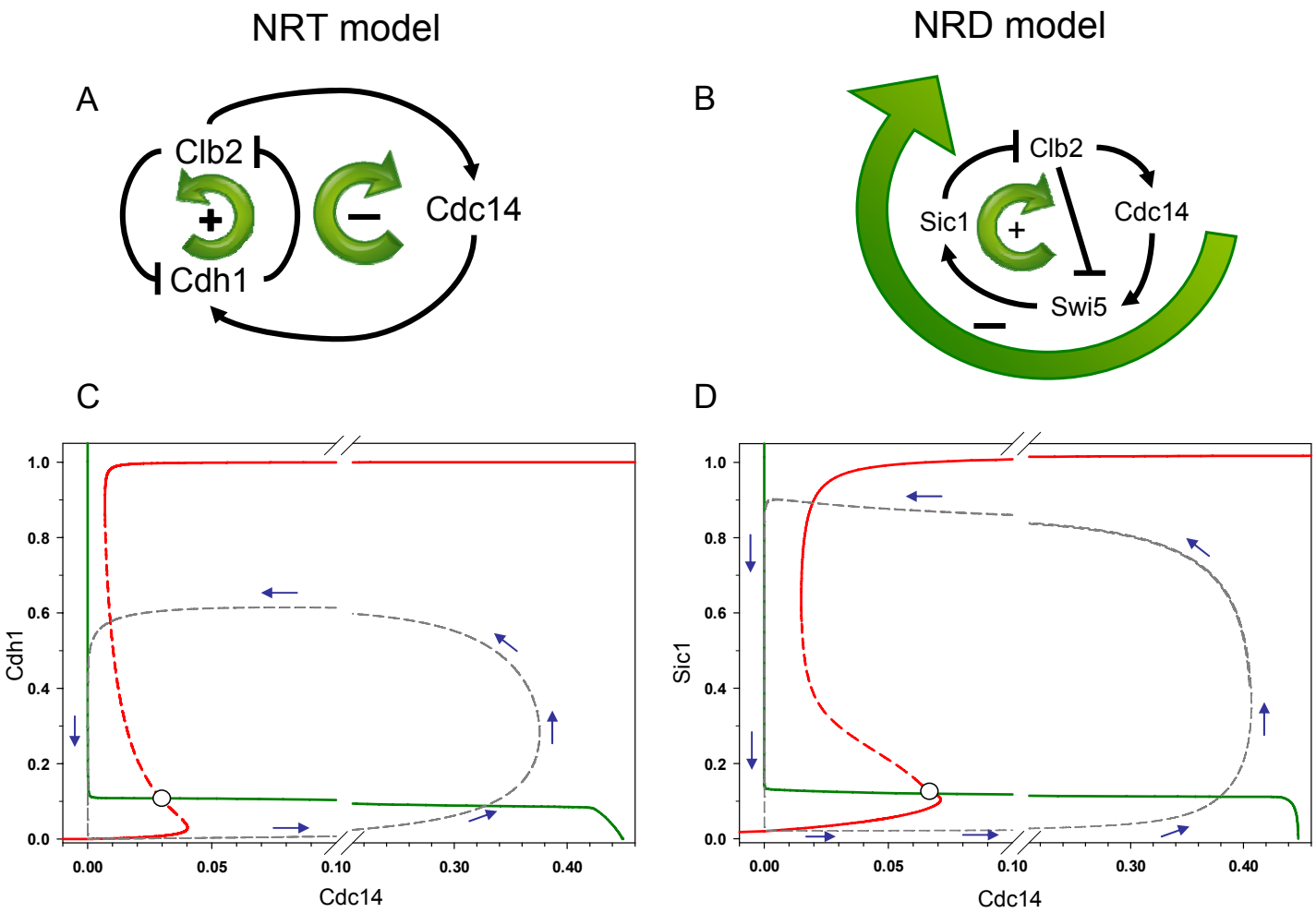


**Figure VI - 6: Cell Cycle Progression in the NRT and NRD models. (A) Network motifs generating the cell cycle oscillations in the NRT model; (B) Network motifs generating the cell cycle oscillations in the NRD model; (C) Phase plane analysis of the NRT model – Cdc14 nullcline is in green and Cdh1 nullcline is in red; (D) Phase plane analysis of the NRD model– Cdc14 nullcline is in green and Sic1 nullcline is in red. In both (C) and (D) the nullclines were calculated as one-parameter bifurcation diagrams with the model using XPPAUT, and combined to create a phase plane portrait.**

# Discussion

## *1. Background*

The mitotic cell cycle is characterised by a series of four phases (G1, S, G2 and M), which promote major physiological and morphological changes in the cell. Ultimately, these changes are responsible for cell reproduction, whereby chromosomes and other cellular components are duplicated and distributed between two daughter cells. This process of nuclear division, otherwise known as mitosis, takes place in M phase. Mitosis itself can be subdivided into four phases: prophase, metaphase, anaphase and telophase.

The term 'mitotic exit' refers to the transition between the latter stages of mitosis (i.e. anaphase and telophase) and the onset of the next G1 phase. In anaphase, the sister chromatids are segregated to opposite poles of the cell, while in telophase, the sister chromatids are repackaged into two identical daughter nuclei. Mitotic exit is a complex undertaking, as each daughter cell must receive an extra copy of the mother cell's genome.

Cell cycle progression is controlled by a complex regulatory protein network. In this thesis, I investigated the molecular mechanisms responsible for the regulation of mitotic exit. Mitotic exit has been the subject of intensive experimental investigation in budding yeast, which has elucidated the key components and interactions which govern its regulatory network. This information is insufficient to extract the network's system's-level properties, however.

With the wealth of the experimental data available, mathematical models can yield useful insights into the operating principles regulating this complex cellular process.

Conversely, the continuous appearance of new experimental data is important to refine the available mathematical descriptions. In this thesis, I studied the control of mitotic exit in budding yeast using a mathematical model. My research was based on both old and recently reported experimental observations, ranging from single to quintuple mutants.

## *2. Designing a Dynamical Model*

The design of a dynamical model of a biological phenomenon is an iterative process. Firstly, using the available experimental data, the model is built according to information about the network's components and interactions. Secondly, the model is parameterised so that its mathematical description fits with the experimental data. Next, the model is tested against experimental results which are distinct from those that were used to build the model. This step is known as the validation step. If the model fails to replicate the experimental results, then the model has failed to pass the validation step and must be redesigned. This can be done at two levels: by changing the values of the parameter set, or by changing the internal structure of the equations. The decision to change the internal structure of the equations reflects a desire to change the way that components interact within the model (i.e. the model's reaction kinetics). If this does not seem necessary, re-parameterization may be sufficient to improve the model.

The main challenge when refining a model (to incorporate new data) is to preserve the capability of the earlier model(s). It is important to refine the model with a minimum number of changes so that the model behaviour does not change dramatically. If the model is modified significantly then it is not only important to address why such optimization was required, but also, why the earlier models exhibit flawed performances.

The validation step must be repeated until the model is able to reproduce all of the experimental results available. As one can see, this process is iterative, because the

validation step determines how many times the model will be modified. The final model must adequately explain all of the available experimental data, and thereby pass the validation step. The final model should be an accurate description of the biological system it represents, and should be able to predict how the system will behave in as yet untested experimental conditions (see Figure 16).

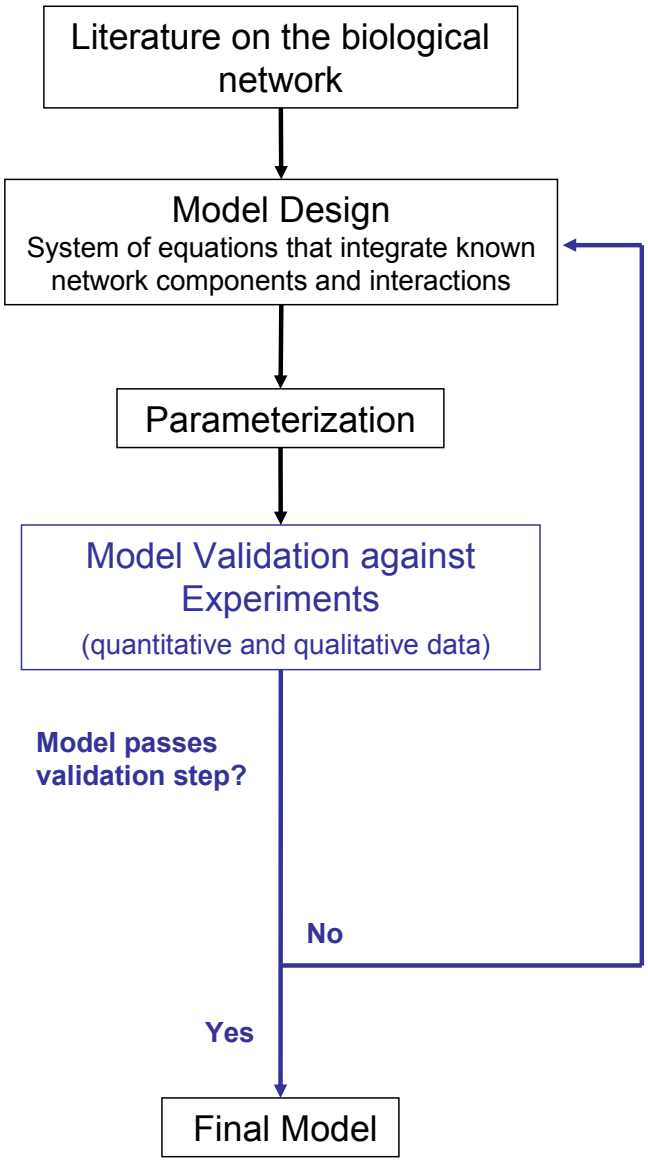


**Figure 16: Flow Chart for building a mathematical model of a biological system.**

## 3. Updating Queralt's Model

In this thesis, I designed a new mathematical model to describe the main events occurring in mitotic exit. This model was as an expansion of the previously-published Queralt's model, and was built in a stepwise manner following the iterative process described in Figure 16.

The new model is described at four distinct stages of its development. Each stage corresponds to an updated version of the model, which was created by modifying the previous version, and was tested against relevant experimental data. In this way, MV1, MV2 and MV3 can be seen as three preliminary mathematical descriptions which were necessary to obtain the final model, MV4. Chapters I to IV describe the specific modifications that were made at each stage of the model's development. They also demonstrate how, at each stage, the model was able to capture new features of the mitotic exit process.

## 4. Model Version 1: The role of Separase in Mitotic Exit

In Chapter I, MV1 examines the role of separase in mitotic exit. MV1 models separase's promotion of sister chromatid segregation through its proteolytic function, and separase's activation of Cdc14 through its proteolytic and non-proteolytic functions.

The importance of separase non-proteolytic function seems to be tightly connected with Clb2 levels within the cell. In the absence of non-proteolytic separase function, cells can still exit mitosis after a delay if Clb2 levels are low; suggesting that separase non-proteolytic contribution to mitotic exit is dispensable. However, when Clb2 levels are high (i.e. in the absence of Cdc20-mediated Clb2 degradation), separase non-proteolytic function becomes essential for mitotic exit. MV1 shows that high levels of Clb2 strongly

inhibit Cdc15, and, under these circumstances, the positive feedback loop on Cdc15 must be activated via (non-proteolytic) separase-dependent Cdc14 release. With this description, MV1 can explain phenotypic differences between the mutants of *cdc20Δ TEV$^{op}$* (Figure I - 5B), *cdc20Δ TEV$^{op}$ SIC1$^{op}$* (Figure I - 5C) and *PDS1-mdb TEV$^{op}$* (Figure I - 6C), in which TEV mimics the proteolytic function of the separase.

A complete loss of separase activity (e.g. in *PDS1*-mdb cells) results in a mitotic arrest where cells cannot segregate the sister chromatids, even in a situation where separase non-proteolytic function is not required (e. g. Clb2 levels are low). This clearly reflects the importance of separase proteolytic function.

Thus, through its dual (proteolytic and non-proteolytic) function, separase is responsible for the temporal coupling of anaphase and Cdc14 release, which is essential for efficient mitotic exit.

## 5. Model Version 2: The role of APC in Mitotic Exit

In Chapter II, MV2 focuses on the role of Cdc20 in mitotic exit. The model indicates that the APC/Cdc20 complex is crucial in driving mitotic exit; it functions as a critical node which controls the downregulation of CDK1 activity and the activation of the CDK1-counteracting phosphatase Cdc14.

According to MV2, Cdc20 promotes mitotic exit via three different pathways, through its interaction with three crucial substrates: Pds1, Clb5 and Clb2. Two complementary pieces of evidence support this conclusion. On one hand, the Cdc20 requirement was suppressed by deletion/inhibition of Cdc20's main substrates (i.e. Pds1, Clb5 and Clb2), while on the other, the Cdc20 requirement is enhanced by expressing stable versions of these substrates in cells (i.e. Pds1-mdb, Clb5-nd, Clb2-kd).

MV2 shows that the degradation of a single APC/Cdc20 substrate is insufficient to drive mitotic exit. However, the combined degradation of Pds1 and Clb5, or Pds1 and Clb2, guarantees mitotic exit by reducing the kinase-to-phosphatase ratio, allowing Cdh1 and Sic1 activation. The requirement of Pds1 degradation is crucial for the activation of the phosphatase branch. Indeed, APC/Cdc20 is able to reduce Clb2/CDK1 kinase activity directly by degrading Clb2 and/or Clb5, but Cdc14 upregulation is driven indirectly through FEAR and MEN. When Pds1 is degraded, separase inhibition is relieved and separase activates both FEAR and MEN through its non-proteolytic and proteolytic functions.

## *6. Model Version 3: The Nuclear Export of Cdc14*

The main topic in Chapter III is the nuclear export of Cdc14. For most of the cell cycle, Cdc14 is bound to Net1 in the nucleolus, and its activity is inhibited. Once Net1 has been phosphorylated, Cdc14 can dissociate from Net1 and leave the nucleolus. At this point, Cdc14's localization within the cell might influence the dynamics of mitotic exit. The main targets of Cdc14-mediated dephosphorylation (e.g. Swi5, Sic1 and Cdh1) all reside in the cytoplasm, which raises the possibility that the migration of Cdc14 between the nucleus and the cytoplasm could be an extra mechanism of Cdc14 regulation.

This possibility was explored in MV3. Here, Cdc14 is no longer regulated solely by Net1 binding and inhibition. Instead, Cdc14 is further regulated by nuclear export into the cytoplasm; this step being controlled by MEN kinases. The results obtained from MV3 indicate that Cdc14 compartmentalisation does indeed play a role in mitotic exit. Without this modification, the model cannot reproduce the phenomenon of Cdc14 endocycles when non-degradable Clb2 is expressed in cells.

Compartmentalisation only regulates Cdc14 partially however. Experiments demonstrated that *net1*Δ*cdc15*Δ mutant is viable (Lu and Cross, 2009a), which implies that Cdc14 is still able to dephosphorylate its substrates – albeit to a lesser extent – while its localization remains restricted to the nucleus.

## 7. Model Version 4: The Mechanism of Net1 Phosphorylation

In Chapter IV, the emphasis of the model is on the mechanism of Net1 phosphorylation. MV4 is in agreement with the two-hit model proposed by Manzoni and colleagues, which proposes that Clb2/CDK1, Cdc5 and MEN kinases are responsible for Net1 phosphorylation, and by extension, the dissociation of Cdc14 from Net1 (Manzoni et al., 2010). According to the two-hit model, Cdc5 is the only kinase that is absolutely required for Net1 phosphorylation, because Clb2 and MEN have partially overlapping roles. According to MV4, Net1 is first phosphorylated by either Clb2 or MEN, which promotes a second step of Net1 phosphorylation by Cdc5. Only once Net1 has been double-phosphorylated can Cdc14 dissociate itself from Net1.

The kinase responsible for the priming phosphorylation of Net1 varies with time. During mitotic progression, Clb2/CDK1 cooperates with Cdc5 to phosphorylate Net1 and induce a transient, FEAR-mediated release of Cdc14. Then, after Cdc20-mediated Clb2 degradation, it is the turn of MEN to cooperate with Cdc5 and trigger a sustained release of Cdc14.

# 8. Model Version 4: Interpretation of the Cdc14 Endocycles

MV4 is the final version of the model proposed in the thesis. It can be used to explain all of the experimental data already addressed by MV1, MV2 and MV3, plus new mutant situations that the previous versions could not account for. MV4 provides the most comprehensive mathematical description of mitotic exit, and is therefore the best equipped to study complex mutant situations such as the recently discovered Cdc14 endocycles (Lu and Cross, 2010; Manzoni et al., 2010).

In MV4, the expression of non-degradable Clb2 above a threshold level blocks mitotic exit. It also promotes the periodic release and recapture of Cdc14; oscillatory behaviour known as Cdc14 endocycles. This phenomenon is known as Cdc14 endocycles and, interestingly, it shows that certain regulators of mitotic exit can oscillate independently of Clb2 oscillations and cell cycle progression. The regulatory network responsible for Cdc14 endocycles in MV4 is based on the descriptions provided by Lu and Cross (2010) and Manzoni et al. (2010). Since MV4 can explain the Cdc14 endocycles, together with other classic experiments in the literature, the model provides a true system's view of Cdc14 endocycles within the mitotic exit process.

Implicitly, MV4 considers that the budding yeast cell cycle should be characterised by one-way switches, and it thoroughly describes the one-way switch controlling the mitotic exit transition. The other known one-way switch in budding yeast, the one controlling START transition, is not explicit in MV4 because MV4 represents a large mother cell, in which this one-way switch does not apply. The one-way switches are the consequence of antagonistic interactions between Clb/CDK1 and their negative regulators (i.e. APC/Cdh1 and Sic1). To turn on these switches, cells make use of

'helper' molecules that are regulated by negative feedback loops (Tyson and Novak, 2008). In MV4, the helper molecules are Cdc20 and Cdc14.

In Chapter V, a phase plane analysis was performed so as to better understand cell cycle progression in MV4. Initially, the results appeared to suggest that cell cycle oscillations are driven by a relaxation oscillator, but this was merely an artefact of MV4 representing a large mother cell (Figure V - 4A). After adapting the model to describe a small daughter cell, the phase plane changes so that a stable G1 steady-state appears, and cell cycle progression is driven by the activation of the START transition (Figure V - 4B).

The phase plane analysis was then extended to the study of the Cdc14 endocycles (Figure V - 4C). The results indicate that the oscillations underlying Cdc14 endocycles are very different from the limit cycles characteristic of mother cells; in the endocycles, high Clb2/CDK1 activity represses many cell cycle regulators (Sic1, Swi5, Cln, MBF, see Figure V - 6). According to our analysis, Cdc14 endocycles are simply the consequence of redundant negative feedback loops in Cdc14 release, generated by the kinases Clb2 and Cdc5 (Figure V - 5). Both kinases trigger Cdc14 release and are targeted for degradation by Cdc14-activated APC/Cdh1. In mutants expressing non-degradable Clb2, the negative feedback loop involving Clb2 degradation cannot be engaged. In these circumstances, Cdc5 can still be degraded by Cdh1, and it is Cdc5 degradation which causes Cdc14 re-sequestration and Cdh1 phosphorylation. After Cdh1 inactivation, Cdc5 is re-synthesised and the repetition of these steps generates the Cdc14 endocycles. Therefore, MV4 portrays the endocycle phenomenon as the outcome of an abnormal cell cycle block caused by high levels of Clb2.

Lu and Cross (2010) do not share this interpretation, however. In their opinion, the Cdc5-dependent negative feedback loop responsible for Cdc14 endocycles must have evolved as an independent oscillator. On the contrary, MV4 is based on the assumption

that these oscillations have no physiological role; instead, they are an experimental artefact. Negative feedback loops are common in biological systems to prevent the sustained activation of various components, and, under certain circumstances (e.g. if they are sufficiently time-delayed), these feedback loops can generate oscillations.

## *9. G1 Phase in the Model Version 4*

The final model, MV4, can reproduce a full budding yeast cell cycle, but its main limitation lies in its description of G1 phase. MV4 contains a simplified description of G1 phase, as it ignores the cell-size dependent activation of G1 transcription factors (i.e. MBF and SBF). In budding yeast cells, the regulation of MBF and SBF activity is under dual control. On one hand, MBF and SBF are inhibited by the activity of Clb/CDK1 complexes during S, G2 and M phases. On the other, they are reactivated once cells reach a critical size during late G1 phase.

During cell division, budding yeast cells give rise to a small daughter cell and a large mother cell. Characteristically, only the small daughter cell is born beneath the critical cell size. The mother cell already exceeds the critical size, and thus cell size is not a rate-limiting factor for MBF and SBF activation. Hence, by neglecting the cell size-dependent regulation of MBF and SBF, MV4 only describes a large mother cell where these transcription factors are reactivated just after mitosis and the cell cycle time is minimum.

## 10. Robustness Analysis of Model Version 4

There is a lack of clear understanding about how cells retain their viability in the face of perturbations. Many hypotheses have been outlined, but due to technical limitations, none have been thoroughly tested. Since MV4 describes a budding yeast cell cycle, this model was used as a platform to study the requirements for robust cell cycle behaviour. In this thesis, I performed an *in silico* analysis, providing a preliminary set of results that may be used as a basis for future studies (both experimental and theoretical).

In Chapter V, I conducted a robustness analysis on MV4 by randomly varying all the parameter values in the network. The aim was to see how much variation could be introduced before the percentage of simulations meeting the viability criteria would fall below 50%. The results indicate that a standard deviation of 25% is possible before this threshold level is crossed (Figure V - 7). Unfortunately, this study cannot rule out the existence of another completely unrelated parameter set that could fit all of the experimental data. Nevertheless, it clearly shows how much the parameter values can deviate from the original parameter set and still produce a phenotype reminiscent of the eukaryotic cell cycle (i.e. that of budding yeast). Significantly, this study represents the first attempt to subject a cell cycle model to global parameter perturbations.

## 11. Using Robustness Analysis to Explore Redundancy in Cell Cycle Control

Bioinformatic evidence from several different species – human (*Homo sapiens*), budding yeast (*Saccharomyces cerevisiae*), fission yeast (*Schizosaccharomyces pombe)*, and arabidopsis (*Arabidopsis thaliana*) – suggest that proteins involved in cell cycle control are regulated by phosphorylation, in addition to transcription and

degradation (de Lichtenberg et al., 2007; Jensen et al., 2006). Given that these redundant layers of cell cycle control are conserved among different species, redundancy may contribute towards the robustness of cell cycle behaviour.

In Chapter VI, I used the results of the previous robustness analysis as a control to evaluate the contribution of different layers of protein regulation to robust behaviour in the face of parameter perturbations. The idea was to compare this control condition with results obtained from the robustness analysis of two additional, 'mutated' versions of MV4. In one version, the NRT model, protein synthesis is not dependent on regulated transcription factors. In the other, the NRD model, proteins are not regulated by targeted degradation.

The results indicate that the NRD model is much more fragile than the wild-type model when subjected to parameter perturbations. As depicted in Figure VI - 2A and 2C, the lack of regulated protein degradation decreases the probability of obtaining an oscillatory solution. Moreover, the period of the oscillations follow a wider distribution of values, with a number of them outside the limits imposed in the viability criteria (Figure VI - 3C). Thus, the regulation of protein degradation appears to play a major role in protecting the oscillatory cell cycle behaviour against parameter perturbations. The NRT model, on the other hand, produces simulations that satisfy the viability criteria with a probability similar to that of the wild-type model (Figure VI - 2A and 2B). The only significant difference is that the average period of the oscillations is considerably shorter (approximately 20 min) than the ones for the wild-type model (Figure VI - 3B).

It is well known that early embryonic cells cycle without gene transcription since they receive all of the essential mRNAs from the mother cell (Murray and Kirschner, 1989a; Murray and Kirschner, 1989b). In early embryos therefore, cell cycle control is achieved through regulated protein degradation and post-translational modifications alone. This is consistent with the results described above, whereby robust oscillatory behaviour can

persist in the face of parameter perturbations, even in the absence of regulated protein transcription.

The results in Chapter VI show that the period of cell cycle oscillations is dependent on the synthesis rate of cell cycle regulators. For example, these period values increase with an increase in the rate constant value of Sic1 (through the extension G1 phase). In addition, the period distributions become much wider with increasing Sic1 synthesis, and thus a greater number of simulations fail to meet the viability criteria (Figure VI - 4 and Figure VI - 5). These observations indicate that regulation at the level of transcription has an important role in controlling cell cycle period.

The regulated transcription of cell cycle proteins also allows the cell to adjust its cycle duration without increasing the spread of its distribution. The importance of regulating cell cycle period becomes clear if one takes cell growth into consideration as well. Balanced growth and division requires that the duration of cell cycle is equal to the characteristic mass doubling time of the cell; otherwise, cell size will drift in successive generations. This balance is achieved by cell size control mechanisms which extend the period of the cell cycle oscillator by stopping it in a stable steady-state. Early embryonic cells rely solely on regulated proteolysis and post-transcriptional modifications to produce robust cell cycle oscillations, bypassing the transcriptional control of cell cycle duration. This could explain why their cell cycles are fast, they do not grow, and their cells become smaller and smaller at each successive division.

The simulated dynamic profiles of the NRD and NRT models show cell cycle oscillations similar to those of the wild-type model (Figure VI - 1A and 1B). This result indicates that – despite major regulatory disruptions – both models retain key features of the regulatory network required to generate a cell cycle oscillator. In the NRT model, antagonism between Clb2/CDK1 and APC/Cdh1 proves sufficient to provide bistability. In the NRD model, which lacks regulated degradation by APC, cell cycle oscillations are

the consequence of antagonism between Clb2/CDK1 and Sic1. Interestingly, the unstable steady-state in the NRD model is very close to the bifurcation point that determines the oscillatory behaviour. Presumably, this explains why the NRD model is less robust than the NRT or wild-type models in maintaining limit cycle oscillations upon perturbations.

To summarise, the robustness analysis of MV4 defined a local region of parameter space in which the model's phenotype is maintained (i.e. 10% SD), and demonstrated how this robust behaviour is lost when that local region is enlarged. In assessing the relative contribution of the redundant layers of protein regulation to cell cycle robustness, it emerged that regulated transcription and regulated degradation make different contributions to cell cycle control. Regulated protein degradation is crucial for generating oscillatory cell cycle behaviour, while regulated transcription is responsible for controlling cell cycle period.

## *12. Major Accomplishments*

This thesis provides an in-depth analysis of the process of mitotic exit by describing the step-wise development of a complex mathematical model. This was achieved by starting from a simple description of mitotic exit with a limited number of components (Queralt et al., 2006), and developing it further. The final outcome is a model of a complete cell cycle, which accounts for both classic and recent experimental findings. With MV4, the recently discovered phenomenon of Cdc14 endocycles can be reproduced and analysed using a full budding yeast cell cycle model. MV4 is the first model to achieve this, since the previous models to address the endocycles phenomenon focused on a smaller part of the molecular network (Manzoni et al., 2010) or used a mechanical approach (Lu and Cross, 2010).

Hence, MV4 has provided valuable quantitative insights into cell cycle regulation. In future, new insights may be gained through further analysis of the structure of the equations and kinetic parameter sensitivity. To give an example of the latter, the robustness analysis of MV4 yielded valuable new information on the governing principles of the cell cycle control network.

## *13. Future Research*

Despite the comprehensiveness of MV4, the work presented in this thesis should be followed up by further studies. Some of the assumptions made during the model's design can be refined, and there are still a small number of mutant situations that the model fails to explain (Appendix 4). Moreover, the robustness analysis presented here should be extended in order to complement our understanding of how the choice of parameters influences the model's performance.

As discussed previously, MV4 is restricted by the fact that it can only represent a mother cell. MV4 could be extended so as to describe the asymmetric cell division that differentiates a mother cell from a daughter cell. A simple way to do this would be to add a new variable representing cell size. Previous budding yeast cell cycle models have incorporated a variable named 'mass' that increases proportionally to a given growth rate during cell cycle progression (Chen et al., 2004; Chen et al., 2000). This variable is then coupled to cyclin synthesis, creating a direct link between cell size and cyclin level in the cell.

Adding the variable 'mass' to MV4 would allow coordination between the START transition and cell size. By coupling Cln synthesis with 'mass' and MBF activation with

Cln upregulation, Clb5 upregulation and Sic1 inactivation would be prevented until the cell reaches a critical size (modelled as a critical 'mass' value).

At division, cell size must be asymmetrically partitioned between mother and daughter cells. For simplicity, the model could assume that the mother cell keeps the same size as immediately prior to budding, and that all growth after bud emergence is restricted to the daughter cell. As a result, MV4's cell cycle description would remain mostly unchanged for a mother cell, and for a daughter cell, the major difference would be an extended G1 phase. This would also be an elegant way to incorporate the START transition into MV4, which is currently not explicit.

The choice of kinetics in MV4 could also be reconsidered. As mentioned in the Methods section, the Goldbeter-Koshland function (Goldbeter and Koshland, 1981) is switch-like; that is, its signal-response curve appears sigmoidal, in particular when the substrate concentration is much higher than the enzyme concentration ("zero order ultrasensitivity"). Thus, when one needs to describe an abrupt sigmoidal response mathematically, the Goldbeter-Koshland function provides a good approximation. The cell cycle regulatory machinery is embedded with molecular switches that promote cell cycle progression, and so, in the cell cycle field, it has become common to model these biochemical reactions with Goldbeter-Koshland kinetics (Chen et al., 2004; Chen et al., 2000; Csikasz-Nagy et al., 2006; Novak et al., 1998), as was the case in this work. However, the use of this kinetics has been questioned recently, because, even if it correctly describes the experimental observations, it does not confirm the molecular mechanism reported.

Many cell cycle proteins undergo multi-site phosphorylation and this may control their enzymatic activity. If an enzyme phosphorylates more than one amino acid residue in a single binding event with the substrate, there is not much difference between a multiple phosphorylation event and a single phosphorylation event. However, if the

phosphorylation of each amino acid residue requires a single binding event, then the resulting kinetics becomes different (Kapuy et al., 2009). Multi-site phosphorylation kinetics has been studied thoroughly, and has already been applied in recent cell cycle models in place of Goldbeter-Koshland kinetics (Barik et al., 2010; Gunawardena, 2005; Kapuy et al., 2009). (Barik et al., 2010; Gunawardena, 2005; Kapuy et al., 2009). It would be interesting to do the same in MV4, and have all the equations described through the law of mass action. As a direct result, one could conduct stochastic simulations with MV4.

In Appendix 5, a number of mutant situations are shown that MV4 cannot simulate. All biological models have limitations, since any phenomenological description will always be a simplified version of the phenomenon itself. Nevertheless, understanding where and why a model fails is fundamental in guiding future research. One aspect that clearly requires further investigation is the mechanism controlling Net1 phosphorylation and subsequent Cdc14 release. MV4 fails to explain four mutant situations as a consequence of this lack of knowledge.

Take, for example, the situation where cells overexpressing separase and carrying the mutated protein Net1-6CDK1 are grown in nocodazole. MV4 predicts that these cells should be arrested in metaphase, with Cdc14 released due to MEN activation. Contrary to this prediction, experimental results indicate that Cdc14 remains sequestered in the nucleolus (Queralt et al., 2006). This suggests that Net1-6CDK1 must also be immune to phosphorylation by MEN kinases, although this theory has not been experimentally verified.

The overexpression of Net1 in cells has been shown to prevent Cdc14 release and arrest cells in telophase (Visintin et al., 1998). Due to the strong inhibitory effect that Net1 phosphorylation has in MV4, the model cannot simulate this mutant. Instead, MV4 predicts that these cells should exit mitosis efficiently. This discrepancy could result from

MV4's assumption that phosphorylated Net1 is completely unable to bind to Cdc14. This not being the case, an overexpression of Net1 may be responsible for Cdc14 sequestration. This hypothesis still needs to be tested experimentally, however.

The precise details of MEN regulation are still a matter of debate. Tem1 is considered necessary to activate Cdc15, yet cells with a Tem1 deletion can activate MEN if Cdc15 is overexpressed (Jaspersen et al., 1998). Thus, Cdc15 may retain some residual activity, even in the absence of Tem1. MV4 does not take this into account, but could be supplemented if more experimental data become available on the independent role of Cdc15 in MEN regulation.

The two-hit mechanism proposed for Net1 phosphorylation fails to explain the mutant *cdc15*Δ GAL-CDC5. MV4 predicts that cells should be arrested in telophase with transient Cdc14 release, yet experiments show that the mutant is viable (Visintin et al., 2003). Experimental results suggest that the overexpression of Cdc5 bypasses the MEN requirement for mitotic exit. A possible explanation is that an excess of Cdc5 could phosphorylate CDK1 sites on Net1. This concept would be interesting to test experimentally.

Recently, a theoretical paper was published focusing on the role of Cdc5 in mitotic exit (Hancioglu and Tyson, 2012). The paper assumes that a single phosphorylation of Net1 is able to release Cdc14, despite the fact that Net1 can suffer a double phosphorylation. This alternative model is successful in explaining several Cdc5 mutant situations, but fails to incorporate the mechanism responsible for Cdc14 endocycles. Ideally, a model should be able to explain all of the relevant mutants. Unfortunately, the current lack of experimental evidence regarding Net1 phosphorylation is clouding theoretical work on this topic.

In chapters V and VI of this thesis, a robustness analysis was performed using a Monte-Carlo method whereby all of the parameters were varied according to a normal

probability distribution. A normal distribution is an appropriate choice because it faithfully captures the distribution of biological noise. However, other probability distributions could also be tested, such as the log-normal probability distribution or the uniform probability distribution.

A log-normal distribution resembles a normal distribution at small standard deviation (SD) values. The advantage of this distribution is that it never allows the parameters to take negative values, even at large SD values. As the present study was conducted at small SD values, the use of a log-normal distribution would not change our results. Nevertheless, it might be interesting to extend our study to include larger SD values. In this situation, it would be preferable to perform the robustness analysis using a log-normal distribution.

According to a uniform probability distribution, a parameter has an equal probability of taking any value within a given interval, and zero probability of taking any other value. This distribution allows the establishment of strict boundaries in parameter values. Thus, replicating the current study using a uniform distribution would add extra information to the robustness analysis; it would establish clear intervals for safe parameter values. For large intervals, however, the new parameter value would tend to lose its connection to the nominal value. In this scenario, the system would probably fail to perform very quickly.

In addition to varying the parameter values using different probability distributions, the robustness analysis could be improved by focusing on specific subsets of parameters. By varying only a chosen subset of parameters instead of the full set, one could investigate how different regulatory reactions affect the system's performance. A good starting point would be the information gathered from the robustness analysis of the NRT and NRD models. These results already provide major clues as to how

parameters related to regulated transcription and degradation can influence the system's performance.

Despite the suggested improvements described here, MV4 is already a comprehensive representation of mitotic exit in budding yeast. In its current form, MV4 can already be used to compare mitotic exit between different eukaryotes. For instance, in *Schizosaccharomyces pombe*, the Cdc14 homolog Clp1/Flp1 inhibits mitotic CDK1 activity. Moreover, Clp1/Flp1 is regulated by a molecular network similar to MEN, known as SIN (Septation Initiation Network) (Bardin and Amon, 2001). In *Caenorhabditis elegans*, the Cdc14 homolog CeCDC-14 is required for cytokinesis (Gruneberg et al., 2002), (Gruneberg et al., 2002), and in humans, Cdc14 has not one but two homologs (hCdc14A and hCdc14B). The role of hCdc14A and hCdc14B in mitotic exit is poorly understood, yet their similarity to budding yeast Cdc14 provides a clue. Indeed, in vitro assays have shown that hCdc14A can dephosphorylate and activate APC/Cdh1 (Bembenek and Yu, 2001).

The organism in which the mitotic exit phenomenon has been most thoroughly studied is budding yeast. Clearly, there is a level of conservation in the events occurring during mitotic exit across different eukaryotes, and thus, this knowledge should help us to better understand what happens in other organisms, including humans. To this end, formulating experiments to discern the similarities and the differences between budding yeast and other species is a logical starting point. MV4 could be used to determine the molecular targets of these experiments and to achieve a more general view of mitotic exit.

# Bibliography


Alexandru, G., Zachariae, W., Schleiffer, A., and Nasmyth, K. (1999). Sister chromatid separation and chromosome re-duplication are regulated by different mechanisms in response to spindle damage. Embo Journal *18*, 2707-2721.

Amon, A., Irniger, S., and Nasmyth, K. (1994). Closing the Cell-Cycle Circle in Yeast - G2 Cyclin Proteolysis Initiated at Mitosis Persists until the Activation of G1 Cyclins in the Next Cycle. Cell *77*, 1037-1050.

Amon, A., Tyers, M., Futcher, B., and Nasmyth, K. (1993). Mechanisms that help the Yeast-Cell Cycle Clock Tick - G2 Cyclins Transcriptionally Active G2 Cyclins and Repress G1 Cyclins. Cell *74*, 993-1007.

Azzam, R., Chen, S. L., Shou, W. Y., Mah, A. S., Alexandru, G., Nasmyth, K., Annan, R. S., Carr, S. A., and Deshaies, R. J. (2004). Phosphorylation by cyclin B-Cdk underlies release of mitotic exit activator Cdc14 from the nucleolus. Science *305*, 516-519.

Bardin, A. J., and Amon, A. (2001). Men and sin: What's the difference? Nature Reviews Molecular Cell Biology *2*, 815-826.

Bardin, A. J., Visintin, R., and Amon, A. (2000). A mechanism for coupling exit from mitosis to partitioning of the nucleus. Cell *102*, 21-31.

Barik, D., Baumann, W. T., Paul, M. R., Novak, B., and Tyson, J. J. (2010). A model of yeast cell-cycle regulation based on multisite phosphorylation. Molecular Systems Biology *6*.

Barral, Y., Jentsch, S., and Mann, C. (1995). G(1) Cyclin Turnover and Nutrient-uptake are controlled by a Common Pathway in Yeast. Genes & Development *9*, 399-409.

Basco, R. D., Segal, M. D., and Reed, S. I. (1995). Negative Regulation of G(1) and G(2) by S-phase Cyclins of Saccharomyces Cerevisine. Molecular and Cellular Biology *15*, 5030-5042.

Bean, J. M., Siggia, E. D., and Cross, F. R. (2005). High functional overlap between MluI cell-cycle box binding factor and Swi4/6 cell-cycle box binding factor in the G1/S transcriptional program in Saccharomyces cerevisiae. Genetics *171*, 49-61.

Bembenek, J., and Yu, H. T. (2001). Regulation of the anaphase-promoting complex by the dual specificity phosphatase human Cdc14a. Journal of Biological Chemistry *276*, 48237-48242.

Bueno, A., and Russell, P. (1992). Dual Functions of CDC6 - A Yeast Protein Required for DNA-Replication also inhibits Nuclear Division. Embo Journal *11*, 2167-2176.

Charvin, G., Oikonomou, C., Siggia, E. D., and Cross, F. R. (2010). Origin of Irreversibility of Cell Cycle Start in Budding Yeast. Plos Biology *8*.

Chen, K. C., Calzone, L., Csikasz-Nagy, A., Cross, F. R., Novak, B., and Tyson, J. J. (2004). Integrative analysis of cell cycle control in budding yeast. Molecular Biology of the Cell *15*, 3841-3862.

Chen, K. C., Csikasz-Nagy, A., Gyorffy, B., Val, J., Novak, B., and Tyson, J. J. (2000). Kinetic analysis of a molecular model of the budding yeast cell cycle. Molecular Biology of the Cell *11*, 369-391.

Christopher P. Fall, E. S. M., John M. Wagner, John J. Tyson (2002). Computational Cell Biology, Springer-Verlag New York).

Ciliberto, A., Lukacs, A., Toth, A., Tyson, J. J., and Novak, B. (2005). Rewiring the exit from mitosis. Cell Cycle *4*, 1107-1112.

CohenFix, O., Peters, J. M., Kirschner, M. W., and Koshland, D. (1996). Anaphase initiation in Saccharomyces cerevisiae is controlled by the APC-dependent degradation of the anaphase inhibitor Pds1p. Genes & Development *10*, 3081-3093.

Cross, F. R. (2003). Two redundant oscillatory mechanisms in the yeast cell cycle. Developmental Cell *4*, 741-752.

Cross, F. R., Yuste-Rojas, M., Gray, S., and Jacobson, M. D. (1999). Specialization and targeting of B-type cyclins. Molecular Cell *4*, 11-19.

Csikasz-Nagy, A., Battogtokh, D., Chen, K. C., Novak, B., and Tyson, J. J. (2006). Analysis of a generic model of eukaryotic cell-cycle regulation. Biophysical Journal *90*, 4361-4379.

D'Amours, D., Stegmeier, F., and Amon, A. (2004). Cdc14 and condensin control the dissolution of cohesin-independent chromosome linkages at repeated DNA. Cell *117*, 455-469.

D'Aquino, K. E., Monje-Casas, F., Paulson, J., Reiser, V., Charles, G. M., Lai, L., Shokat, K. M., and Amon, A. (2005). The protein kinase Kin4 inhibits exit from mitosis in response to spindle position defects. Molecular Cell *19*, 223-234.

De Antoni, A., Pearson, C. G., Cimini, D., Canman, J. C., Sala, V., Nezi, L., Mapelli, M., Sironi, L., Faretta, M., Salmon, E. D., and Musacchio, A. (2005). The Mad1/Mad2 complex as a template for Mad2 activation in the spindle assembly checkpoint. Current Biology *15*, 214-225.

de Lichtenberg, U., Jensen, T. S., Brunak, S., Bork, P., and Jensen, L. J. (2007). Evolution of cell cycle control: Same molecular machines, different regulation. Cell Cycle *6*, 1819-1825.

Dirick, L., Bohm, T., and Nasmyth, K. (1995). Roles and Regulation of Cln-Cdc28 Kinases at the Start of the Cell-Cycle of Saccharomyces-Cerevisiae. Embo Journal *14*, 4803-4813.

Drapkin, B. J., Lu, Y., Procko, A. L., Timney, B. L., and Cross, F. R. (2009). Analysis of the mitotic exit control system using locked levels of stable mitotic cyclin. Molecular Systems Biology *5*.

Drury, L. S., Perkins, G., and Diffley, J. F. X. (1997). The Cdc4/34/53 pathway targets Cdc6p for proteolysis in budding yeast. Embo Journal *16*, 5966-5976.

Elledge, S. J. (1996). Cell cycle checkpoints: Preventing an identity crisis. Science *274*, 1664-1672.

Ermentrout, B., Author, Mahajan, A., and Reviewer (2003). Simulating, Analyzing, and Animating Dynamical Systems: A Guide to XPPAUT for Researchers and Students. Applied Mechanics Reviews *56*, B53.

Evans, T., Rosenthal, E. T., Youngblom, J., Distel, D., and Hunt, T. (1983). Cyclin - A Protein Specified by Maternal Messenger-RNA in Sea-Urchin eggs that is destroyed at each Cleavage Division. Cell *33*, 389-396.

Fang, G. W., Yu, H. T., and Kirschner, M. W. (1998). Direct binding of CDC20 protein family members activates the anaphase-promoting complex in mitosis and G1. Molecular Cell *2*, 163-171.

Fesquet, D., Fitzpatrick, P. J., Johnson, A. L., Kramer, K. M., Toyn, J. H., and Johnston, L. H. (1999). A Bub2p-dependent spindle checkpoint pathway regulates the Dbf2p kinase in budding yeast. Embo Journal *18*, 2424-2434.

Fitch, I., Dahmann, C., Surana, U., Amon, A., Nasmyth, K., Goetsch, L., Byers, B., and Futcher, B. (1992). Characterization of 4 B-Type Cyclin Genes of the Budding Yeast Saccharomyces-Cerevisiae. Molecular Biology of the Cell *3*, 805-818.

Geymonat, M., Spanos, A., Walker, P. A., Johnston, L. H., and Sedgwick, S. G. (2003). In vitro regulation of budding yeast Bfa1/Bub2 GAP activity by Cdc5. Journal of Biological Chemistry *278*, 14591-14594.

Goldbeter, A., and Koshland, D. E. (1981). An Amplified Sensitivity arising from Covalent Modifications in Biological-Systems. Proceedings of the National Academy of Sciences of the United States of America-Biological Sciences *78*, 6840-6844.

Gruneberg, U., Campbell, K., Simpson, C., Grindlay, J., and Schiebel, E. (2000). Nud1p links astral microtubule organization and the control of exit from mitosis. Embo Journal *19*, 6475-6488.

Gruneberg, U., Glotzer, M., Gartner, A., and Nigg, E. A. (2002). The CeCDC-14 phosphatase is required for cytokinesis in the Caenorhabditis elegans embryo. Journal of Cell Biology *158*, 901-914.

Gunawardena, J. (2005). Multisite protein phosphorylation makes a good threshold but can be a poor switch. Proceedings of the National Academy of Sciences of the United States of America *102*, 14617-14622.

Hancioglu, B., and Tyson, J. J. (2012). A mathematical model of mitotic exit in budding yeast: the role of Polo kinase. PloS one *7*, e30810.

Harper, J. W., and Elledge, S. J. (1998). The role of Cdk7 in CAK function, a retro-retrospective. Genes & Development *12*, 285-289.

Hartwell, L. H., and Weinert, T. A. (1989). Checkpoints - Controls That Ensure the Order of Cell-Cycle Events. Science *246*, 629-634.

Hershko, A., and Ciechanover, A. (1998). The ubiquitin system. Annual Review of Biochemistry *67*, 425-479.

Higuchi, T., and Uhlmann, F. (2005). Stabilization of microtubule dynamics at anaphase onset promotes chromosome segregation. Nature *433*, 171-176.

Hopfner, K. P. (2003). Chromosome cohesion: Closing time. Current Biology *13*, R866-R868.

Hu, F., and Elledge, S. J. (2002). Bub2 is a cell cycle regulated phospho-protein controlled by multiple checkpoints. Cell Cycle *1*, 351-355.

Hu, F. H., Wang, Y. C., Liu, D., Li, Y. M., Qin, J., and Elledge, S. J. (2001). Regulation of the Bub2/Bfal GAP complex by Cdc5 and cell cycle checkpoints. Cell *107*, 655-665.

Hwang, L. H., Lau, L. F., Smith, D. L., Mistrot, C. A., Hardwick, K. G., Hwang, E. S., Amon, A., and Murray, A. W. (1998). Budding yeast Cdc20: A target of the spindle checkpoint. Science *279*, 1041-1044.

Irniger, S. (2002). Cyclin destruction in mitosis: a crucial task of Cdc20. Febs Letters *532*, 7-11.

Ivanov, D., and Nasmyth, K. (2005). A topological interaction between cohesin rings and a circular minichromosome. Cell *122*, 849-860.

Jacobson, M. D., Gray, S., Yuste-Rojas, M., and Cross, F. R. (2000). Testing cyclin specificity in the exit from mitosis. Molecular and Cellular Biology *20*, 4483-4493.

Jaquenoud, M., van Drogen, F., and Peter, M. (2002). Cell cycle-dependent nuclear export of Cdh1p may contribute to the inactivation of APC/CCdh1. Embo Journal *21*, 6515-6526.

Jaspersen, S. L., Charles, J. F., Tinker-Kulberg, R. L., and Morgan, D. O. (1998). A late mitotic regulatory network controlling cyclin destruction in Saccharomyces cerevisiae. Molecular Biology of the Cell *9*, 2803-2817.

Jaspersen, S. L., and Morgan, D. O. (2000). Cdc14 activates Cdc15 to promote mitotic exit in budding yeast. Current Biology *10*, 615-618.

Jensen, L. J., Jensen, T. S., de Lichtenberg, U., Brunak, S., and Bork, P. (2006). Co-evolution of transcriptional and posttranslational cell-cycle regulation. Nature *443*, 594-597.

Jensen, S., Geymonat, M., Johnson, A. L., Segal, M., and Johnston, L. H. (2002). Spatial regulation of the guanine nucleotide exchange factor Lte1 in Saccharomyces cerevisiae. Journal of Cell Science *115*, 4977-4991.

Johnson, K. A., and Goody, R. S. (2011). The Original Michaelis Constant: Translation of the 1913 Michaelis-Menten Paper. Biochemistry *50*, 8264-8269.

Johnston, G. C., Pringle, J. R., and Hartwell, L. H. (1977). Coordination of Growth with Cell-Division in Yeast Saccharomyces-Cerevisiae. Experimental Cell Research *105*, 79-98.

Jorgensen, P., and Tyers, M. (2004). How cells coordinate growth and division. Current Biology *14*, R1014-R1027.

Kaizu, K., Moriya, H., and Kitano, H. (2010). Fragilities Caused by Dosage Imbalance in Regulation of the Budding Yeast Cell Cycle. Plos Genetics *6*.

Kapuy, O., Barik, D., Sananes, M. R. D., Tyson, J. J., and Novak, B. (2009). Bistability by multiple phosphorylation of regulatory proteins. Progress in Biophysics & Molecular Biology *100*, 47-56.

King, R. W., Deshaies, R. J., Peters, J. M., and Kirschner, M. W. (1996). How proteolysis drives the cell cycle. Science *274*, 1652-1659.

Kitano, H. (2004). Biological robustness. Nature Reviews Genetics *5*, 826-837.

Komarnitsky, S. I., Chiang, Y. C., Luca, F. C., Chen, J. J., Toyn, J. H., Winey, M., Johnston, L. H., and Denis, C. L. (1998). DBF2 protein kinase binds to and acts through the cell cycle-regulated MOB1 protein. Molecular and Cellular Biology *18*, 2100-2107.

Lew, D. J., and Burke, D. J. (2003). The spindle assembly and spindle position checkpoints. Annual Review of Genetics *37*, 251-282.

Lew, D. J., and Reed, S. I. (1995). A Cell-Cycle Checkpoint Monitors Cell Morphogenesis in Budding Yeast. Journal of Cell Biology *129*, 739-749.

Liakopoulos, D., Kusch, J., Grava, S., Vogel, J., and Barral, Y. (2003). Asymmetric loading of Kar9 onto spindle poles and microtubules ensures proper spindle alignment. Cell *112*, 561-574.

Lim, H. H., Goh, P. Y., and Surana, U. (1998). Cdc20 is essential for the cyclosome-mediated proteolysis of both Pds1 and Clb2 during M phase in budding yeast. Current Biology *8*, 231-234.

Loog, M., and Morgan, D. O. (2005). Cyclin specificity in the phosphorylation of cyclin-dependent kinase substrates. Nature *434*, 104-108.

Lopez-Aviles, S., Kapuy, O., Novak, B., and Uhlmann, F. (2009). Irreversibility of mitotic exit is the consequence of systems-level feedback. Nature *459*, 592-595.

Lu, Y., and Cross, F. (2009a). Mitotic Exit in the Absence of Separase Activity. Molecular Biology of the Cell *20*, 1576-1591.

Lu, Y., and Cross, F. (2009b). Mitotic exit in the absence of separase activity. Mol Biol Cell *20*, 1576-1591.

Lu, Y., and Cross, F. R. (2010). Periodic Cyclin-Cdk Activity Entrains an Autonomous Cdc14 Release Oscillator. Cell *141*, 268-279.

Luca, F. C., and Winey, M. (1998). MOB1, an essential yeast gene required for completion of mitosis and maintenance of ploidy. Molecular Biology of the Cell *9*, 29-46.

Maddox, P. S., Bloom, K. S., and Salmon, E. D. (2000). The polarity and dynamics of microtubule assembly in the budding yeast Saccharomyces cerevisiae. Nature Cell Biology *2*, 36-41.

Maekawa, H., Usui, T., Knop, M., and Schiebel, E. (2003). Yeast Cdk1 translocates to the plus end of cytoplasmic microtubules to regulate bud cortex interactions. Embo Journal *22*, 438-449.

Mah, A. S., Jang, J., and Deshaies, R. J. (2001). Protein kinase Cdc15 activates the Dbf2-Mob1 kinase complex. Proceedings of the National Academy of Sciences of the United States of America *98*, 7325-7330.

Manzoni, R., Montani, F., Visintin, C., Caudron, F., Ciliberto, A., and Visintin, R. (2010). Oscillations in Cdc14 release and sequestration reveal a circuit underlying mitotic exit. Journal of Cell Biology *190*, 209-222.

McMillan, J. N., Theesfeld, C. L., Harrison, J. C., Bardes, E. S. G., and Lew, D. J. (2002). Determinants of Swe1p degradation in Saccharomyces cerevisiae. Molecular Biology of the Cell *13*, 3560-3575.

Mendenhall, M. D. (1993). An Inihibitor of P34(CDC28) Protein-Kinase Activity from Saccharomyces-Cerevisiae. Science *259*, 216-219.

Mendenhall, M. D., al-Jumaily, W., and Nugroho, T. T. (1995). The Cdc28 inhibitor p40SIC1. Progress in cell cycle research *1*, 173-185.

Menten, L., and Michaelis, M. I. (1913). Die Kinetik der Invertinwirkung. Biochemische Zeitschrift *49*, 333-369.

Mirchenko, L., and Uhlmann, F. (2010). Sli15(INCENP) Dephosphorylation Prevents Mitotic Checkpoint Reengagement Due to Loss of Tension at Anaphase Onset. Current Biology *20*, 1396-1401.

Mirsky, H. P., Liu, A. C., Welsh, D. K., Kay, S. A., and Doyle, F. J., III (2009). A model of the cell-autonomous mammalian circadian clock. Proceedings of the National Academy of Sciences of the United States of America *106*, 11107-11112.

Mitchison, J. M. (2003). Growth during the cell cycle. International Review of Cytology - a Survey of Cell Biology, Vol 226 *226*, 165-258.

Mohl, D. A., Huddleston, M. J., Collingwood, T. S., Annan, R. S., and Deshaies, R. J. (2009). Dbf2-Mob1 drives relocalization of protein phosphatase Cdc14 to the cytoplasm during exit from mitosis. Journal of Cell Biology *184*, 527-539.

Moll, T., Tebb, G., Surana, U., Robitsch, H., and Nasmyth, K. (1991). The Role of Phosphorylation and the Cdc28 Protein-Kinase in Cell-Cycle Regulated Nuclear Import of the Saccharomyces-Cerevisiae Transcription Factor-Swi5. Cell *66*, 743-758.

Morgan, D. O. (1999). Regulation of the APC and the exit from mitosis. Nature Cell Biology *1*, E47-E53.

Morgan, D. O. (2007a). The Cell Cycle Principles of Control).

Morgan, D. O. (2007b). The Cell Cycle Principles of Control, Oxford University Press).

Morohashi, M., Winn, A. E., Borisuk, M. T., Bolouri, H., Doyle, J., and Kitano, H. (2002). Robustness as a measure of plausibility in models of biochemical networks. Journal of Theoretical Biology *216*, 19-30.

Murray, A. W., and Kirschner, M. W. (1989a). Cyclin Synthesis Drives the Early Embryonic-Cell Cycle. Nature *339*, 275-280.

Murray, A. W., and Kirschner, M. W. (1989b). Dominoes and Clocks - the Union of 2 Views of the Cell-Cycle. Science *246*, 614-621.

Nasmyth, K. (1996). Viewpoint: Putting the cell cycle in order. Science *274*, 1643-1645.

Nasmyth, K., Peters, L. M., and Uhlmann, F. (2000). Splitting the chromosome: Cutting the ties that bind sister chromatids. Science *288*, 1379-1384.

Novak, B., Csikasz-Nagy, A., Gyorffy, B., Nasmyth, K., and Tyson, J. J. (1998). Model scenarios for evolution of the eukaryotic cell cycle. Philosophical Transactions of the Royal Society of London Series B-Biological Sciences *353*, 2063-2076.

Novak, B., Toth, A., Csikasz-Nagy, A., Gyorffy, B., Tyson, J. J., and Nasmyth, K. (1999). Finishing the cell cycle. Journal of Theoretical Biology *199*, 223-233.

Novak, B., and Tyson, J. J. (2008). Design principles of biochemical oscillators. Nature Reviews Molecular Cell Biology *9*, 981-991.

Novak, B., Tyson, J. J., Gyorffy, B., and Csikasz-Nagy, A. (2007). Irreversible cell-cycle transitions are due to systems-level feedback. Nature Cell Biology *9*, 724-728.

Nurse, P. (1985). Cell-Cycle Control Genes in Yeast. Trends in Genetics *1*, 51-55.

Orlicky, S., Tang, X. J., Willems, A., Tyers, M., and Sicheri, F. (2003). Structural basis for phosphodependent substrate selection and orientation by the SCF(Cdc4) ubiquitin ligase. Cell *112*, 243-256.

Pereira, G., Hofken, T., Grindlay, J., Manson, C., and Schiebel, E. (2000). The Bub2p spindle checkpoint links nuclear migration with mitotic exit. Molecular Cell *6*, 1-10.

Pereira, G., Manson, C., Grindlay, J., and Schiebel, E. (2002). Regulation of the Bfa1p-Bub2p complex at spindle pole bodies by the cell cycle phosphatase Cdc14p. Journal of Cell Biology *157*, 367-379.

Pereira, G., and Schiebel, E. (2003). Separase regulates INCENP-Aurora B anaphase spindle function through Cdc14. Science *302*, 2120-2124.

Pereira, G., and Schiebel, E. (2005). Kin4 kinase delays mitotic exit in response to spindle alignment defect. Molecular Cell *19*, 209-221.

Piatti, S., Lengauer, C., and Nasmyth, K. (1995). CDC6 is an unstable protein whose de-novo synthesis in G(1) is important for the onset of S-Phase and for preventing a reductional Anaphase in the Budding Yeast Saccharomyces-Cerevisiae. Embo Journal *14*, 3788-3799.

Pic-Taylor, A., Darieva, Z., Morgan, B. A., and Sharrocks, A. D. (2004). Regulation of cell cycle-specific gene expression through cyclin-dependent kinase-mediated phosphorylation of the forkhead transcription factor Fkh2p. Molecular and Cellular Biology *24*, 10036-10046.

Prinz, S., Hwang, E. S., Visintin, R., and Amon, A. (1998). The regulation of Cdc20 proteolysis reveals a role for the APC components Cdc23 and Cdc27 during S phase and early mitosis. Current Biology *8*, 750-760.

Queralt, E., Lehane, C., Novak, B., and Uhlmann, F. (2006). Downregulation of PP2A(Cdc-95) phosphatase by separase initiates mitotic exit in budding yeast. Cell *125*, 719-732.

Queralt, E., and Uhlmann, F. (2008). Cdk-counteracting phosphatases unlock mitotic exit. Current Opinion in Cell Biology *20*, 661-668.

Richardson, H. E., Wittenberg, C., Cross, F., and Reed, S. I. (1989). An Essential G1 Function for Cyclin-like proteins in Yeast. Cell *59*, 1127-1133.

Ross, K. E., and Cohen-Fix, O. (2004). The FEAR pathway, but not the Mitotic Exit Network, affects nuclear positioning during anaphase in budding yeast. Molecular Biology of the Cell *15*, 257A-257A.

Russell, P., Moreno, S., and Reed, S. I. (1989). Conservation of Mitotic Controls in Fission and Budding Yeasts. Cell *57*, 295-303.

Schwab, M., Lutum, A. S., and Seufert, W. (1997). Yeast Hct1 is a regulator of Clb2 cyclin proteolysis. Cell *90*, 683-693.

Schwob, E., Bohm, T., Mendenhall, M. D., and Nasmyth, K. (1994). The B-Type Cyclin Kinase Inhibitor P40(SIC1) Controls the G1 to S Transition in Saccharomyces-Cerevisiae. Cell *79*, 233-244.

Seshan, A., Bardin, A. J., and Amon, A. (2002). Control of Lte1 localization by cell polarity determinants and Cdc14. Current Biology *12*, 2098-2110.

Shirayama, M., Matsui, Y., and Tohe, A. (1994). The Yeast Tem1 Gene, Which Encodes a Gtp-Binding Protein, Is Involved in Termination of M-Phase. Molecular and Cellular Biology *14*, 7476-7482.

Shirayama, M., Toth, A., Galova, M., and Nasmyth, K. (1999). APC(Cdc20) promotes exit from mitosis by destroying the anaphase inhibitor Pds1 and cyclin Clb5. Nature *402*, 203-207.

Shou, W. Y., Azzam, R., Chen, S. L., Huddleston, M. J., Baskerville, C., Charbonneau, H., Annan, R. S., Carr, S. A., and Deshaies, R. J. (2002). Cdc5 influences phosphorylation of Netl and disassembly of the RENT complex. Bmc Molecular Biology *3*.

Shou, W. Y., Seol, J. H., Shevchenko, A., Baskerville, C., Moazed, D., Chen, Z. W. S., Jang, J., Charbonneau, H., and Deshaies, R. J. (1999). Exit from mitosis is triggered by Tem1-dependent release of the protein phosphatase Cdc14 from nucleolar RENT complex. Cell *97*, 233-244.

Sia, R. A. L., Bardes, E. S. G., and Lew, D. J. (1998). Control of Swe1p degradation by the morphogenesis checkpoint. Embo Journal *17*, 6678-6688.

Siegmund, R. F., and Nasmyth, K. A. (1996). The Saccharomyces cerevisiae start-specific transcription factor Swi4 interacts through the ankyrin repeats with the mitotic Clb2/Cdc28 kinase and through its conserved carboxy terminus with Swi6. Molecular and Cellular Biology *16*, 2647-2655.

Skowyra, D., Craig, K. L., Tyers, M., Elledge, S. J., and Harper, J. W. (1997). F-box proteins are receptors that recruit phosphorylated substrates to the SCF ubiquitin-ligase complex. Cell *91*, 209-219.

Stegmeier, F., Huang, J., Rahal, R., Zmolik, J., Moazed, D., and Amon, A. (2004). The replication fork block protein Fob1 functions as a negative regulator of the FEAR network. Current Biology *14*, 467-480.

Stegmeier, F., Visintin, R., and Amon, A. (2002). Separase, polo kinase, the kinetochore protein Slk19 and Spo12 function in a network that controls Cdc14 localization during early anaphase. Cell *108*, 207-220.

Strogatz, S. H. (1994). Nonlinear Dynamics and Chaos, Westview Press).

Sudakin, V., Ganoth, D., Dahan, A., Heller, H., Hershko, J., Luca, F. C., Ruderman, J. V., and Hershko, A. (1995). The Cyclosome, a Large Complex Containing Cyclin-Selective Ubiquitin Ligase Activity, Targets Cyclins for Destruction at the End of Mitosis. Molecular Biology of the Cell *6*, 185-197.

Sullivan, M., Holt, L., and Morgan, D. O. (2008). Cyclin-specific control of ribosomal DNA segregation. Molecular and Cellular Biology *28*, 5328-5336.

Sullivan, M., Lehane, C., and Uhlmann, F. (2001). Orchestrating anaphase and mitotic exit: separase cleavage and localization of Slk19. Nature Cell Biology *3*, 771-777.

Sullivan, M., and Uhlmann, F. (2003). A non-proteolytic function of separase links the onset of anaphase to mitotic exit. Nature Cell Biology *5*, 249-254.

Thornton, B. R., Chen, K. C., Cross, F. R., Tyson, J. J., and Toczyski, D. P. (2004). Cycling without the cyclosome - Modeling a yeast strain lacking the APC. Cell Cycle *3*, 629-633.

Thornton, B. R., and Toczyski, D. P. (2003a). Securin and B-cyclin/CDK are the only essential targets of the APC. Nat Cell Biol *5*, 1090-1094.

Thornton, B. R., and Toczyski, D. P. (2003b). Securin and B-cyclin/CDK are the only essential targets of the APC. Nature Cell Biology *5*, 1090-1094.

Toyn, J. H., Johnson, A. L., Donovan, J. D., Toone, W. M., and Johnston, L. H. (1997). The Swi5 transcription factor of Saccharomyces cerevisiae has a role in exit from mitosis through induction of the cdk-inhibitor Sic1 in telophase. Genetics *145*, 85-96.

Traverso, E. E., Baskerville, C., Liu, Y., Shou, W. Y., James, P., Deshaies, R. J., and Charbonneau, H. (2001). Characterization of the Net1 cell cycle-dependent regulator of the Cdc14 phosphatase from budding yeast. Journal of Biological Chemistry *276*, 21924-21931.

Tyers, M. (1996). The cyclin-dependent kinase inhibitor p40(SIC1) imposes the requirement for Cln G1 cyclin function at start. Proceedings of the National Academy of Sciences of the United States of America *93*, 7772-7776.

Tyson, J. J. (2007). Bringing cartoons to life. Nature *445*, 823-823.

Tyson, J. J., Chen, K., and Novak, B. (2001). Network dynamics and cell physiology. Nature Reviews Molecular Cell Biology *2*, 908-916.

Tyson, J. J., Chen, K. C., and Novak, B. (2003). Sniffers, buzzers, toggles and blinkers: dynamics of regulatory and signaling pathways in the cell. Current Opinion in Cell Biology *15*, 221-231.

Tyson, J. J., and Novak, B. (2001). Regulation of the eukaryotic cell cycle: Molecular antagonism, hysteresis, and irreversible transitions. Journal of Theoretical Biology *210*, 249-263.

Tyson, J. J., and Novak, B. (2008). Temporal organization of the cell cycle. Current Biology *18*, R759-R768.

Uhlmann, F., Wernic, D., Poupart, M. A., Koonin, E. V., and Nasmyth, K. (2000). Cleavage of cohesin by the CD clan protease separin triggers anaphase in yeast. Cell *103*, 375-386.

Verma, R., Annan, R. S., Huddleston, M. J., Carr, S. A., Reynard, G., and Deshaies, R. J. (1997). Phosphorylation of Sic1p by G(1) Cdk required for its degradation and entry into S phase. Science *278*, 455-460.

Visintin, C., Tomson, B. N., Rahal, R., Paulson, J., Cohen, M., Taunton, J., Amon, A., and Visintin, R. (2008). APC/C-Cdh1-mediated degradation of the Polo kinase Cdc5

promotes the return of Cdc14 into the nucleolus (vol 22, pg 79, 2008). Genes & Development *22*, 1560-1560.

Visintin, R., and Amon, A. (2001). Regulation of the mitotic exit protein kinases Cdc15 and Dbf2. Molecular Biology of the Cell *12*, 2961-2974.

Visintin, R., Craig, K., Hwang, E. S., Prinz, S., Tyers, M., and Amon, A. (1998). The phosphatase Cdc14 triggers mitotic exit by reversal of CDK-dependent phosphorylation. Molecular Cell *2*, 709-718.

Visintin, R., Hwang, E. S., and Amon, A. (1999). Cfi1 prevents premature exit from mitosis by anchoring Cdc14 phosphatase in the nucleolus. Nature *398*, 818-823.

Visintin, R., Prinz, S., and Amon, A. (1997). CDC20 and CDH1: A family of substrate-specific activators of APC-dependent proteolysis. Science *278*, 460-463.

Visintin, R., Stegmeier, F., and Amon, A. (2003). The role of the polo kinase Cdc5 in controlling Cdc14 localization. Molecular Biology of the Cell *14*, 4486-4498.

Wang, B. D., Yang-Gonzalez, V., and Strunnikov, A. V. (2004). Cdc14p/FEAR pathway controls segregation of nucleolus in S-cerevisiae by facilitating condensin targeting to rDNA chromatin in anaphase. Cell Cycle *3*, 960-967.

Wasch, R., and Cross, F. R. (2002). APC-dependent proteolysis of the mitotic cyclin Clb2 is essential for mitotic exit. Nature *418*, 556-562.

Widlund, P. O., Lyssand, J. S., Anderson, S., Niessen, S., Yates, J. R., and Davis, T. N. (2006). Phosphorylation of the chromosomal passenger protein Bir1 is required for localization of Ndc10 to the spindle during anaphase and full spindle elongation. Molecular Biology of the Cell *17*, 1065-1074.

Wilmes, G. M., Archambault, V., Austin, R. J., Jacobson, M. D., Bell, S. P., and Cross, F. R. (2004). Interaction of the S-phase cyclin Clb5 with an 'RXL' docking sequence in the initiator protein Orc6 provides an origin-localized replication control switch. Genes & Development *18*, 981-991.

Yeh, E., Skibbens, R. V., Cheng, J. W., Salmon, E. D., and Bloom, K. (1995). Spindle Dynamics and Cell-Cycle Regulation of Dynein in the Budding Yeast, Saccharomyces-Cerevisiae. Journal of Cell Biology *130*, 687-700.

Yeong, F. M., Lim, H. H., Padmashree, C. G., and Surana, U. (2000). Exit from mitosis in budding yeast:biphasic inactivation of the Cdc28-Clb2 mitotic kinase and the role of Cdc20. Cell Biology International *24*.

Yoshida, S., and Toh-e, A. (2002). Budding yeast Cdc5 phosphorylates Net1 and assists Cdc14 release from the nucleolus. Biochemical and Biophysical Research Communications *294*, 687-691.

Zachariae, W., Schwab, M., Nasmyth, K., and Seufert, W. (1998). Control of cyclin ubiquitination by CDK-regulated binding of Hct1 to the anaphase promoting complex. Science *282*, 1721-1724.

# Appendices

# 1. Scripts for WINPP

Each script incorporates new components and/or protein interactions which are highlighted in blue writing.

## a. MV1 Parameter set and System of ODEs

```
# INITIAL CONDITIONS from Cdc20 block

init CLB2T=0.998, Cdc20=0
init Cdh1=0
init Pds1T=0.6, Esp1T=0.25, Esp1b=0.249
init Net1=0.464, RENT=0.497
init PoloT=0.999, Polo=0.945
init Tem1=0.0039, Cdc15=0.0827
init MEN=0.0003
init Sic1T=0


# PARAMETERS

p ksclb2=0.03, kdclb2=0.03, kdclb2'=0.2, kdclb2"=2
p ks20=0.015, kd20=0.05, kd20'=2
p kdcdh=0.01, kdcdh'=1, kpcdh=0, kpcdh'=1, Jcdh=0.0015
p kspds=0, kdpds=0, kdpds'=2, ksesp=0.001, kdesp=0.004
p lapds=500, ldpds=1
p Net1T=1, kd'=0.1, kd=0.45, kp=0.2, kp'=2, Jnet=0.05
p Cdc14T=0.5, lanet=500, ldnet=1
p kspolo=0.01, kdpolo=0.01, kdpolo'=0.25
p kapolo=0, kapolo'=0.5, kipolo=0.1, Jpolo=0.25
p katem=0, katem'=0.6, kitem=0.1, kitem'=1, kitem"=20, Jtem1=0.005
p kac15=0.05, kac15'=1, kic15=0.03, kic15'=0.3, Jcdc15=1
p lamen=100, ldmen=0.1
p PPT=1, kpp=0.1, ki=40
p kssic=0, kdsic=0.005
p Kdiss=0.001


# SET OF EQUATIONS

# Clb2T is synthesised by a background rate; degradation rate is a
function of Cdc20 and Cdh1

CLB2T' = ksclb2 - (kdclb2 + kdclb2'*Cdc20 + kdclb2"*Cdh1)* CLB2T

CLB2 = (CLB2T - Trimer)

aux CLB2=CLB2
```

```
# Cdc20 protein is synthesised at constant rate and destroyed by Cdh1

Cdc20' = ks20 - (kd20 + kd20'*Cdh1)*Cdc20

# Cdh1 is activated by Cdc14 and inactivated by Clb2

Cdh1'= (kdcdh + kdcdh'*Cdc14)*(1 - Cdh1)/(Jcdh+1-Cdh1)  - (kpcdh +
kpcdh'*CLB2)*Cdh1/(Jcdh+Cdh1)
# Pds1 is synthesised at a constant rate and degraded by Cdc20

Pds1T' = kspds - (kdpds + kdpds'*Cdc20)*Pds1T

# Esp1 is synthesised and degraded at a constant rates

Esp1T' = ksesp - kdesp*Esp1T

# The complex of Pds1:Esp1 is made by association and it disappears by
dissociation, and by degradation of Pds1 or Esp1

Esp1b' = lapds*Pds1*Esp1 - (ldpds + kdesp + kdpds + kdpds'*Cdc20)*Esp1b

Pds1 = Pds1T - Esp1b

Esp1 = Esp1T - Esp1b

aux Esp1 = Esp1

# Net1 is dephosphorylated by Cdc14 and PP2A, and phosphorylated by CDK1
and MEN kinases

Net1' = (kd'*Cdc14 + kd*PP)*(Net1T - Net1 - RENT)/(Jnet + Net1T - Net1 -
RENT) -  (kp*CLB2 + kp'*MEN)*Net1/(Jnet + Net1 + RENT) -
lanet*Net1*Cdc14 + ldnet*RENT

# The complex RENT is made by association of free Cdc14 and
unphosphorylated Net1, and it disappears by dissociation, and by
phosphorylation by CDK1 and MEN kinases

RENT' = lanet*Net1*Cdc14 - ldnet*RENT - (kp*CLB2 + kp'*MEN)*RENT/(Jnet +
Net1 +RENT)

aux Net1deP = Net1 + RENT

Cdc14 = Cdc14T - RENT

aux Cdc14 = Cdc14

# PoloT is synthesised by a background rate; degradation rate is a
function of Cdh1

PoloT' = kspolo - (kdpolo + kdpolo'*Cdh1)*PoloT

# Polo is activated by Clb2 and has a background inactivation

Polo' = (kapolo + kapolo'*CLB2)*(PoloT-Polo)/(Jpolo + PoloT - Polo) -
kipolo*Polo/(Jpolo + Polo) - (kdpolo + kdpolo'*Cdh1)*Polo
```

```
# Tem1 is activated by Polo and its inactivation is controlled by Esp1

Tem1' = (katem + katem'*Polo)*(1 - Tem1)/(Jtem1 + 1 - Tem1) - (kitem +
kitem'/(1 + kitem"*Esp1))*Tem1/(Jtem1 + Tem1)

# Cdc15 is activated by CDc14 and inactivated by Clb2

Cdc15' = (kac15 + kac15'*Cdc14)*(1 - Cdc15)/(Jcdc15 + 1 - Cdc15) -
(kic15 + kic15'*CLB2)*Cdc15/(Jcdc15 + Cdc15)

# MEN active form is made from active Tem1 and Cdc15 (association and
dissociation)

MEN'= lamen*(Tem1-MEN)*(Cdc15-MEN) - ldmen*MEN - (kitem + kitem'/(1 +
kitem"*Esp1))*MEN/(Jtem1 + Tem1) - (kic15 + kic15'*CLB2)*MEN/(Jcdc15 +
Cdc15)

# The PP2A phosphatase is inhibited by Esp1 (free)

PP = PPT*(1 + kpp*ki*Esp1)/(1 + ki*Esp1)

aux PP = PPT*(1 + kpp*ki*Esp1)/(1 + ki*Esp1)

# The CDK1 inhibitor (Sic1) binds reversibly to Clb2/CDK1

Sic1t' = kssic - kdsic*Sic1t

a = CLB2t*Sic1t
b = CLB2t+Sic1t+Kdiss
Trimer = 2*a / ( b + sqrt(b^2 - 4*a))

aux Trimer = 2*a / ( b + sqrt(b^2 - 4*a))

done
```

### b. MV2 Parameter set and System of ODEs

```
# INITIAL CONDITIONS from Cdc20 block

init Clb2T=0.993, Trim2=0.0005, Mcm=0.9918
init Clb5T=0.3, Trim5=0, Cdc20=0
init Cdh1=0, Sic1T=0.0006, Swi5=0.0007
init Pds1T=0.6, Esp1T=0.25, Esp1b=0.249
init Net1=0.482, RENT=0.498
init PoloT=1.041, Polo=1.016
init Tem1=0.0065, Cdc15=0.0827
init MEN=0.0005

# PARAMETERS

p ksclb2=0.01, ksclb2'=0.02, kdclb2=0.03, kdclb2'=0.2, kdclb2"=2
p kasic2=20, kdisic2=0.1, kdsic'=0.001, kdsic"=2, kdsic=1
p kasic5=10, kdsic5=0.1
p ksmcm'=0.01, ksmcm=6, kdmcm=0.5, Jmcm=0.1
p ksclb5=0, kdclb5'=0, kdclb5=1
p ks20=0.001, ks20'=0.01, kd20=0.05, kd20'=0.5
p kdcdh=0.01, kdcdh'=1, kpcdh=0, kpcdh'=0.5, Jcdh=0.0015, kpcdh"=1
p kssic'=0.001, kssic=0.05
p kaswi=0.01, kaswi'=1, Jswi=0.01, kiswi=0.1, kiswi'=0.1, Swi5t=1
p kspds=0, kdpds=0, kdpds'=2, ksesp=0.001, kdesp=0.004
p lapds=500, ldpds=1
p Net1T=1, kd'=0.1, kd=0.45
p kp=0, kp'=0.04, kp"=0.1, kp"'=2
p Jnet=0.05, Cdc14T=0.5, lanet=500, ldnet=1
p kspolo=0.001, kspolo'=0.02, kdpolo=0.02, kdpolo'=0.5
p kapolo=0, kapolo'=1, kipolo=0.2, Jpolo=0.1
p katem=0, katem'=0.6, kitem=0.1, kitem'=1, kitem"=20, Jtem1=0.005
p kac15=0.05, kac15'=1, kic15=0.03, kic15'=0.3, Jcdc15=1
p lamen=100, ldmen=0.1
p PPT=1, kpp=0.1, ki=40


# SET OF EQUATIONS

# Clb2T is synthesised through Mcm1 and by a slow background rate;
degradation rate is a function of Cdc20 and Cdh1

Clb2T' = ksclb2 + ksclb2'*Mcm - V2* Clb2T

V2 = kdclb2 + kdclb2'*Cdc20 + kdclb2"*Cdh1

# The CDK1 inhibitor (Sic1) binds reversibly to Clb2/CDK1

Trim2' = kasic2*(Clb2T-Trim2)*(Sic1T-Trim2-Trim5) - kdisic2*Trim2 - (V2
+ vdsic)*Trim2

vdsic = kdsic' + kdsic"*Clb5 + kdsic*Clb2

Clb2 = Clb2T - Trim2
```

```
aux Clb2=Clb2

# The TF for Clb2 (Mcm1) is activated by Clb2 kinase

Mcm' = (ksmcm' + ksmcm*Clb2)*(1 - Mcm)/(Jmcm+1-Mcm) - kdmcm*Mcm/(Jmcm +
Mcm)

# Clb5T is synthesised by constant synthesis; degradation rate (V6) is a
function of Cdc20 (see V6)

Clb5T' = ksclb5 - V6* Clb5T

V6 = kdclb5' + kdclb5*Cdc20

# the CDK1 inhibitor (Sic1) binds reversibly to Clb5/CDK1

Trim5' = kasic5*(Clb5T-Trim5)*(Sic1T-Trim2-Trim5) - kdsic5*Trim5 - (V6 +
Vdsic)*Trim5

Clb5=Clb5T - Trim5

aux Clb5=Clb5T - Trim5

# Cdc20 protein is synthesised through Mcm1 and its degradation rate is
a function of Cdh1

Cdc20' = ks20 + ks20'*Mcm - (kd20 + kd20'*Cdh1)*Cdc20

# Cdh1 is activated by Cdc14 and inactivated by Clb2 and Clb5

Cdh1'= (kdcdh + kdcdh'*Cdc14)*(1 - Cdh1)/(Jcdh+1-Cdh1)  - (kpcdh +
kpcdh'*Clb2 + kpcdh"*Clb5)*Cdh1/(Jcdh+Cdh1)

# Sic1 is synthesised through Swi5 and by a slow background rate;
degradation rate is a function of Clb2 and Clb5

Sic1T' = kssic' + kssic*Swi5 - vdsic*Sic1T

# Swi5 is activated by Cdc14 and inactivated by Clb2

Swi5' = (kaswi + kaswi'*Cdc14)*(Swi5T - Swi5)/(Jswi + Swi5T - Swi5)  -
(kiswi + kiswi'*Clb2)*Swi5/(Jswi + Swi5)

# Pds1 is synthesised at a constant rate and its degradation rate is a
function of Cdc20 (see Vdpds)

Pds1T' = kspds - (kdpds + kdpds'*Cdc20)*Pds1T

# Esp1 is synthesised at a constant rate and degraded by first order
kinetics

Esp1T' = ksesp - kdesp*Esp1T

# The complex of Pds1:Esp1 is made by association and it disappears by
dissociation, and by degradation of Pds1 or Esp1
```

```
Esp1b' = lapds*Pds1*Esp1 - (ldpds + kdesp + kdpds + kdpds'*Cdc20)*Esp1b

Pds1 = Pds1T - Esp1b

# Active (free) Esp1 is the difference between Esp1(total) and the
Pds1:Esp1 complex

Esp1 = Esp1T - Esp1b

aux Esp1 = Esp1

# Net1 unP'd form (free and the complex with Cdc14) is created by
background and PP2A, and P'd by background, CDK1 and MEN kinases (see
Vp)

Net1' = (kd'*Cdc14 + kd*PP)*(Net1T - Net1 - RENT)/(Jnet + Net1T - Net1 -
RENT) -  Vp*Net1/(Jnet + Net1 + RENT) - lanet*Net1*Cdc14 + ldnet*RENT

RENT' = lanet*Net1*Cdc14 - ldnet*RENT - Vp*RENT/(Jnet + Net1 +RENT)

Vp= (kp+ kp'*Polo + kp"*Clb2 + kp"'*MEN)

aux Net1deP = Net1 + RENT

Cdc14 = Cdc14T - RENT

aux Cdc14 = Cdc14

# Polo1T = Polo protein level: synthesis through Mcm1 and constant
background rate; degradation rate is a function of Cdh1

PoloT' = kspolo + kspolo'*Mcm - (kdpolo + kdpolo'*Cdh1)*PoloT

# Polo is activated by Clb2/CDK1 and has a background inactivation

Polo' = (kapolo + kapolo'*Clb2)*(PoloT-Polo)/(Jpolo + PoloT - Polo) -
kipolo*Polo/(Jpolo + Polo) - (kdpolo + kdpolo'*Cdh1)*Polo

# Tem1 is activated by Polo and its inactivation is controlled by Esp1

Tem1' = (katem + katem'*Polo)*(1 - Tem1)/(Jtem1 + 1 - Tem1) - (kitem +
kitem'/(1 + kitem"*Esp1))*Tem1/(Jtem1 + Tem1)

# Cdc15 is activated by CDc14 and inactivated by Clb2/CDK1

Cdc15' = (kac15 + kac15'*Cdc14)*(1 - Cdc15)/(Jcdc15 + 1 - Cdc15) -
(kic15 + kic15'*Clb2)*Cdc15/(Jcdc15 + Cdc15)

# MEN active form is made from active Tem1 and Cdc15 (association and
dissociation)

MEN'= lamen*(Tem1-MEN)*(Cdc15-MEN) - ldmen*MEN - (kitem + kitem'/(1 +
kitem"*Esp1))*MEN/(Jtem1 + Tem1) - (kic15 + kic15'*Clb2)*MEN/(Jcdc15 +
Cdc15)

# The PP2A phosphatase is inhibited by Esp1 (free)
```

```
PP = PPT*(1 + kpp*ki*Esp1)/(1 + ki*Esp1)

aux PP = PPT*(1 + kpp*ki*Esp1)/(1 + ki*Esp1)

done
```

### *c. MV3 Parameter set and System of ODEs*

```
# INITIAL CONDITIONS from Cdc20 block

init Clb2T=0.981, Trim2=0.0011, Mcm=0.997
init Clb5T=0.333, Trim5=0, Cdc20=0
init Cdh1=0, Sic1T=0.0015, Swi5=0.0005
init Pds1T=0.6, Esp1T=0.25, Esp1b=0.249
init Net1=0.484, RENT=0.498
init PoloT=1.007, Polo=0.991, Cdc14n=0.002
init Tem1=0.0061, Cdc15=0.0685
init MEN=0.0004

# PARAMETERS

p Clb2nd=0, ksclb2=0.015, ksclb2'=0.005
p kdclb2=0.02, kdclb2'=0.1, kdclb2"=0.4
p kasic2=20, kdisic2=0.1, kdsic'=0.1, kdsic"=2, kdsic=2
p kasic5=10, kdsic5=0.1
p ksmcm'=0.01, ksmcm=1, kdmcm=0.25, Jmcm=0.01
p ksclb5=0.01, kdclb5'=0.03, kdclb5=1.5
p ks20=0.001, ks20'=0.01, kd20=0.05, kd20'=0.5
p kdcdh=0.03, kdcdh'=0.3, kpcdh=0.001, kpcdh'=0.1
p Jcdh=0.01, kpcdh"=0.75
p kssic'=0.004, kssic=0.2
p kaswi=0.01, kaswi'=1, Jswi=0.01, kiswi=0.1, kiswi'=0.1, Swi5t=1
p kspds=0.012, kdpds=0.02, kdpds'=2, ksesp=0.001, kdesp=0.004,
lapds=500, ldpds=1
p Net1T=1, kd'=0.1, kd=0.45
p kp=0, kp'=0.04, kp"=0.1, kp"'=3
p Jnet=0.05, Cdc14T=0.5, lanet=500, ldnet=1
p kexp=0.01, kexp'=10, kexp"=0, kimp=1
p kspolo=0.001, kspolo'=0.05, kdpolo=0.05, kdpolo'=0.5
p kapolo=0, kapolo'=1, kipolo=0.1, Jpolo=0.1
p katem=0, katem'=0.6, kitem=0.1, kitem'=1, kitem"=20, Jtem1=0.005
p kac15=0.03, kac15'=0, kac15"=1, kic15=0.03, kic15'=0.2, Jcdc15=1
p lamen=100, ldmen=0.1
p PPT=1, kpp=0.1, ki=40


# SET OF EQUATIONS

# Clb2T is synthesised through Mcm1 and by a slow background rate;
degradation rate is a function of Cdc20 and Cdh1

Clb2T' = ksclb2 + ksclb2'*Mcm - V2* Clb2T

V2 = kdclb2 + kdclb2'*Cdc20 + kdclb2"*Cdh1

# The CDK1 inhibitor (Sic1) binds reversibly to Clb2/CDK1

Trim2' = kasic2*Clb2*(Sic1T-Trim2-Trim5) - kdisic2*Trim2 - (V2 +
vdsic)*Trim2
```

```
vdsic = kdsic' + kdsic"*Clb5 + kdsic*Clb2

Clb2 = Clb2T - Trim2 + Clb2nd

aux Clb2=Clb2

# The TF for Clb2 (Mcm1) is activated by Clb2 kinase

Mcm' = (ksmcm' + ksmcm*Clb2)*(1 - Mcm)/(Jmcm+1-Mcm) - kdmcm*Mcm/(Jmcm +
Mcm)

# Clb5T is synthesised by constant synthesis; degradation rate (V6) is a
function of Cdc20 (see V6)

Clb5T' = ksclb5 - V6* Clb5T

V6 = kdclb5' + kdclb5*Cdc20

# The CDK1 inhibitor (Sic1) binds reversibly to Clb5/CDK1

Trim5' = kasic5*(Clb5T-Trim5)*(Sic1T-Trim2-Trim5) - kdsic5*Trim5 - (V6 +
Vdsic)*Trim5

Clb5=Clb5T - Trim5

aux Clb5=Clb5T - Trim5

# Cdc20 protein is synthesised through Mcm1 and by a slow background
rate, and destroyed by Cdh1

Cdc20' = ks20 + ks20'*Mcm - (kd20 + kd20'*Cdh1)*Cdc20

# Cdh1 is activated by Cdc14 and inactivated by Clb2 and Clb5

Cdh1'= (kdcdh + kdcdh'*Cdc14c)*(1 - Cdh1)/(Jcdh+1-Cdh1)  - (kpcdh +
kpcdh'*Clb2 + kpcdh"*Clb5)*Cdh1/(Jcdh+Cdh1)

# Sic1 is synthesised by Swi5; degradation rate is a function of Clb2
and Clb5

Sic1T' = kssic' + kssic*Swi5 - vdsic*Sic1T

# Swi5 is activated by Cdc14 and inactivated by Clb2/CDK1

Swi5' = (kaswi + kaswi'*Cdc14c)*(Swi5T - Swi5)/(Jswi + Swi5T - Swi5)  -
(kiswi + kiswi'*Clb2)*Swi5/(Jswi + Swi5)

# Pds1 is synthesised at a constant rate and degraded by Cdc20 (see
Vdpds)

Pds1T' = kspds - (kdpds + kdpds'*Cdc20)*Pds1T

# Esp1 is synthesised at a constant rate and degraded by first order
kinetics

Esp1T' = ksesp - kdesp*Esp1T
```

```
# The complex of Pds1:Esp1 is made by association and it disappears by
dissociation, and by degradation of Pds1 or Esp1

Esp1b' = lapds*Pds1*Esp1 - (ldpds + kdesp + kdpds + kdpds'*Cdc20)*Esp1b

Pds1 = Pds1T - Esp1b

# Active (free) Esp1 is the difference between Esp1(total) and the
Pds1:Esp1 complex

Esp1 = Esp1T - Esp1b

aux Esp1 = Esp1

# Net1 unP'd form (free and the complex with Cdc14) is created by
background and PP2A, and P'd by background, CDK1 and MEN kinases (see
Vp)

Net1' = (kd'*Cdc14n + kd*PP)*(Net1T - Net1 - RENT)/(Jnet + Net1T - Net1
- RENT) -  Vp*Net1/(Jnet + Net1 + RENT) - lanet*Net1*Cdc14n + ldnet*RENT

RENT' = lanet*Net1*Cdc14n - ldnet*RENT - Vp*RENT/(Jnet + Net1 +RENT)

Vp= (kp+ kp'*Polo + kp"*Clb2 + kp"'*MEN)

aux Net1deP = Net1 + RENT

# Cdc14n is the free nuclear form which is released by Net
phosphorylation. This form is then exported to the cytoplasm (Cdc14c).

Cdc14n' = Vp * RENT/(Jnet + Net1 + RENT) - lanet*Net1*Cdc14n +
ldnet*RENT - vexp*Cdc14n + kimp*(Cdc14T-Cdc14n-RENT)

vexp = kexp + kexp'*MEN + kexp"*Clb2

Cdc14c = Cdc14T - Cdc14n - RENT

aux Cdc14c = Cdc14T - Cdc14n - RENT

# Polo1T = Polo protein level: synthesis through Mcm1 and constant
background rate; degradation rate is a function of Cdh1

PoloT' = kspolo + kspolo'*Mcm - (kdpolo + kdpolo'*Cdh1)*PoloT

# Polo is activated by Clb2/CDK1 and has a background inactivation

Polo' = (kapolo + kapolo'*Clb2)*(PoloT-Polo)/(Jpolo + PoloT - Polo) -
kipolo*Polo/(Jpolo + Polo) - (kdpolo + kdpolo'*Cdh1)*Polo

# Tem1 is activated by Polo and its inactivation is controlled by Esp1

Tem1' = (katem + katem'*Polo)*(1 - Tem1)/(Jtem1 + 1 - Tem1) - (kitem +
kitem'/(1 + kitem"*Esp1))*Tem1/(Jtem1 + Tem1)

# Cdc15 is activated by CDc14 and inactivated by CDK1
```

```
Cdc15' = (kac15 + kac15'*Cdc14n + kac15"*Cdc14c )*(1 - Cdc15)/(Jcdc15 +
1 - Cdc15) - (kic15 + kic15'*Clb2)*Cdc15/(Jcdc15 + Cdc15)

# MEN active form is made from active Tem1 and Cdc15 (association and
dissociation)

MEN'= lamen*(Tem1-MEN)*(Cdc15-MEN) - ldmen*MEN - (kitem + kitem'/(1 +
kitem"*Esp1))*MEN/(Jtem1 + Tem1) - (kic15 + kic15'*Clb2)*MEN/(Jcdc15 +
Cdc15)

# The PP2A phosphatase is inhibited by Esp1 (free)

PP = PPT*(1 + kpp*ki*Esp1)/(1 + ki*Esp1)

aux PP = PPT*(1 + kpp*ki*Esp1)/(1 + ki*Esp1)

done
```

### *d. MV4 Parameter set and System of ODE*

```
# INITIAL CONDITIONS from Cdc20 block
init Clb2T=0.999, Trim2=0.0014, Mcm=0.9967
init Clb5T=0.202, Cln=0.0407, Trim5=0, Cdc20=0
init Cdh1=0, Sic1T=0.0016, Swi5=0
init Pds1T=0.6019, Esp1T=0.25, Esp1b=0.248
init Net1deP=0.9598, Net1PP=0.0119, RENT=0.497, RENTP=0.01433
init PoloT=1.016, Polo=1.0002, Cdc14n=0.002
init Tem1=0.006, Cdc15=0.067
init MEN=0.00041, MBF=0.0019

# PARAMETERS

p Clb2nd=0, ksclb2=0.015, ksclb2'=0.005, kdclb2=0.02
p kdclb2'=0.1, kdclb2"=0.4
p kasic2=40, kdisic2=0.1, kasic5=10, kdsic5=0.1
p kssic=0.004, kssic'=0.2, kdsic=0.04, kdsic'=2, kdsic"=2, kdsic'"=1.5
p ksmcm=0.01, ksmcm'=1, kdmcm=0.25, Jmcm=0.01
p ksclb5=0.002, ksclb5'=0.01, kdclb5=0.01, kdclb5'=1
p kscln=0.01, kscln'=0.1, kdcln=0.25
p ks20=0.001, ks20'=0.05, kd20=0.1, kd20'=1
p kdcdh=0.03, kdcdh'=0.3, kpcdh=0.001, kpcdh'=0.04, kpcdh"=0.75
p Jcdh=0.01
p kaswi=0.2, kaswi'=1, Jswi=0.1, kiswi=0.01, kiswi'=0.5, kiswi"=0.75
p Swi5t=1
p kspds=0.006, kspds'=0.01, kdpds=0.01, kdpds'=2
p ksesp=0.001, kdesp=0.004, lapds=500, ldpds=1
p Net1T=1, kd'=0.1, kd=0.45
p kp'=2, kp"=0.2, kp"'=3
p Jnet=0.05, Cdc14T=0.5, lanet=500, ldnet=1
p kexp=0.01, kexp'=20, kimp=1
p kspolo=0.001, kspolo'=0.05, kdpolo=0.05, kdpolo'=0.5
p kapolo=0, kapolo'=1, kipolo=0.1, Jpolo=0.1
p katem=0, katem'=0.6, kitem=0.1, kitem'=1, kitem"=20, Jtem1=0.005
p kac15=0.03, kac15'=0.5, kic15=0.03, kic15'=0.2, Jcdc15=1
p lamen=100, ldmen=0.1
p kambf=0.1, kimbf'=0.5, kimbf"=0.5, Jmbf=0.01
p PPT=1, kpp=0.1, ki=40


# SET OF EQUATIONS


# Clb2T is synthesised through Mcm1 and by a slow background rate;
degradation rate is a function of Cdc20 and Cdh1

Clb2T' = ksclb2 + ksclb2'*Mcm - V2* Clb2T

V2 = kdclb2 + kdclb2'*Cdc20 + kdclb2"*Cdh1

# the CDK1 inhibitor (Sic1) binds reversibly to Clb2/CDK1
```

```
Trim2' = kasic2*Clb2*(Sic1T-Trim2-Trim5) - kdisic2*Trim2 - (V2 +
vdsic)*Trim2

vdsic = kdsic + kdsic'*Clb5 + kdsic"*Clb2 + kdsic'"*Cln

Clb2 = Clb2T - Trim2 + Clb2nd

aux Clb2=Clb2

# The TF for Clb2 (Mcm1) is activated by Clb2 kinase

Mcm' = (ksmcm + ksmcm'*Clb2)*(1 - Mcm)/(Jmcm+1-Mcm) - kdmcm*Mcm/(Jmcm +
Mcm)

# Clb5T is synthesised through constant synthesis; degradation rate (V6)
is a function of Cdc20 (see V6)

Clb5T' = ksclb5+ ksclb5'*MBF - V6* Clb5T

V6 = kdclb5 + kdclb5'*Cdc20 + kdclb5"*Cdh1

Cln' = kscln + kscln'*MBF - kdcln*Cln

# the CDK1 inhibitor (Sic1) binds reversibly to Clb5/CDK1

Trim5' = kasic5*(Clb5T-Trim5)*(Sic1T-Trim2-Trim5) - kdsic5*Trim5 - (V6 +
Vdsic)*Trim5

Clb5=Clb5T - Trim5

aux Clb5=Clb5T - Trim5

# Cdc20 protein is synthesised through Mcm1 and by a slow background
rate, and destroyed by Cdh1

Cdc20' = ks20 + ks20'*Mcm - (kd20 + kd20'*Cdh1)*Cdc20

# Cdh1 is activated by Cdc14 and inactivated by Clb2 and Clb5

Cdh1'= (kdcdh*Cdc14n + kdcdh'*Cdc14c)*(1 - Cdh1)/(Jcdh+1-Cdh1)  - (kpcdh
+ kpcdh'*Clb2 + kpcdh"*Clb5)*Cdh1/(Jcdh+Cdh1)

# Sic1 is synthesised by Swi5; degradation rate is a function of Clb2
and Clb5

Sic1T' = kssic + kssic'*Swi5 - vdsic*Sic1T

# Swi5 is activated by Cdc14 and inactivated by Clb2

Swi5' = (kaswi*Cdc14n + kaswi'*Cdc14c)*(Swi5T - Swi5)/(Jswi + Swi5T -
Swi5)  - (kiswi + kiswi'*Clb2 + kiswi"*Clb5)*Swi5/(Jswi + Swi5)

# Pds1 is synthesised through MBF and by a slow background rate, and
degraded by Cdc20 (see Vdpds)

Pds1T' = kspds + kspds'*MBF - (kdpds + kdpds'*Cdc20)*Pds1T
```

```
# Esp1 is synthesised at a constant rate and degraded by first order
kinetics

Esp1T' = ksesp - kdesp*Esp1T

# The complex of Pds1:Esp1 is made by association and it disappears by
dissociation, and by degradation of Pds1 or Esp1

Esp1b' = lapds*Pds1*Esp1 - (ldpds + kdesp + kdpds + kdpds'*Cdc20)*Esp1b

Pds1 = Pds1T - Esp1b

# Active (free) Esp1 is the difference between Esp1(total) and the
Pds1:Esp1 complex

Esp1 = Esp1T - Esp1b

aux Esp1 = Esp1

# Net1 is unphosphorylated by by background, Cdc14 and PP2A.
# Net1 is primarly phosphorylated by Clb2/CDK1 and MEN kinases (see Vp)
# Net1P is further phosphorylated by Polo kinase
# Only Net1deP and Net1P can bind to Cdc14

Net1deP' = Vd*(Net1T - Net1deP) -  Vp*Net1deP

Net1PP' = kp'*Polo*(Net1T - Net1deP - Net1PP) - Vd*Net1PP

RENT' = lanet*(Net1T - Net1PP - RENT)*Cdc14n - ldnet*RENT -
kp'*Polo*RENTP

RENTP' = Vp*(RENT-RENTP) - Vd*RENTP + lanet*(Net1T - Net1deP - Net1PP -
RENTP)*Cdc14n - ldnet*RENTP - kp'*Polo*RENTP

Vd = (kd*PP + kd'*Cdc14n)/(Jnet + Net1T - Net1deP)

Vp= (kp + kp"*Clb2 + kp"'*MEN)/(Jnet + Net1deP)

aux Net1CP = Net1T - Net1deP

# Cdc14n is the free nuclear form which is released by Net
phosphorylation. This form is then exported to the cytoplasm (Cdc14c).

Cdc14n' = kp'*Polo*RENTP - lanet*(Net1T - Net1PP - RENT)*Cdc14n +
ldnet*RENT - vexp*Cdc14n + kimp*Cdc14c
vexp = kexp + kexp'*MEN + kexp"*Clb2

Cdc14c = Cdc14T - Cdc14n - RENT

aux Cdc14c = Cdc14T - Cdc14n - RENT

# Polo1T = Polo protein level: synthesis through Mcm1 and constant
background rate; degradation rate is a function of Cdh1

PoloT' = kspolo + kspolo'*Mcm - (kdpolo + kdpolo'*Cdh1 +
kdpolo"*Cdc20)*PoloT
```

```
# Polo is activated by CDK1 and has a background inactivation

Polo' = (kapolo + kapolo'*Clb2)*(PoloT-Polo)/(Jpolo + PoloT - Polo) -
kipolo*Polo/(Jpolo + Polo) - (kdpolo + kdpolo'*Cdh1 +
kdpolo"*Cdc20)*Polo

# Tem1 is activated by Polo and its inactivation is controlled by Esp1

Tem1' = (katem + katem'*Polo)*(1 - Tem1)/(Jtem1 + 1 - Tem1) - (kitem +
kitem'/(1 + kitem"*Esp1))*Tem1/(Jtem1 + Tem1)

# Cdc15 is activated by Cdc14 and inactivated by Clb2

Cdc15' = (kac15 + kac15'*Cdc14n + kac15"*Cdc14c)*(1 - Cdc15)/(Jcdc15 + 1
- Cdc15) - (kic15 + kic15'*Clb2)*Cdc15/(Jcdc15 + Cdc15)

# MEN active form is made from active Tem1 and Cdc15 (association and
dissociation)

MEN'= lamen*(Tem1-MEN)*(Cdc15-MEN) - ldmen*MEN - (kitem + kitem'/(1 +
kitem"*Esp1))*MEN/(Jtem1 + Tem1) - (kic15 + kic15'*Clb2)*MEN/(Jcdc15 +
Cdc15)

# MBF is inactivated by Clb2/CDK1 and Clb5/CDK1 kinase

MBF' = kambf*(1 - MBF)/(Jmbf + 1 - MBF) - (kimbf + kimbf'*Clb2 +
kimbf"*Clb5)*MBF/(Jmbf + MBF)

# The PP2A phosphatase is inhibited by Esp1 (free)

PP = PPT*(1 + kpp*ki*Esp1)/(1 + ki*Esp1)

aux PP = PPT*(1 + kpp*ki*Esp1)/(1 + ki*Esp1)

#Numerics
#@ TOTAL=300, METH=stiff, toll=3e-16, toler=3e-16, XHI=500, YLO=0,
YHI=2, BOUND=1000, maxstorage=10000

#AUTO settings
#@dsmax=.01, dsmin=.0001, ds=.5, ntst=30, nmax=1000, npr=1000, parmin=-
10, parmax=10
#@autoximn=0, autoxmax=3, autoymin=0, autoymax=3

done
```

## 2. Conservation of Parameters among Chapters

**In blue and yellow are shown parameters that conserved the same values among different versions of the model. Blue represents conservation with earlier versions and yellow represents conservation with the final version.**

| MV1 | | | MV2 | | | MV3 | | | MV4 | |
|---|---|---|---|---|---|---|---|---|---|---|
| **Parameters** | **Value** | | **Parameters** | **Value** | | **Parameters** | **Value** | | **Parameters** | **Value** |
| | | | | | | Clb2nd | 0 | | Clb2nd | 0 |
| ksclb2 | 0.03 | | ksclb2 | 0.01 | | ksclb2 | 0.015 | | ksclb2 | 0.015 |
| kdclb2 | 0.03 | | ksclb2' | 0.02 | | ksclb2' | 0.005 | | ksclb2' | 0.005 |
| kdclb2' | 0.2 | | kdclb2 | 0.03 | | kdclb2 | 0.02 | | kdclb2 | 0.02 |
| kdclb2" | 2 | | kdclb2' | 0.2 | | kdclb2' | 0.1 | | kdclb2' | 0.1 |
| | | | kdclb2" | 2 | | kdclb2" | 0.4 | | kdclb2" | 0.4 |
| Kdiss | 0.001 | | kasic2 | 20 | | kasic2 | 20 | | kasic2 | 40 |
| | | | kdisic2 | 0.1 | | kdisic2 | 0.1 | | kdisic2 | 0.1 |
| | | | kasic5 | 10 | | kasic5 | 10 | | kasic5 | 10 |
| | | | kdsic5 | 0.1 | | kdsic5 | 0.1 | | kdsic5 | 0.1 |
| kssic | 0 | | kssic' | 0.001 | | kssic' | 0.004 | | kssic | 0.004 |
| | | | kssic | 0.05 | | kssic | 0.2 | | kssic' | 0.2 |
| kdsic | 0.005 | | kdsic' | 0.001 | | kdsic' | 0.1 | | kdsic | 0.04 |
| | | | kdsic" | 2 | | kdsic" | 2 | | kdsic' | 2 |
| | | | kdsic | 1 | | kdsic | 2 | | kdsic" | 2 |
| | | | | | | | | | kdsic'" | 1.5 |
| | | | ksmcm' | 0.01 | | ksmcm' | 0.01 | | ksmcm | 0.01 |
| | | | ksmcm | 6 | | ksmcm | 1 | | ksmcm' | 1 |
| | | | kdmcm | 0.5 | | kdmcm | 0.25 | | kdmcm | 0.25 |
| | | | Jmcm | 0.1 | | Jmcm | 0.01 | | Jmcm | 0.01 |
| | | | ksclb5 | 0 | | ksclb5 | 0.01 | | ksclb5 | 0.002 |
| | | | | | | | | | ksclb5' | 0.01 |
| | | | kdclb5' | 0 | | kdclb5' | 0.03 | | kdclb5 | 0.01 |
| | | | kdclb5 | 1 | | kdclb5 | 1.5 | | kdclb5' | 1 |
| | | | | | | | | | kdclb5" | 0 |
| | | | | | | | | | kscln | 0.01 |
| | | | | | | | | | kscln' | 0.1 |
| | | | | | | | | | kdcln | 0.25 |
| ks20 | 0.015 | | ks20 | 0.001 | | ks20 | 0.001 | | ks20 | 0.001 |
| | | | ks20' | 0.01 | | ks20' | 0.01 | | ks20' | 0.05 |
| kd20 | 0.05 | | kd20 | 0.05 | | kd20 | 0.05 | | kd20 | 0.1 |
| kd20' | 2 | | kd20' | 0.5 | | kd20' | 0.5 | | kd20' | 1 |
| kdcdh | 0.01 | | kdcdh | 0.01 | | kdcdh | 0.03 | | kdcdh | 0.03 |
| kdcdh' | 1 | | kdcdh' | 1 | | kdcdh' | 0.3 | | kdcdh' | 0.3 |
| kpcdh | 0 | | kpcdh | 0 | | kpcdh | 0.001 | | kpcdh | 0.001 |
| kpcdh' | 1 | | kpcdh' | 0.5 | | kpcdh' | 0.1 | | kpcdh' | 0.04 |
| | | | kpcdh" | 1 | | kpcdh" | 0.75 | | kpcdh" | 0.75 |
| Jcdh | 0.0015 | | Jcdh | 0.0015 | | Jcdh | 0.01 | | Jcdh | 0.01 |

| MV1 | | | MV2 | | | MV3 | | | MV4 | |
|---|---|---|---|---|---|---|---|---|---|---|
| **Parameters** | **Value** | | **Parameters** | **Value** | | **Parameters** | **Value** | | **Parameters** | **Value** |
| | | | | | | Clb2nd | 0 | | Clb2nd | 0 |
| | | | kaswi | 0.01 | | kaswi | 0.01 | | kaswi | 0.2 |
| | | | kaswi' | 1 | | kaswi' | 1 | | kaswi' | 1 |
| | | | Jswi | 0.01 | | Jswi | 0.01 | | Jswi | 0.1 |
| | | | kiswi | 0.1 | | kiswi | 0.1 | | kiswi | 0.01 |
| | | | kiswi' | 0.1 | | kiswi' | 0.1 | | kiswi' | 0.5 |
| | | | | | | | | | kiswi" | 0.75 |
| | | | Swi5t | 1 | | Swi5t | 1 | | Swi5t | 1 |
| kspds | 0 | | kspds | 0 | | kspds | 0.012 | | kspds | 0.006 |
| | | | | | | | | | kspds' | 0.01 |
| kdpds | 0 | | kdpds | 0 | | kdpds | 0.02 | | kdpds | 0.01 |
| kdpds' | 2 | | kdpds' | 2 | | kdpds' | 2 | | kdpds' | 2 |
| ksesp | 0.001 | | ksesp | 0.001 | | ksesp | 0.001 | | ksesp | 0.001 |
| kdesp | 0.004 | | kdesp | 0.004 | | kdesp | 0.004 | | kdesp | 0.004 |
| lapds | 500 | | lapds | 500 | | lapds | 500 | | lapds | 500 |
| ldpds | 1 | | ldpds | 1 | | ldpds | 1 | | ldpds | 1 |
| Net1T | 1 | | Net1T | 1 | | Net1T | 1 | | Net1T | 1 |
| kd' | 0.1 | | kd' | 0.1 | | kd' | 0.1 | | kd' | 0.1 |
| kd | 0.45 | | kd | 0.45 | | kd | 0.45 | | kd | 0.45 |
| | | | kp | 0 | | kp | 0 | | kp | 0 |
| | | | kp' | 0.04 | | kp' | 0.04 | | kp' | 2 |
| kp | 0.2 | | kp" | 0.1 | | kp" | 0.1 | | kp" | 0.2 |
| kp' | 2 | | kp"' | 2 | | kp"' | 3 | | kp"' | 3 |
| Jnet | 0.05 | | Jnet | 0.05 | | Jnet | 0.05 | | Jnet | 0.05 |
| Cdc14T | 0.5 | | Cdc14T | 0.5 | | Cdc14T | 0.5 | | Cdc14T | 0.5 |
| lanet | 500 | | lanet | 500 | | lanet | 500 | | lanet | 500 |
| ldnet | 1 | | ldnet | 1 | | ldnet | 1 | | ldnet | 1 |
| | | | | | | kexp | 0.01 | | kexp | 0.01 |
| | | | | | | kexp' | 10 | | kexp' | 20 |
| | | | | | | kexp" | 0 | | kexp" | 0 |
| | | | | | | kimp | 1 | | kimp | 1 |
| | | | kspolo | 0.001 | | kspolo | 0.001 | | kspolo | 0.001 |
| kspolo | 0.01 | | kspolo' | 0.02 | | kspolo' | 0.05 | | kspolo' | 0.05 |
| kdpolo | 0.01 | | kdpolo | 0.02 | | kdpolo | 0.05 | | kdpolo | 0.05 |
| kdpolo' | 0.25 | | kdpolo' | 0.5 | | kdpolo' | 0.5 | | kdpolo' | 0.5 |
| | | | | | | | | | kdpolo" | 0 |
| kapolo | 0 | | kapolo | 0 | | kapolo | 0 | | kapolo | 0 |
| kapolo' | 0.5 | | kapolo' | 1 | | kapolo' | 1 | | kapolo' | 1 |
| kipolo | 0.1 | | kipolo | 0.2 | | kipolo | 0.1 | | kipolo | 0.1 |
| Jpolo | 0.25 | | Jpolo | 0.1 | | Jpolo | 0.1 | | Jpolo | 0.1 |
| katem | 0 | | katem | 0 | | katem | 0 | | katem | 0 |
| katem' | 0.6 | | katem' | 0.6 | | katem' | 0.6 | | katem' | 0.6 |
| kitem | 0.1 | | kitem | 0.1 | | kitem | 0.1 | | kitem | 0.1 |
| kitem' | 1 | | kitem' | 1 | | kitem' | 1 | | kitem' | 1 |
| kitem" | 20 | | kitem" | 20 | | kitem" | 20 | | kitem" | 20 |
| Jtem1 | 0.005 | | Jtem1 | 0.005 | | Jtem1 | 0.005 | | Jtem1 | 0.005 |

| MV1 | | | MV2 | | | MV3 | | | MV4 | |
|---|---|---|---|---|---|---|---|---|---|---|
| **Parameters** | **Value** | | **Parameters** | **Value** | | **Parameters** | **Value** | | **Parameters** | **Value** |
| kac15 | 0.05 | | kac15 | 0.05 | | kac15 | 0.03 | | kac15 | 0.03 |
| | | | | | | kac15' | 0 | | kac15' | 0 |
| kac15' | 1 | | kac15' | 1 | | kac15" | 1 | | kac15" | 0.5 |
| kic15 | 0.03 | | kic15 | 0.03 | | kic15 | 0.03 | | kic15 | 0.03 |
| kic15' | 0.3 | | kic15' | 0.3 | | kic15' | 0.2 | | kic15' | 0.2 |
| Jcdc15 | 1 | | Jcdc15 | 1 | | Jcdc15 | 1 | | Jcdc15 | 1 |
| lamen | 100 | | lamen | 100 | | lamen | 100 | | lamen | 100 |
| ldmen | 0.1 | | ldmen | 0.1 | | ldmen | 0.1 | | ldmen | 0.1 |
| | | | | | | | | | kambf | 0.1 |
| | | | | | | | | | kimbf | 0 |
| | | | | | | | | | kimbf' | 0.5 |
| | | | | | | | | | kimbf" | 0.5 |
| | | | | | | | | | Jmbf | 0.01 |
| PPT | 1 | | PPT | 1 | | PPT | 1 | | PPT | 1 |
| kpp | 0.1 | | kpp | 0.1 | | kpp | 0.1 | | kpp | 0.1 |
| ki | 40 | | ki | 40 | | ki | 40 | | ki | 40 |

## 3. Mutants Simulated with MV4

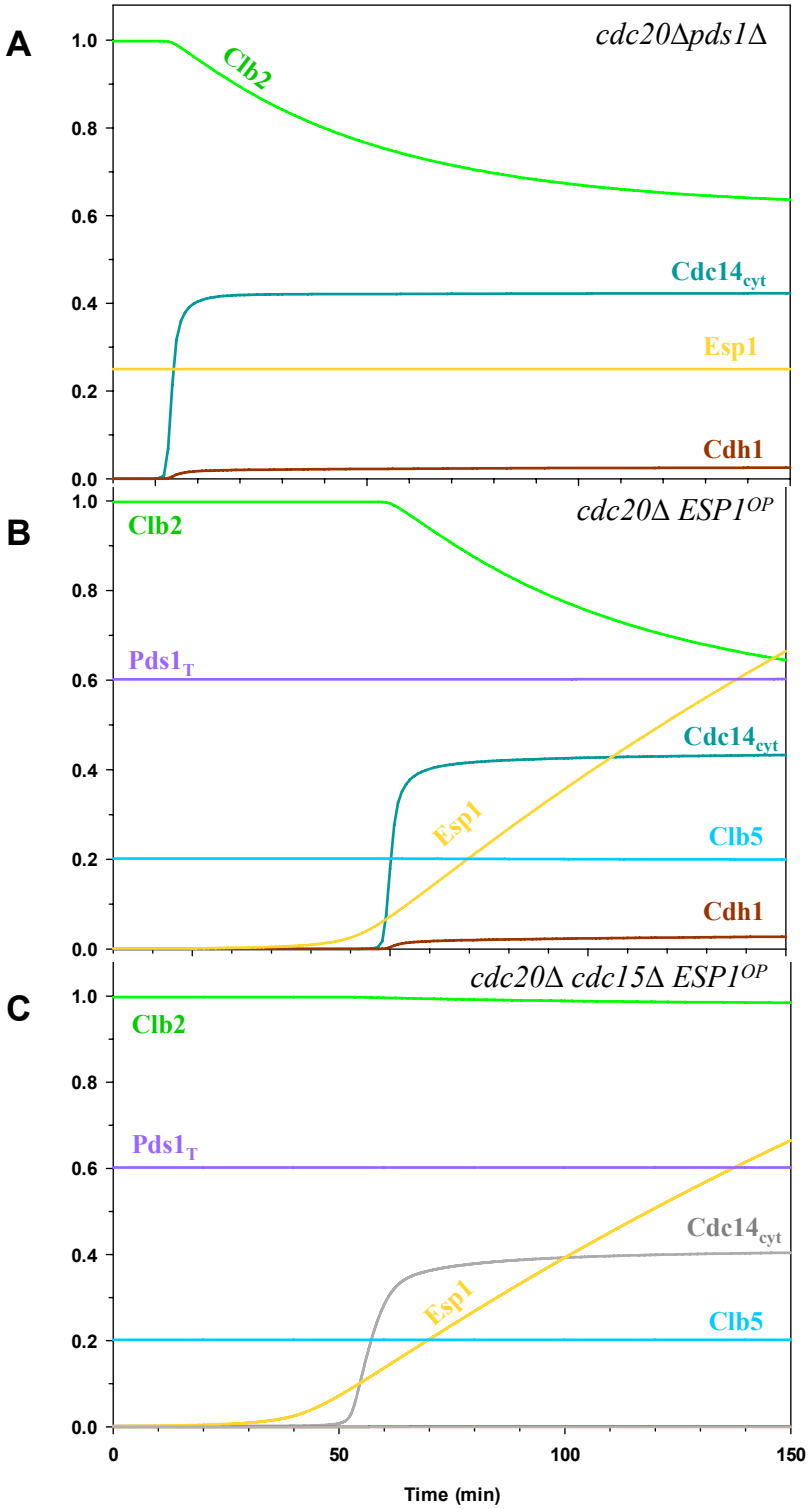


**Figure A3 - 1: Numerical simulations of mitotic progression in metaphase-blocked cells ($k_{s20} = k_{s20}' = 0$) with a (A) Pds1 deletion ($k_{dpds1} = k_{dpds1}' = 0$; Initial Conditions: $[Pds1_T] = 0$, $[Esp1_B] = 0$]), (B) overexpressing separase ($k_{sesp} = 0.01\ min^{-1}$) and (C) with Cdc15 deletion ($k_{ac15} = k_{ac15}' = 0$).**

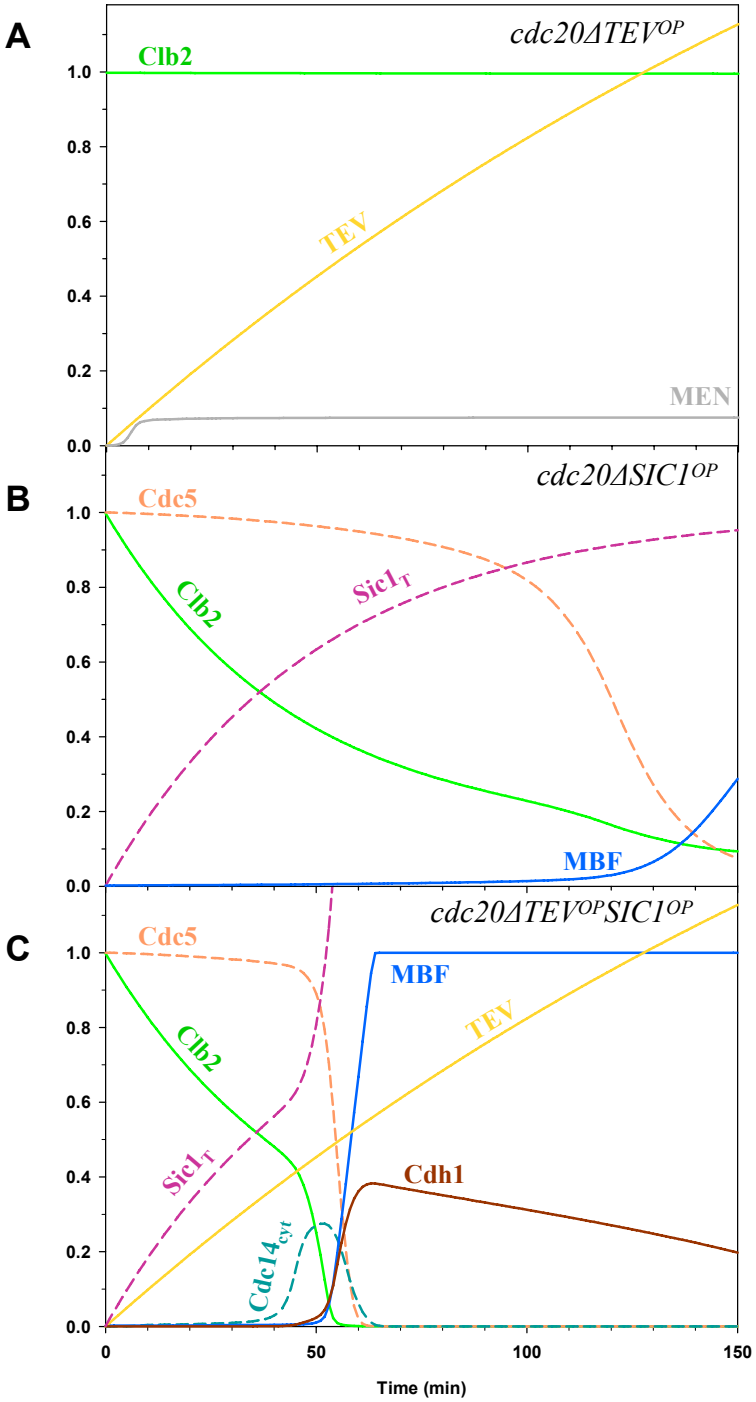


**Figure A3 - 2: Efficient exit from the *cdc20*Δ stable mitotic state requires both inhibition of CDK1 and activation of Cdc14. (A) A ten-fold TEV expression over separase level ($k_{sesp}$ = 0.01 $min^{-1}$, $k_i$ = 0, $l_{apds}$ = 0; Initial Conditions: [$Esp1_T$] = 0; [$Esp1_B$] = 0) in a Cdc20 block ($k_{s20}$ = $k_{s20}$' = 0) can only induce partial MEN activation but no Cdc14 release nor mitotic exit. (B) Non-degradable Sic1 overexpression ($k_{ssic}$=0.02 $min^{-1}$, $k_{ssic}$'=0.2 $min^{-1}$, $k_{dsic}$=0.02 $min^{-1}$, $k_{dsic}$'= $k_{dsic}$''= $k_{dsic}$'''=0) in a Cdc20 block brings about mitotic exit after a long delay because Cdc14 is not activated. (C) Overexpression of TEV andnon-degradable Sic1 in a Cdc20 block activates Cdc14 release and mitotic exit.**

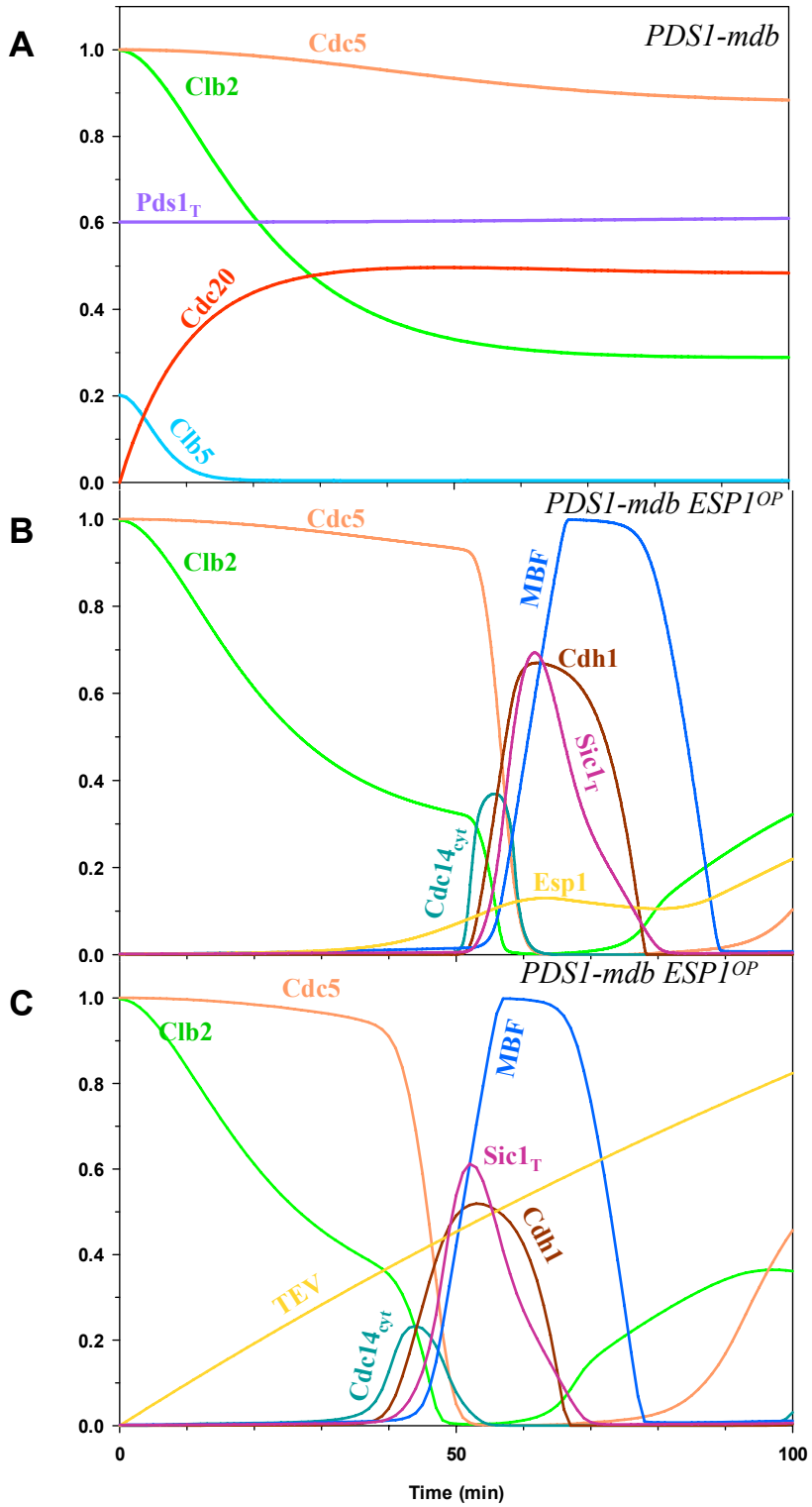


**Figure A3 - 3: Numerical simulation of mitotic progression after Cdc20 release in cells (A) expressing endogenous levels of undegradable Pds1 ($k_{dpds}$' = 0), and (B) overexpressing separase ($k_{sesp}$ = 0.01 $min^{-1}$) or (C) TEV ($k_{sesp}$ = 0.01 $min^{-1}$, $k_i$ = 0, $l_{apds}$ = 0; Initial Conditions: $[Esp1_T]$ = 0; $[Esp1_B]$ = 0).**

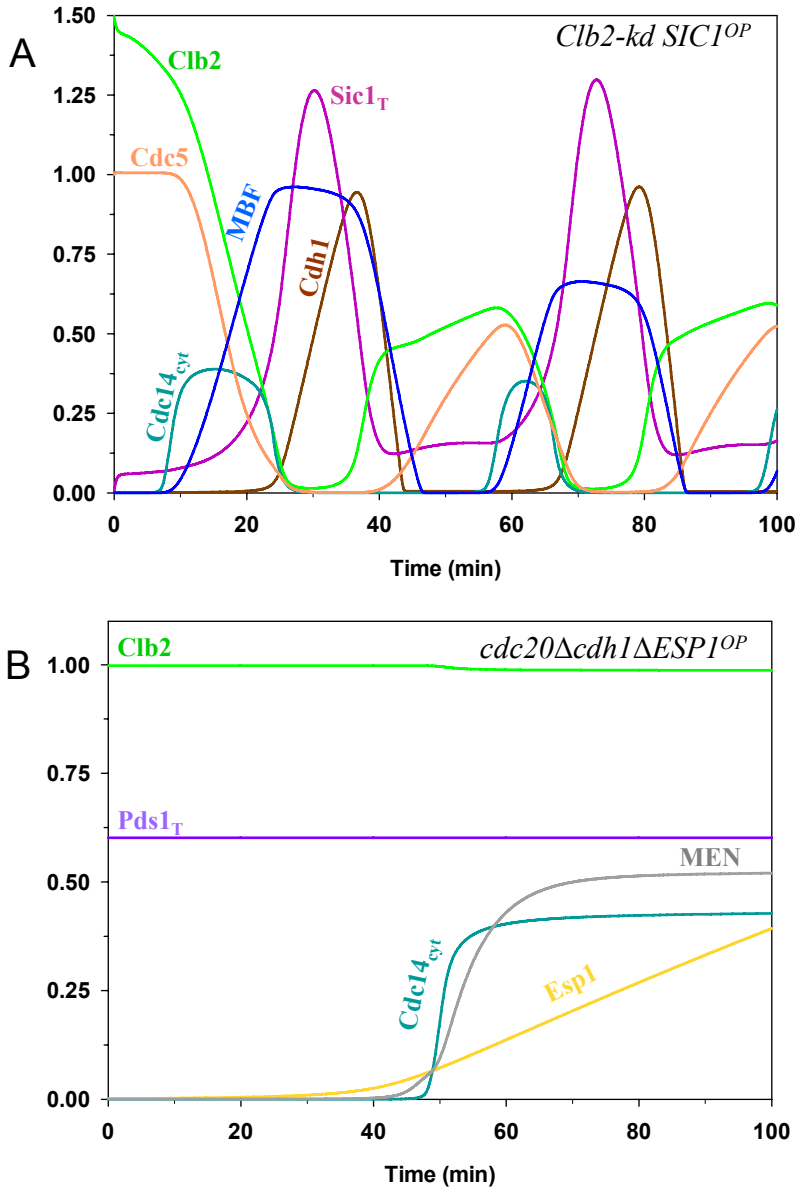


**Figure A3 - 4: Numerical simulations of mitotic progression: (A) after Cdc20 release in cells expressing Clb2-kd (undegradable Clb2 lacking KEN and destruction boxes) (Clb2nd = 0.5) and overexpressing Sic1 ($k_{ssic}$ = 0.2 $min^{-1}$); (C) in cells depleted of Cdc20 ($k_{s20} = k_{s20}' = 0$), overexpressing separase ($k_{sesp}$ = 0.01 $min^{-1}$) and with a Cdh1 deletion ($k_{dcdh} = k_{dcdh}' = 0$).**

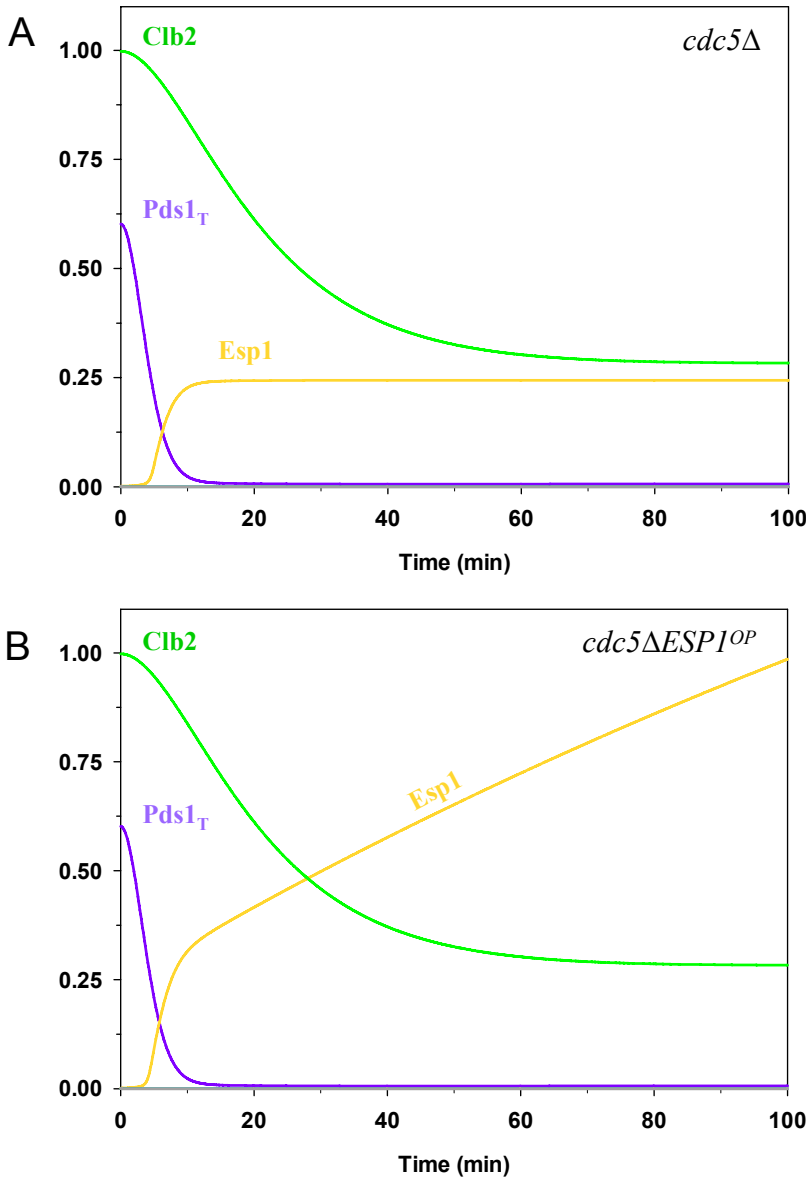


**Figure A3 - 5: Numerical simulations of mitotic progression after Cdc20 release in cells: (A) with inactivated Cdc5 ($k_{spolo}$ = $ks_{polo}$' = 0, Initial Conditions: [$Polo_T$] = [Polo] = 0), and (B) with Esp1 overexpression ($k_{sesp}$ = 0.01 $min^{-1}$).**

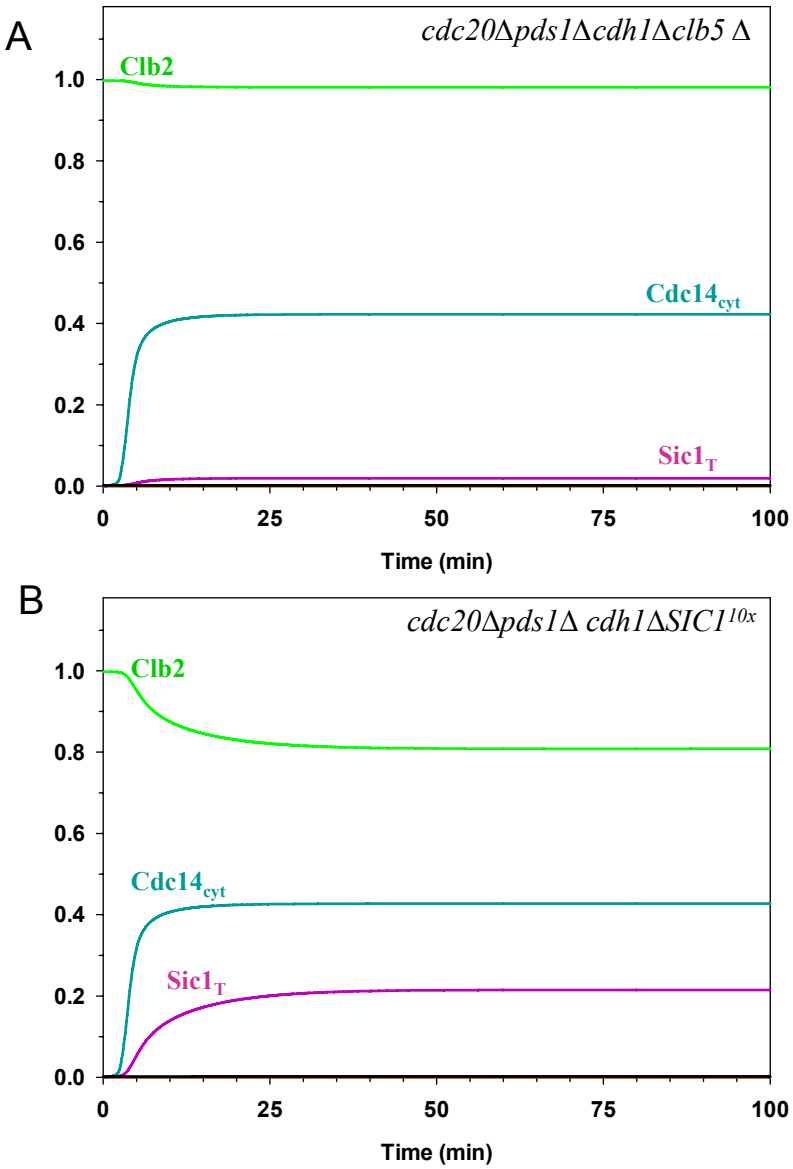


**Figure A3 - 6: Cdh1 becomes essential in *cdc20Δpds1Δclb5Δ* and *cdc20Δpds1ΔSIC1$^{10x}$* genetic backgrounds. Simulations of (A)*cdc20Δpds1Δcdh1clb5Δ*, and (B) *cdc20ΔpdsΔcdh1ΔSIC1$^{10x}$* were started from the stable steady state of *cdc20Δ* ($k_{s20}$'= $k_{s20}$=0).**
**Pds1 deletion: $k_{spds}$' = $k_{spds}$ =0, Initial Conditions [$Pds1_T$] = [$Esp1_B$] =0.**
**Cdh1 deletion: $k_{dcdh}$' = $k_{dcdh}$ =0.**
**Clb5 deletion: $k_{sclb5}$=0.001 min$^{-1}$, $k_{sclb5}$' = 0.005 (panel A).**
**Sic1 overexpression: $k_{ssic}$' =2 min$^{-1}$ (panel B).**

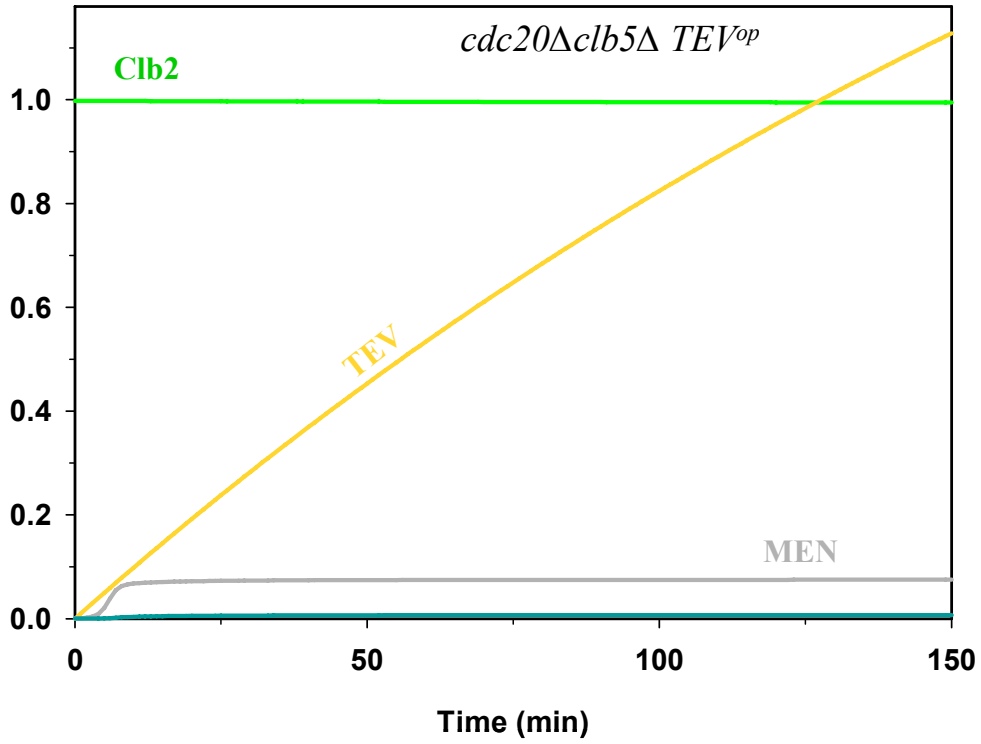


**Figure A3 - 7: TEV overexpression in *cdc20Δclb5Δ* cells cannot induce mitotic exit. The simulation was run from a *cdc20Δ* ($k_{s20}$'= $k_{s20}$=0) situation with Clb5 deleted ($k_{sclb5}$=0.001 $min^{-1}$, $k_{sclb5}$' = 0.005 $min^{-1}$) and TEV expressed ($k_{sesp}$ = 0.01 $min^{-1}$, $k_i$ = 0, $l_{apds}$ = 0; Initial Conditions: [$Esp1_T$] = 0; [$Esp1_B$] = 0).**

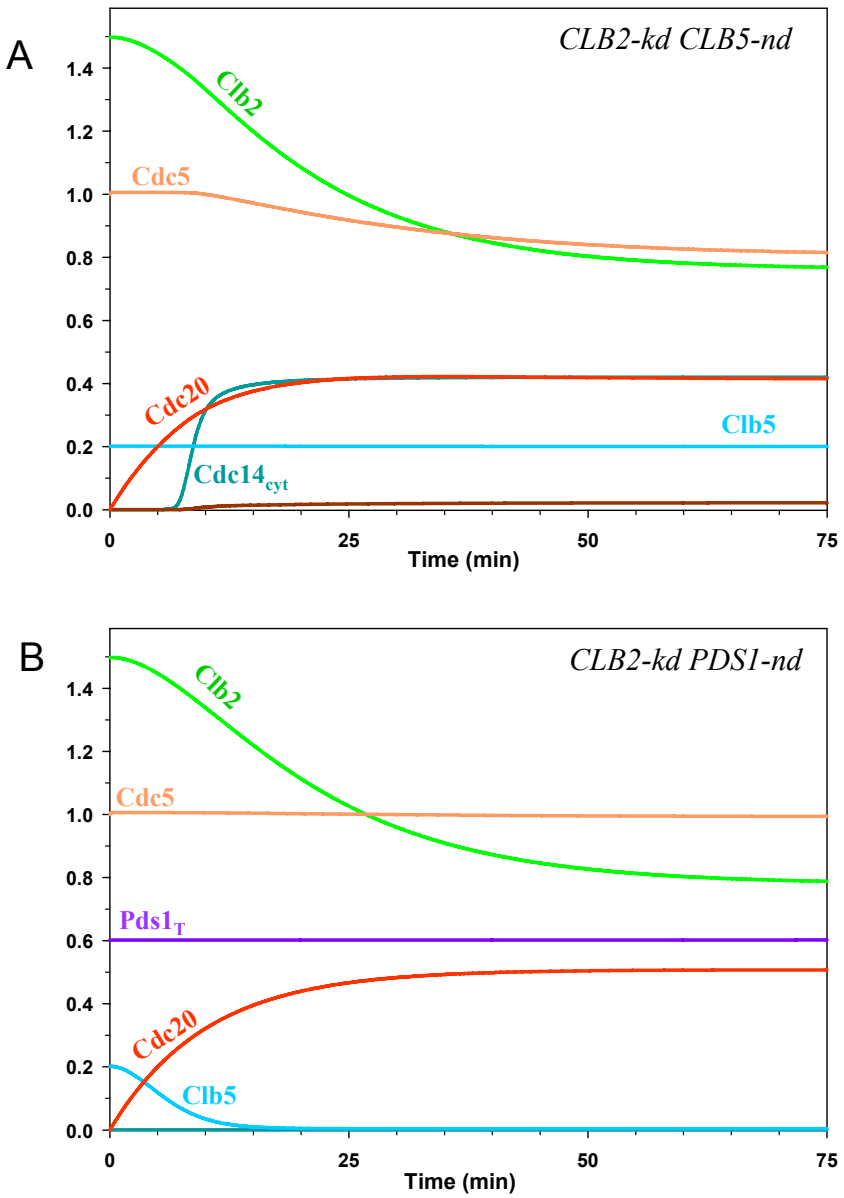


**Figure A3 - 8: Numerical simulations of mitotic progression after Cdc20 release in cells with non-degradable Clb2 (Clb2nd = 0.5). (A) Clb2-kd cells with non-degradable Clb5 ($k_{dclb5}$' = 0). (B) Clb2-kd cells with non-degradable Pds1 ($k_{dpds}$ = 0).**

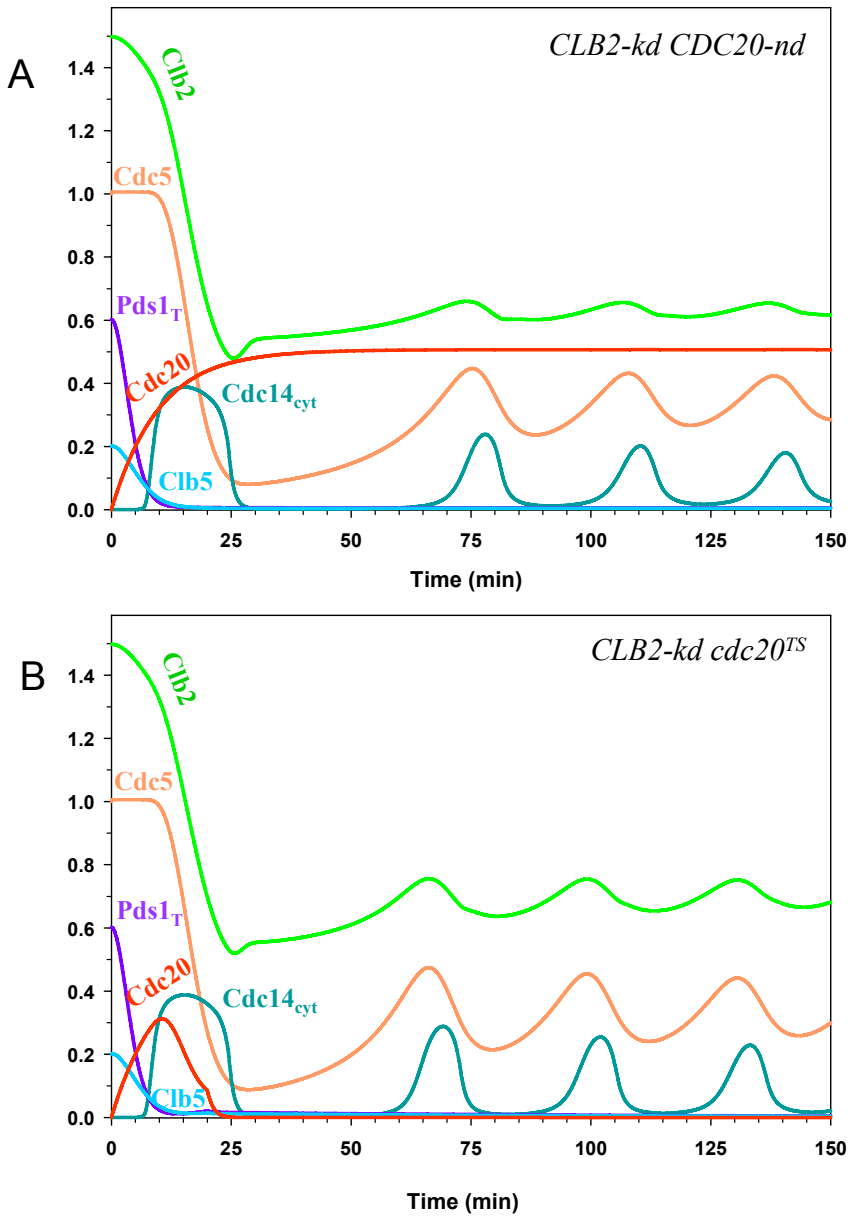


**Figure A3 - 9: Numerical simulations of mitotic progression after Cdc20 release in cells with non-degradable Clb2 (Clb2nd = 0.5). (A) Clb2-kd cells with non-degradable Cdc20 ($k_{ds20}$' = 0). (B) Clb2-kd cells with temperature sensitive Cdc20 (Cdc20 was inactivated after 20 min , $k_{s20}$'= $k_{s20}$=0, and Pds1 and Clb5 were not allowed to be re-synthesised, $k_{spds}$ = $k_{spds}$ = 0 and $k_{sclb5}$ = $k_{sclb5}$' =0).**

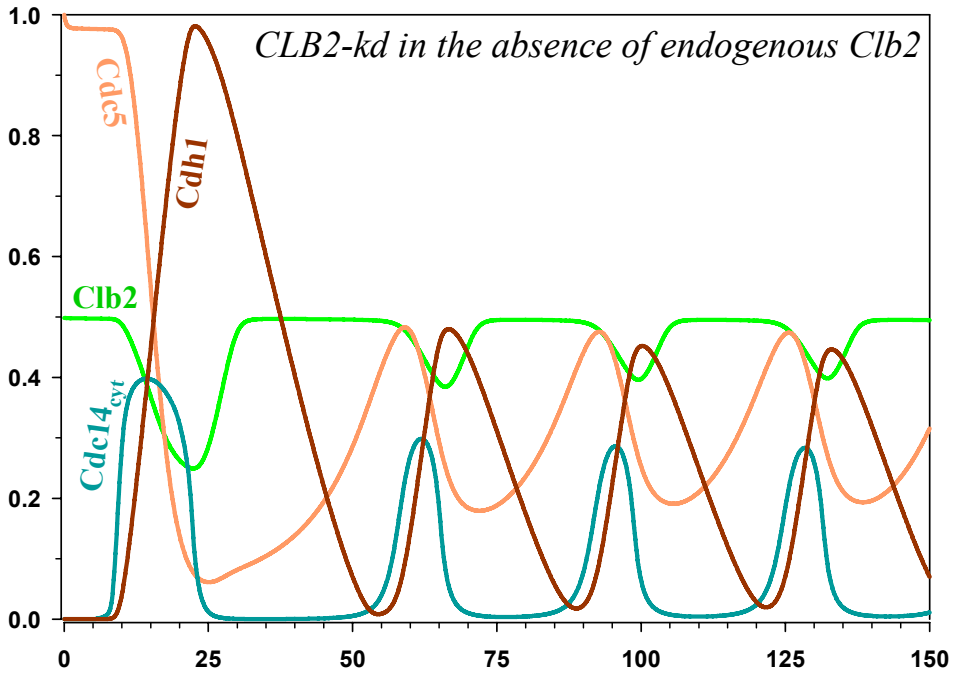


**Figure A3 - 10: Numerical simulation of mitotic progression after Cdc20 release in cells with non-degradable Clb2 (Clb2nd = 0.5) but with no expression of endogenous Clb2 ($k_{sclb2} = k_{sclb2}' = 0$).**

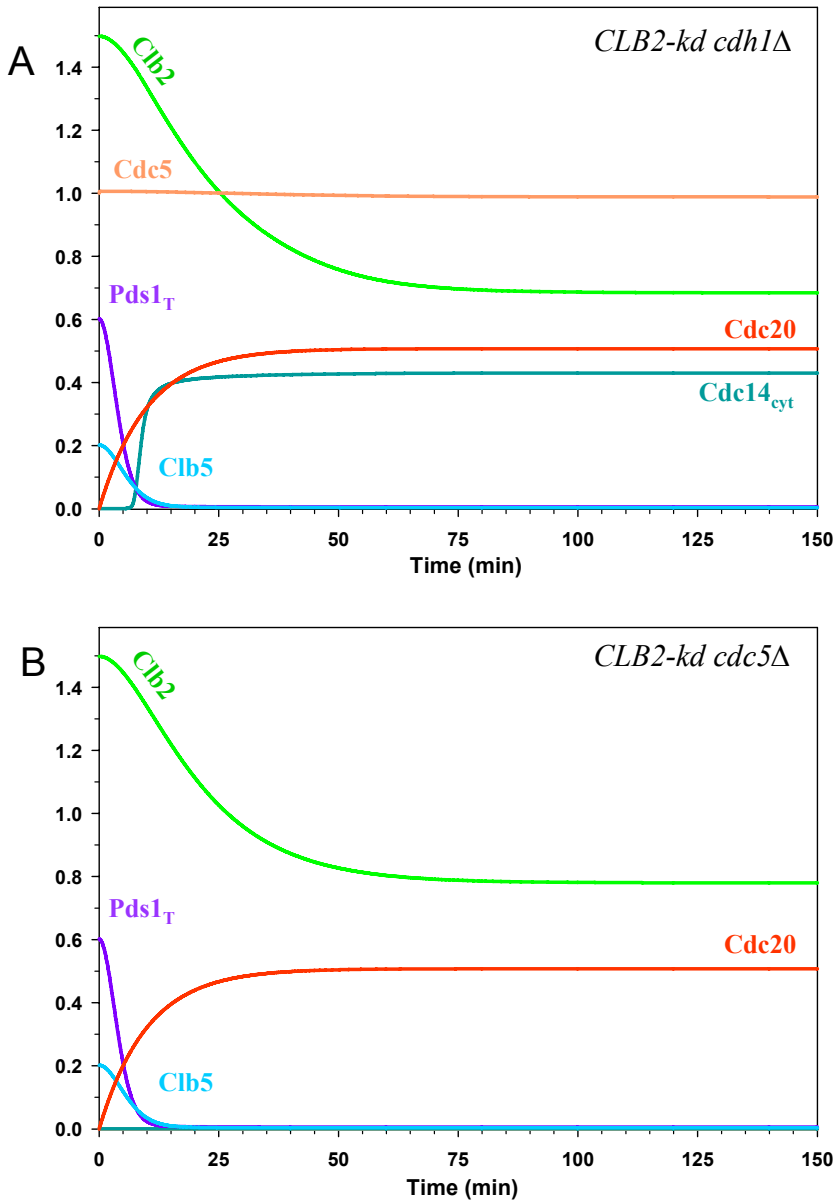


**Figure A3 - 11: Numerical simulations of mitotic progression after Cdc20 release in cells with non-degradable Clb2 (Clb2nd = 0.5). (A) Clb2-kd cells with Cdh1 deletion ($k_{dcdh} = k_{dcdh}' = 0$), or (B) with Cdc5 deletion ($k_{dpolo} = k_{dpolo}' = 0$, Initial Conditions $[Polo_T] = [Polo] = 0$).**

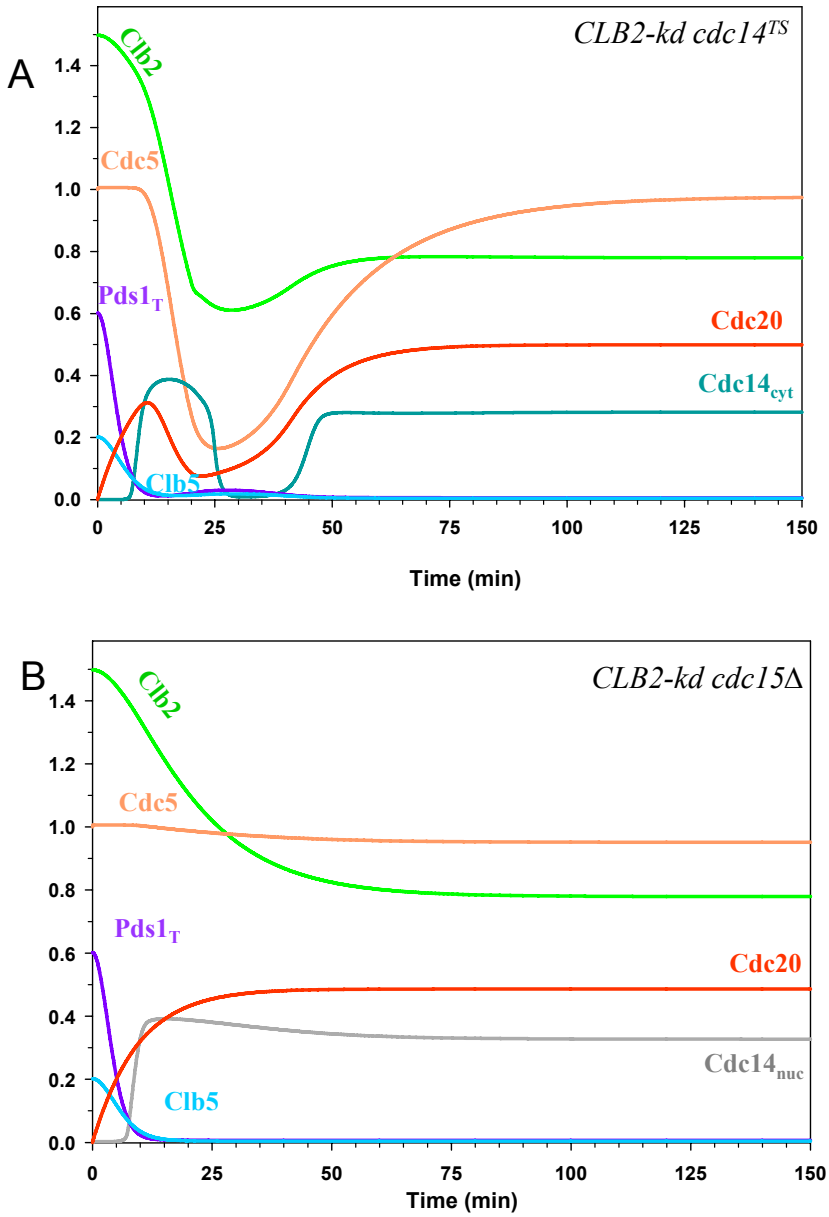


**Figure A3 - 12: Numerical simulations of mitotic progression after Cdc20 release in cells with non-degradable Clb2 (Clb2nd = 0.5). (A) Clb2-kd cells with Cdc14 inactivated after 20min from Cdc20 release (temperature sensitive allele – $k_{dcdh} = k_{dcdh}' = k_{aswi} = k_{aswi}' = k_{ac15}' = k_{ac15}'' = 0$) and (B) Clb2-kd cells with Cdc15 deletion ($k_{ac15} = k_{ac15}' = k_{ac15}'' = 0$).**

## 4. Mitotic Exit Mutant Situations that MV4 fails to explain

| Genotype | Observed Phenotype | Simulation Details | Simulated Phenotype | Notes |
|---|---|---|---|---|
| *cdh1Δsic1Δ GAL-CDC20* | Viable cells (Cross, 2003) | $k_{dcdh} = k_{dcdh}' = 0$<br>$k_{ssic} = k_{ssic}' = 0$<br>$k_{s20}$=0.1 $min^{-1}$ | Cell cycle block without Clb's | In the model, Cdc20 post-translational regulation is ignored which causes constitutively active Cdc20 which degrades all the Clb cyclins. |
| *bub2 pds1Δ* in nocodazole | Mitotic exit and re-replication (Alexandru et al., 1999) | $k_{s20} = k_{s20}' = 0$<br>$k_{spds} = k_{spds}' = 0$<br>$k_{item} = k_{item}' = 0$<br>Initial Conditions:<br>$Pds1_t = 0$<br>$Esp1_b = 0$ | Telophase block | Although Cdc14 gets activated in the model, Clb cyclins are not degraded. |
| GAL-ESP1 *Net1-6CDK1* in nocodazole | No Cdc14 release (Queralt et al., 2006) | $k_{s20} = k_{s20}' = 0$<br>$k_{sesp}$ = 0.01 $min^{-1}$<br>$k_p" = 0$ | Cdc14 release | The observed phenotype can only be explained if *Net1-6CDK1* compromises Net1 phosphorylation by MEN as well. |
| GAL-NET1 | Telophase arrest (Visintin et al., 1999) | $Net1_T = 10$ | Mitotic exit | Phosphorylated Net1 should have some residual activity for Cdc14 in the model. |
| *tem1Δ* GAL-CDC15 | Viable cells (Jaspersen et al., 1998) | $k_{atem} = k_{atem}' = 0$<br>$k_{ac15}$ = 0.5 $min^{-1}$ | Telophase block with transient Cdc14 release | In the model Tem1 is an essential MEN component, but the experiment suggests that $Cdc15^{OP}$ bypasses the Tem1 requirement. |
| *cdc15Δ* GAL-CDC5 | Viable cells (Visintin et al., 2003) | $k_{ac15} = k_{ac15}' = 0$<br>$k_{spolo}$ = 0.5 $min^{-1}$ | Telophase block with transient Cdc14 release | In the experiment $Cdc5^{OP}$ bypasses the MEN requirement for ME, but not in the model. |

# 5. Scripts for MATLAB

## a. ALLParameters.m

```
% Script written by Paula Freire
% Reproduction of parameters from MV4 model

% Parameters

Clb2nd      = 0     ; p0(1)   = Clb2nd    ;
ksclb2      = 0.015 ; p0(2)   = ksclb2    ;
ksclb2_p    = 0.005 ; p0(3)   = ksclb2_p  ;
kdclb2      = 0.02  ; p0(4)   = kdclb2    ;
kdclb2_p    = 0.1   ; p0(5)   = kdclb2_p  ;
kdclb2_pp   = 0.4   ; p0(6)   = kdclb2_pp ;
kasic2      = 40    ; p0(7)   = kasic2    ;
kdisic2     = 0.1   ; p0(8)   = kdisic2   ;
kasic5      = 10    ; p0(9)   = kasic5    ;
kdsic5      = 0.1   ; p0(10)  = kdsic5    ;
kssic       = 0.004 ; p0(11)  = kssic     ;
kssic_p     = 0.2   ; p0(12)  = kssic_p   ;
kdsic       = 0.04  ; p0(13)  = kdsic     ;
kdsic_p     = 2     ; p0(14)  = kdsic_p   ;
kdsic_pp    = 2     ; p0(15)  = kdsic_pp  ;
kdsic_ppp   = 1.5   ; p0(16)  = kdsic_ppp ;
ksmcm       = 0.01  ; p0(17)  = ksmcm     ;
ksmcm_p     = 1     ; p0(18)  = ksmcm_p   ;
kdmcm       = 0.25  ; p0(19)  = kdmcm     ;
Jmcm        = 0.01  ; p0(20)  = Jmcm      ;
ksclb5      = 0.002 ; p0(21)  = ksclb5    ;
ksclb5_p    = 0.01  ; p0(22)  = ksclb5_p  ;
kdclb5      = 0.01  ; p0(23)  = kdclb5    ;
kdclb5_p    = 1     ; p0(24)  = kdclb5_p  ;
kdclb5_pp   = 0     ; p0(25)  = kdclb5_pp ;
kscln       = 0.01  ; p0(26)  = kscln     ;
kscln_p     = 0.1   ; p0(27)  = kscln_p   ;
kdcln       = 0.25  ; p0(28)  = kdcln     ;
ks20        = 0.001 ; p0(29)  = ks20      ;
ks20_p      = 0.05  ; p0(30)  = ks20_p    ;
kd20        = 0.1   ; p0(31)  = kd20      ;
kd20_p      = 1     ; p0(32)  = kd20_p    ;
kdcdh       = 0.03  ; p0(33)  = kdcdh     ;
kdcdh_p     = 0.3   ; p0(34)  = kdcdh_p   ;
kpcdh       = 0.001 ; p0(35)  = kpcdh     ;
kpcdh_p     = 0.04  ; p0(36)  = kpcdh_p   ;
kpcdh_pp    = 0.75  ; p0(37)  = kpcdh_pp  ;
Jcdh        = 0.01  ; p0(38)  = Jcdh      ;
kaswi       = 0.2   ; p0(39)  = kaswi     ;
kaswi_p     = 1     ; p0(40)  = kaswi_p   ;
Jswi        = 0.1   ; p0(41)  = Jswi      ;
kiswi       = 0.01  ; p0(42)  = kiswi     ;
kiswi_p     = 0.5   ; p0(43)  = kiswi_p   ;
```

```
kiswi_pp    = 0.75  ; p0(44)  = kiswi_pp  ;
Swi5t       = 1     ; p0(45)  = Swi5t     ;
kspds       = 0.006 ; p0(46)  = kspds     ;
kspds_p     = 0.01  ; p0(47)  = kspds_p   ;
kdpds       = 0.01  ; p0(48)  = kdpds     ;
kdpds_p     = 2     ; p0(49)  = kdpds_p   ;
ksesp       = 0.001 ; p0(50)  = ksesp     ;
kdesp       = 0.004 ; p0(51)  = kdesp     ;
lapds       = 500   ; p0(52)  = lapds     ;
ldpds       = 1     ; p0(53)  = ldpds     ;
Net1T       = 1     ; p0(54)  = Net1T     ;
kd_p        = 0.1   ; p0(55)  = kd_p      ;
kd          = 0.45  ; p0(56)  = kd        ;
kp          = 0     ; p0(57)  = kp        ;
kp_p        = 2     ; p0(58)  = kp_p      ;
kp_pp       = 0.2   ; p0(59)  = kp_pp     ;
kp_ppp      = 3     ; p0(60)  = kp_ppp    ;
Jnet        = 0.05  ; p0(61)  = Jnet      ;
Cdc14T      = 0.5   ; p0(62)  = Cdc14T    ;
lanet       = 500   ; p0(63)  = lanet     ;
ldnet       = 1     ; p0(64)  = ldnet     ;
kexp        = 0.01  ; p0(65)  = kexp      ;
kexp_p      = 20    ; p0(66)  = kexp_p    ;
kexp_pp     = 0     ; p0(67)  = kexp_pp   ;
kimp        = 1     ; p0(68)  = kimp      ;
kspolo      = 0.001 ; p0(69)  = kspolo    ;
kspolo_p    = 0.05  ; p0(70)  = kspolo_p  ;
kdpolo      = 0.05  ; p0(71)  = kdpolo    ;
kdpolo_p    = 0.5   ; p0(72)  = kdpolo_p  ;
kdpolo_pp   = 0     ; p0(73)  = kdpolo_pp ;
kapolo      = 0     ; p0(74)  = kapolo    ;
kapolo_p    = 1     ; p0(75)  = kapolo_p  ;
kipolo      = 0.1   ; p0(76)  = kipolo    ;
Jpolo       = 0.1   ; p0(77)  = Jpolo     ;
katem       = 0     ; p0(78)  = katem     ;
katem_p     = 0.6   ; p0(79)  = katem_p   ;
kitem       = 0.1   ; p0(80)  = kitem     ;
kitem_p     = 1     ; p0(81)  = kitem_p   ;
kitem_pp    = 20    ; p0(82)  = kitem_pp  ;
Jtem1       = 0.005 ; p0(83)  = Jtem1     ;
kac15       = 0.03  ; p0(84)  = kac15     ;
kac15_p     = 0     ; p0(85)  = kac15_p   ;
kac15_pp    = 0.5   ; p0(86)  = kac15_pp  ;
kic15       = 0.03  ; p0(87)  = kic15     ;
kic15_p     = 0.2   ; p0(88)  = kic15_p   ;
Jcdc15      = 1     ; p0(89)  = Jcdc15    ;
lamen       = 100   ; p0(90)  = lamen     ;
ldmen       = 0.1   ; p0(91)  = ldmen     ;
kambf       = 0.1   ; p0(92)  = kambf     ;
kimbf       = 0     ; p0(93)  = kimbf     ;
kimbf_p     = 0.5   ; p0(94)  = kimbf_p   ;
kimbf_pp    = 0.5   ; p0(95)  = kimbf_pp  ;
Jmbf        = 0.01  ; p0(96)  = Jmbf      ;
PPT         = 1     ; p0(97)  = PPT       ;
kpp         = 0.1   ; p0(98)  = kpp       ;
ki          = 40    ; p0(99)  = ki        ;
kdcdh_pp    = 0     ; p0(100) = kdcdh_pp  ;
```

```
kaswi_pp    = 0     ; p0(101) = kaswi_pp  ;
Cdh1T       = 1     ; p0(102) = Cdh1T     ;
Tem1T       = 1     ; p0(103) = Tem1T     ;
Cdc15T      = 1     ; p0(104) = Cdc15T    ;
MBFT        = 1     ; p0(105) = MBFT      ;

save p0.dat p0 -ascii
```

### b. ParameterDistribution.m

```
% Script written by Paula Freire
% Generation of different parameter sets in Matlab
% New parameter sets are generated from a normal distribution with
% required Standard Deviation (SD).

% Parameters

label=char('Clb2nd', 'ksclb2', 'ksclb2_p', 'kdclb2', 'kdclb2_p', ...
    'kdclb2_p_p', 'kasic2', 'kdisic2', 'kasic5', 'kdsic5', 'kssic',...
    'kssic_p', 'kdsic', 'kdsic_p', 'kdsic_p_p', 'kdsic_p_p_p', ...
    'ksmcm', 'ksmcm_p', 'kdmcm', 'Jmcm', 'ksclb5', 'ksclb5_p', ...
    'kdclb5', 'kdclb5_p', 'kdclb5_p_p', 'kscln', 'kscln_p', 'kdcln', ...
    'ks20', 'ks20_p', 'kd20', 'kd20_p', 'kdcdh', 'kdcdh_p', 'kpcdh', ...
    'kpcdh_p', 'kpcdh_p_p', 'Jcdh', 'kaswi', 'kaswi_p', 'Jswi', ...
    'kiswi', 'kiswi_p', 'kiswi_p_p', 'Swi5t', 'kspds', 'kspds_p', ...
    'kdpds', 'kdpds_p', 'ksesp', 'kdesp', 'lapds', 'ldpds', 'Net1T',...
    'kd_p', 'kd', 'kp', 'kp_p', 'kp_p_p', 'kp_p_p_p', 'Jnet', 'Cdc14T',...
    'lanet', 'ldnet', 'kexp', 'kexp_p', 'kexp_p_p', 'kimp', 'kspolo',...
    'kspolo_p', 'kdpolo', 'kdpolo_p', 'kdpolo_p_p', 'kapolo', ...
    'kapolo_p', 'kipolo', 'Jpolo', 'katem', 'katem_p', 'kitem', ...
    'kitem_p', 'kitem_p_p', 'Jtem1', 'kac15', 'kac15_p', 'kac15_p_p', ...
    'kic15', 'kic15_p', 'Jcdc15', 'lamen', 'ldmen', 'kambf', 'kimbf', ...
    'kimbf_p', 'kimbf_p_p', 'Jmbf', 'PPT', 'kpp', 'ki', 'kdcdh_p_p', ...
    'kaswi_p_p','Cdh1T','Tem1T','Cdc15T','MBFT');

load p0.dat % This file was generated from ALLParameters.m

SD=0.10*p0; % Standard Deviation
viablemutants=0;
index_J=[20 38 41 61 77 83 89 96]; % Michaelis constants

% z is a vector of the same length of p0.
% All its entries are 1 except in the ones where p0 is zero.
% When p0 is zero, z becomes zero as well.
% z is an auxiliar vector to prevent zeroed out parameters to assume
% non zero values in the newly generated parameter set.
z=true(1,length(p0));
for i=1:length(p0)
        if p0(i)==0
           z(i)=0;
        end
end

for k=1:10000
    p_set_SD10(k,:)=(p0+randn(1,105).*SD).*z; % New sets of parameter
                                              % values
    neg_index=[];
    neg_index=find(p_set_SD10(k,:)<0); % Negative parameter values are
                                       % set to zero.
    for i=1:length(neg_index);
        p_set_SD10(k,neg_index(i))=0;
    end
```

```
    for j=1:length(index_J)
        if p_set_SD10(k,index_J(j))==0 % Michaelis constants cannot be
                                       % zero.
            p_set_SD10(k,index_J(j))=0.00001;
        end
    end
end


save p_set_SD10.dat p_set_SD10 -ascii
```

### c. *MB_set.m*

```
% Script written by Paula Freire
% MV4 Model in Matlab
% Parameters from a metaphase block

% Parameters

load p_set_SD10.dat

p_MB_SD10=p_set_SD10;
% ks20 and ks20_p are set to zero in all parameter sets.
p_MB_SD10(:,29:30)=zeros(length(p_MB_SD10),2);

save p_MB_SD10.dat p_MB_SD10 -ascii
```

### d. InitialConditions.m

```
% Script written by Paula Freire
% MV4 Model in Matlab
% Solves system of ODEs with parameters from Metaphase Block
% This file generates Initial Conditions according to the given
% parameter set

% Parameters

load p_MB_SD10.dat
% load Init_Cond_SD10.dat

% Initial Conditions
CLB2Ti   = 0 ;
TRIM2i   = 0 ;
MCMi     = 0 ;
CLB5Ti   = 0 ;
CLNi     = 0 ;
TRIM5i   = 0 ;
CDC20i   = 0 ;
CDH1i    = 0 ;
SIC1Ti   = 0 ;
SWI5i    = 0 ;
PDS1Ti   = 0 ;
ESP1Ti   = 0 ;
ESP1Bi   = 0 ;
NET1DEPi = 0 ;
NET1PPi  = 0 ;
RENTi    = 0 ;
RENTPi   = 0 ;
CDC14Ni  = 0 ;
POLOTi   = 0 ;
POLOi    = 0 ;
TEM1i    = 0 ;
CDC15i   = 0 ;
MENi     = 0 ;
MBFi     = 0 ;

check = 0 % This variable helps following the progression of the
          % simulation.

for k=1:10000
% Solving the system
init_cond = [CLB2Ti TRIM2i MCMi CLB5Ti CLNi TRIM5i CDC20i CDH1i SIC1Ti ...
    SWI5i PDS1Ti ESP1Ti ESP1Bi NET1DEPi NET1PPi RENTi RENTPi CDC14Ni ...
    POLOTi POLOi TEM1i CDC15i MENi MBFi];
tspan = [0 1000];
[t,x] = ode23s(@(t1,y1) MV4(t1,y1,p_MB_SD10(k,:)),tspan,init_cond);

Init_Cond_SD10(k,:)=x(length(x),1:24);

check = check+1
```

```
end

% Save last concentrations to be used as initial conditions for each
% parameter set
save Init_Cond_SD10.dat Init_Cond_SD10 -ascii
```

### e. *MV4.m*

```
% Function to solve system of ODE's

function yprime = MV4(t,x,p)
yprime = [ p(2)+p(3)*x(3)-x(1)*(p(4)+p(5)*x(7)+p(6)*x(8)); ... %
x(1)=Clb2T

    p(7)*(x(1)-x(2)+p(1))*(x(9)-x(2)-x(6))-p(8)*x(2)-
x(2)*(p(4)+p(5)*x(7)+p(6)*x(8)+p(13)+p(14)*(x(4)-x(6))+p(15)*(x(1)-
x(2)+p(1))+p(16)*x(5)); ... % x(2)=Trim2

    (p(17)+p(18)*(x(1)-x(2)+p(1)))*(1-x(3))/(p(20)+1-x(3))-
p(19)*x(3)/(p(20)+x(3)); ... % x(3)=Mcm1

    p(21)+p(22)*x(24)-x(4)*(p(23)+p(24)*x(7)+p(25)*x(8)); ... %
x(4)=Clb5T

    p(26)+ p(27)*x(24)-p(28)*x(5); ... % x(5)=Cln

    p(9)*(x(4)-x(6))*(x(9)-x(2)-x(6))-p(10)*x(6)-
x(6)*(p(23)+p(24)*x(7)+p(25)*x(8)+p(13)+p(14)*(x(4)-x(6))+p(15)*(x(1)-
x(2)+p(1))+p(16)*x(5)); ... % x(6)=Trim5

    p(29)+x(3)*p(30)-x(7)*(p(31)+p(32)*x(8)); ... % x(7)=Cdc20
    (p(100)+p(33)*x(18)+p(34)*(p(62)-x(18)-x(16)))*(p(102)-
x(8))/(p(38)+p(102)-x(8))-(p(35)+p(36)*(x(1)-x(2)+p(1))+p(37)*(x(4)-
x(6)))*x(8)/(p(38)+x(8)); ... % x(8)=Cdh1

    p(11)+p(12)*x(10)-x(9)*(p(13)+p(14)*(x(4)-x(6))+p(15)*(x(1)-
x(2)+p(1))+p(16)*x(5)); ... % x(9)=Sic1t
    (p(101)+p(39)*x(18)+p(40)*(p(62)-x(18)-x(16)))*(p(45)-
x(10))/(p(41)+p(45)-x(10))-x(10)*(p(42)+p(43)*(x(1)-
x(2)+p(1))+p(44)*(x(4)-x(6)))/(x(10)+p(41)); ... x(10)=Swi5

    p(46)+p(47)*x(24)-(p(48)+p(49)*x(7))*x(11); ... % x(11)=Pds1T

    p(50)-p(51)*x(12); ... % x(12)=Esp1T

    p(52)*(x(11)-x(13))*(x(12)-x(13))-
x(13)*(p(53)+p(51)+p(48)+p(49)*x(7)); ... % x(13)=Esp1b
    (p(54)-x(14))*(p(56)*(p(97)*(1+p(98)*p(99)*(x(12)-
x(13)))/(1+p(99)*(x(12)-x(13))))+p(55)*x(18))/(p(61)+p(54)-x(14))-
x(14)*(p(57)+p(59)*(x(1)-x(2)+p(1))+p(60)*x(23))/(p(61)+x(14)); ... %
x(14)=Net1deP

    p(58)*x(20)*(p(54)-x(14)-x(15))-
x(15)*(p(56)*(p(97)*(1+p(98)*p(99)*(x(12)-x(13)))/(1+p(99)*(x(12)-
x(13))))+p(55)*x(18))/(p(61)+p(54)-x(14)); ...% x(15)=Net1PP

    p(63)*(p(54)-x(15)-x(16))*x(18)-p(64)*x(16)-p(58)*x(20)*x(17); ... %
x(16)=RENT
```

```
    (p(57)+p(59)*(x(1)-x(2)+p(1))+p(60)*x(23))/(p(61)+x(14))*(x(16)-
x(17))-(p(56)*(p(97)*(1+p(98)*p(99)*(x(12)-x(13)))/(1+p(99)*(x(12)-
x(13))))+p(55)*x(18))/(p(61)+p(54)-x(14))*x(17)+p(63)*(p(54)-x(14)-
x(15)-x(17))*x(18)-p(64)*x(17)-p(58)*x(20)*x(17); ... % x(17)=RENTP

    p(58)*x(20)*x(17)-p(63)*(p(54)-x(15)-x(16))*x(18)+p(64)*x(16)-
(p(65)+p(66)*x(23)+p(67)*(x(1)-x(2)+p(1)))*x(18)+p(68)*(p(62)-x(18)-
x(16)); ... % x(18)=Cdc14n

    p(69)+p(70)*x(3)-(p(71)+p(72)*x(8)+p(73)*x(7))*x(19); ... %
x(19)=PoloT
    (p(74)+p(75)*(x(1)-x(2)+p(1)))*(x(19)-x(20))/(p(77)+x(19)-x(20))-
p(76)*x(20)/(p(77)+x(20))-(p(71)+p(72)*x(8)+p(73)*x(7))*x(20); ... %
x(20)=Polo

    (p(78)+p(79)*x(20))*(p(103)-x(21))/(p(83)+p(103)-x(21))-
(p(80)+p(81)/(1+p(82)*(x(12)-x(13))))*x(21)/(p(83)+x(21)); ... %
x(21)=Tem1

    (p(84)+p(85)*x(18)+p(86)*(p(62)-x(18)-x(16)))*(p(104)-
x(22))/(p(89)+p(104)-x(22))-(p(87)+p(88)*(x(1)-
x(2)+p(1)))*x(22)/(p(89)+x(22)); ... % x(22)=Cdc15

    p(90)*(x(21)-x(23))*(x(22)-x(23))-p(91)*x(23)-
(p(80)+p(81)/(1+p(82)*(x(12)-x(13))))*x(23)/(p(83)+x(21))-
(p(87)+p(88)*(x(1)-x(2)+p(1)))*x(23)/(p(89)+x(22)); ... % x(23)=MEN

    p(92)*(p(105)-x(24))/(p(96)+p(105)-x(24))-(p(93)+p(94)*(x(1)-
x(2)+p(1))+p(95)*(x(4)-x(6)))*x(24)/(p(96)+x(24)); ... % x(24)=MBF
    ];
```

### f. MitoticExit.m

```
% Script written by Paula Freire
% MV4 Model in Matlab
% Script uses the function 'checkviability.m' to evaluate mutant
% viability

% Parameters

load p0.dat
load p_set_SD10.dat


% Initial Conditions
load Init_Cond_SD10.dat

tspan = [0 600];  % Time interval for simulation
XT=1;             % Total Amount of general kinase/phosphatase substrate
kp=2;
viablemutants=0; % Before running the code the number of viable mutants
                 % should be null.
check=0          % This variable lets you check how the code is
                 % running.
n=1;


for k=1:10000

    p=p_set_SD10(k,:);% New set of parameter values
    init_cond=Init_Cond_SD10(k,:); % New set of initial conditions
                                   % corresponding to the
                                   % parameter set


    % Solving the system
    [t,x] = ode23s(@(t1,y1) MV4(t1,y1,p),tspan,init_cond);

    % Other Components
    x(:,25) = x(:,1)-x(:,2)+p(1); % Clb2
    x(:,26) = x(:,4)-x(:,6); % Clb5
    x(:,27) = x(:,12)-x(:,13); % Esp1
    x(:,28) = x(:,11)-x(:,13); % Pds1
    x(:,29) = p(62)-x(:,18)-x(:,16); % Cdc14c
    x(:,30) = x(:,9)-x(:,2)-x(:,6); % Sic1
    x(:,31) = x(:,25)+x(:,26); % Clb2+Clb5
    % x(:,32) = (x(:,25)+x(:,26))./(x(:,29)+0.2*x(:,18)+ppase);
    % Clb2+Clb5/(Cdc14c+ppase)
    % x(:,33) = x(:,25)./(x(:,29)+0.2*x(:,18)+ppase);
    % Clb2/(Cdc14c+ppase)
    x(:,32) = x(:,25)*XT./(x(:,25)+kp*(x(:,29)+x(:,18)*0.2)); % General
                                                    % Clb2/Cdc14 substrate
    x(:,33) = x(:,31)*XT./(x(:,31)+kp*(x(:,29)+x(:,18)*0.2)); % General
                                                  % Clb2,5/Cdc14 substrate
```

```
    c=checkviability(x,p,t);

    % Check if mutant is viable, count number of viable mutants, store
    % index of inviable mutants in 'list_p'
    if checkviability(x,p,t)==1
        viablemutants=viablemutants+1;
    else
        list_p(n,:)=[k c];
        n=n+1;
    end

    check=check+1

end

% list_p=list_p';
save list_p_inv_SD10.dat list_p -ascii % Stores indexes of inviable
                                       % mutants
save viablemutants_SD10.dat viablemutants -ascii % Stores the number of
                                                 % viable mutants
```

### g. checkviability.m

```
% Function to check if a mutant is viable

function viablemutant = checkviability(z,p,t)

    % Verification that there are oscillations

    % 1st derivative for Clb2
    for i=1:length(z(:,1))
        der(i,1) = p(2)+p(3)*z(i,3)-
z(i,1)*(p(4)+p(5)*z(i,7)+p(6)*z(i,8)); ... % z(i,1)=Clb2T
        der(i,2) = p(7)*(z(i,1)-z(i,2)+p(1))*(z(i,9)-z(i,2)-z(i,6))-
p(8)*z(i,2)-z(i,2)*(p(4)+p(5)*z(i,7)+p(6)*z(i,8)+p(13)+p(14)*(z(i,4)-
z(i,6))+p(15)*(z(i,1)-z(i,2)+p(1))+p(16)*z(i,5)); ... % z(i,2)=Trim2
        der(i,3) = der(i,1)-der(i,2); % Clb2
    end

    s_max=0;
    s_min=0;
    maxlist=[];
    index_max=[];

    % For x(i) to be a maximum, the derivative must be zero and this is
    % equivalent to think that the derivative changes signs at that
    % point. Moreover, in a maximum, the derivative goes from positive
    % to negative.
    % If these conditions are verified then take the corresponding
    % time-point.

    % These two entries tell you where the Clb2 derivative changes
    % signs.
    change_signs = der(1:length(t)-1,3).*der(2:length(t),3);
    index = find(change_signs <= 0);

    % This for loop first separates the index for maximums and
    % then for minimums
    for i=1:length(index)
        if der(index(i),3)>0
            s_max=s_max+1;
            index_max(s_max)=index(i);
            maxlist(s_max)=t(index(i)); % This stores the times where a
                                        % maximum occurs
        end
    end


   % Period is calculated as the round value to the closest integer.
   period=[];
    for i=3:s_max
        period(i-2)=round(maxlist(i)-maxlist(i-1)); % To calculate the
                                                    % period, we don't
                                                    % want the first
```

```
                                                    % maximum value.
    end

    % Check if period is kept (within 1 min boundary)
    j=1;
    for i=2:length(period)
        if abs((period(i-1)-period(i))/mean(period))<=mean(period)*0.05
            j=j+1;
        end
    end

    % Make sure that period(2) exists for the simulation
    if length(period)<2
        period=[-1 -1];
    end

     % Check if mutant is viable

    viablemutant=0;
%     period
    s = length(index_max);

        if j>2 && period(length(period))>=30 &&
period(length(period))<=100
            % We want to look at what is happening between the two last
            % maximum peaks (last period interval).
            Clb2subs     = [z(index_max(s-1):index_max(s),32)
t(index_max(s-1):index_max(s))];
            Clb5Clb2subs = [z(index_max(s-1):index_max(s),33)
t(index_max(s-1):index_max(s))];
            Esp1         = [z(index_max(s-1):index_max(s),27)
t(index_max(s-1):index_max(s))];

            MExit    = 0;
            StartM   = 0;
            Anaphase = 0;

            % Mitotic Exit - Kinase activity is low enough to allow
            % relicensing.
            tresh_Clb5Clb2subs = find(Clb5Clb2subs(:,1)<=0.4,1);
            MExit = Clb5Clb2subs(tresh_Clb5Clb2subs,2);

            % If there is no thresh_Clb5Clb2, the code doesn't go into
            % this if loop, StartM and Anaphase won't be calculated.
            if isempty(tresh_Clb5Clb2subs)
               MExit  = 0;
               StartM = 0;
            else % Start Mitosis & Check Anaphase
               tresh_Clb2subs =
find(Clb2subs(tresh_Clb5Clb2subs:length(Clb2subs(:,1)),1)>=0.6,1)+tresh_
Clb5Clb2subs; % We are looking at Start of Mitosis only after the cell
              % has exited mitosis.
               StartM = Clb2subs(tresh_Clb2subs,2);
               if isempty(tresh_Clb2subs)
                   StartM = 0;
```

```
        end
        aux4 = length(Clb2subs(:,1));
        if isempty(aux4)
            Anaphase = 0;
        elseif Esp1(aux4,1)>=0.1
            Anaphase = 1;
        end
    end

    if  MExit<StartM && Anaphase==1
        viablemutant=1;
    end

end
```

### h. Calc_Period_Ampl.m

```
% Script written by Paula Freire
% MV4 Model in Matlab
% From a given parameter set, this script stores the period and
% the amplitude of every simulation which have a limit cycle behaviour
% This script also stores how many they are.

load p_set_SD10.dat
load Init_Cond_SD10.dat

tspan = [0 600];

check = 0

for k=1:10000
    p=p_set_SD10(k,:);% New set of parameter values
    init_cond=Init_Cond_SD10(k,:); % New set of initial conditions
                                   % corresponding to the parameter set

    % Solving the system
    [t,x] = ode23s(@(t1,y1) MV4(t1,y1,p),tspan,init_cond);

    % Other Components
    x(:,25) = x(:,1)-x(:,2)+p(1); % Clb2
    x(:,26) = x(:,4)-x(:,6); % Clb5
    x(:,27) = x(:,12)-x(:,13); % Esp1
    x(:,28) = x(:,11)-x(:,13); % Pds1
    x(:,29) = p(62)-x(:,18)-x(:,16); % Cdc14c
    x(:,30) = x(:,9)-x(:,2)-x(:,6); % Sic1

    % 1st derivative for Clb2
    for i=1:length(x(:,1))
        der(i,1) = p(2)+p(3)*x(i,3)-
x(i,1)*(p(4)+p(5)*x(i,7)+p(6)*x(i,8)); ... % x(i,1)=Clb2T
        der(i,2) = p(7)*(x(i,1)-x(i,2)+p(1))*(x(i,9)-x(i,2)-x(i,6))-
p(8)*x(i,2)-x(i,2)*(p(4)+p(5)*x(i,7)+p(6)*x(i,8)+p(13)+p(14)*(x(i,4)-
x(i,6))+p(15)*(x(i,1)-x(i,2)+p(1))+p(16)*x(i,5)); ... % x(i,2)=Trim2
        der(i,3) = der(i,1)-der(i,2); % Clb2
    end

    % Verification that there are oscillations

    s_max=0;
    s_min=0;
    maxlist=[];
    index_max=[];
    index_min=[];
    amplitude=0;

    % For x(i) to be a maximum, the derivative must be zero and this is
    % equivalent to think that the derivative changes signs at that
    % point. Moreover, in a maximum, the derivative goes from positive
```

```
 % to negative.
 % If these conditions are verified then take the corresponding
 % time-point.

 % These two entries tell you where the Clb2 derivative changes
 % signs.
 change_signs = der(1:length(t)-1,3).*der(2:length(t),3);
 index = find(change_signs <= 0);

 % This for loop first separates the index for maximums and
 % then for minimums.
 for i=1:length(index)
     if der(index(i),3)>0
         s_max=s_max+1;
         index_max(s_max)=index(i);
         maxlist(s_max)=t(index(i)); % This stores the times where
                                     % a maximum occurs.
     end
     if der(index(i),3)<0
         s_min=s_min+1;
         index_min(s_min)=index(i);
     end

 end

% Amplitude of the oscillation
if length(index_max)>1 && length(index_min)>1
    middle=round(length(index_max)/2); % Constant that helps to
                                       % calculate the amplitude
                                       % roughly around the middle of
                                       % the simulation.
    amplitude = x(index_max(middle),25)-x(index_min(middle),25);
else
    amplitude = 0;
end

% Period is calculated as the round value to the closest integer.
period=[];
 for i=3:s_max
     period(i-2)=round(maxlist(i)-maxlist(i-1)); % To calculate the
                                                 % period we don't
                                                 % want the first
                                                 % maximum value.
 end

 % Check if period is kept (within 1 min boundary)
 viablemutant=0;
 j=1;
 for i=2:length(period)
     if abs((period(i-1)-period(i))/mean(period))<=mean(period)*0.05
         j=j+1;
     end
 end
```

```
  if j>2
       n = length(period_list)+1;
       period_list(n)=period(j);
       amplitude_list(n)=amplitude;
       simulations(n)=k;
   end

    check=check+1

end

save('SD10.mat','period_list','-mat');
save('SD10.mat','amplitude_list','-append','-mat');
save('SD10.mat','simulations','-append','-mat');
```

### *i. Parameters_noTransc.m*

```
% Script written by Paula Freire
% MV4 Model in Matlab
% Parameters for No Regulated Transcription

% Parameters

Clb2nd      = 0     ; p(1)   = Clb2nd    ;
ksclb2      = 0.015 ; p(2)   = ksclb2    ;
ksclb2_p    = 0     ; p(3)   = ksclb2_p  ;
kdclb2      = 0.02  ; p(4)   = kdclb2    ;
kdclb2_p    = 0.1   ; p(5)   = kdclb2_p  ;
kdclb2_pp   = 0.4   ; p(6)   = kdclb2_pp ;
kasic2      = 40    ; p(7)   = kasic2    ;
kdisic2     = 0.1   ; p(8)   = kdisic2   ;
kasic5      = 10    ; p(9)   = kasic5    ;
kdsic5      = 0.1   ; p(10)  = kdsic5    ;
kssic       = 0.004  ; p(11)  = kssic    ;
kssic_p     = 0     ; p(12)  = kssic_p   ;
kdsic       = 0.04  ; p(13)  = kdsic     ;
kdsic_p     = 2     ; p(14)  = kdsic_p   ;
kdsic_pp    = 2     ; p(15)  = kdsic_pp  ;
kdsic_ppp   = 1.5   ; p(16)  = kdsic_ppp ;
ksmcm       = 0.01  ; p(17)  = ksmcm     ;
ksmcm_p     = 1     ; p(18)  = ksmcm_p   ;
kdmcm       = 0.25  ; p(19)  = kdmcm     ;
Jmcm        = 0.01  ; p(20)  = Jmcm      ;
ksclb5      = 0.002 ; p(21)  = ksclb5    ;
ksclb5_p    = 0     ; p(22)  = ksclb5_p  ;
kdclb5      = 0.01  ; p(23)  = kdclb5    ;
kdclb5_p    = 1     ; p(24)  = kdclb5_p  ;
kdclb5_pp   = 0     ; p(25)  = kdclb5_pp ;
kscln       = 0.01  ; p(26)  = kscln     ;
kscln_p     = 0     ; p(27)  = kscln_p   ;
kdcln       = 0.25  ; p(28)  = kdcln     ;
ks20        = 0.01  ; p(29)  = ks20      ;
ks20_p      = 0     ; p(30)  = ks20_p    ;
kd20        = 0.1   ; p(31)  = kd20      ;
kd20_p      = 1     ; p(32)  = kd20_p    ;
kdcdh       = 0.03  ; p(33)  = kdcdh     ;
kdcdh_p     = 0.3   ; p(34)  = kdcdh_p   ;
kpcdh       = 0.001 ; p(35)  = kpcdh     ;
kpcdh_p     = 0.04  ; p(36)  = kpcdh_p   ;
kpcdh_pp    = 0.75  ; p(37)  = kpcdh_pp  ;
Jcdh        = 0.01  ; p(38)  = Jcdh      ;
kaswi       = 0.2   ; p(39)  = kaswi     ;
kaswi_p     = 1     ; p(40)  = kaswi_p   ;
Jswi        = 0.1   ; p(41)  = Jswi      ;
kiswi       = 0.01  ; p(42)  = kiswi     ;
kiswi_p     = 0.5   ; p(43)  = kiswi_p   ;
kiswi_pp    = 0.75  ; p(44)  = kiswi_pp  ;
Swi5t       = 1     ; p(45)  = Swi5t     ;
kspds       = 0.006 ; p(46)  = kspds     ;
kspds_p     = 0     ; p(47)  = kspds_p   ;
kdpds       = 0.01  ; p(48)  = kdpds     ;
kdpds_p     = 2     ; p(49)  = kdpds_p   ;
ksesp       = 0.001 ; p(50)  = ksesp     ;
```

```
kdesp       = 0.004 ; p(51)  = kdesp     ;
lapds       = 500   ; p(52)  = lapds     ;
ldpds       = 1     ; p(53)  = ldpds     ;
Net1T       = 1     ; p(54)  = Net1T     ;
kd_p        = 0.1   ; p(55)  = kd_p      ;
kd          = 0.45  ; p(56)  = kd        ;
kp          = 0     ; p(57)  = kp        ;
kp_p        = 2     ; p(58)  = kp_p      ;
kp_pp       = 0.2   ; p(59)  = kp_pp     ;
kp_ppp      = 3     ; p(60)  = kp_ppp    ;
Jnet        = 0.05  ; p(61)  = Jnet      ;
Cdc14T      = 0.5   ; p(62)  = Cdc14T    ;
lanet       = 500   ; p(63)  = lanet     ;
ldnet       = 1     ; p(64)  = ldnet     ;
kexp        = 0.01  ; p(65)  = kexp      ;
kexp_p      = 20    ; p(66)  = kexp_p    ;
kexp_pp     = 0     ; p(67)  = kexp_pp   ;
kimp        = 1     ; p(68)  = kimp      ;
kspolo      = 0.05  ; p(69)  = kspolo    ;
kspolo_p    = 0     ; p(70)  = kspolo_p  ;
kdpolo      = 0.05  ; p(71)  = kdpolo    ;
kdpolo_p    = 0.5   ; p(72)  = kdpolo_p  ;
kdpolo_pp   = 0     ; p(73)  = kdpolo_pp ;
kapolo      = 0     ; p(74)  = kapolo    ;
kapolo_p    = 1     ; p(75)  = kapolo_p  ;
kipolo      = 0.1   ; p(76)  = kipolo    ;
Jpolo       = 0.1   ; p(77)  = Jpolo     ;
katem       = 0     ; p(78)  = katem     ;
katem_p     = 0.6   ; p(79)  = katem_p   ;
kitem       = 0.1   ; p(80)  = kitem     ;
kitem_p     = 1     ; p(81)  = kitem_p   ;
kitem_pp    = 20    ; p(82)  = kitem_pp  ;
Jtem1       = 0.005 ; p(83)  = Jtem1     ;
kac15       = 0.03  ; p(84)  = kac15     ;
kac15_p     = 0     ; p(85)  = kac15_p   ;
kac15_pp    = 0.5   ; p(86)  = kac15_pp  ;
kic15       = 0.03  ; p(87)  = kic15     ;
kic15_p     = 0.2   ; p(88)  = kic15_p   ;
Jcdc15      = 1     ; p(89)  = Jcdc15    ;
lamen       = 100   ; p(90)  = lamen     ;
ldmen       = 0.1   ; p(91)  = ldmen     ;
kambf       = 0.1   ; p(92)  = kambf     ;
kimbf       = 0     ; p(93)  = kimbf     ;
kimbf_p     = 0.5   ; p(94)  = kimbf_p   ;
kimbf_pp    = 0.5   ; p(95)  = kimbf_pp  ;
Jmbf        = 0.01  ; p(96)  = Jmbf      ;
PPT         = 1     ; p(97)  = PPT       ;
kpp         = 0.1   ; p(98)  = kpp       ;
ki          = 40    ; p(99)  = ki        ;
kdcdh_pp    = 0     ; p(100) = kdcdh_pp  ;
kaswi_pp    = 0     ; p(101) = kaswi_pp  ;
Cdh1T       = 1     ; p(102) = Cdh1T     ;
Tem1T       = 1     ; p(103) = Tem1T     ;
Cdc15T      = 1     ; p(104) = Cdc15T    ;
MBFT        = 1     ; p(105) = MBFT      ;

save p0_noTransc.dat p -ascii
```

### *j. Parameters_noDeg.m*

```
% Script written by Paula Freire
% MV4 Model in Matlab
% Parameters for No Regulated Degradation

% Parameters

Clb2nd      = 0      ; p(1)   = Clb2nd    ;
ksclb2      = 0.015  ; p(2)   = ksclb2    ;
ksclb2_p    = 0.005  ; p(3)   = ksclb2_p  ;
kdclb2      = 0.05   ; p(4)   = kdclb2    ;
kdclb2_p    = 0      ; p(5)   = kdclb2_p  ;
kdclb2_pp   = 0      ; p(6)   = kdclb2_pp ;
kasic2      = 40     ; p(7)   = kasic2    ;
kdisic2     = 0.1    ; p(8)   = kdisic2   ;
kasic5      = 10     ; p(9)   = kasic5    ;
kdsic5      = 0.1    ; p(10)  = kdsic5    ;
kssic       = 0.004  ; p(11)  = kssic     ;
kssic_p     = 0.2    ; p(12)  = kssic_p   ;
kdsic       = 0.2    ; p(13)  = kdsic     ;
kdsic_p     = 0      ; p(14)  = kdsic_p   ;
kdsic_pp    = 0      ; p(15)  = kdsic_pp  ;
kdsic_ppp   = 0      ; p(16)  = kdsic_ppp ;
ksmcm       = 0.01   ; p(17)  = ksmcm     ;
ksmcm_p     = 1      ; p(18)  = ksmcm_p   ;
kdmcm       = 0.25   ; p(19)  = kdmcm     ;
Jmcm        = 0.01   ; p(20)  = Jmcm      ;
ksclb5      = 0.002  ; p(21)  = ksclb5    ;
ksclb5_p    = 0.01   ; p(22)  = ksclb5_p  ;
kdclb5      = 0.01   ; p(23)  = kdclb5    ;
kdclb5_p    = 0      ; p(24)  = kdclb5_p  ;
kdclb5_pp   = 0      ; p(25)  = kdclb5_pp ;
kscln       = 0.01   ; p(26)  = kscln     ;
kscln_p     = 0.1    ; p(27)  = kscln_p   ;
kdcln       = 0.25   ; p(28)  = kdcln     ;
ks20        = 0.001  ; p(29)  = ks20      ;
ks20_p      = 0.05   ; p(30)  = ks20_p    ;
kd20        = 0.1    ; p(31)  = kd20      ;
kd20_p      = 0      ; p(32)  = kd20_p    ;
kdcdh       = 0.03   ; p(33)  = kdcdh     ;
kdcdh_p     = 0.3    ; p(34)  = kdcdh_p   ;
kpcdh       = 0.001  ; p(35)  = kpcdh     ;
kpcdh_p     = 0.04   ; p(36)  = kpcdh_p   ;
kpcdh_pp    = 0.75   ; p(37)  = kpcdh_pp  ;
Jcdh        = 0.01   ; p(38)  = Jcdh      ;
kaswi       = 0.2    ; p(39)  = kaswi     ;
kaswi_p     = 1      ; p(40)  = kaswi_p   ;
Jswi        = 0.1    ; p(41)  = Jswi      ;
kiswi       = 0.01   ; p(42)  = kiswi     ;
kiswi_p     = 0.5    ; p(43)  = kiswi_p   ;
kiswi_pp    = 0.75   ; p(44)  = kiswi_pp  ;
Swi5t       = 1      ; p(45)  = Swi5t     ;
kspds       = 0.006  ; p(46)  = kspds     ;
kspds_p     = 0      ; p(47)  = kspds_p   ;
kdpds       = 0.1    ; p(48)  = kdpds     ;
kdpds_p     = 0      ; p(49)  = kdpds_p   ;
```

```
ksesp       = 0.001  ; p(50)  = ksesp     ;
kdesp       = 0.004  ; p(51)  = kdesp     ;
lapds       = 500    ; p(52)  = lapds     ;
ldpds       = 1      ; p(53)  = ldpds     ;
Net1T       = 1      ; p(54)  = Net1T     ;
kd_p        = 0.1    ; p(55)  = kd_p      ;
kd          = 0.45   ; p(56)  = kd        ;
kp          = 0      ; p(57)  = kp        ;
kp_p        = 2      ; p(58)  = kp_p      ;
kp_pp       = 0.2    ; p(59)  = kp_pp     ;
kp_ppp      = 3      ; p(60)  = kp_ppp    ;
Jnet        = 0.05   ; p(61)  = Jnet      ;
Cdc14T      = 0.5    ; p(62)  = Cdc14T    ;
lanet       = 500    ; p(63)  = lanet     ;
ldnet       = 1      ; p(64)  = ldnet     ;
kexp        = 0.01   ; p(65)  = kexp      ;
kexp_p      = 20     ; p(66)  = kexp_p    ;
kexp_pp     = 0      ; p(67)  = kexp_pp   ;
kimp        = 1      ; p(68)  = kimp      ;
kspolo      = 0.001  ; p(69)  = kspolo    ;
kspolo_p    = 0.05   ; p(70)  = kspolo_p  ;
kdpolo      = 0.05   ; p(71)  = kdpolo    ;
kdpolo_p    = 0      ; p(72)  = kdpolo_p  ;
kdpolo_pp   = 0      ; p(73)  = kdpolo_pp ;
kapolo      = 0      ; p(74)  = kapolo    ;
kapolo_p    = 1      ; p(75)  = kapolo_p  ;
kipolo      = 0.1    ; p(76)  = kipolo    ;
Jpolo       = 0.1    ; p(77)  = Jpolo     ;
katem       = 0      ; p(78)  = katem     ;
katem_p     = 0.6    ; p(79)  = katem_p   ;
kitem       = 0.1    ; p(80)  = kitem     ;
kitem_p     = 1      ; p(81)  = kitem_p   ;
kitem_pp    = 20     ; p(82)  = kitem_pp  ;
Jtem1       = 0.005  ; p(83)  = Jtem1     ;
kac15       = 0.03   ; p(84)  = kac15     ;
kac15_p     = 0      ; p(85)  = kac15_p   ;
kac15_pp    = 0.5    ; p(86)  = kac15_pp  ;
kic15       = 0.03   ; p(87)  = kic15     ;
kic15_p     = 0.2    ; p(88)  = kic15_p   ;
Jcdc15      = 1      ; p(89)  = Jcdc15    ;
lamen       = 100    ; p(90)  = lamen     ;
ldmen       = 0.1    ; p(91)  = ldmen     ;
kambf       = 0.1    ; p(92)  = kambf     ;
kimbf       = 0      ; p(93)  = kimbf     ;
kimbf_p     = 0.5    ; p(94)  = kimbf_p   ;
kimbf_pp    = 0.5    ; p(95)  = kimbf_pp  ;
Jmbf        = 0.01   ; p(96)  = Jmbf      ;
PPT         = 1      ; p(97)  = PPT       ;
kpp         = 0.1    ; p(98)  = kpp       ;
ki          = 40     ; p(99)  = ki        ;
kdcdh_pp    = 0      ; p(100) = kdcdh_pp  ;
kaswi_pp    = 0      ; p(101) = kaswi_pp  ;
Cdh1T       = 1      ; p(102) = Cdh1T     ;
Tem1T       = 1      ; p(103) = Tem1T     ;
Cdc15T      = 1      ; p(104) = Cdc15T    ;
MBFT        = 1      ; p(105) = MBFT      ;

save p0_noDeg.dat p -ascii
```

## *6. Papers published during DPhil studies*

Novak B, Vinod PK, Freire P, Kapuy O. (2010). Systems-level feedback in cell-cycle control. Biochemical Society Transactions. 38(5):1242-6.

Vinod PK*, Freire P*, Rattani A, Ciliberto A, Uhlmann F and Novak B (2011). Computational modelling of mitotic exit in budding yeast – the role of separase and Cdc14 endocycles, Journal of the Royal, Interface. 8(61),1128-41.

** These authors contributed equally to this work.*

Freire P, Zhang T (2011). Two legs are better than one. Cell Cycle. 10(8):1189-90.

Freire P, Vinod PK, Novak B (2012). Interplay of Transcriptional and Proteolytic Regulation in driving Robust Cell Cycle Progression. Molecular. BioSystems. DOI: 10.1039/C2MB05406J (published online).